FAST - RESPONSE MEASUREMENTS OF THE CONCENTRATION OF SULPHUR (AND PHOSPHORUS) COMPOUNDS IN THE ATMOSPHERE

BY

Andrew Hadjitofi, B.Sc. (Hons).

AUGUST, 1978

A thesis submitted for the degree of Doctor of Philosophy of the University of London and for the Diploma of Imperial College.

Chemical Engineering Department,
Imperial College,
London, S.W.7. 2BY.

PREFACE

The work described in this thesis was carried out in the Department of Chemical Engineering, Imperial College of Science and Technology, University of London, between October 1973 and September 1976 under the supervision of Dr. M.J.G. Wilson.

The work is original and has not been submitted for a degree at any other university.

I would like to thank Dr. M.J.G. Wilson for his valuable help during the course of this work.

I would also like to thank the technical staff of the department, in particular Mr. Dick Woods of the electronics workship, the Dover Harbour Board, and Mr. Loveday - head groundsman at Harlington Sports ground.

The author gratefully acknowledges the three year studentship received from the Science Research Council and for their subsequent sponsorship of the project.

ABSTRACT

A flame photometric detector has been designed and constructed to respond to concentration fluctuations of sulphur and phosphorus compounds in the atmosphere often lasting only tens of milliseconds. The 90% response times for both sulphur and phosphorus channels are the shortest yet achieved being 80 milliseconds for the sulphur channel and 8 milliseconds for the phosphorus channel.

The detector has been used in experiments to record the concentration of sulphur dioxide emitted into the atmosphere from a variety of single identified sources at a range of distances. A major aim of analysing the data was to develop a simple statistic that utilises the concentration fluctuations in an attempt to produce a relation between source distance and concentration fluctuations. The results calculated using the statistic show that it is possible to distinguish between near and far sources particularly in unstable and neutral atmospheric conditions. The technique may help to provide a method of estimating the distance of an unknown source.

The detector has also been used to record the concentration of both sulphur and phosphorus compounds emitted from two coincident sources and two separate sources.

C O N T E N T S

CHAPTER 1

INTRODUCTION

Systematic measurements of air pollution - smoke and sulphur dioxide - were started in 1914 in the United Kingdom by the voluntary efforts of a Committee for Investigation of Atmospheric Pollution. From its humble beginnings in 1914 the Investigation had grown enormously by the time the Clean Air Act 1956 came into force and since 1961, under the auspices of the Warren Spring Laboratory, a National Survey is now compiled containing daily data on smoke and sulphur dioxide from well over 1300 sites in the United Kingdom.

In a typical year up to half a million measurements - on sulphur dioxide alone - are stored on computer tape at the Warren Spring Laboratory and these are used to compute monthly, seasonal and annual averages for each site. These results are published in Annual Tables under the general title "The Investigation of Air Pollution National Survey, Smoke and Sulphur Dioxide" obtainable from the Warren Spring Laboratory, together with the highest daily mean and the number of days when the pollution exceeds a certain level.

Possible effects of pollution on health are continuously studied under the surveillance of the Medical Research Council's Air Pollution Unit at St. Bartholomew's Hospital and organisations, such as the Central Electricity Generating Board (C.E.G.B.), have begun to use mobile laboratories which can measure several pollutants in a few minutes at a given site and visit many sites in succession.

Briefly, with respect to Air Pollution Measurements in the United States of America the situation is aptly typified by the warnings that have been expressed in the past five years or so concerning the "data for data's sake" approach.

However, despite the proliferation of air pollution measurements, at present, instruments for measuring air pollution can only collect a small fraction of the information that is available and might be considered useful. In many cases instruments cannot even match the response time and sensitivity of the human nose, still less the performance of some insects detecting pheromones.

Fairly well developed and reasonably satisfactory theory now exists for the prediction of stochastic mean concentrations in turbulent diffusion. However, the theory only treats a restricted aspect of the turbulent

diffusion process; namely the first moment of the probability distribution of the random variable - the mean concentration. At long sampling times, it is known that concentration is generally distributed log-normally, both in space and time; this is convenient because the results can be characterised by the geometric mean and the standard geometric deviation. Very little is known, however, about the rapid fluctuations that last only a second or less and yet this is long enough for smell to be perceived or other physiological effects to be initiated. From an engineering point of view the prediction or assessment of pollution nuisance or hazard can only be incomplete if based on mean-field theory alone because of the inability of the theory to predict reasonable estimates of instantaneous concentration profiles. Even where the theory has been developed it is of little practical use because of the lack of suitable experimental data.

It is, therefore, the first aim of this work to record new information about the way the concentration of air pollution fluctuates with time. A fast-response instrument has been developed which can follow fluctuations in sulphur concentration that are too rapid to be measured with other instruments.

The nature and approximate direction of an unknown source of pollution may be quickly determinable, but means of estimating its distance are still lacking. An approximate estimate would often be useful in detecting the presence of nearby sources or in distinguishing between two sources at very different distances. Thus, a method is to be developed that uses the concentration fluctuations to gain information about the source or sources of pollution and so help make it possible to estimate the distance of an unknown source.

The speed of response that has been achieved may make it possible to give a realistic description of the concentration pattern that would be experienced by an insect in a plume of pheromone and the development of methods of detecting plumes with the use of a fast-response instrument is relevant to the location of orebodies.

Simultaneous recording of the concentration of two elements (sulphur and phosporous) in the atmosphere, using a fast-response instrument, offers more interesting possibilities. Such measurements may help develop real-time methods and criteria for detecting pollution from sources that emit more than one pollutant and may also help in

identifying the origin of individual puffs of pollution. Therefore, the second aim of this work is to demonstrate the use of a twin channel instrument for the simultaneous detection of two elements in the air.

A survey of analytical techniques available for the measurement of the concentration of sulphur compounds in the atmosphere is also included in this work.

CHAPTER 2

ANALYTICAL TECHNIQUES AND INSTRUMENTATION

2.1 Introduction

The aim of this chapter is to give a brief outline of some of the common analytical techniques currently employed in atmospheric pollution monitoring activities and to relate the applicability of the techniques to fast-response measurements of the concentration of sulphur compounds, sulphur dioxide in particular. Operational principles are not discussed in detail since these are well documented in the literature, but some of the practical difficulties apparent during an instruments use are highlighted.

There are many review articles on the subjects of instrumentation and techniques for air pollution monitoring. The state of the art can be typically represented by the following reviews.

KATZ (1969) gives a good account of the principles of air sampling and analysis. The text reads rather like a menu but is most informative with respect to the wet chemistry techniques and to some of the more traditional automatic techniques, such as colorimetry and conductimetry.

STEVENS and O'KEEFFE (1970) give an authoritative but somewhat brief and self-indulgent review, discussing instrumentation with improved sensitivity and specificity. There is little mention of spectroscopic techniques with more attention given to analysers based on chemiluminescent principles. The authors appear to be bent on the hope that in the future they will "have a part in the development of still more advanced air pollution instruments," which indeed they have had.

FORREST and NEWMAN (1973) provide an overview of the analytical techniques used in ambient air monitoring for sulphur compounds. In their own words, "the review is not designed to be exhaustive."

A comprehensive review by SALTZMAN and CUDDEBACK (1975) covers material from mid 1972 to late 1974 not covered in a previous review (MUELLER and KOTHNY, 1973) and selected as being of particular interest for air sampling and analyses. The article has well over 400 references relating to various topics in "Air Pollution" and there are good sections on Source Analyses, Remote Sensing and Field Studies - Methods, Evaluation and Standardisation.

More complete information on "Sulphur Dioxide Analyser Instrumentation and Air Monitoring" in general can be obtained from the ENVIRONMENTAL INSTRUMENTAL GROUP (1972; Updates: Feb. 1973, Dec. 1973). Included in this thorough survey are references, reviews of individual instruments and recommendations for analytical instrumentation.

Other useful review articles and references are given throughout the chapter.

2.2 Current Instrumentation

At present there are a large variety of instruments available which utilise some chemical or physical property of the species to be measured. This is not surprising when it is considered that the range of concentration experienced in the background environment to the urban environment - including stack emissions - may be as high as 10^6. So the determination of any one pollutant by a specific technique would require that the technique be capable of giving results of the necessary precision and accuracy over this wide concentration range, as well as overcome the problems of interferences and sample treatment. The result of this is that instruments, techniques and general analytical procedures are designed for application to specified concentration ranges as broadly represented by the following three classes:-

a) Background.

This relates to the atmosphere unaffected by the activities of Mankind and, for background analysis, concentration and trapping techniques involving long averaging times and large volumes are frequently used. These techniques are adequate because the background concentrations are not, generally, time or space dependent.

b) Ambient.

This is the atmosphere in cities and other major population centres as influenced by the activities of Man. Techniques involving long averaging times are not particularly useful for ambient analysis because they do not give adequate information about dangerous peaks and there is, therefore, a need for fast-response and highly sensitive instruments.

c) The Emission Class.

This class involves both stack and automobile emissions. Here the analytical problem is one of sample treatment for high moisture and particulate content and once the sample has been prepared the analytical technique is a relatively easy operation.

There is, of course, a good deal of overlap in these three classes with respect to instrumentation. For

example, an ambient analyser may well be suitable for background and emission source analysis, although, a background analyser would not be necessarily suitable for ambient analysis.

On the basis of these three classes, Tables 2.1, 2.2 and 2.3 have been formulated to show the range of instruments currently available to measure sulphur compounds in the background, ambient and emission environments, respectively.

The Tables and related comments have been compiled from the following sources:-

i) Environmental Instrumental Group (1972, 1973).

ii) Manufacturer's Specifications, when obtainable.

iii) Various references found in the literature pertaining to development and use of analytical techniques.

iv) Visits made to Harwell, Medical Research Council's Air Pollution Unit at St. Bartholomew's hospital and to a "Commission for the European Communities" campaign held at Drax, Yorkshire.

Prior to discussing the contents of Tables 2.1, 2.2 and 2.3, it is to be noted that the precision and accuracy of many of the instruments have not been thoroughly investigated and there is a great deal of doubt as to the significance of the data generated by these instruments.

PRINCIPLE OF OPERATION	SENSITIVITY	INTERFERENCES	MANNER OF MEASUREMENT
BARIUM SULPHATE TURBIDIMETRY	2μg SO_2/3ML ABSORBENT SOLUTION OR BETTER	HYDROGEN SULPHIDE AND SULPHURIC ACID MIST	POINT
SODIUM TETRABORATE TITRIMETRY	$1\mu g M^{-3}$ IN $10M^3$ AIR	METALLIC OXIDES AND AMMONIA	POINT
SODIUM TETRACHLORO-MERCURATE COLORIMETRY	$1\mu g\ M^{-3}$		POINT
COLLECTION ON IMPREGNATED FILTER PAPER/DETERMINING SULPHUR DIOXIDE AS SULPHATE COLORIMETRICALLY	$1\text{-}2\mu g M^{-3}$ IN $1M^3$ AIR	PREFILTERS REQUIRED BECAUSE IMPURITIES AFFECT THE SENSITIVITY	POINT
ABSORPTION IN HYDROGEN PEROXIDE/DETERMINING SULPHUR DIXOIDE COLORIMETRICALLY	$1\text{-}2\mu g M^{-3}$ IN $1\ M^3$ AIR	PREFILTERS REQUIRED BECAUSE IMPURITIES AFFECT THE SENSITIVITY	POINT

TABLE 2.1 SULPHUR DIOXIDE BACKGROUND ANALYSERS

PRINCIPLE OF OPERATION	MANUFACTURER	MEASURING RANGE μgm^{-3}	RESPONSE TIME	MANNER OF MEASUREMENT	MULTI-PARAMETER CAPABILITY
CONDUCTIMETRIC.	CALIBRATED INSTRUMENTS	10 - 10000	1.5 MIN	POINT	
	LEEDS AND NORTHRUP	12 - 5000	2-6 MIN	POINT	
	SCIENTIFIC INDUSTRIES	20 - 12000	30 SEC	POINT	
COLORIMETRIC.	ATLAS	5 - 25000	1-6 MIN	POINT	ALDEHYDES
	HOUSTON ATLAS	20 - 100%	2 MIN	POINT	TOTAL SULPHUR, H_2S
AMPEROMETRIC.	ATLAS	2 - 25000	2 MIN	POINT	OZONE
	PHILLIPS	10 - 10000	2 MIN	POINT	H_2S, MERCAPTANS
ELECTROCHEMICAL—TRANSDUCER.	ENVIROMETRICS	20 - 50000000	5-10 SEC	POINT	H_2S, NO_x, CO, NO_2
	THETA SENSORS	20 - 2450	23 SEC	POINT	
FLAME-PHOTOMETRIC—	BENDIX	10 - 2450	30 SEC	POINT	TOTAL SULPHUR, PHOSPHORUS
DETECTOR.	MELOY	20 - 2450	12 SEC	POINT	TOTAL SULPHUR, PHOSPHORUS
FLAME-PHOTOMETRIC— DETECTOR/GAS —	TRACOR	10 - 5000	3 MIN	POINT	SULPHUR COMPOUNDS
CHROMATOGRAPHY.	BENDIX	10 - 2450	5 MIN	POINT	SULPHUR COMPOUNDS
CORRELATION— SPECTROSCOPY.	BARRINGER	2 - 2450	20 SEC	POINT/LONG-PATH	NO_2
SECOND-DERIVATIVE— SPECTROSCOPY	SPECTROMETRICS	7 - 25000	24 SEC	POINT	NO, NO_2, O_3, NH_3 ETC.
FLUORESCENCE - DETECTION.	NOT COMMERCIALLY AVAILABLE	20 - 5000	1 MIN	POINT	

Table 2.2 Sulphur Dioxide Ambient Analysers.

PRINCIPLE OF OPERATION	MANUFACTURER	MEASURING RANGE μgm^{-3}	RESPONSE TIME	MANNER OF MEASUREMENT	MULTI-PARAMETER CAPABILITY
CONDUCTIMETRIC.	CALIBRATED INSTRUMENTS	2450 - 20000000	2 MIN	POINT	CO_2
COLORIMETRIC.	HOUSTON ATLAS	20 - 100%	2 MIN	POINT	TOTAL SULPHUR, H_2S
AMPEROMETRIC.	BARTON	100 - 2500000	5 MIN	POINT	H_2S, MERCAPTANS
ELECTROCHEMICAL —	DYNASCIENCES	25000 - 12000000	90 SEC - 3 MIN	POINT	NO_x, CO, H_2O, NO_2
TRANSDUCER.	ENVIROMETRICS	20 - 50000000	5 - 10 SEC	POINT	H_2S, NO_x, CO, NO_2
NONDISPERSIVE — ABSORPTION —	DUPONT (U.V)	20000 - 12000000	15 SEC	POINT	NO_x, Hg, NO_2
SPECTROSCOPY.	INTERTECH (I.R.)	2450 - 100%	0.5 SEC	POINT	NO, NO_x, CO, ETC.
DISPERSIVE — ABSORPTION — SPECTROSCOPY.	ENVIRONMENTAL DATA (I.R.)	250 - 7000000	30 SEC	POINT	CO, NO_x, ETC.
CORRELATION — SPECTROSCOPY.	COMBUSTION EQUIPMENT	24500 - 12000000	20 SEC	POINT/LONG-PATH	
SECOND-DERIVATIVE — SPECTROSCOPY.	SPECTROMETRICS	245 - 100%	1 SEC	POINT	NO, NO_2, O_3, NH_3 ETC.
RAMAN — BACKSCATTERING.	a	1000- 100%	a	REMOTE/LONG PATH	NO_2, NO, NO_x, CO, CO_2, ETC.
RESONANCE — FLUORESCENCE— BACKSCATTERING.	a	a	a	REMOTE	NO_2, CO, Hg, C_6H_6.
PIEZOELECTRIC.	NOT COMMERCIALLY	50 - 735000	a	POINT	H_2S
LIDAR.	a	a	a	REMOTE	AEROSOL CONCENTRATION

"a" Information not available

Table 2.3 Sulphur Dioxide Emission Source Analysers.

Furthermore, there is a great lack of data and information on instrument operation in the field and although manufacturers go to great lengths to supply information concerning an instrument's operation in the laboratory, it is still very difficult to formulate any objective opinion on the merits of a given instrument.

The instruments are primarily divided into background, ambient and emission-source analysers and then according to the principles of operation. The measuring range implies the minimum and maximum concentrations measured and the response time is that time necessary for a 90% reading after a step positive input, exclusive of dead time. Additional equipment is usually necessary for "multiparameter capability" - the capability of measuring the concentration of more than one compound using the same principle technique.

The manner of making the measurement will have a marked influence on the significance of the results and for this reason a column headed "Manner of Measurement" has been included in the Tables. This heading is described by the three following divisions:

a) Point Measurements.

These are made at a specific point in space and are usually made continuously. They are, therefore, not space averaged but can be time averaged.

b) Remote Measurements.

These measurements are obtained from an analytical instrument usually placed at an appreciable distance from the portion of the atmosphere under investigation. The measurement is not necessarily time averaged or space averaged.

c) Long Path Mode Measurements.

A long path mode measurement is made over a long distance and is a space average but may or may not be a time average .

The features of sulphur dioxide analysers that are currently available - as summarised in the Tables - are now discussed in more detail.

Wet-Chemistry Analysers

There are a number of simple wet-chemistry analytical methods that can be used to measure background sulphur dioxide concentrations of the order of 5 $\mu g\ m^{-3}$ or below. KATZ (1969) outlines the principles underlying some of the methods and gives references for fuller technical details. HEALY and ATKINS (1975), also briefly review some simple "non-instrumental" sampling and analytical methods used for the determination of sulphur dioxide in air, in a paper that discusses the determination of atmospheric sulphur dioxide after collection on impregnated filter paper. The ability of such workers in covering this field make it unnecessary to discuss these techniques any further except to say that a number of them are listed in Table 2.1.

All of these techniques are suitable for background analysis and although they have slow response times they are generally used for ambient and emission -source analysis.

Wet-Chemistry techniques tend to be cheap and extremely simple to use requiring little expertise and maintenance to operate which is why many of them are still in use today.

Conductimetric Analysers

First developed in the late 1920's, these analysers remain popular today and have been used for ambient and emission-source analysis. The basic principle involves measuring the conductance of an absorbing solution into which sulphur dioxide has been dissolved by contact of the solution with air. A solution of distilled water and diluted acidified hydrogen perxiode is commonly used to oxidise the SO_2 to H_2SO_4 primarily because there is no interference from carbon dioxide with this solution. These analysers generally have high sensitivity and response times of the order of thirty seconds to one minute. They are simple in operation but are susceptible to interference by non-sulphur dioxide gases that form or remove ions in solution and because of this there is a move to the use of the more specific Amperometric and colorimetric techniques.

Amperometric Analysers

Amperometric analysers, more commonly called Coulometric analysers, measure the generating current required to oxidise or reduce a desired constituent, the magnitude of this current is proportional to the amount of absorbed pollutant gas. In connection with sulphur dioxide the

current necessary to maintain a constant halogen concentration is measured. Any compound that is able to react with the halogen or with the reduced component - halide - is a potential interferent of which the most noted groups are: hydrogen sulphide and organic sulphides. Without filters, sensitivities to these sulphur compounds may be comparable to sulphur dioxide, however, most commercially available amperometric systems are made specific by the use of suitable prefilters. The major advantage of these analysers is the minimal maintenance required, due in part to the regeneration of the reagent. They have been used for ambient and emission-source analysis even though their slow response time make them generally unsuitable for ambient monitoring.

HALL (1974) investigated the problems in using various instruments for measuring the concentration of sulphur - containing odourants in stack emissions. Of the amperometric analysers he used, he found that a Barton coulometer suffered from a short term instability lasting seconds due to the cell and flow system dynamics. The cell zero also showed a drift over a period of a day or less. This variation was affected by barometric pressure changes, temperature changes, electrolyte condition and to a greater extent by changes in the "constant" flow rate of total gas.

However, the system was simple to operate which was more than Hall could say for the Dohrmann Microcoulometer. This analyser had many operating requirements which were difficult to achieve in the field such as daily calibration, changing the cell electrolyte and constant skilled attention to keep the instrument in adjustment.

Colorimetric Analysers

In colorimetry the quantity of a coloured component is determined by measuring the relative amount of absorption of light passing through a solution of the pollutant of interest. Colorimetric determination for sulphur dioxide is usually dependent upon the ability of sulphur dioxide to form sulphurous acid. Commercial analysers use pararosaniline or related dyes to detect the sulphurous acid. The chemical apparatus and detailed analytical procedure are described by WEST and GAEKE (1956). The advantages of colorimetric analysers are simplicity, high sensitivity and good specificity but colour intensity is usually sensitive to temperature, pH, development time, purity of reagents, age of solutions and some atmospheric interferents. These analysers are slow in response and are widely used for background and emission-source analysis.

Electrochemical Transducer Analysers

For the determination of sulphur dioxide the electrochemical transducer is a galvanic cell in which the current generated by the oxidation of sulphur dioxide is measured at a sensing electrode. SHAW (1968) describes electrochemical transducer analysers operating on the principle of electro-oxidation and electroreduction of the species. Sulphur dioxide selectively diffuses through a semi-permeable membrane and, as a dissolved gas, diffuses through a thin film electrolyte to a sensing electrode where it is absorbed thus creating a charge which is measured. Selectivity is determined by the choice of membrane and electrolyte materials. Information regarding electrolytes and electrode materials used in E.C.T. analysers have not been revealed by the manufacturers.

These analysers have a potentially wide area of application but there is little information published to illustrate this. They are simple in operation, having low maintenance requirements, fast-response and excellent portability and because there are no external reagents as such, multi-parameter capability is possible through the use of different transducers that are easily installed. On the negative side, the membrane is adversely affected by

material in the sample that may adhere to it and transducer replacement can be expensive.

Flame Photometric and Gas Chromatography - Flame Photometric Detectors (FPD, GC-FPD)

When sulphur compounds are burned in a hydrogen rich flame, a strong blue chemiluminescence is emitted. The emitting molecule is the excited S_2^* species. Since two atoms are involved the intensity of emission is proportional to the square of the sulphur compound concentration, for compounds containing only one S-atom. The original F.P.D. was described by DRAEGER (1962). CRIDER (1965) and BRODY and CHANEY (1966) both describe a flame photometric detector sensitive to phosphorus and sulphur compounds using interference filters that transmit at 526 nm and 394 nm respectively. Where determinations of specific sulphur compounds are required a gas chromatograph can be used in conjunction with the F.P.D.

Flame photometric detectors have high sensitivity, fast response - of the order of seconds - and good selectivity for sulphur compounds. There are no solutions and the only required reagents are hydrogen for the flame and perhaps clean air for utilising as an emission-source analyser with a dilution system. Disadvantages may be the need for a

compressed hydrogen supply and the inability to discriminate among sulphur compounds without selective filters.

HALL (1974) evaluated the use of two commercially available GC-F.P.D.'s - a Bendix and a Tracor model - for their performance in the field, along with the coulometric instruments already mentioned. He describes the Tracor model 250 H as having a "function selector box for electronic controls that was inoperable as received and reasons for this could not be diagnosed with the incomplete operating manual supplied." The Bendix GC-F.P.D. (unfortunately no model name or number is given) comes the closest to satisfactory performance - in Hall's words - and has a zero reading normally constant within 0.5% of scale. The model on test required rebalancing at the end of six months in the field.

One convenient characteristic of flame photometric detectors is the ease with which they can be calibrated in the field. However, typical problems associated with these instruments include baseline instability, difficulties in lighting the flame and noisy signals due to hydrogen flow fluctuations.

Two features commonly noted with flame photometric detectors are:

a) The Log-Log plot of the calibration curve is not linear at concentrations of sulphur dioxide greater than 5000 $\mu g\ m^{-3}$.

b) The gradient of the calibration curve over the linear portion is not equal to two and is, in actual fact, consistently less than two in most commercial analysers. Some analysers even have calibration curves split into two distinct sections relating to two different concentration ranges.

Explanations for these features are given in Chapter 3.

Spectroscopic Analysers

The most promising instrumental developments for air monitoring are those techniques based upon spectroscopy because these techniques offer wide multi-parameter capability, versatility in operation and high sensitivities especially as the sensitivity is amenable to improvement using suitable noise reduction techniques, such as correlation. Many of the spectroscopic instruments listed in Tables

2.2 and 2.3 are either in early commercial stages or in advanced prototype stage. HODGESON, McCLENNY and HANST (1973) provide a critically constructive review with fifty-six references and comment on a variety of spectroscopic methods used to detect air pollution in the gas phase.

Spectroscopic techniques based upon absorption spectrophotometry include short-path point instruments, microwave and second derivative instruments.

A short-path point instrument has the radiation source, sample cell and radiation detector all contained in one package. The sample of air from a specific region in space is drawn into the sample cell and the attenuation of the radiant power is continuously measured photometrically. The path length may range from several centimetres to several meters. The radiation regions normally employed are in the ultra-violet and infra-red, since the pollutants of interest generally show little or no absorption in the visible. Short-path instruments are rarely employed for ambient and background analysis because of lack of sensitivity but they are useful for emission-source analysis. Dispersive and non-dispersive absorption spectrophotometers (ultra-violet and infra-red) are two examples of such instruments.

In rotational microwave spectroscopy a polar molecule absorbs energy at specific frequencies in the microwave region when it is a freely rotating body. The frequencies are determined only by the energy separating two rotational levels of the entire molecule. Thus, the absorption spectrum in this region for a given compound is unique to that compound. Specificity is high owing to the sharpness of the spectral peaks, but sensitivity is low.

The second derivative spectrometer processes the Transmission vs wavelength function of an ordinary spectrometer to produce an output signal proportional to the second derivative with respect to the wavelength of the function. Ultraviolet light is collected and focused onto an oscillating entrance slit of a grating spectrometer. By slowly changing the grating oscillation, the "exiting" light has a slowly scanning centre wavelength with sinusoidal wavelength modulation created by the oscillating entrance slit. This radiation passes through the gas sample and is detected with a photomultiplier tube. The signal is then electronically processed to produce a second derivative spectrum.

These instruments have fast response and are very sensitive, thus they have good potential as background, ambient and emission-source analysers. However, they are relatively new and require field testing before a definitive evaluation can be made.

WILLIAMS and HAGGER (1970) have discussed the theory and construction of a derivative spectrometer.

With the development of laser technology in recent years, absorption techniques are still receiving a great deal of attention because of improved sensitivities and extensive multiparameter capability using tuning lasers (MEASURES and PILON, 1972).

Laser sources and techniques based on lasers have also been applied to optical measurements of pollutants based on phenomena other than absorption of radiation. A few of the more prominent techniques include Raman Backscattering, Resonance Fluorescence, Lidar and Correlation Spectroscopy.

A Raman spectrum results from inelastic collisions of monochromatic photons with molecular species during scattering, resulting in bands or lines of shifted wavelength in the scattered radiation relative to those in the

exciting radiation. This wavelength shift is a function of the molecular vibrational states and permits unique identification of the molecule by comparison with "library" records. The Raman signal is proportional to the Raman cross-section of the species, the atmospheric transmittance, the laser energy per pulse and the species concentration. Beyond about 1 km the scheme is severely limited because of small Raman signal and loss of laser exciting radiation by atmospheric scattering and so is only useful as an emission-source analyser.

In fluorescence backscattering the exciting radiation is absorbed in a well-defined spectral region, causing a molecular transition. Radiation is simultaneously emitted at a lower frequency accompanied by an intermediate transition within the molecule. The molecule ultimately achieves the ground state by nonradiative processes. The absorption region and the emitted frequency are specific to each species so great selectivity and sensitivity are possible at moderate distances (100 metres or so). However, the major disadvantage of this technique is the difficulty in evaluating concentrations.

Many of the factors that affect signal intensity at the detector for the Raman and Fluorescence analysers are

discussed quantitatively by KILDAL and BYER (1971).

Lidar (Light Detection and Ranging) is the most versatile of the remote sensing techniques. It is usually operated with the transmitter and receiver at the same site by projecting a laser beam and measuring the light backscattered from particles and gas molecules in the beam. Scatter from smoke plumes by lidar at a range of 3 kilometres with an atmospheric visibility of 5 kilometres has been reported by HAMILTON (1969). Plumes from stacks can be tracked by lidar over long periods and used to predict ground-level concentrations of pollution. Plume-rise can also be measured. A more important application has been the measurement of the height of the mixing layer, the layer of the lower atmosphere below a stable layer (inversion) in which emitted pollutants are dispersed and mixed. The top of the mixing layer is distinguished by a sharp decrease in lidar backscatter.

In correlation spectroscopy the incoming light signal is dispersed by a grating spectrometer. Instead of the normal exit slit there is a correlation mask (an array of slits). This is a photographic replica of the spectrum of the compound, with slits corresponding to the main absorption peaks. When this mask is vibrated across the

spectrum a beat signal is obtained when the incident light bears the absorption pattern of the monitored component. Although absorption of other gases may produce overlaps with some peaks, nothing else will correlate over the whole array and so the signal from the desired component is much enhanced, therefore, a photomultiplier tube will observe a minimum when peaks of the sample spectrum line up with troughs on the mask spectrum and a maximum when the peaks of the sample spectrum line up with peaks of the mask spectrum. The difference in light intensities seen by the photomultiplier is a measure of the sulphur dioxide concentration between the light source and the detector. Models now use a rotating mask instead of a vibrating refractor plate driven by a tuning fork.

Advantages are high specificity, fast response and capabilities for point and long-path mode sensing in background, ambient and emission environments. However, the analyser cannot detect local wide fluctuations from the mean, when used in the long-path mode.

A general discussion of correlation spectroscopy has been given by DAVIES (1970) and WILLIAMS and KOLLITZ (1968). KAY (1967) describes an instrument applying the technique to ambient sulphur dioxide detection and BARRINGER

et al (1968, 1969A 1969B) discuss the design, development and application of commercial instruments.

New Techniques

Piezoelectric Analysers.

SHACKELFORD and GUILBAULT (1974) describe a relatively new device - a piezoelectric crystal sensor - and discuss its use for measurement of organophosphorus insecticides in the air. These detectors consist of a vibrating quartz crystal which is coated with a substrate which selectively and reversibly absorbs the desired pollutant when exposed to air contaminated with the pollutant. The frequency of vibration of the crystal depends on the weight of the coating and the weight of the material absorbed onto the coating. Thus, the concentration of the pollutant in the air is measured by observing changes in the frequency of the vibrations of the coated crystal. Shackelford and Guilbault claimed a sensitivity to allow detection of organophosphorus insecticides at less than 0.01 p.p.m ($^{v}/_{v}$) as operated in a sample injection flow system. Moisture in the air, Nitrogen Dioxide and Ammonia pose interference problems but work is in progress to produce new crystals to increase selectivity of the detector.

KARMARKAR, WEBBER and GUILBAULT (1976) used a piezoelectric analyser for the measurement of sulphur dioxide and hydrogen sulphide in automobile exhausts and industrial stack gases.

Fluorescence Analysers.

SCHWARZ, OKABE and WHITTAKER (1974) report the use of a fluorescence analyser with a detection limit of 20 $\mu g\, m^{-3}$ for sulphur dioxide with a counting time of one minute. The principle of the analyser is based on photon counting of the sulphur dioxide fluorescence excited by the zinc 214 nm line. Fluorescence detection has yet to be accepted as a technique for analysing sulphur dioxide in ambient air and problems involving the interaction of sulphur dioxide with water layers on the internal surfaces still have to be studied.

2.3 Summary

The past ten years have seen a tremendous upsurge in the variety of techniques now available to measure concentrations of pollutants in the atmosphere, not only for sulphur dioxide, although there is still a lot to be done for standardisation and calibration. Continued research means that present instruments will soon be obsolete as new

ones take their place even though the older instruments have not been fully evaluated.

Instruments, at present, are limited to response times of the order of seconds and more likely tens of seconds for air pollution analysis. Instruments, in general, have not been designed to respond in seconds or less since they then tend to become more costly to manufacture and to operate - there simply is very little demand for instruments with response times of milliseconds, although Epidemiologists may argue otherwise. It is difficult to assess the potential of a particular technique for this work because workers and manufacturers do not relate an instrument's response time to signal detection; to decide whether an instrument can respond "faithfully" to fast fluctuating signals not only requires knowledge of the instrument's response time but also of the flow characteristics of the inlet sampling line and reaction cell.

The choice of an analytical technique for this project rests on the fact that flame photometric detection is the fastest method that has sufficient sensitivity for ambient analysis, as well as this Department having had previous experience (BARYNIN, 1970) in the development and application of a flame photometric detector and so it is this that is used for further development in this research.

CHAPTER 3

INSTRUMENT DEVELOPMENT

Introduction

Chapter three discusses the development of the flame photometric detector used in this work. The objective of developing a new detector is to produce an instrument capable of responding rapidly to fluctuating concentrations of sulphur and phosphorus compounds released into the atmosphere.

A review of the literature concerning the mechanisms of sulphur and phosphorus compound chemiluminescence is first considered as this will aid in the design of the instrument, after which the work relating to design, testing and characterisation of the instrument is discussed.

3.1 Sulphur Compound Chemiluminescence

Up to the present day there has been a wealth of literature concerning chemiluminescence of sulphur compounds. The phenomenon has been described in several review articles, GLOVER (1975), STEVENS and HODGESON (1973) being the least inadequate articles. Analytical applications have also been discussed - RUDOLF SEITZ and NEARY (1974), ISACSSON and WETTERMARK (1974) - and reviews specifically on the applications to the measurements of air pollutants are most abundant; STEVENS and HODGESON (1973) is one of the more complete review articles.

Spectroscopic work directed towards identifying the emitters of radiation from various sulphur containing systems has been summarised by KONDRATIEV (1962) and GAYDON (1974). When the concentration of the sulphur compound is high, a strong continuum is generally observed extending through most of the visible into the ultra violet. Superimposed on this is the spectrum emitted by electronically excited S_2, FOWLER and VAIDYA (1931). This spectrum is the one also observed when most sulphur compounds, organic or inorganic, are added to low temperature flames with excess hydrogen or with a diffusion flame of air burning in an atmosphere of hydrogen, SUGDEN, BULEWICZ and DEMERDACHE (1962) and SUGDEN and DEMERDACHE (1962), and it is this system that is now discussed.

DAGNALL, THOMPSON and WEST (1967) investigated the light emission of sulphur in cool flames. Using a hydrogen-nitrogen diffusion flame burning in air they measured the S_2 emission at 384 nm (the maximum emission intensity being displayed at 394 nm, GAYDON 1974); the emission intensity was shown to be dependent on flame temperature, being reduced as the temperature was increased. EVERETT, WEST and WILLIAMS (1974) report that between 0-10 p.p.m of sulphur dioxide the light emission intensity is proportional to the square of the sulphur concentration but between 10-40 p.p.m self-absorption affects the emission process and self-quenching dominates above 40 p.p.m.

SYTY and DEAN (1968) discuss what they call a rational reaction mechanism for fuel rich hydrogen flames. Theyexplain that a high concentration of hydroxyl (OH) species evident in such flames is largely consumed by the excess hydrogen producing excess hydrogen atoms when the gases are cooled, so that a high concentration of OH prevails only in the region above the reaction zone of the flame. Thus, cooling of the hydrogen-air diffusion flame reduces the background emission of the OH species. GAYDON (1974) discusses the combustion mechanism of hydrogen-oxygen and hydrogen-air flames in more detail.

ALDOUS, DAGNALL and WEST (1970) note that the highly reducing nature and low incidence of molecular or atomic oxygen in the cool flame are other contributing factors that support the production of intensely emitting

species in diffusion flames. A variety of burner configurations have been reported in the literature notably in the work by VEILLON and PARK (1972), CRIDER (1965) and SYTY and DEAN (1968) - all of these workers use a glass shield to surround the flame whose main function appears to be the isolation of the flame from entrained air, particularly oxygen. Figure 3.1 shows a typical burner.

Previous work, FAIR and THRUSH (1969A), for which there are equilibrium and kinetic constants, indicates that S_2 chemiluminescence arises from two processes:

1. A two body combination of S atoms.
2. A three body gas phase recombination of S atoms.

Mechanisims 1 and 2 are now discussed especially in relation to spectroscopy.

1. Light emission arises from the two body inverse predissociation.

$$S + S \rightleftharpoons S_2^* \ (B, v' = 10) \qquad \text{Equation 3.1}$$

$$S_2^* \longrightarrow S_2(X) + h\nu \qquad \text{Equation 3.2}$$

B and X refer to electronic energy states.

The pseudo equilibrum constant for equation 3.1 has been calculated to be 0.39 cm^3 $mole^{-1}$ at 298 K, FAIR and THRUSH (1969A).

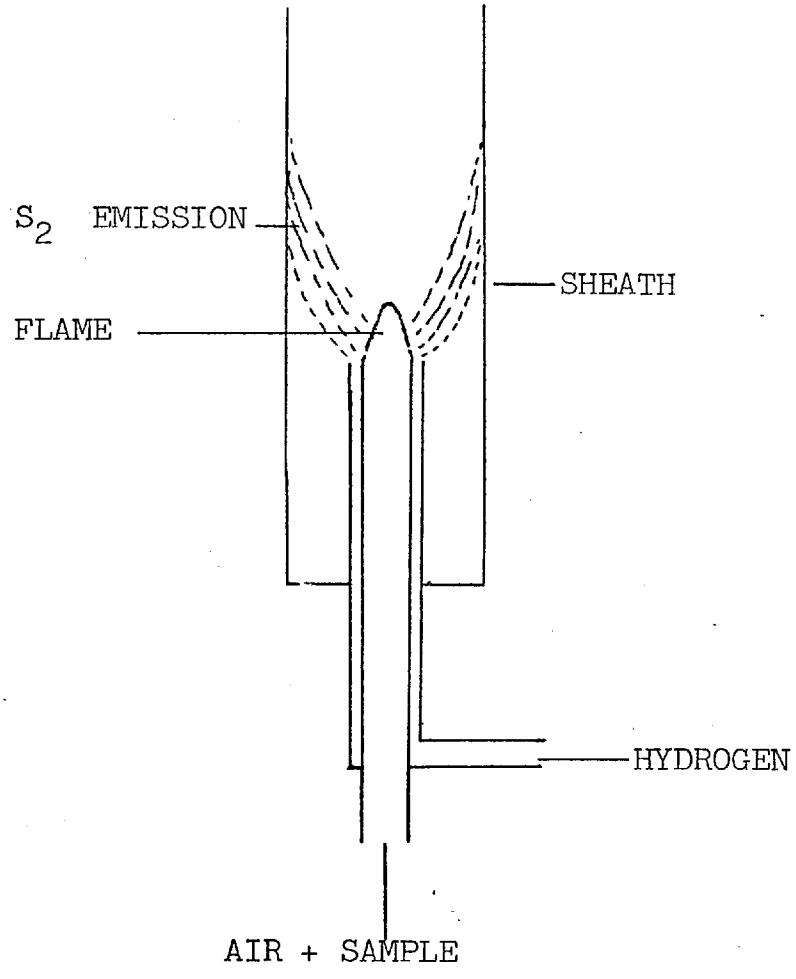

Figure 3.1. Typical Burner and Sheath Configuration.

2. Light emission from a three body recombination reaction into lower levels arises from:

$$S + S + M \xrightarrow{K_{3.3}} S_2^* \qquad \text{Equation 3.3}$$

$$S_2^* \longrightarrow S_2 + h\nu \qquad \text{Equation 3.4}$$

A value of $k_{3.3}$ has been calculated to be 10^3 M^6 $Mole^{-2}$ sec^{-1} for M = Argon, FAIR and THRUSH (1969A).

While discussing S_2 emission from hydrogen rich flames containing sulphur, CULLIS and MULCAHY (1972) quote a value of $10^{5.7}$ M^6 $Mole^{-2}$ sec^{-1} for the rate constant $k_{3.5}$ of the following recombination reaction

$$S + S + M \xrightarrow{k_{3.5}} S_2 + M(B, V' \leq 9) \qquad \text{Equation 3.5}$$

M = Carbon Dioxide.

This value of $k_{3.5}$ (FOWLES, DE SORGO, YARWOOD, STRAUSZ and GUNNING 1967) was obtained from the half life of the growth curve of S_2 and the concentration of S atoms formed during the flash photoysis of carbonyl sulphide in the prescence of a large excess of carbon dioxide. In reconciling the difference between $K_{3.3}$ and $k_{3.5}$, CULLIS and MULCAHY suggest that only a small fraction of the S_2 molecules are formed in the excited state. They state that "it appears that light emission in addition to arising from a three body recombination also results from a two body combination process (equations 3.1 and 3.2) and it is this process which is responsible for much of the S_2 emission from hydrogen rich flames containing sulphur." This comment is not endorsed from an examination of the spectroscopic results available in the literature.

3.1.1 Spectroscopy

In their work Fair and Thrush (1969A)added small flows of hydrogen sulphide to a stream of hydrogen atoms which then gave rise to a pale blue chemiluminescence in a discharge flow system. The spectrum of the emission was shown to be due to the $B \rightarrow X$ state transition of the S_2 molecule. Vibrational levels of the B state up to $V' = 10$ were populated and the most outstanding feature of the spectrum was the strong emission from levels $V' = 9,8,7,6$. However, this intensity distribution is different from that found in flames where emission from $V' = 0$ is normally the most intense, GAYDON and WHITTINGHAM (1947). GAYDON and WOLFHARD (1952) discuss the spectra of atomic flames and note that the spectrum of a carbon disulphide/atomic hydrogen flame was unusual. In normal flame sources, bands with low initital vibrational quantum numbers are the strongest and the strong $V' = 0$ progression λ 3645-4046 gives the system a "fairly simple appearance." However, as GAYDON and WHITTINGHAM observe, in addition to these bands being present in atomic flames there are other significant bands at shorter wavelengths λ 2799 - 2989, in other words bands with V' of 9 and 10 seem especially favoured in the atomic flame.

Therefore, the assertion of CULLIS and MULCAHY that the two body combination process is responsible for emission from hydrogen rich flames containing sulphur is not realised because excitation of trace quantities of sulphur in flames is restricted to rich hydrogen ones

and the spectrum always shows the v' = 0 progression as the dominant one. For this reason, doubt is also cast on the applicability of the three body recombination reaction to S_2 emission from hydrogen rich flames.

One other mechanism is given in the literature for S_2 chemiluminescence for which there are no equilibrium or kinetic constants available.

BRINSLEY and STEPHENS (1946) considered the equilibria existing in the flame of a coal gas-air mixture containing slightly less than the theoretical amount of air and suggested that the sulphur (S_2) may arise from the reaction.

$$2\ SO \rightleftharpoons SO_2 + \tfrac{1}{2}\ S_2 \qquad \text{Equation 3.6}$$

At the temperature existing in the flame this system is composed predominantly of SO, and a considerable fall in temperature is necessary for the formation of S_2 in sufficient concentration to give a visible glow.

The excitation of S_2 to excited S_2^* was suggested to GAYDON (1974) by Mr. H.G. Crone who thought the reaction might be

$$H + H + S_2 \longrightarrow S_2^* + H_2 \qquad \text{Equation 3.7}$$

Mr. H.G. Crone pointed out that this reaction gave sufficient energy but without much excess.

The following points are a summary of the review of the literature on sulphur chemiluminescence and are

considered useful as design criteria for a suitable burner for a fast response flame photometric detector:

1. Shielding and cooling of the diffusion flame are necessary to reduce the OH radiation intensity.

2. The oxygen fraction in the flame should just be sufficient to maintain combustion.

3. Convective eddies that would give rise to back mixing in the burner should be reduced so that any sulphur atoms should pass through the diffusion flame once only, (BARYNIN, 1970).

3.2 Phosphorus Chemiluminescence

Along with the violet emission from flames containing sulphur, a green emission from flames containing phosphorus has been observed. The earliest references to these observations may be found in the work of SALET (1869) and in that of GEUTER (1907). SALET reported seeing these emissions when an air-hydrogen diffusion flame was allowed to impinge upon a vertical glass surface that was cooled from the back with a flow of cold water. LUDLUM (1935) and RUMPF (1938) incorrectly attributed these bands to a PH molecule in air-hydrogen flames.

BRODY and CHANEY (1966) and DAGNALL, THOMPSON and WEST (1968) showed that the visible emission has a banded structure with a strong maximum around 526 nm and weaker maxima at 510 nm and 560 nm. SYTY and DEAN (1968) observed a phosphorus continuum underlying the band system. They found

that in a shielded fuel rich air-hydrogen diffusion flame, the intensity of the continuum was about one half the intensity of the band system. Studies by LAM THANH MY and PEYRON (1963) of the emission of moist atomic hydrogen reaction with phosphorus, show that the bands are due to the triatomic emitter HPO and that the continuous emission from phosphorus compounds in hydrogen flames must be due to HPO. Observations of the intensity of the green glow around the base of a shielded flame and within the periphery of the inner cone show that the intensity of emission is proportional to (FENIMORE and JONES, 1964):

$$\left[\text{Phosphorus}\right]^{0.4\pm0.1} \cdot \frac{[H]^2 [H_2O]^{0.5\pm0.5}}{[H_2]^{1.0\pm0.5}} \cdot \exp\left[-(5\pm5)/RT\right]$$

Equation 3.8

Fenimore and Jones offer the following possible reaction route as an "interpretation" of equation 3.8 and which is consistent with the identification of the emitter HPO:

$$P_2 + PO \rightleftharpoons P + PO \qquad \text{Equation 3.9}$$

$$P + OH \rightleftharpoons PO + H \qquad \text{Equation 3.10}$$

$$H + PO + M \rightleftharpoons HPO^* + M \qquad \text{Equation 3.11}$$

$$H + PO^* \rightleftharpoons HPO^* \qquad \text{Equation 3.12}$$

where M is a catalytic body.

The flame radiation intensity is proportional to $[H]\,[PO]$, and the phosphorus is present mostly as P_2 molecules in accordance with reactions 3.9 and 3.10.

As Fenimore and Jones admit, the flame result can also be interpreted by an intensity proportional to [H] [P] with the same equilibria among P_2, HPO and P. GAYDON (1974) gives the wavelengths, wavenumbers, vibrational quantum numbers for the S_2 and HPO band systems.

Note that according to the reaction sequences, Equation 3.11 and Equation 3.12, the HPO molecule is excited upon formation whereas the S_2 molecule is excited after it has formed.

No kinetic or equilibria data is available for HPO chemiluminescence but the following observations reported in the literature are accepted as useful design criteria:

a. Excess oxygen removes the HPO molecules by reaction and so is detrimental to the existence of the HPO molecule though not to the PO molecule.

b. The green HPO emission is observed only in fuel rich hydrogen flames and is strongest at the hydrogen orifice of the burner.

c. Both shielded and unshielded air-hydrogen diffusion flames emit the HPO bands, however, only when shielded does a hydrogen-oxygen-argon flame give appreciable emission. Apparently the third body M can either be nitrogen molecules or the inner surface of the shield. GILBERT in a private communication to Syty and Dean, however, suggests that the enhancement of the HPO molecule by a shield is due not to the action of the surface as a third body but to the cooling effect of the wall or of an entrained inert. SYTY

and DEAN (1968) explain that both viewpoints have merit because reaction 3.10 would be favoured in regions where excess OH prevailed - in the lower part of the burner above the primary reaction zone; reactions 3.11 and 3.12 could follow owing to the excess concentrations of H atoms and the presence of a suitable third body.

3.3 Limitations of Existing Flame Photometric Detectors

Further design criteria can be obtained by examining some of the limitations of existing commercial flame photometric detectors.

There are now a number of commercial forms of the flame photometric detector and it has been used in gas-chromatographic studies of atmospheric pollution, STEVENS, MULIK, O'KEEFFE and KROST (1971). The detector consists of a small flame, fed with a hydrogen and inert gas mixture, the primary combustion zone of which is shielded and the cooler secondary zone displays the emission, which is viewed via an interference filter by the photomultiplier. Figure 3.2 shows a flame photometric detector as used by BRODY and CHANEY (1966).

The sampling line flow characteristics represent a major limitation of existing flame photometric detectors. Even if an instrument has a so-called 90% response time of one second the instrument may be quite inadequate for this work because it may have a sampling line with large internal volumes that act to smooth-out the concentration gradients in the gas flow if the residence time of the gases in the sampling line is also large. The length of the sampling line is also important because fluid elements of fully developed laminar flow in a tube will have a wide distribution of residence times. Therefore, it is desirable to shorten the inlet tube so that the flow does not fully develop and operate with as short a residence time as is possible.

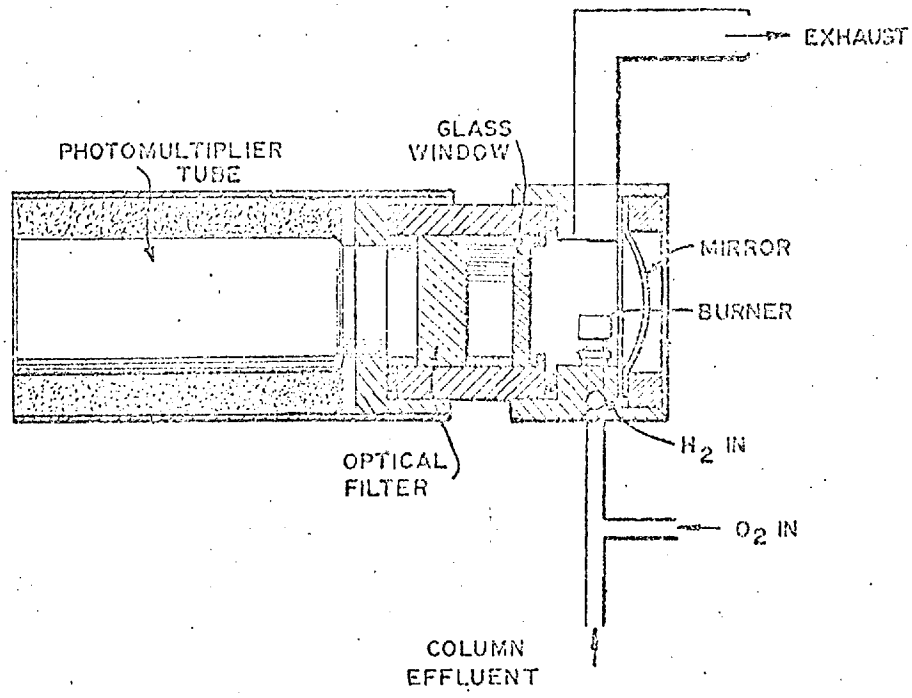

Figure 3.2 This figure is an elevation view of the flame photometer as patented by Brody and Chaney.

An important aspect concerning the design of flame photometric detectors is the choice of the materials of construction of the inlet gas sampling line.

Studies of absorption of sulphur and phosphorus compounds on various materials have been sparse and where the work has been carried out, it has been of a limited nature with respect to flow ranges, humidity ranges and sizes of materials used - WOHLERS, TRIEFF, NEWSTEIN and STEVENS (1967) present some results. However, it is known that fluorinated ethylene propylene (F.E.P. Teflon), stainless steel and glass absorb less sulphur and phosphorus compounds than many other materials such as neoprene. Teflon, being the most suitable material in this respect, has found an important application as column packing in Gas Chromatographic/Flame Photometric Detectors used to detect sulphur and phosphorus compounds at the thousand parts per million level; STEVENS, MULIK, O'KEEFFE and KROST (1971).

Commercial flame photometric detectors typically use small bore - 0.15cm. - teflon tubing about one metre in length to sample atmospheric air. When the tubing is clean the instrument should meet its specification rating for the response time and sensitivity, however, depending on the operating time and the environment from which it samples there may well be a particulate buildup on the teflon tubing's walls. The particulate matter often absorbs, for example, incoming sulphur dioxide consequently affecting the instrument's performance - the response time being increased whilst the sensitivity will be reduced. Thus, this emphasizes why the sampling line should have a low internal volume and surface area.

Many commercial detectors referred to in the literature have calibration curves (i.e. log-log plots of light emission intensity usually measured as the photo-multiplier signal output in millivolts vs concentration) for sulphur compounds containing one sulphur atom with gradients of well under two over a wide range of concentration (i.e. 0.01 p.p.m. to 10 p.p.m.). A possible explanation for this is that it may be due to the fact that commercial flame photometric detectors have burner compartments with internal volumes of between 2 to 3 cm^3 in which convective eddies may give rise to backmixing of the products of combustion in the flame. The effect of this would be to lower the gradient of the calibration curve from its value of about 2 because the sulphur atoms would pass through the flame more than once thus emitting more light for a given number of sulphur species present.

Clearly, this situation is not desirable for fast-response detection. A simple solution involves reducing the internal volume of the burner compartment and inverting the burner - the products of combustion are heavier than the reactants for this particular reaction - thus reducing backmixing.

3.4 Burner and Detector Design

A burner and detector containing several features described by BARYNIN (1970) and FROSTLING and BRANTTE (1972) have been designed and built. Figure 3.3. illustrates the burner used, figure 3.4 shows the flow system employed in the detector and figures 3.5A and 3.5 B are photographs of the front and back of the detector respectively.

Atmospheric air is continuously sampled at a rate of 220 millilitre minute^{-1} through a very short and narrow sampling system consisting of a teflon tube and a quartz glass capillary - see figure 3.3 - and burned upside down in a water cooled fuel rich diffusion flame with 1.1 litre minute^{-1} hydrogen. The right angled teflon tube provides a means of securing a light tight cover over the top of the burner. The burner is made from quartz except from the neck downwards (A in figure 3.3), which is pyrex; pyrex being preferable to quartz in the emission-viewing area because it is a better absorber of ultra-violet radiation and is therefore useful in blocking the OH radiation from the flame centred at about 300 nm.

The dimensions of the cooling jacket are similar to thos as described by BARYNIN (1970), the length of the jacket being such so as shield flame radiation up to the region where maximum sulphur emission occurs - about 2 cm below the flame tip. The emission from phosphorus in the flame occurs directly at the flame tip and so HPO chemiluminescent radiation is unfortunately also blocked by the water jacket.

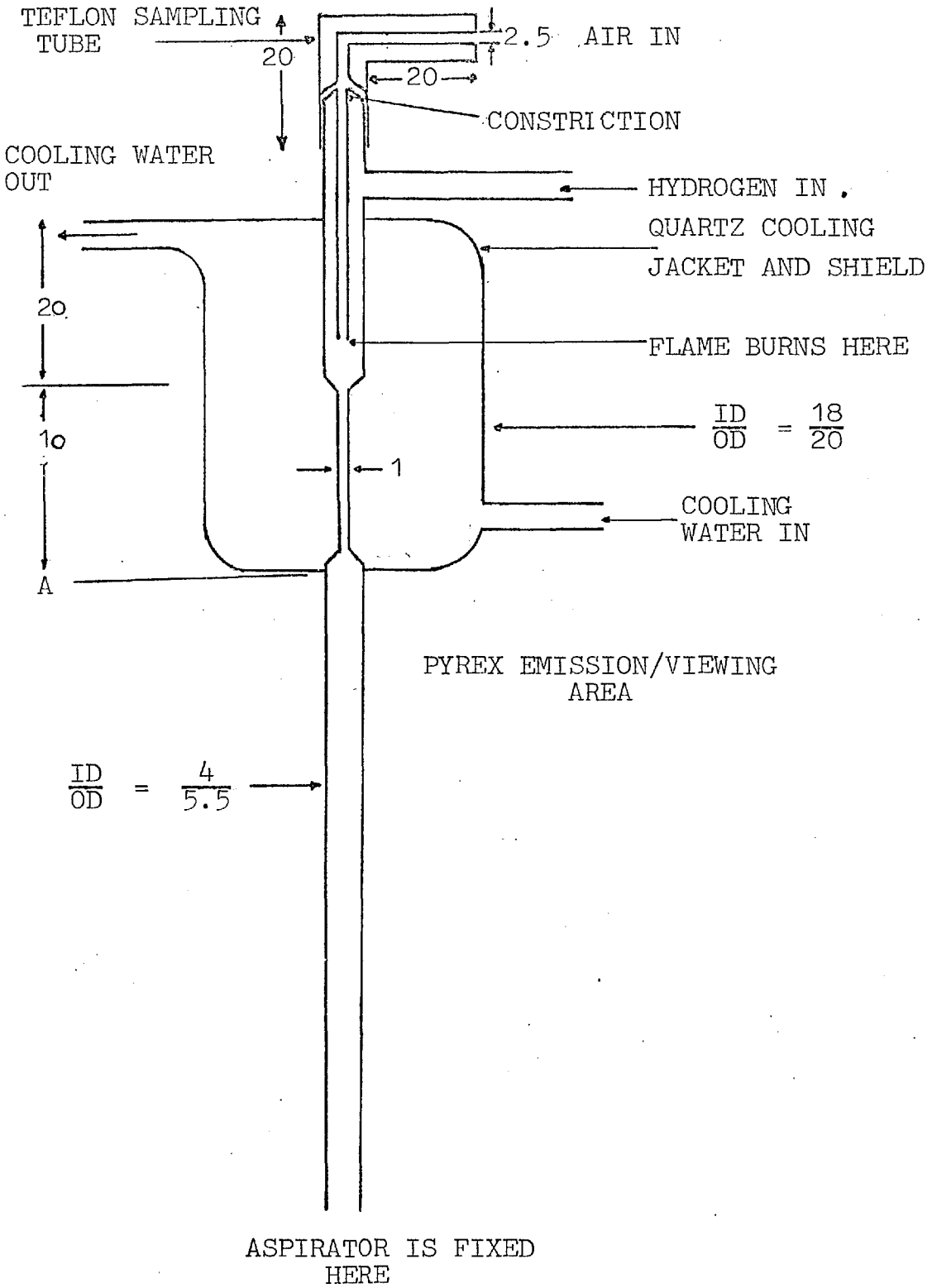

Figure 3.3 This figure shows the burner used in the detector. (All dimensions in mm.)

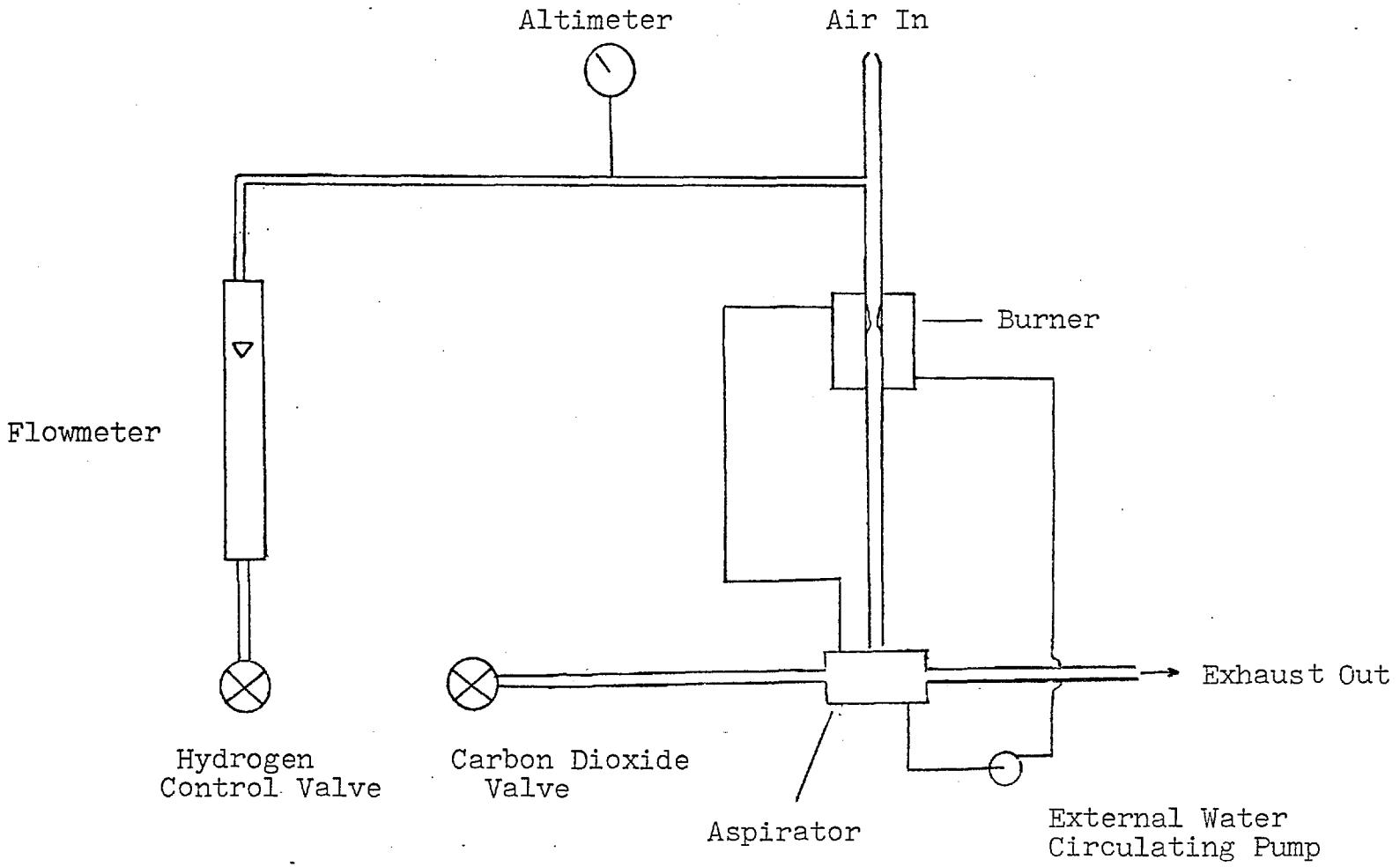

Figure 3.4 The Detector's Flow System

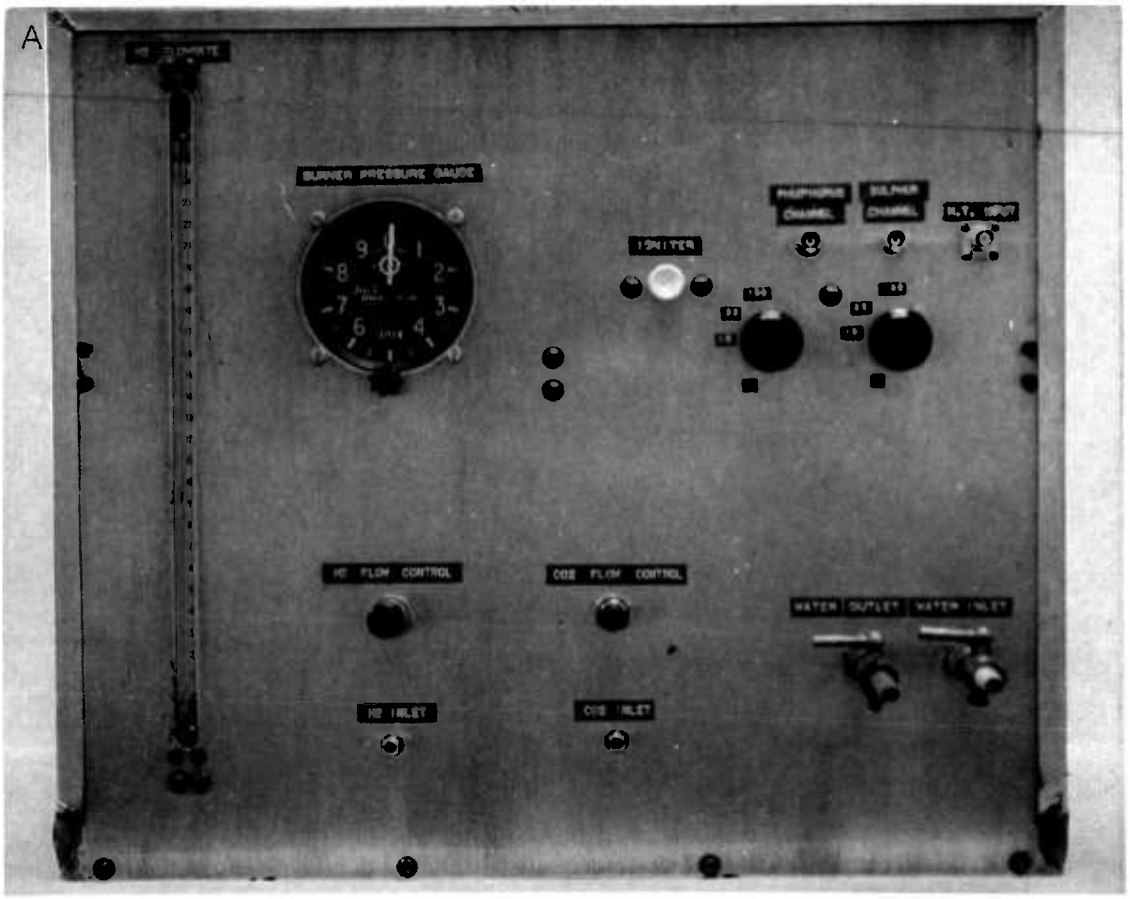

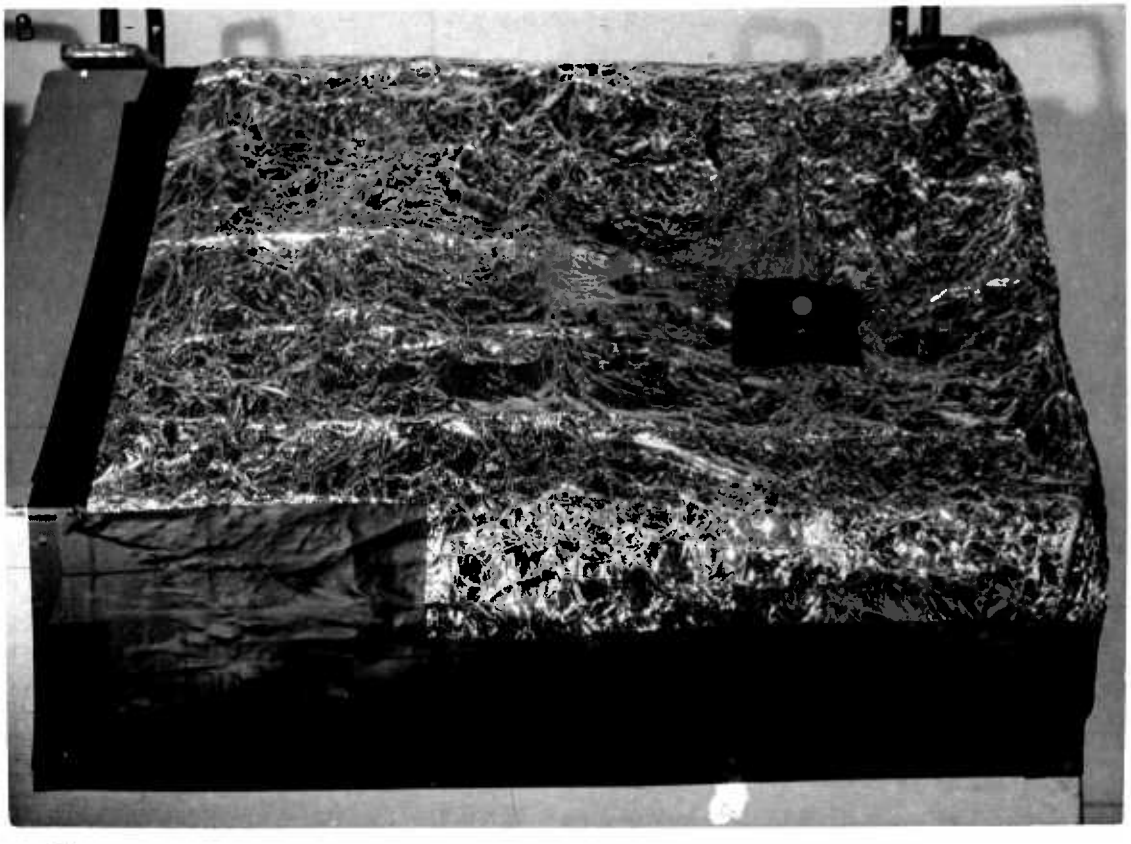

Figure 3.5 These two figures show the detector.
A = front of the detector
B = back of the detector (showing sampling tube)

Light from the burner passes to two photomultipliers placed perpendicular to each other and especially selected for low dark current and good transmission in the blue end of the spectrum. One photomultiplier is fitted with an interference fitter appropriate for light emitted by sulphur having a peak wavelength of 396 nm and a bandwidth of 11 nm whilst the other photomultiplier has an interference filter suitable for phosphorus with a peak wavelength of 526 nm and a bandwidth of 9 nm. Both photomultiplier tube housings are lagged with 2 cm glass fibre wrap and the distance between the front of the interference filters and the burner is 4 cm for both photomultipliers.

An aluminium reflecting surface with two plane mirrors positioned so as to reflect light to the photomultipliers from the burner, surrounds the burner and photomultipliers. The burner and optics are all fastened onto a 0.5 cm thick steel plate chassis for stability and this with all of the other components of the detector are contained within a 0.1 cm thick plate-metal, light-tight box that measures 46cm x 46cm x 41cm at the extremities. Internal surfaces including the burner cooling jacket are coated with matt black paint and the external surface is painted silver. The sampling point at the back of the detector's sloping roof (see figure 3.5B) is covered with two layers of p.v.c. and one layer of reflecting aluminium foil all secured with insulating tape and completely light tight. This area of the detector also serves as an explosion vent.

The required air flow and pressure conditions within the burner have been obtained by carefully grinding the constriction at the top of the burner - see figure 3.3. The pressure drop between the inside of the burner and the atmosphere - about 0.1 atmospheres - serves to reduce the effects of wind gusts at the sampling inlet on the hydrogen/air flow ratios inside the burner and is continuously measured using an altimeter, since this was found to be the only pressure guage available with the necessary sensitivity.

A piezoelectric igniter is used to ignite the hydrogen-air mixture via two nickel electrodes sealed into the top of the burner. An aspirator, which is driven by carbon dioxide and is connected to the burner using silicon tubing, is used to suck hydrogen and air through the burner and also acts as a safety precaution by diluting the excess hydrogen exhaust with carbon dioxide before discharging to the atmosphere. Cooling water at $40^{o}C$ is supplied from a "TECHNE" thermostatic water circulator to cool the burner and prevent condensation within the aspirator. The hydrogen gas flow is controlled and metered using a "Brooks" needle valve and a "Rotameter" flowmeter respectively, and the carbon dioxide gas flow is regulated using a "Hoke" needle valve. The cooling water pipes are 0.8 cm. i.d copper tubing and are lagged whilst all of the other plumbing in the detector is 0.2 cm. i.d stainless steel tubing connected with "Swagelock" fittings.

The electrical co-axial cables used for signal carrying and the high tension supply are placed above the water pipes and connections are made at the front of the detector using co-axial adaptors. The load resistors used for the two photomultipliers can be varied independently (1 kΩ to 200 kΩ) using a variable resistance box and a single high tension supply is used for both photomultipliers Start-up procedure and operating instructions are given in Chapter 5.1.3.

3.5 Response Time Testing

It was necessary to build an apparatus that was capable of measuring the response time of the detector. A manual method (BARYNIN, 1970) of step testing has previously been used, however, this method suffered from two major disadvantages:

1. The so-called step change could never really be a step change because the sample point did not traverse an interface but a continuous boundary of steep concentration gradients.

2. The step test consisted of a given step change from pure air to polluted air (a rise) and a step change from polluted air to pure air (a fall). However, because of the manual method employed, the waveform of the rise signal may have been entirely different to that of the fall signal thus making the interpretation of the results rather difficult.

The new piece of apparatus - named the Oscillating Calibrator - was designed with a view to reduce or overcome the above limitations. Figure 3.6b shows the apparatus. The apparatus consists of two teflon tubes - 1 cm. diameter and 12 cm. long mounted on a brass plate. One tube carries a flow of phosphorus pentafluoride in air and the other carries a flow of sulphur dioxide in air. The gas presented to the burner orifice via any one of the teflon tubes is suddenly changed from the pure air to the polluted air and vice-versa. This change is initiated by actuating one of two solenoids with a switch. The apparatus cannot overcome the first disadvantage listed above, but can only reduce the time that the steep concentration gradients are sampled from by having a fast acceleration through the concentration gradients, and the effect of the second disadvantage should be significantly reduced.

As a further development of the step test, a continuous oscillating calibrator was constructed to investigate the effect of various input signal frequencies on the detector output by continuously alternating between pure and polluted air - see figure 3.6a. As in the step method, the gases flow through two teflon tubes mounted on a brass guide plate that contains a slot into which a guide pin sits. The guide pin is secured to a motor and rotates in an eccentric orbit and the speed of oscillation can be varied using a rheostat.

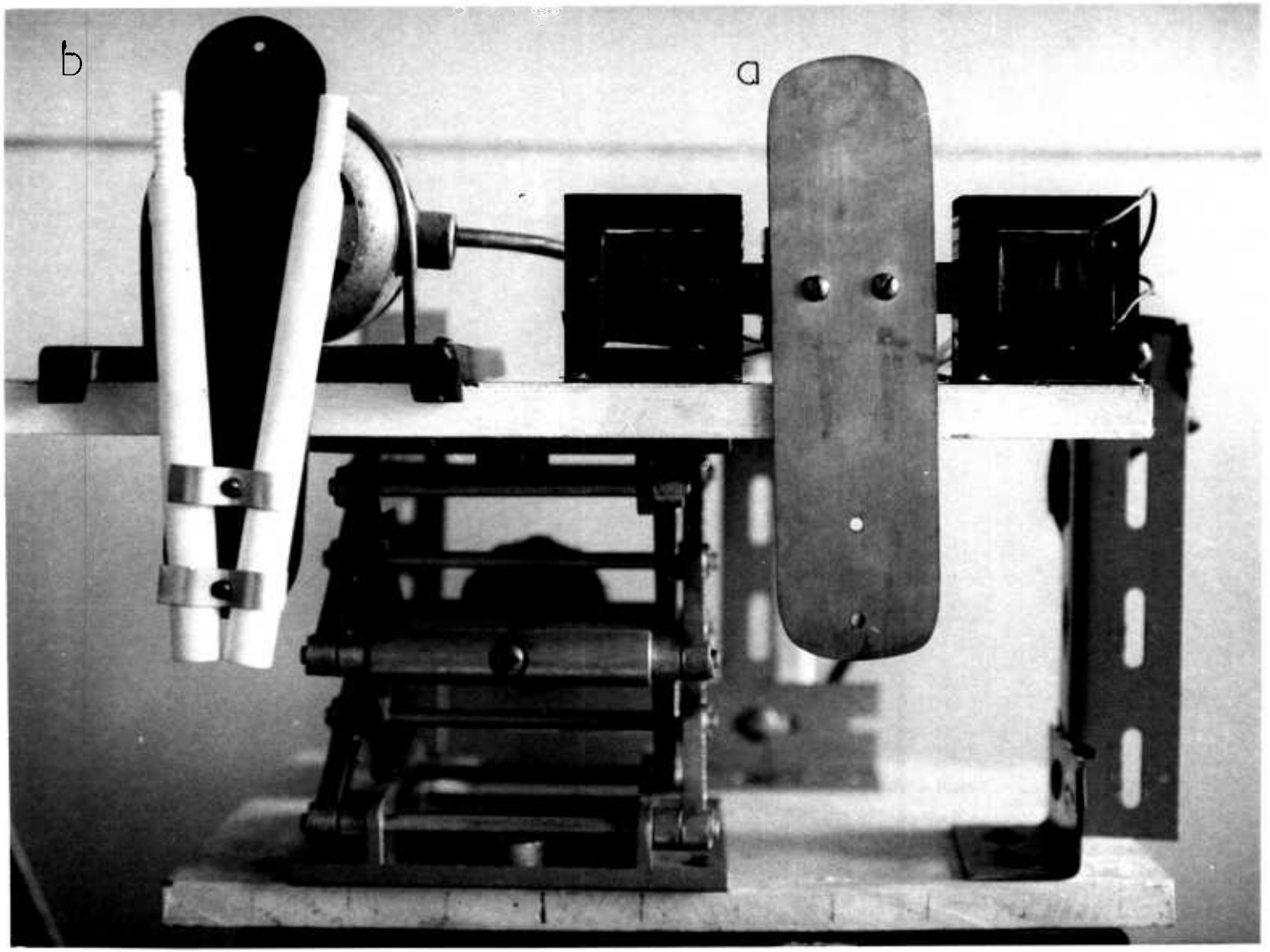

Figure 3.6 This figure shows the Oscillating Calibrator a = step apparatus b = continuous apparatus.

The two halves of the oscillating calibrator are mounted onto a wooden base that is fixed to a "Labjack", so that the calibrator can be raised or lowered over the burner inlet orifice.

The calibration flow system used to give a supply of polluted air is shown in figure 3.7. Sulphur dioxide permeation tubes are used as a source of sulphur and a cylinder of 25 p.p.m. phosphorus pentafluoride - in - air B.O.C. Special Gas mixture is used as a source of phosphorus. The polluted air can be humidified from 0 to 100% and the air is supplied from B.O.C. gas cylinders. The detector, with the roof removed, is set-up as explained in Chapter 5.1.1 and the oscillating calibrator placed in position over the burner. The response tests can then be carried out and the detector output signals are displayed on an oscilloscope with storage and photographic facilities.

The permeation tubes were constructed according to the method of LINDQVIST and LANTING (1972), with one alteration; the glass vials are cooled with liquid nitrogen to freeze the sulphur dioxide as opposed to using a dry ice/acetone mixture as suggested by LINDQVIST and LANTING (1972). This gives more time to seal the vials before the solid sulphur dioxide vapourises, thus making the sealing operation easier and safer.

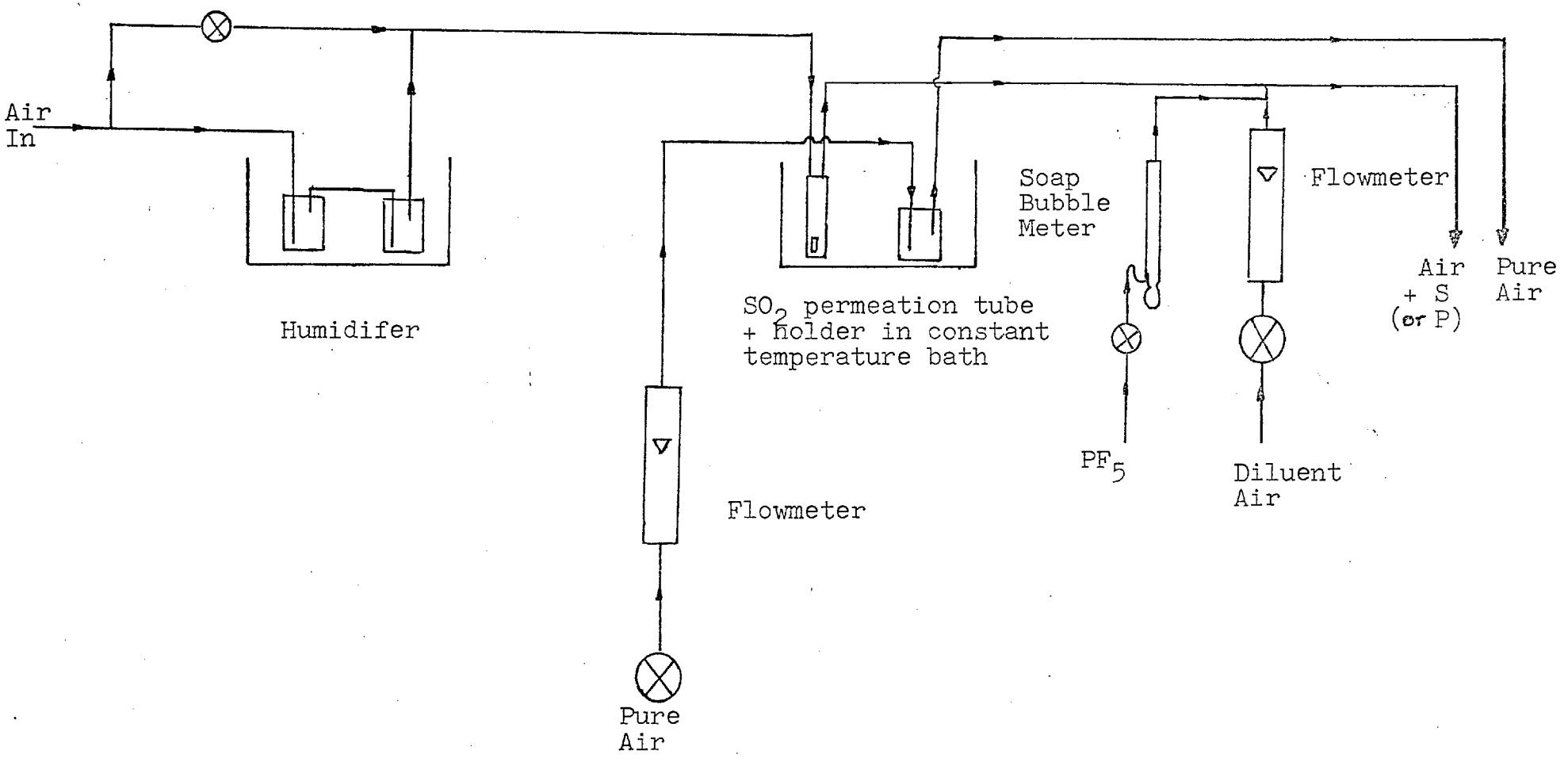

Figure 3.7 Flow System used to Supply Pure Air and Air + SO_2 and/or Air + PF_5 to the Detector.

3.6 Results on Response Time Tests

3.6.1 Step Tests with Sulphur

Table 3.1 shows the results for different step concentration intervals. The response times are averages of three runs for each step interval. Figure 3.8a shows a photograph of a typical rise curve for the response of the detector to a step input obtained from a change in gas concentration of pureair to polluted air. Analysis of the photograph reveals that the detector responds to 90% of a step rise in concentration in under 100 milliseconds and to 100% in under one second. Figure 3.8b is a photograph of the corresponding fall curve for the response of the detector to a step input obtained from a change in gas concentration of polluted air to pure air. The detector responds to 90% of a step fall in concentration in under 20 milliseconds and to 100% in under 50 milliseconds. In both cases the concentration of sulphur dioxide is 200 micrograms per cubic metre.

3.6.2 Step Tests with Phosphorus

Table 3.2 shows the results for different step intervals and the response times are averages of three runs for each step interval - as in the case of sulphur. Figures 3.9a and 3.9b show photographs of a rise and fall respectively with a concentration of phosphorus pentafluoride of 300 microgrammes per cubic metre. In both cases the detector responds to 100% of a step input in under 15 milliseconds.

SULPHUR

RUN	STEP INTERVAL $\mu g\ M^{-3}$	RESPONSE TIME $t_{90\%}$ M.Secs		RESPONSE TIME $t_{100\%}$ M.Secs	
		RISE	FALL	RISE	FALL
1	0 - 80	88	15	890	48
2	0 - 200	75	17	970	53
3	0 - 1500	83	17	930	44

Table 3.1 This table shows the response time of the detector for different step intervals.

$t_{90\%}$ is the time, in milliseconds, for the output to reach 90% of the final signal level.

$t_{100\%}$ is the time, in milliseconds, for the output to reach 100% of the final signal level.

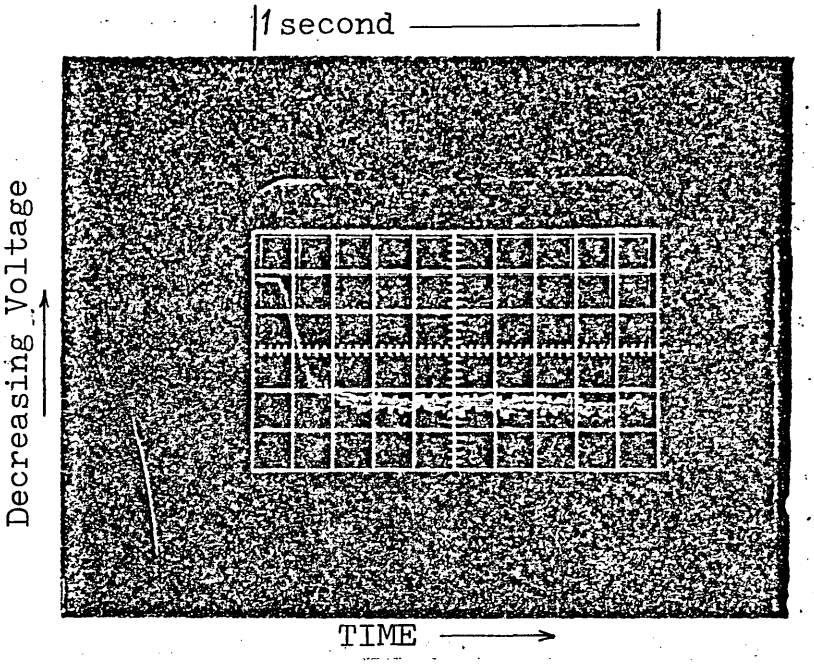

Figure 3.8a The detection response to a positive step input of sulphur (rise) No S — S

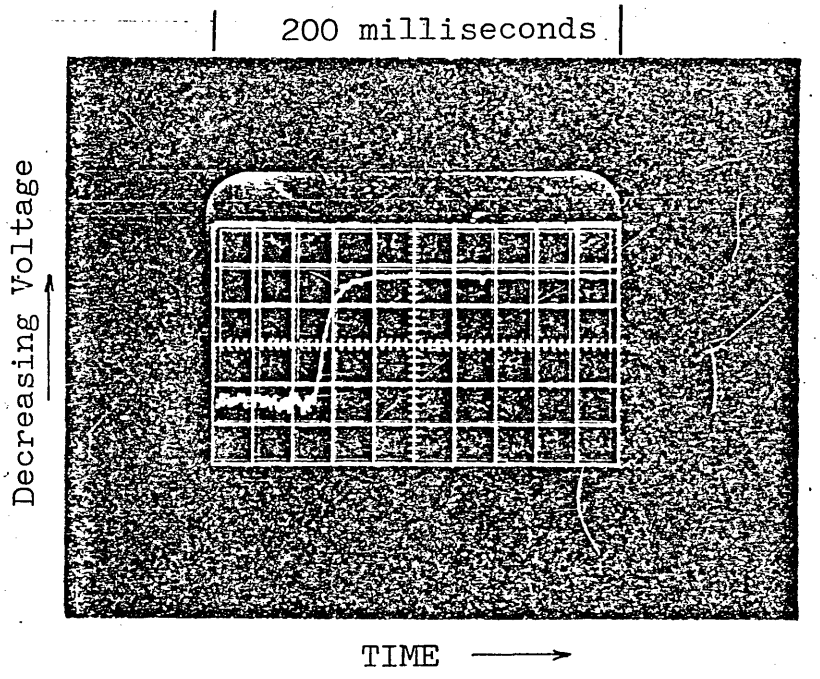

Figure 3.8b The detection response to a negative step input of sulphur (fall) S — No S

PHOSPHORUS

RUN	STEP INTERVAL $\mu g\ M^{-3}$	RESPONSE TIME $t_{90\%}$ M.Secs		RESPONSE TIME $t_{100\%}$ M.Secs	
		RISE	FALL	RISE	FALL
1	0 - 100	7	8	15	13
2	0 - 300	8	9	15	14
3	0 - 1400	8	8	17	15

Table 3.2 This table shows the response time of the detector for different step intervals.
$t_{90\%}$ and $t_{100\%}$ are the times, in milliseconds, for the output to reach 90% and 100% of the final signal level respectively.

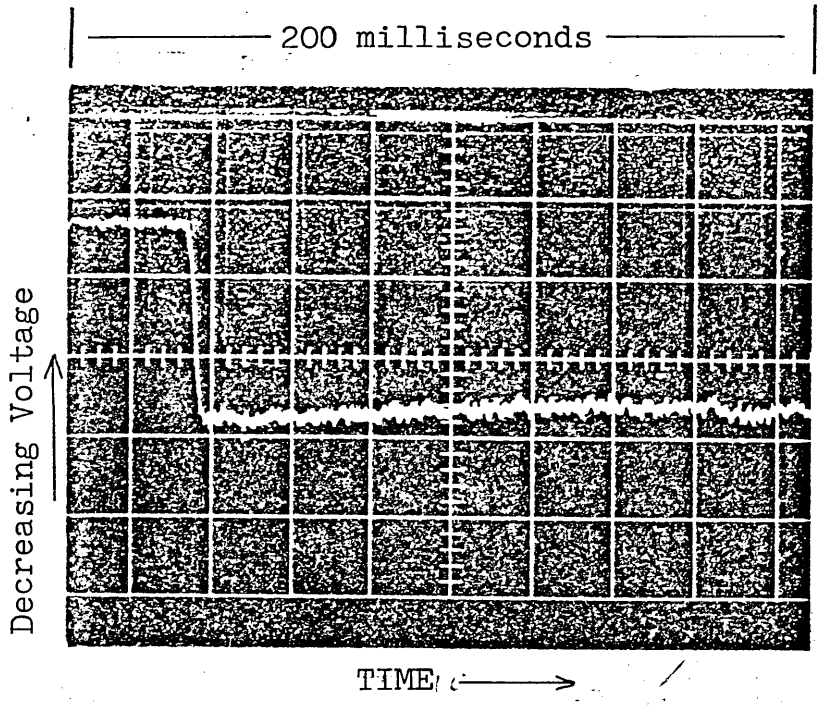

Figure 3.9a The detector's response to a positive step input of phosphorus No P — P

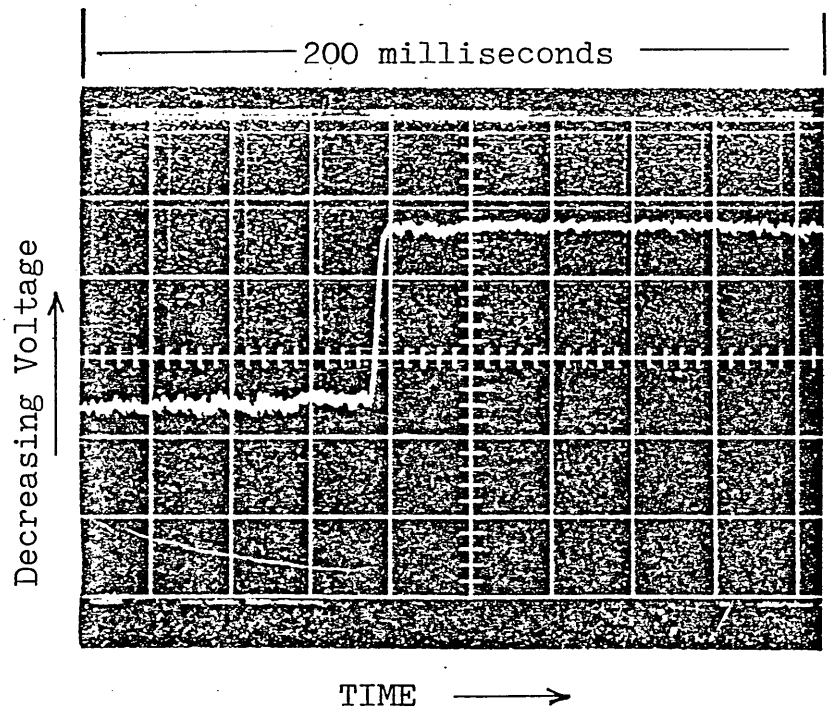

Figure 3.9b The detector's response to negative step input of phosphorus P — No P

3.6.3. Frequency testing with sulphur and Phosphorus.

Using the continuous part of the oscillating calibrator - as described in 3.5 - tests at different frequencies were made with concentrations of 200 microgrammes of sulphur dioxide per cubic metre and 460 microgrammes of phosphorus pentafluoride per cubic metre. Figures 3.10a and 3.10b show photographs of the detector's response to approximate square waves at these concentrations with a frequency of about 5Hz for sulphur and 15 Hz for phosphorus. The amplitude of the output from the detector shows no detectable attenuation up to these frequencies.

3.6.4 Effect of Humidity on the Response Time.

The effect of humidity on the response time of the detector was investigated using a humidified supply of polluted air and pure air. Several runs were carried out for different step intervals at relative humidities of 40, 70 and 90%, however, no noticeable change in response time was recorded for sulphur and phosphorus. The step intervals were the same as those used for the step testing procedure.

3.6.5 Effect of History on the Response Time.

The duration for which the burner samples from either the pure atmospheric air or polluted air was found to have no effect on the response time. Duration times of milliseconds up to minutes were used in these tests.

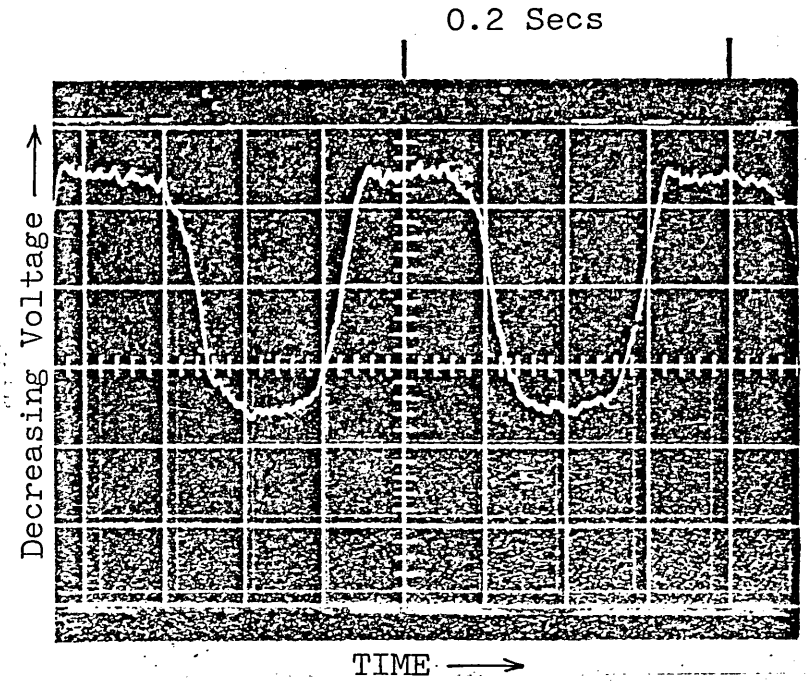

Figure3.10a The detector's response to an approximate square wave with sulphur.

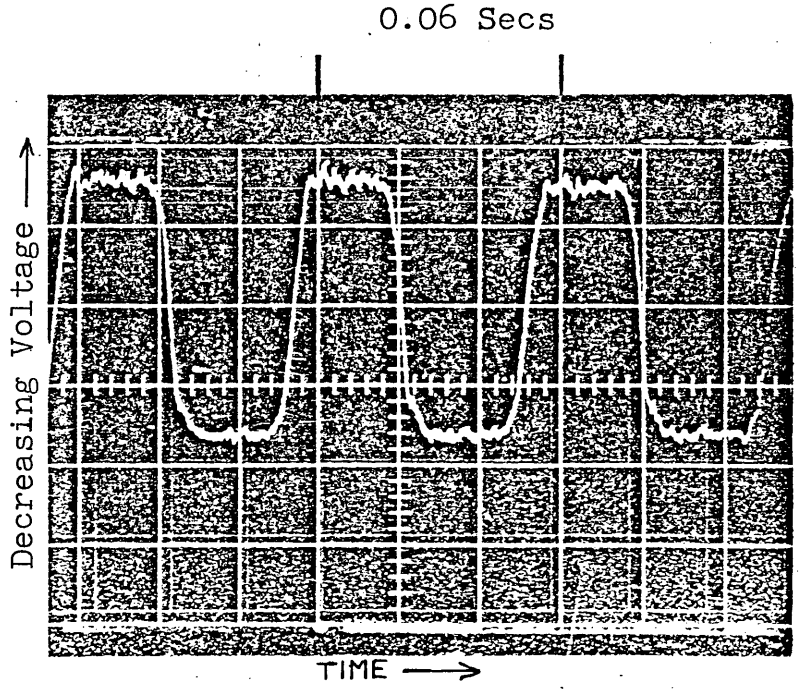

Figure 3.10b The detector's response to an approximate square wave with phosphorus.

3.6.6 Effect of the Teflon Sampling Tube on the Response Time.

The previous tests were carried out without the teflon sampling tube and so it was necessary to determine whether the tube had any serious effects on the results. A straight version of the tube was made with as near as possible the same dimensions as the one shown in figure 3.3 and the tests were carried out in exactly the same way as previously described. No difference was detected for the step and frequency tests; the only effect of the sampling tube was to introduce a dead time (the residence time of the gases in the input sampling tube).

3.6.7 Transient and Frequency Response of the Detector.

The transient response is of interest when determining the suitability of instruments to measure step changes in concentration. The most complete dynamic description of a system is its transfer function which is the ratio of the Laplace transformed output signal to the Laplace transformed input signal. Knowledge of the transfer function implies knowledge about the output from a system for any given input. Frequency response curves are essentially a graphical record of the transfer function and are therefore useful to depict the dynamic response of a system.

The first stage in this calculation is to produce the transient response from figures 3.8a, 3.8b, 3.9a and 3.9b. The figures are magnified and projected onto suitable graph paper using an Epidiascope. This enables the deflections

and corresponding times to be easily read from the graph so that the transient response can then be determined for the various systems.

a. Sulphur Rise.

Graph 3.1 shows a rise fitted by a non-linear equation from groups of results typical of figure 3.8a. The equation

$$Y_{out} = 1 - e^{-t/7} - 0.16e^{-t/195} + 0.16e^{-10t} \quad \text{Equation 3.13}$$

where t is in milliseconds, contains two time constants and a "dummy" parameter. The first term in equation - $e^{-t/7}$ - describes the very fast initial rise in the signal whilst the second term allows for the much slower secondary process occurring in the rise. The final term, e^{-10t}, plays no part in the function apart from ensuring that the function has a value of zero when t is zero.

The transfer function can now be calculated by differentiating the transient response to give the impluse response. After laplace transforming and converting to the frequency domain a magnitude, M, (1-attenuation) vs frequency graph can be plotted.

Therefore

$$\left[\frac{dy}{dt}\right]_{out} = \frac{1}{0.007} e^{-t/0.007} + \frac{0.16}{0.195} e^{-t/0.195} - 1600\, e^{-10000t} \quad \text{Equation 3.14}$$

t is in seconds

and the Transfer Function

$$G(S) = \frac{L\left[\frac{dy}{dt}\right]_{out}}{L\left[\frac{dy}{dt}\right]_{in}} \quad \text{Equation 3.15}$$

can be calculated using the following simplifying assumptions:-

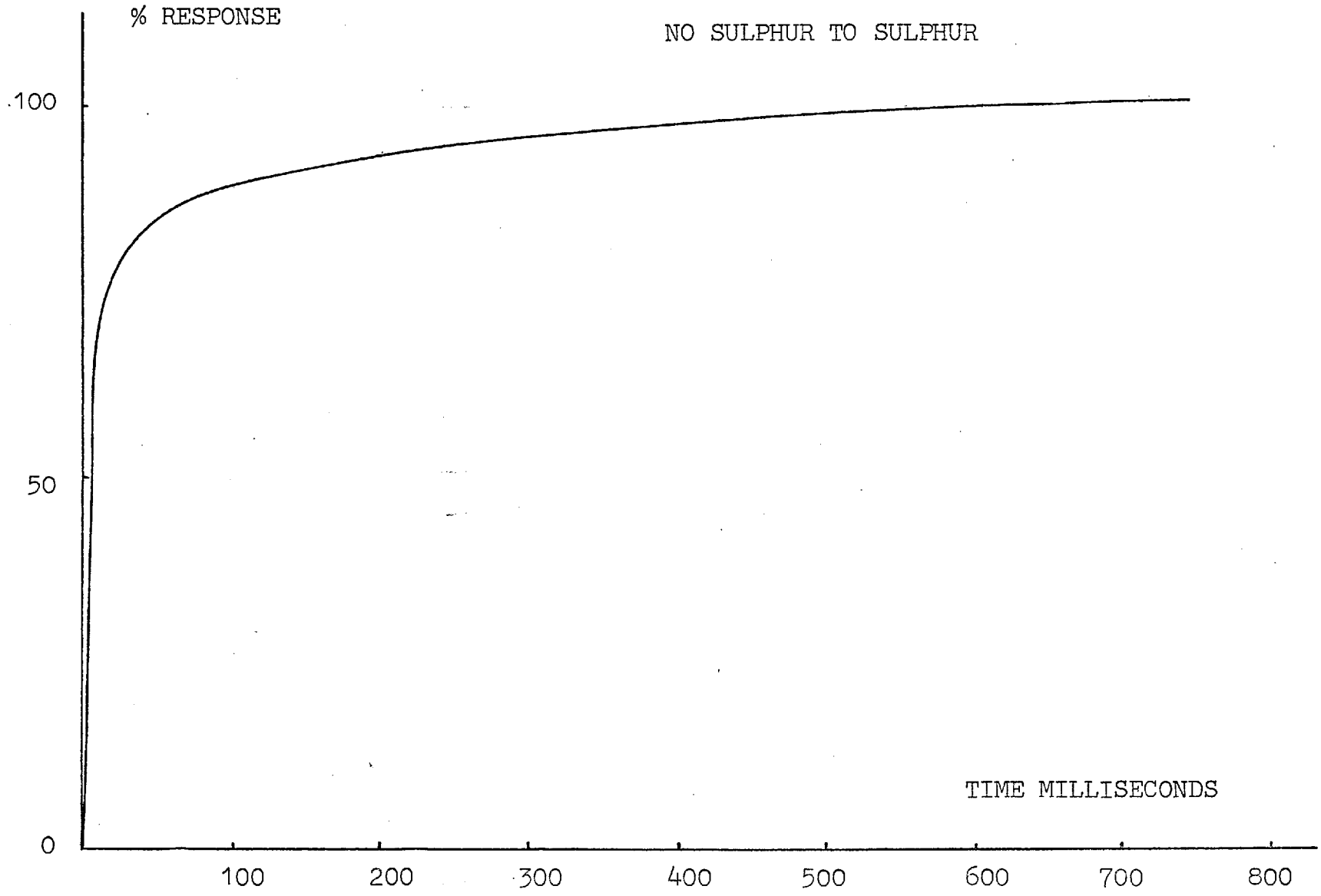

Graph 3.1 This graph is a "rise" curve plotted from the regression equation 3.13.

i) The dead time has been removed from the transfer function because it represents a relatively small time constant. The inclusion of this time constant would not affect the shape of the response curve but only displace the curve in time.

The dead time has been calculated for a flow of 220 ml minute^{-1} air through the sampling tube and an internal volume of 5.12 x 10^{-2} cm^3 -inclusive of the internal volume of the teflon tube and quartz capillary as in figure 3.3. The value for the dead time θ_{TC} is

$$\theta_{TC} = 14 \text{ milliseconds.}$$

where T and C denote tubing and capillary respectively.

ii) The input step signal to the detector is considered to be ideal so that

$$L\left[\frac{dy}{dt}\right]_{in} = \underline{1}$$

The input step signal is actually non-ideal but its waveform is not precisely known. The error in this assumption - for the sulphur case - will become significant only at high input signal frequencies (80-100Hz).

Therefore, on substituting Equation 3.14 into Equation 3.15 and converting to the frequency domain, the Magnitude and frequency can be calculated. Values are shown in Table 3.3.

M	W
1	0
0.99	1
0.93	5
0.88	10
0.85	20
0.83	30
0.82	40
0.8	50
0.78	60
0.76	70
0.74	80
0.72	90
0.69	100

Table 3.3.

Table 3.3. shows the Magnitude for various values of frequency-wHerz.

A plot of M vs w (Hz) is shown in graph 3.2.

b. Sulphur Fall.

The same procedure is carried out as for the Sulphur rise. Graph 3.3 shows a fall fitted by a non-linear equation containing only one time constant:

$$Y_{out} = 1 - e^{-t/10} \qquad 3.16$$

where t is in milliseconds. Graph 3.4 is a plot of magnitude vs w (Hz).

c. Phosphorus Rise and Fall.

Graph 3.5 shows the transient response of the detector to a rise (A) and a fall (B) in phosphorus concentration. The curves are essentially linear for at least 90% response, however, a non-linear equation has been approximated to both the rise and fall - since they are similar - and this accounts for the "trailing-off" on the signal:

$$Y_{out} = 1 = e^{-t/4} \qquad 3.17$$

where t is in milliseconds. It is considered meaningless to determine the frequency response of the detector to phosphorus simply because the transient response has not been measured. The oscillating calibrator is not fast enough either in the step mode or continuous mode to determine the transient response, this point is discussed in more detail in 3.6.8 .

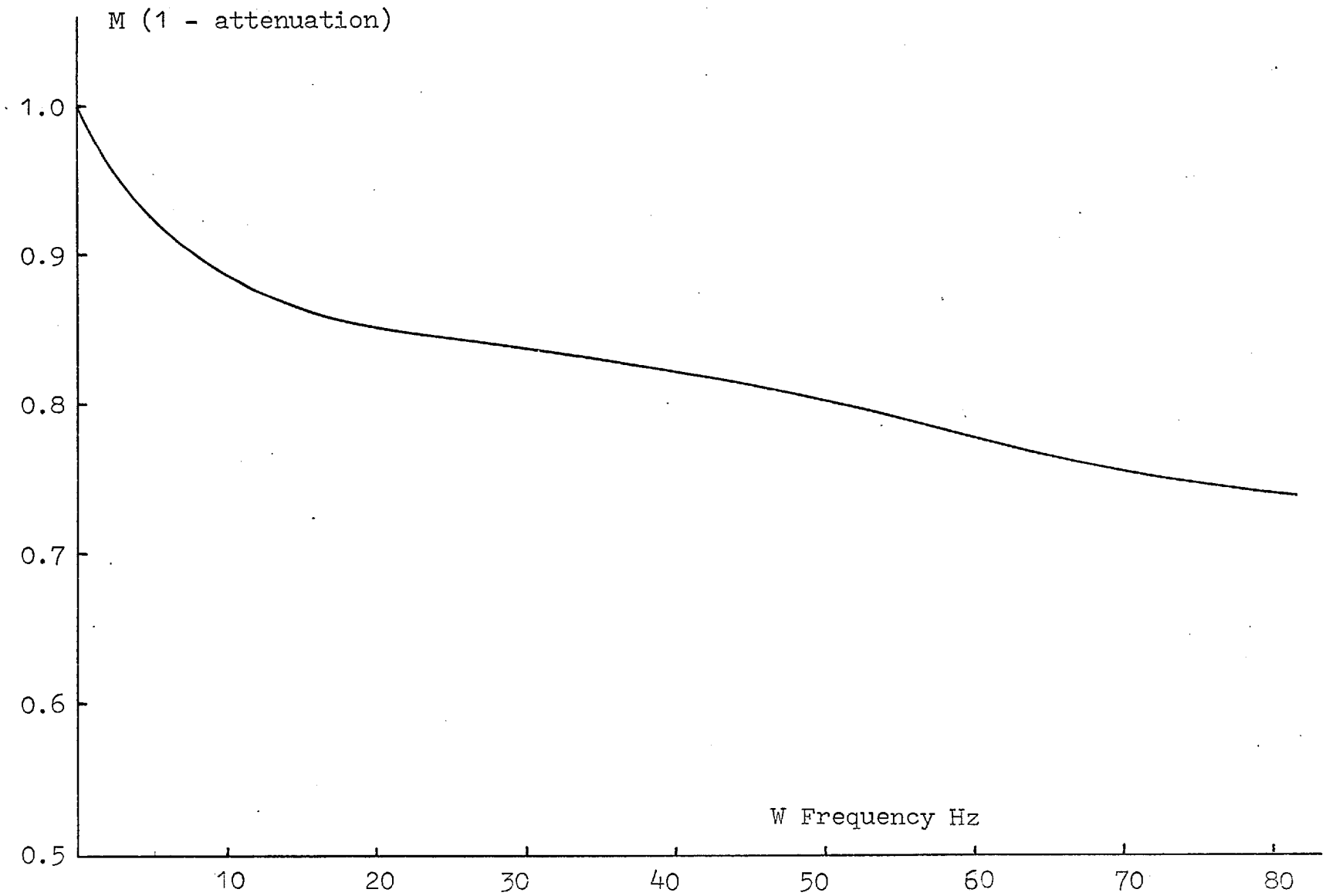

Graph 3.2 This graph is a plot of the magnitude (M) vs Frequency (W Hz) for a rise.

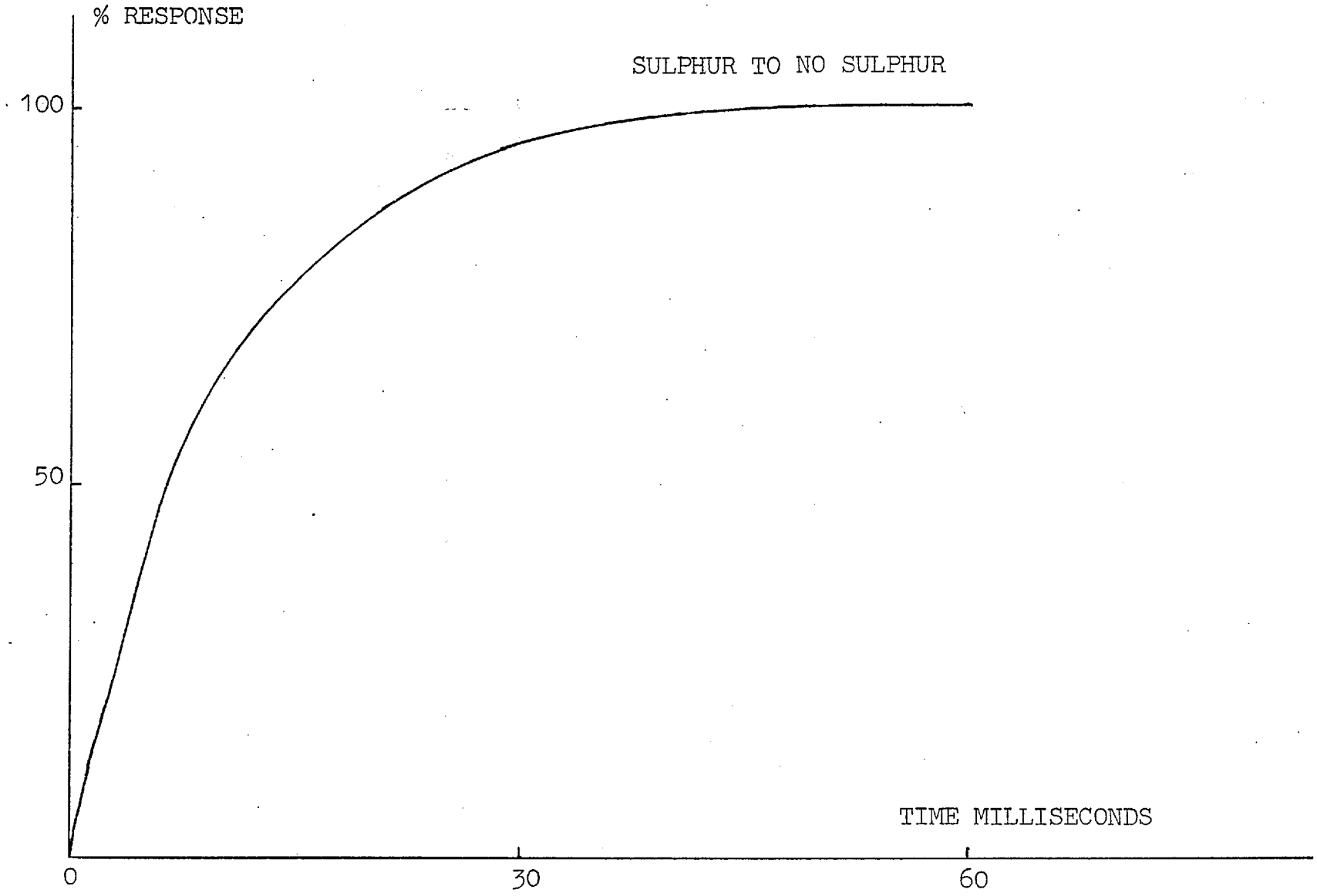

Graph 3.3 This is a "fall" curve plotted from the regression equation 3.16

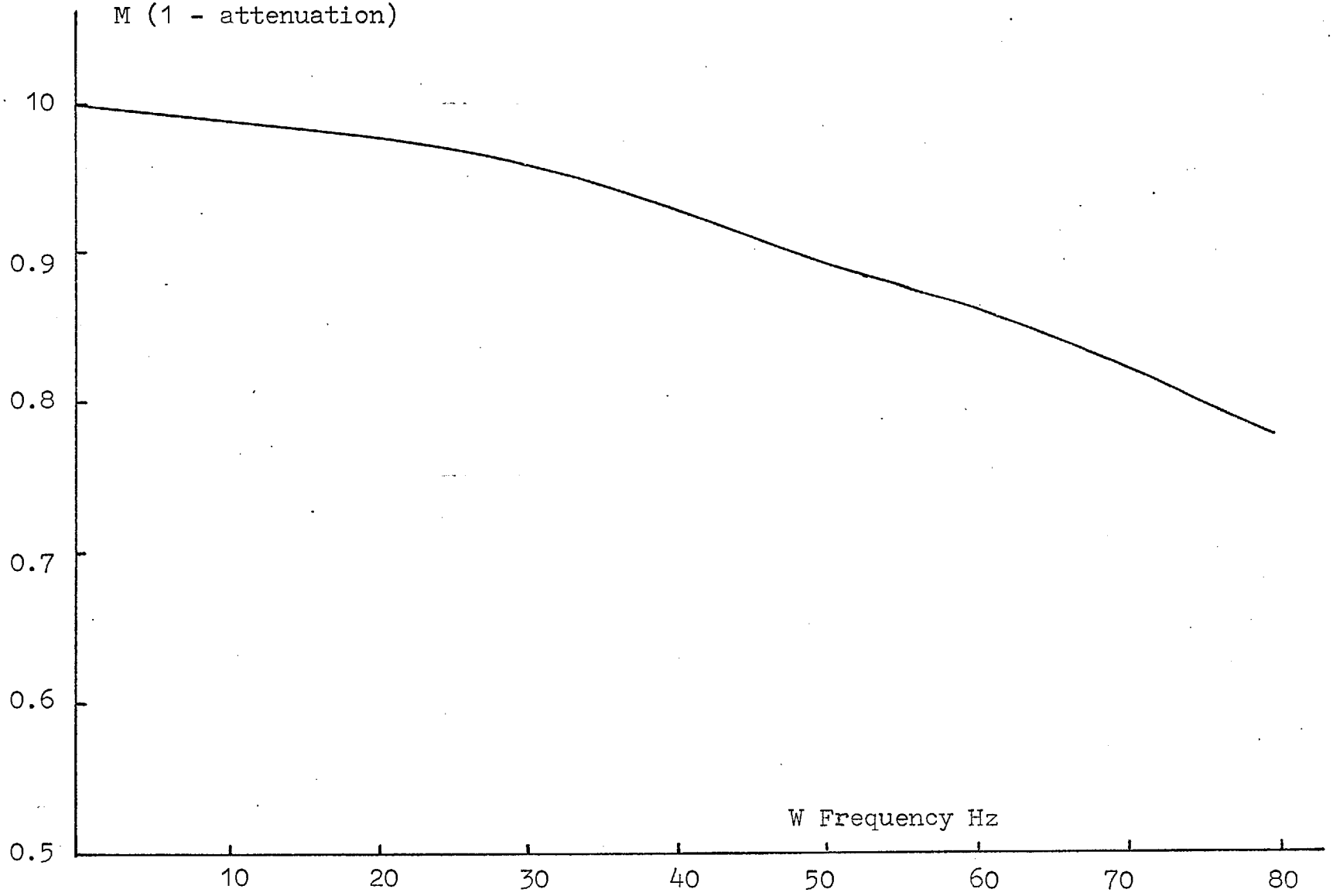

Graph 3.4 This graph is a plot of the Magnitude (M) vs Frequency (W Hz) for a fall.

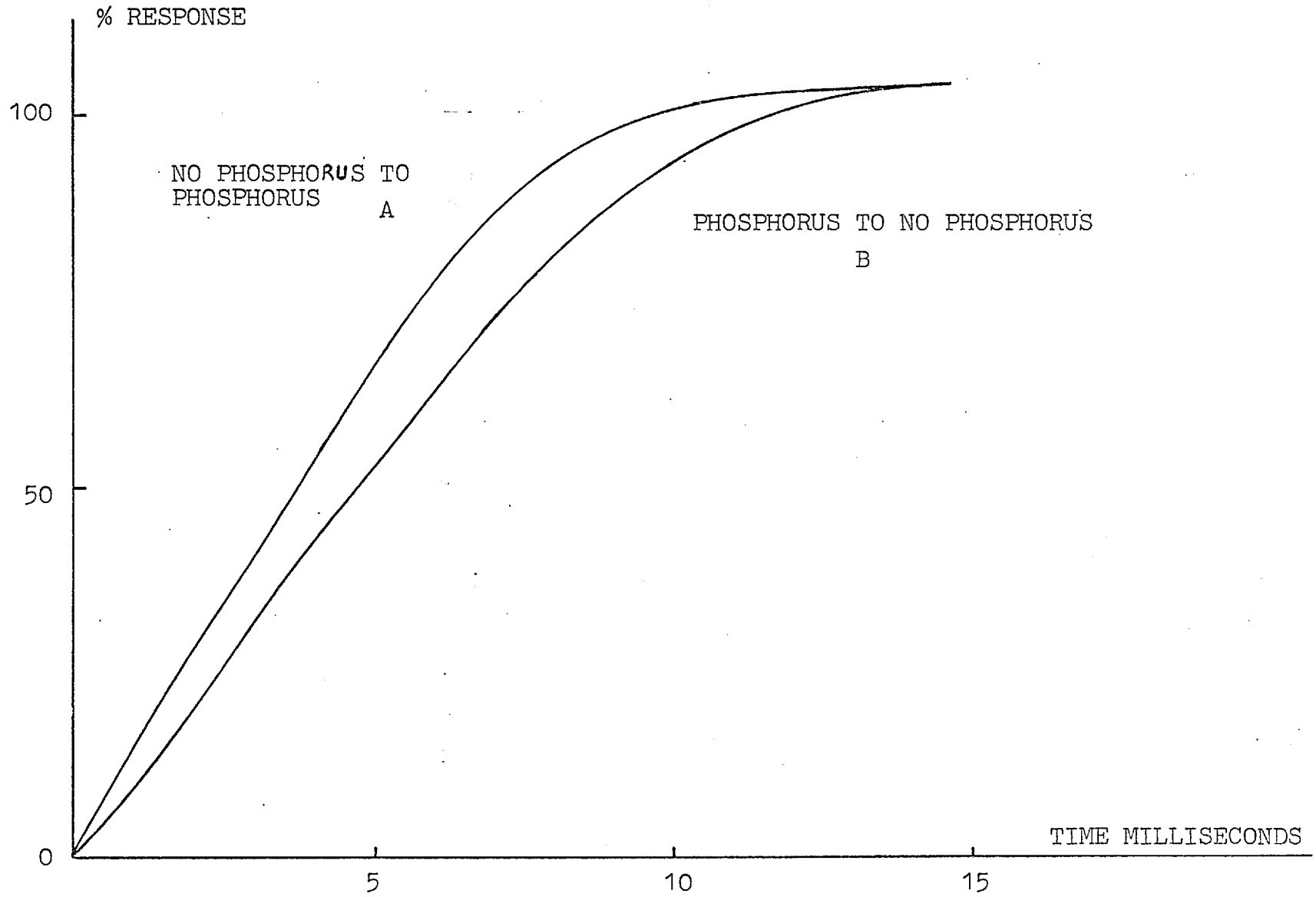

Graph 3.5 This graph shows a rise,A, and a fall curve, B, for the phosphorus response of the detector.

3.6.8 Discussions of Response Time Results.

Response - time testing devices using solenoid valves, for example, that can be switched between any two flows of different concentrations have been used in the past, although, the literature contains sparse and inadequate descriptions of such apparatus. This type of apparatus may work well with the conventional sulphur flame photometric detectors because response times are of the order of 20 to 50 times slower and this makes the problem much easier with respect to testing. However, for this detector, a device with the speed of the oscillating calibrator is essential in order to tailor the desired signal.

The results from the step tests can be described by the values of the three following time constants:

a) A time constant describing the time for which it takes the calibrator to produce a change of concentration.

The value of this time constant is dependent on the speed of movement of the calibrator across the burner inlet and the concentration gradients existing at the burner inlet. The traverse time of the calibrator has been measured using microswitches and displaying the elapsed time between a contact opening and closing on an oscilloscope, and this was found to be about 10 milliseconds.

b) A time constant describing the time for which the detector indicates a change in concentration of sulphur.

c) A time constant describing the time for which the detector indicates a change in concentration of phosphorus.

In recalling the results of 3.6.2 - Step Tests with Phosphorus - it is noted that the 100% response time on the phosphorus channel is only 15 milliseconds for both a step rise and a step fall. This value is comparable to the value of 10 milliseconds for the traverse time of the calibrator and for this reason the phosphorus response time is considered to be an indication of the non-ideality of the step input to the burner. The response time of the detector to reach 100% of a step rise or fall in phosphorus concentration is 15 milliseconds at the very most.

Graph 3.5 shows the transient response of the detector to a step rise (A) and a step fall (B) in phosphorus concentration and it is seen that a maximum difference between the rise and fall curve of about 2 milliseconds exists on the time scale. This difference could be due to the fact that the calibrator's speed of travel in the two directions was slightly different or possibly due to a peculiarity of the detector's response on the phosphorus channel.

The results for sulphur are more interesting than those for phosphorus. Graph 3.1 shows a rise curve and graph 3.3 shows a fall curve for sulphur. The 90% response time for the fall is approximately six times faster than the rise and the form of the rise is not the same as the fall with the rise having a much slower secondary process controlling the response after the first 100 milliseconds. The difference

in the form of the curves cannot be wholly accounted for by the speed of the calibrator because the calibrator's movement only occupies about 20% of the total response time for the fall. This difference may be a function of the reaction mechanism occurring within the burner.

The values for the response times are maximum times, again because of the non-ideal step input. The step tests and frequency tests both show the response of the sulphur channel to be flat up to 5Hz and appreciable attenuation (20%) occurs only at 50 HZ - for a rise. As previously shown, the response of the sulphur channel is non-linear - the rise being of a different form than the fall - and this will inevitably give rise to harmonic distortion especially with signals that rise or fall in times faster than 100 milliseconds, since then rises will be significantly attenuated but falls will not be. Given the non-linear response of this instrument it would be more desirable to use a pulse test as opposed to a step test because, theoretically, only one pulse simultaneously excites the system with all frequencies and if carefully constructed will produce significant response in the frequency range of interest. The step test, however, is only valid for the particular input function that generated the response and so is of limited use. Unfortunately to tailor a pulse of the necessary width and height to generate the frequency response of this instrument is extremely difficult to do and so a step test is used in this work because it is a relatively easy task to construct and use a step test as an input to this instrument.

SHILLER and CAMPBELL (1971) note that the sensitivity of a flame photometric detector to sulphur falls in the presence of large concentrations of hydrocarbons. The introduction of 1200 p.p.m. into the detector via a chromatographic column destroyed the S_2 emission. Shiller and Campbell suggest that the destruction of the emission is due to carbon building on the walls of the burner and the S_2 reacting to give carbon disulphide. This explanation was put forwardbecause when the flow of propane was stopped the emission returned at a rate that depended on the duration of the hydrocarbon flow. In section 3.6.5 the effect of sampling history on the response time of the burner was examined but no indication of possible particulate building on the walls affected the results. Of course, the respective concentrations in this experiment, using room air as a source of particulate material, and Shiller and Campbell's work are completely different as is the chemical nature of the particles.

3.7 Calibration of the Sulphur and Phosphorus Channels

The detector was calibrated with the use of the flow system shown in figure 3.7 to provide flows of gases of known concentration. The calibration was carried out under static conditions using pure air from cylinders and the sulphur and phosphorus sources as mentioned in section 3.5. The photomultiplier signal output voltage - using a given load resistance of 100 KΩ was recorded on a graph recorder for different power supply levels (E.H.T. levels) and, after a suitable equilibration period, for different gas concentrations.

3.7.1 Sulphur

Graph 3.6 is a log-log plot of the concentration of sulphur dioxide (Cso_2 μgM^{-3}) against the photomultiplier signal output (Pso_2 millivolts MV) at different E.H.T. levels. For a given photomultiplier signal output and E.H.T. level the concentration of sulphur dioxide can be accurately estimated from

$$C_{so_2}\ (394) = A \cdot (P_{so_2} - BAKGRS)^B \quad \mu gM^{-3} \text{ at } 394 \text{ nm}$$

Equation 3.18

where the values for A and B are determined from the intercept and gradient respectively of graph 3.6 and BAKGRS is the photomultiplier signal output obtained by viewing the flame radiation without the presence of sulphur species.

The graph suggests the following relationship:

$$\text{Emission Intensity} \propto (\text{Concentration})^2$$

Table 3.4 lists the values of A, B and BAKGRS for different E.H.T. levels.

3.7.2 Phosphorus

Graph 3.7 is a log-log plot of the concentration of phosphorus pentafluoride (C_{PF_5} $\mu g\ M^{-3}$) against the photomultiplier signal output (P_{PF_5} MV) at different E.H.T. levels.

For a given photomultiplier signal output and E.H.T level the concentration of phosphorus pentafluoride can be accurately estimated from

$$C_{PF_5}\ (526) = D \cdot (P_{PF_5} - BAKGRP)^E \ \mu gM^{-3} \text{ at } 526 \text{ nm.}$$

Equation 3.19

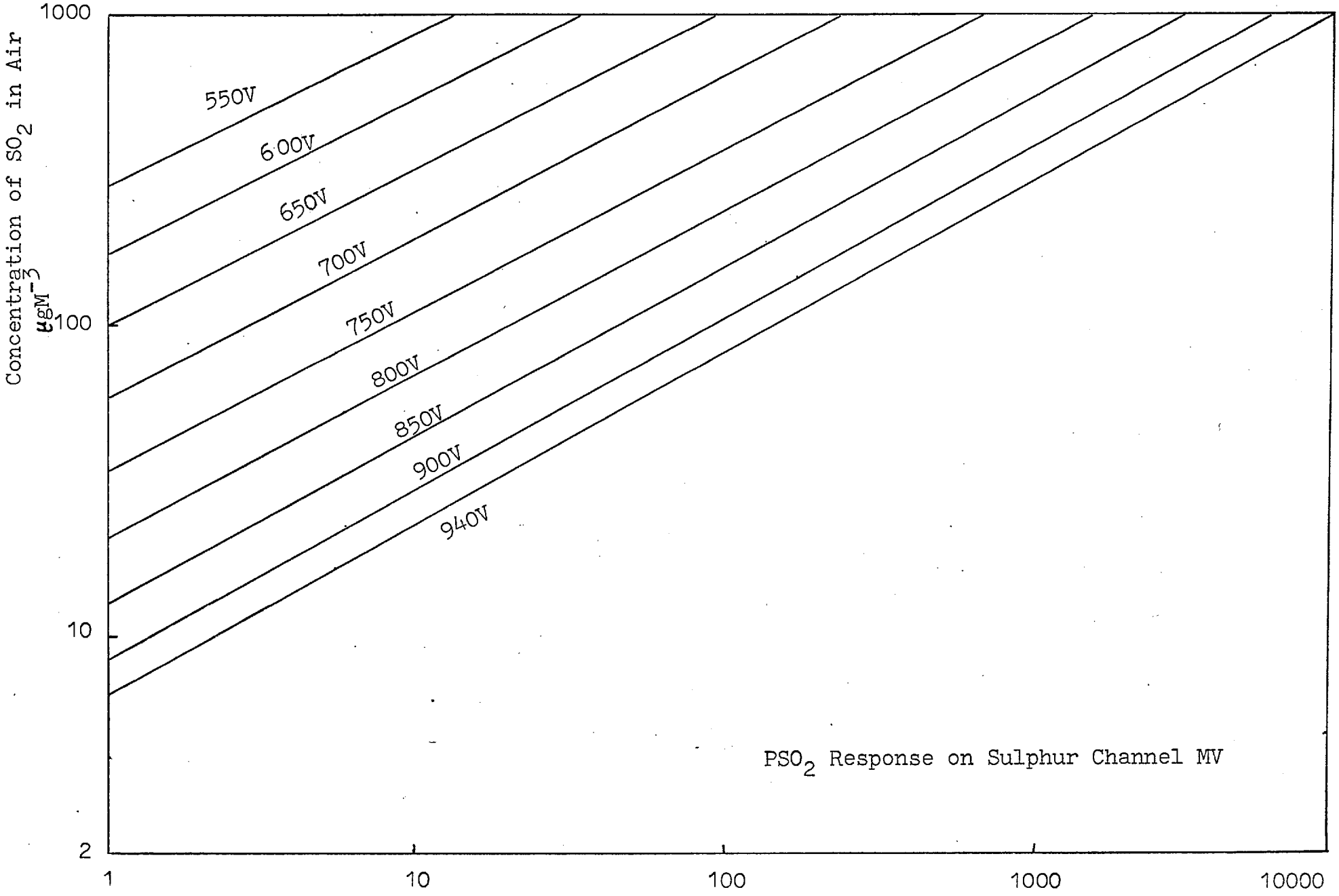

Graph 3.6 Detector response (PSO_2 millivolts) VS Concentration of SO_2 in Air (μgM^{-3}) for different E.H.T. levels (volts).

TABLE 3.4 SULPHUR

E.H.T.	550	600	650	700	750	800	850	900	940
A	280	170	100	58	34	20.5	12.5	8.5	6.5
B	0.49	0.5	0.51	0.52	0.52	0.53	0.54	0.55	0.55
BAKGRS	-	-	0.1	0.4	0.9	2.2	4.5	9	16

This table shows values for the constants A, B and BAKGRS for various photomultiplier power supplies (E.H.T. levels) for the sulphur channel.

TABLE 3.5 PHOSPHORUS

E.H.T.		600	650	700	750	800	850	900	940
D		520	185	15	11.6	10.4	8.6	4.7	2.8
E		1.1	1.1	1.1	1	1	0.97	0.92	0.9
BAKGRP		0.1	0.5	1.3	3.2	7.3	16	32	50

This table shows values for the constants D, E and BAKGRP for various E.H.T. levels for the phosphorus channel.

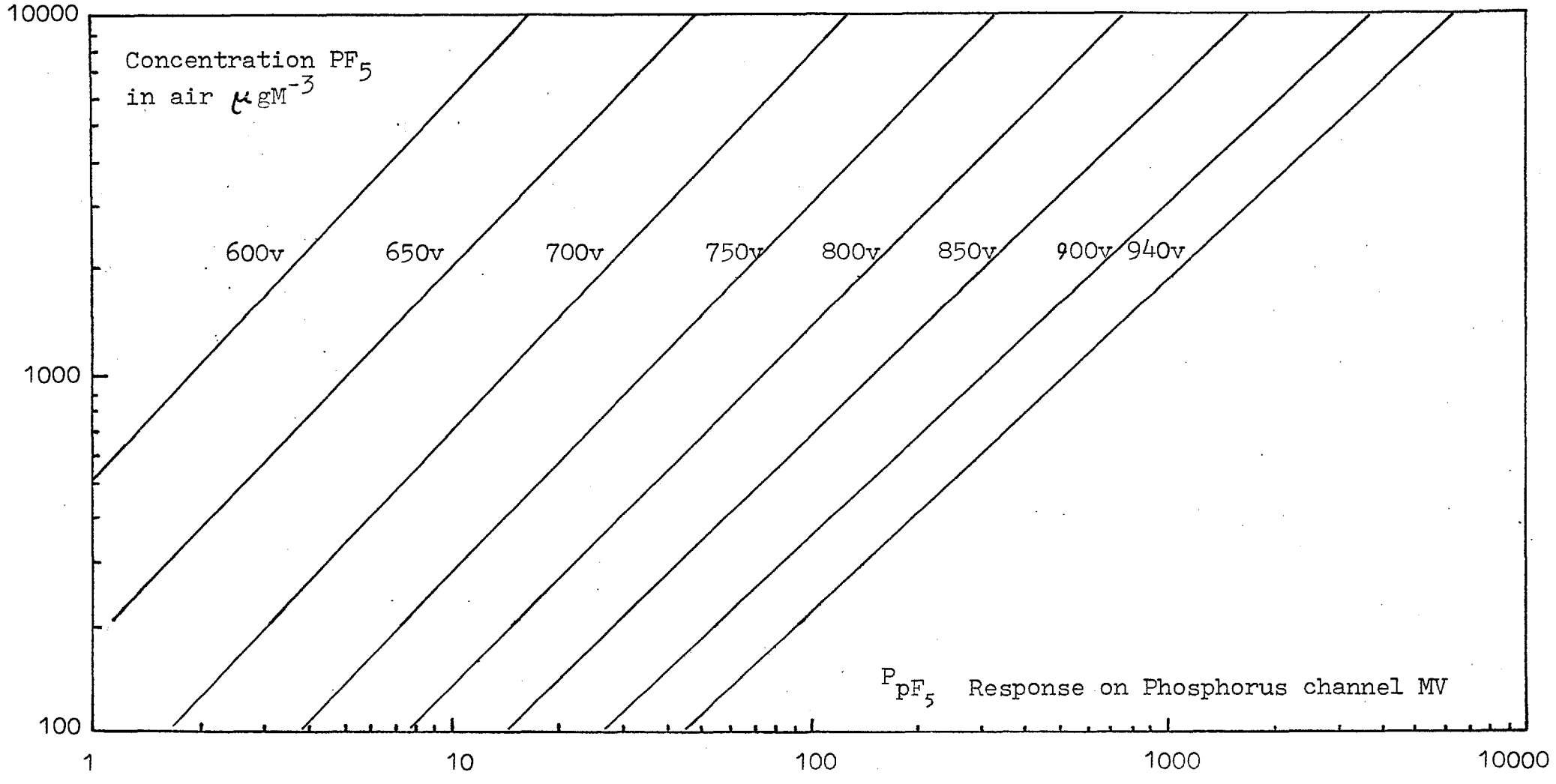

GRAPH 3.7 Detector response (P_{PF_5} millivolts) VS concentration of PF_5 in air ($\mu g\ M^{-3}$) for different E.H.T. levels (volts).

where the values for D and E are determined from the intercept and gradient respectively of graph 3.7 and BAKGRP is the photomultiplier signal output obtained by viewing the flame radiation without the prescence of phosphorus species.

The graph suggests the relationship

Emission Intensity $\propto$ Concentration

Table 3.5 lists the values of D and E and BAKGRP for different E.H.T. levels.

3.7.3 Sulphur/Phosphorus Interference

Since the spectra of sulphur and phosphorus overlap there is mutual interference between sulphur and phosphorus and this is reflected in graph 3.8 which shows the interference of phosphorus on the sulphur channel (394 nm) and graph 3.9 shows the interference of sulphur on the phosphorus channel (526 nm) for different power supply levels. Both graphs are Log-Log plots.

a. Phosphorus interference on the Sulphur Channel.

The response to phosphorus is linear with respect to concentration on the sulphur channel and can be estimated. in μgM^{-3} given photomultiplier signal output and E.H.T. level from

$$C_{PF_5}\ (394) = F \cdot (P_{PF_5\text{-}SO_2} - BAKGRS)^G\ \mu g\ M^{-3} \text{ at } 394 \text{ nm}$$

Equation 3.20

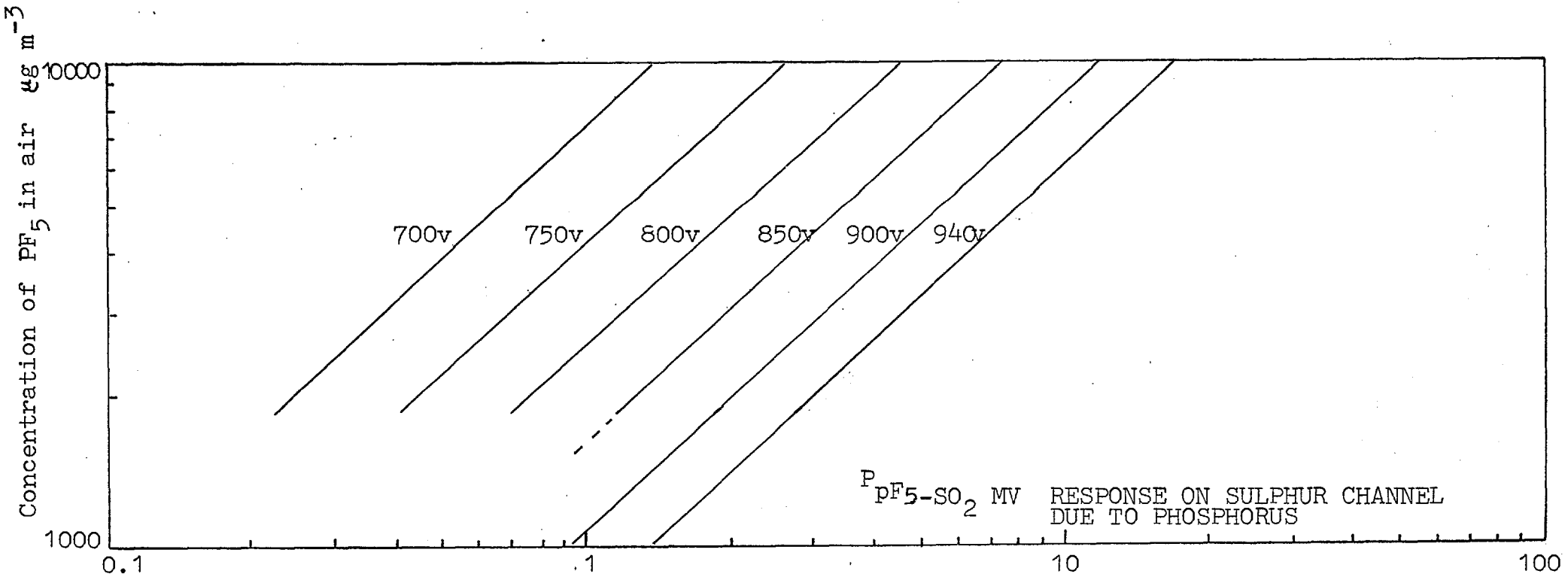

GRAPH 3.8 Detector response on the sulphur channel ($P_{PF_5-SO_2}$ MV) due to phosphorus vs concentration of PF_5 in air ($\mu g\ m^{-3}$) at different E.H.T. levels (volts).

Graph 3.8 is a Log-Log plot of the concentration of phosphorus pentafluoride (C_{PF_5} $\mu g\ M^{-3}$) against the photomultiplier signal output ($P_{PF_5\text{-}SO_2}$ MV) at different E.H.T. levels. Table 3.6 shows the values of F and G obtained from graph 3.8 and BAKGRS is the photomultiplier signal output due to radiation emitted from the sulphur/phosphorus-free flame.

b. Sulphur interference on the Phosphorus Channel.

Graph 3.9 is a Log-Log plot of the concentration of sulphur (C_{SO_2} $\mu g\ M^{-3}$) against the photomultiplier signal output ($P_{SO_2\text{-}PF_5}$ MV) at different E.H.T. levels. The response to sulphur on the phosphorus channel is exponential and can be estimated (in $\mu g\ M^{-3}$) for a given photomultiplier signal output and E.H.T. level from:

$$C_{SO_2}(526) = H \cdot (P_{SO_2\text{-}PF_5} - BAKGRP)^I \ \mu g\ M^{-3} \text{ at } 526 \text{ nm}$$

Equation 3.21

Table 3.7 lists the values of H and I obtained from graph 3.9 and BAKGRP is the photomultiplier signal output due to radiation emitted from the sulphur/phosphorus-free flame.

The total response R at 394 nm - in terms of output MV - is therefore

$$R(394) = P_{SO_2}(394) + P_{PF_5\text{-}SO_2}(394) \text{ MV}$$ Equation 3.22

and at 526 nm

$$R(526) = P_{SO_2\text{-}PF_5}(526) + P_{PF_5}(526) \text{ MV}$$ Equation 3.2

TABLE 3.6 Phosphorus Interference on the Sulphur Channel

EHT	700	750	800	850	900	940			
F	7200	4100	2700	1700	1070	700			
G	0.91	0.89	0.89	0.88	0.88	0.88			
BAKGRS	0.4	0.9	2.2	4.5	9	16			

This table shows values for the constants F, G and BAKGRS for various photomultiplier power supplies (E.H.T. levels) obtained for phosphorus interference on the sulphur channel.

TABLE 3.7 Sulphur Interference on the Phosphorus Channel

EHT	600	650	700	750	800	850	900	940	
H	330	203	140	94	64	46	36	26	
I	0.49	0.49	0.48	0.48	0.47	0.46	0.46	0.46	
BAKGRP	0.1	0.5	1.3	3.2	7.3	16	32	50	

This table shows values for the constants H, I, and BAKGRP for various E.H.T. levels for sulphur interference on the phosphorus channel.

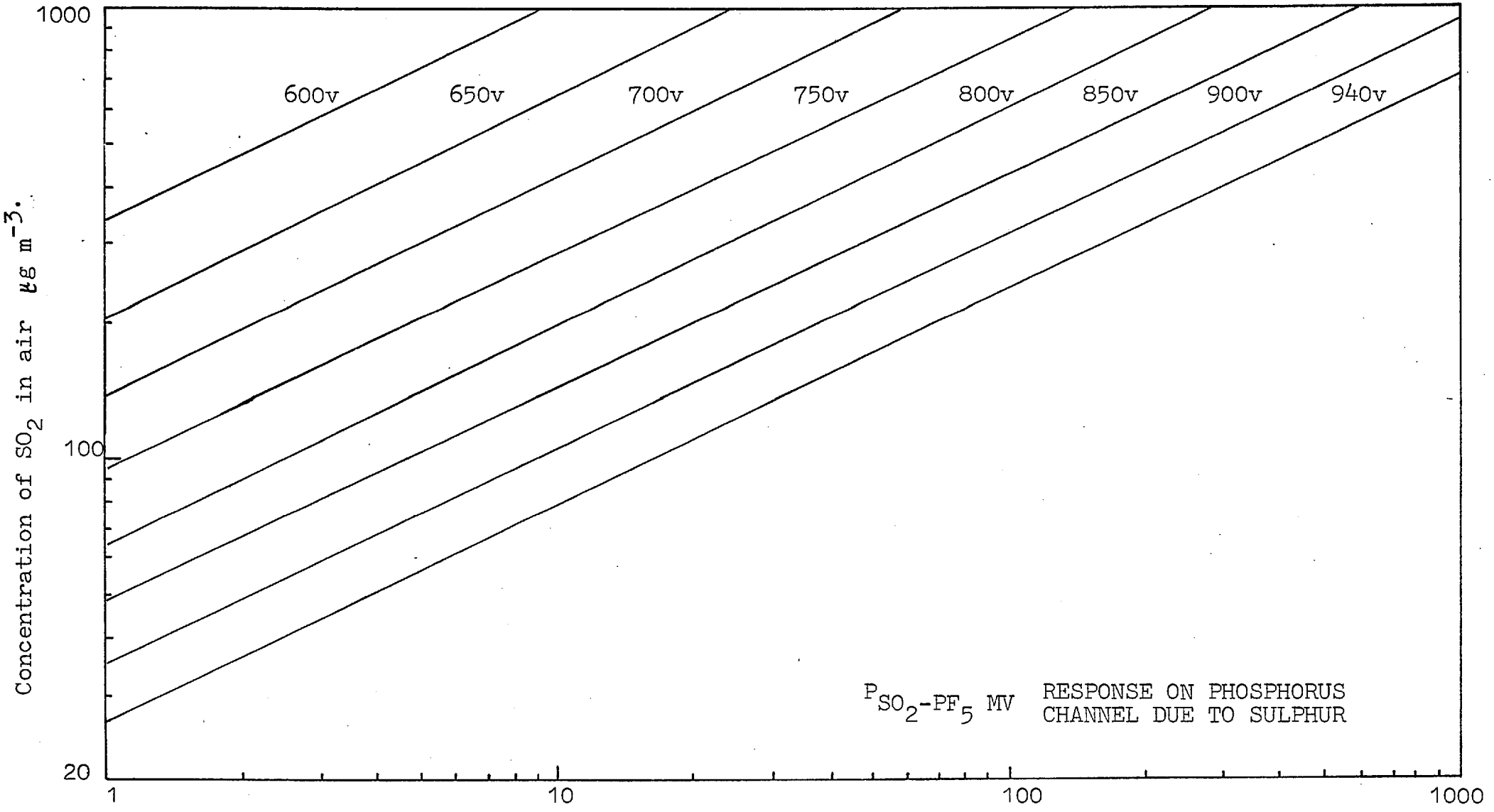

GRAPH 3.9 Detector response on the phosphorus channel ($P_{SO_2-PF_5}$ MV) due to sulphur vs concentration of SO_2 in air ($\mu g\ m^{-3}$) at different E.H.T. levels (volts).

Since both channels respond to both sulphur and phosphorus care must be exercised in interpreting detector outputs. Data interpretation is aided by substution into equations 3.22 and 3.23 for C_{SO_2} and C_{PF_5} and solving simultaneously.

Although graphs 3.6, 3.7, 3.8 and 3.9 do not reflect optimum detector performance they do illustrate two important characteristics of the detector:

i.) Since the response to phosphorus is linear and that to sulphur exponential, detector selectivity is dependent on concentration. By definition, selectivity has a value of 1.0 at those points at which the sulphur and phosphorus curves intersect. This being the case, the selectivity of the sulphur channel increases with increasing concentration whereas that of the phosphorus channel increases with decreasing concentration.

ii.) Also because the response to sulphur is exponential it has been suggested - CRIDER and SLATER (1969) - that such a flame photometric detector can operate on the most sensitive part of the calibration curve simply by adding a flow of sulphur dioxide gas to either the hydrogen or air gas flows. For the detector described here this can be achieved by inserting a permeation tube holder and a permeation tube into the hydrogen supply line, but this was not attempted in this work.

3.8 Notable Interferences

SHILLER and CAMPBELL (1971) report that hydrocarbons - in "large quantities" - elongate the hydrogen flame to the point that it may enter into the field of view of the optical system resulting in interference both on the sulphur and the phosphorus channel. CRIDER and SLATER (1969) note that chlorinated hydrocarbons chemiluminesce at 490 nm in a hydrogen-air diffusion flame after a luminescent background has been established with sulphur dioxide.

During laboratory and field trials of the fast-response detector it was noticed that particulate matter when sucked into the burner gave a characteristic emission signal varying in amplitude but always typical of the signal shown in figure 3.11. This effect was apparent in the results of BARYNIN (1970) but was, unfortunately, not reported.

3.9 Noise on the Photomultiplier Output

The a.c. fluctuations on a d.c. signal have been measured on both the sulphur and phosphorus channels by recording the maximum peak to trough deflection recorded on an oscilloscope for a sampling time of 3 minutes.

The Root Mean Square (R.M.S.) Noise is given by

$$\text{R.M.S. Noise} = \frac{\text{MAXIMUM DEFLECTION}}{2\sqrt{2}}$$

Graph 3.10 is a plot of the mean signal recorded on the sulphur channel against the R.M.S. noise for different E.H.T. levels. As can be seen the mean signal level/r.m.s. noise ratio increases as the mean signal level increases for

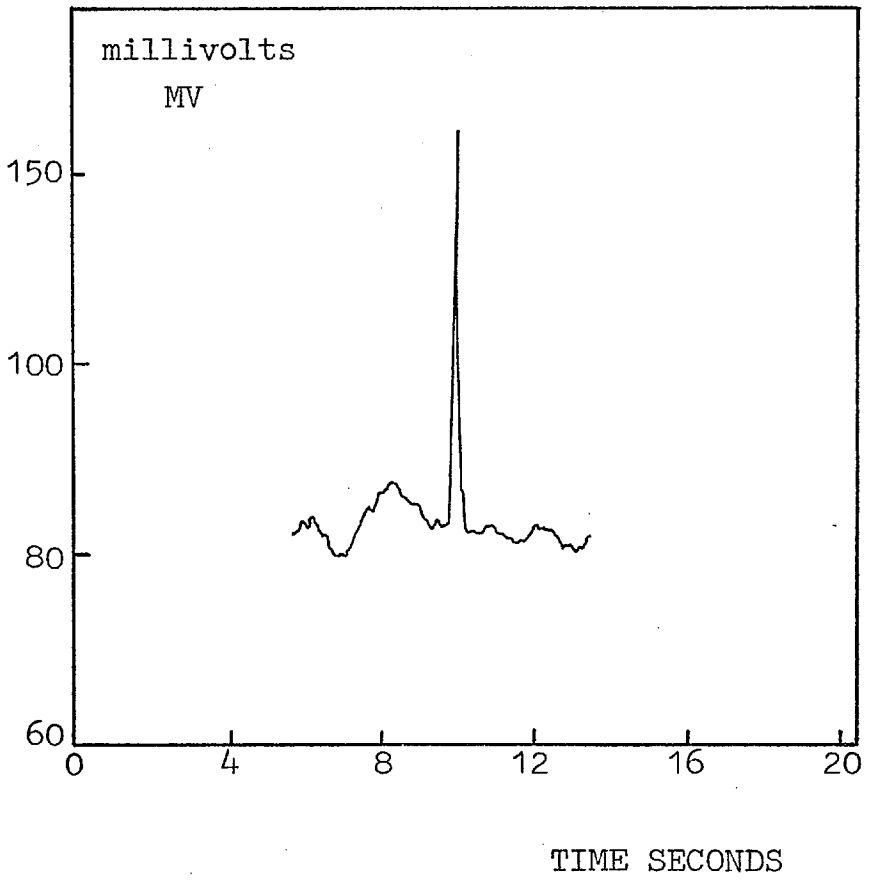

Figure 3.11

This figure shows a characteristic response on the sulphur channel from a particle entering the burner.

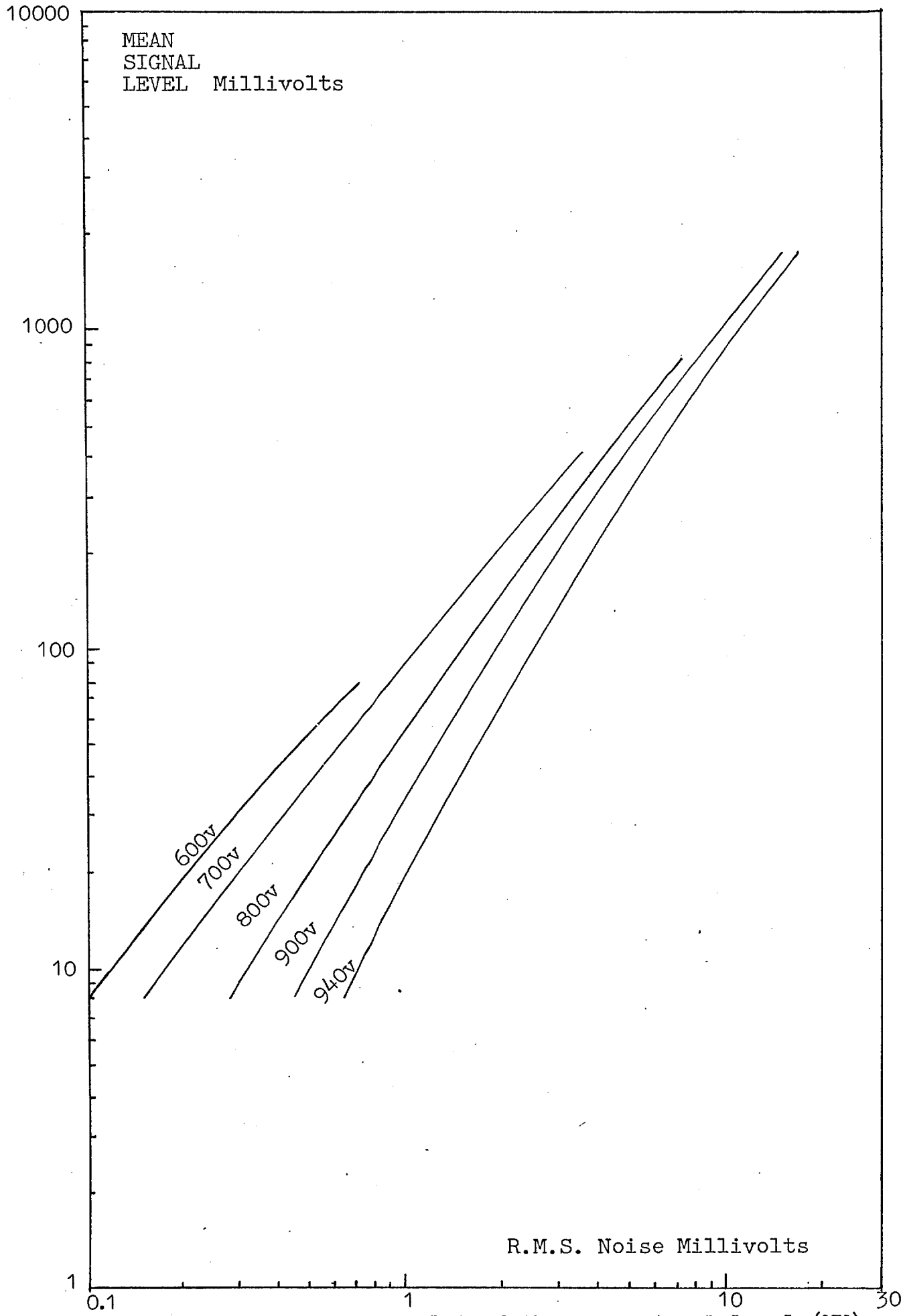

Graph 3.10 This is a plot of the mean signal level (MV) VS R.M.S. noise (MV) for various E.H.T. levels on the sulphur channel.

a given E.H.T. - the ratio increasing from about 10:1 to about 110:1. The graph suggests that it pays to operate at a lower E.H.T. because for a given mean signal level the mean signal level/r.m.s. noise ratio is greater at the lower E.H.T.

The fluctuations on a given signal have also been recorded on a cassette data logger (see Chapter 5.1) digitising at 50 readings a second and sampling for about three minutes. The resulting cumulative distribution obtained from the digitised record has been plotted on normal-probability paper and graph 3.11 shows the result. The straight line on graph 3.11 indicates that the fluctuations are normally distributed. These signal fluctuations are believed to originate from the statistical fluctuations associated with the emission process from each grid within the photomultiplier tube and not from flame noise. This has been verified with the use of a torch bulb and battery. Using the torch bulb as a source of light, the same mean signal level output from the photomultiplier for a given E.H.T. supply was obtained as when the flame was used as a source of light. In both cases, the torch bulb and flame gave the same r.m.s. noise results. The torch bulb is useful in this context because it has all optical frequencies present with approximately the same intensity and is therefore useful as a reasonably steady non-fluctuating source of light.

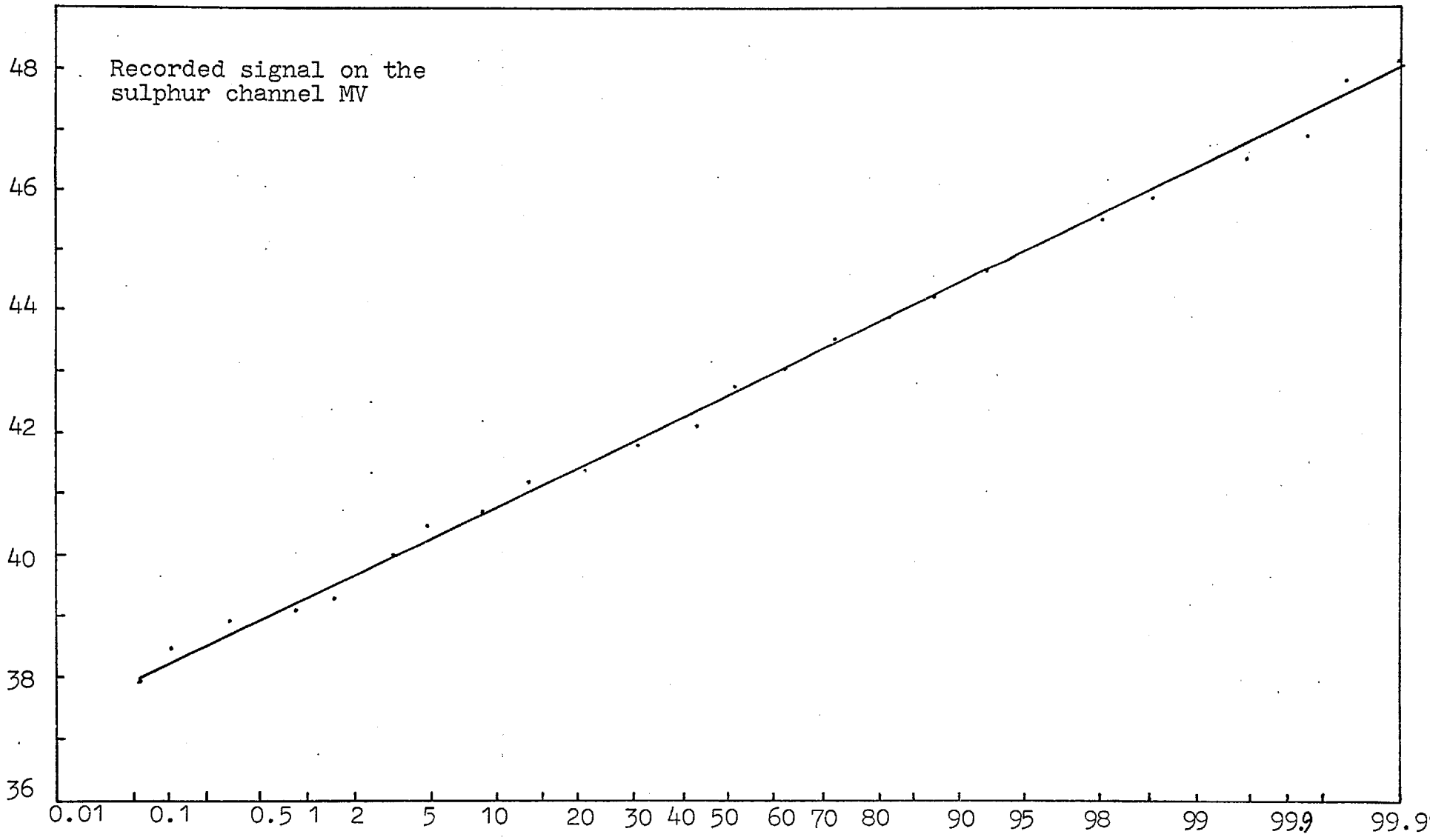

GRAPH 3.11 NORMAL PROBABILITY PLOT FOR FLUCTUATIONS ON SULPHUR CHANNEL.

Graph 3.12 is a plot of the mean signal level recorded on the phosphorus channel against the r.m.s. Noise. The mean signal level/r.m.s. noise remains constant as the mean signal level increases for any given E.H.T. level. The ratio being equal to about 22:1. Again, the fluctuations on a given signal have been recorded on a cassette data logger and the results when plotted on normal-probability paper yield graph 3.13. The fluctuations are approximately normally distributed but the torch bulb experiment reveals that the signal fluctuations from the flame are greater than those obtained when the torch bulb is used as a source of light thus indicating that the fluctuations originate from a source other than from photo-multiplier noise. The fluctuations on the phosphorus channel could be due to flame noise.

3.10 Minimum Detection Limit

The minimum detection limit, for this work, is defined as that concentration that will produce a signal equal to twice the background root mean square noise level.

On the sulphur channel, at the most sensitive operating E.H.T. photomultiplier supply voltage - 940 V - the minimum detection limit is 10 $\mu g\ M^{-3}$ SO_2 since this situation produces a signal of 2 MV at a root mean square noise level of 0.9 MV.

On the phosphorus channel, at the same E.H.T. level, as for the sulphur channel, the minimum detection limit is 11$\mu g\ M^{-3}$ PF_5 since this concentration produces a signal of 5.1 MV at a root mean square noise level of 2.5 MV.

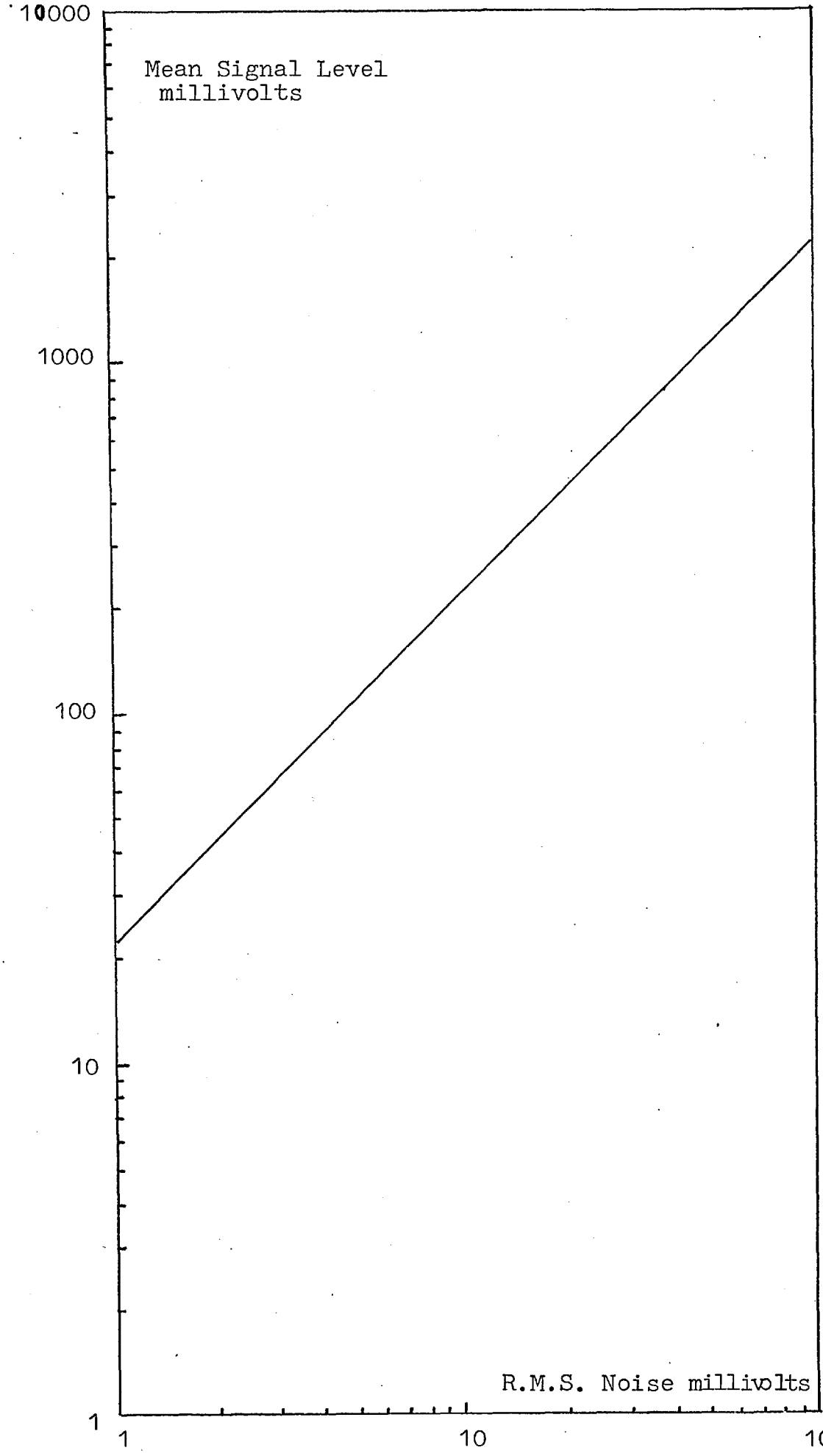

Graph 3.12 This is a plot of the mean signal level (mv) vs R.M.S. noise (MV) for the hos horus channel

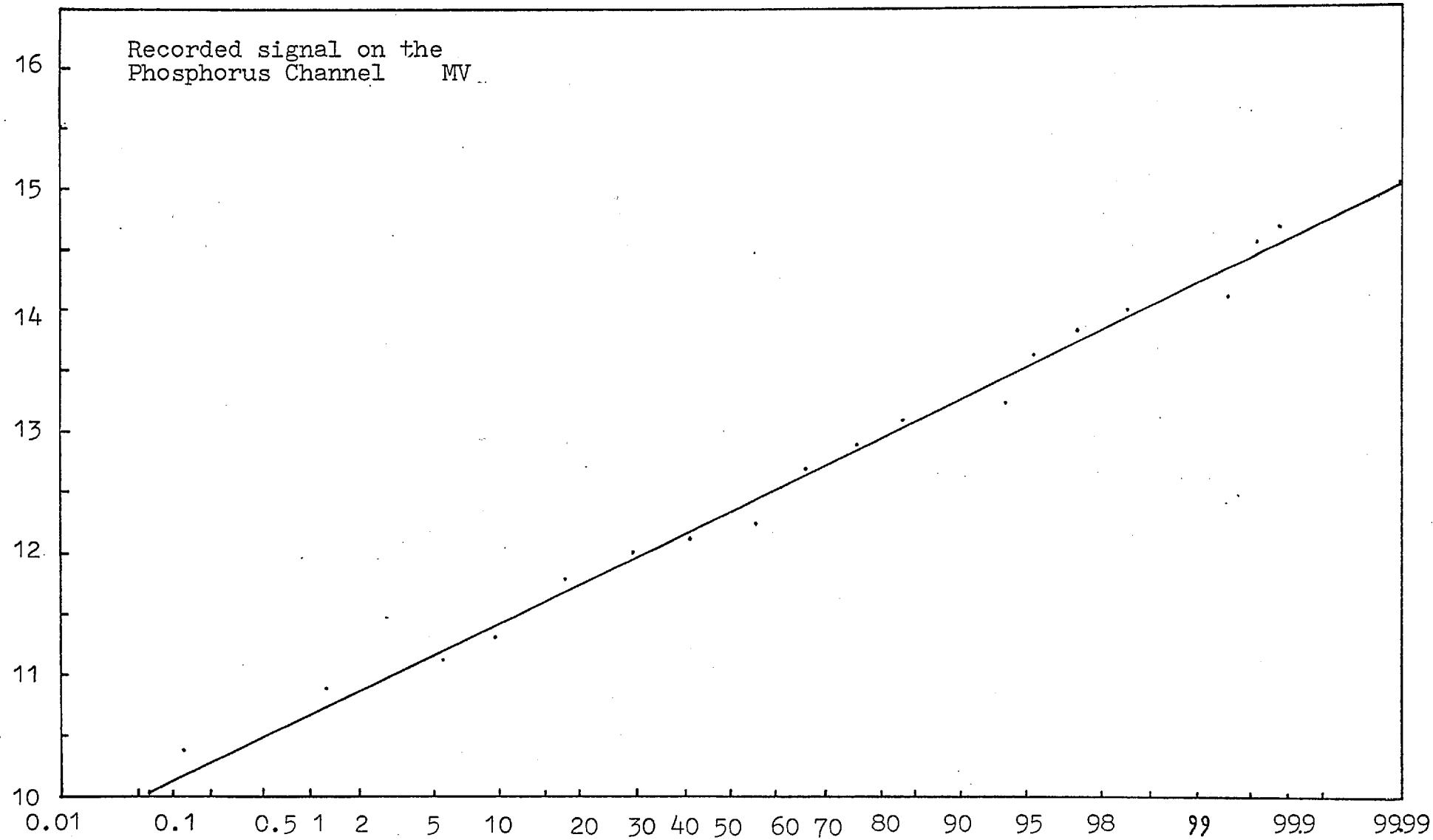

Graph 3.13 NORMAL PROBABILITY PLOT FOR FLUCTUATIONS ON PHOSPHORUS CHANNEL.

CHAPTER 4

THEORY

Introduction

The theory to be discussed provides background information concerning a variety of relevant and important aspects of diffusion in the lower layers of the atmosphere. The treatment here will be qualitative and further details can be obtained from the references given. A small section on stability of the atmosphere is also included.

Conclusions from the theory relating to this research work are given at the end of the chapter.

4.1 Stability

In its simplest terms, the stability of the atmosphere is its tendency to resist or enhance vertical motion, or alternatively to suppress or augment existing turbulence. Stability is related both to wind shear and temperature structure in the vertical, but it is generally the latter which is used as an indicator of the conditions.

4.1.1 Dry Adiab atic Lapse Rate

When a small volume of air is forced upward in the atmosphere it will encounter lower pressure, expand and cool. If it is assumed that there is no exchange of heat between the environment and the small volume, a rate at which cooling occurs during the ascent can be defined as the dry adiabatic lapse rate ($-1^{\circ}C/100$ metres). Such a process never actually occurs in the atmosphere, since turbulence tends to destroy the theoretically isolated volume, and exchange of heat does occur, but the concept has value as a yardstick to assess the turbulent characteristics of the atmosphere.

4.1.2. Potential Temperature

If a parcel of dry air were brought adiabatically from its initial state to the arbitrarily selected standard pressure of 1000 mb, it would assume a new temperature, θ known as the "potential temperature." The quantity is

closely related to the dry adiabatic lapse rate, since an atmosphere having a decrease in ambient temperature with height of $-1^{o}C/100$ metres has a potential temperature that is constant with height. An increase of potential temperature with height implies stability and a decrease, instability, as explained in the following sections.

4.1.3 Environmental Lapse Rate

The actual distribution of temperature in the vertical is known as the "environmental lapse rate" and it seldom approximates the adiabatic lapse rate in the lowest 100 metres over any extended period.

4.1.4 Superadiabatic

On days when strong solar heating is occurring or when cold air is being transported over a much warmer surface, the rate of decrease of temperature with height usually exceeds $-1^{o}C/100$ metres, implying that any small volume displaced upward would become less dense than its surroundings and tend to continue its upward motion. A super adiabatic condition favours strong convection, instability, and turbulence. Superadiabatic conditions are usually confined to the lowest 200 metres of the atmosphere.

4.1.5 Neutral

A neutral condition, in which the lapse rate in the atmosphere is nearly identical to the dry adiabatic lapse rate, implies no tendency for a displaced parcel to

gain or lose buoyancy. A neutral condition is usually associated with overcast skies and moderate to strong wind speeds.

4.1.6 Subadiabatic

An atmosphere in which the temperature decreases more gradually than $-1^{\circ}C/100$ metres is actually slightly stable, since a small parcel displaced upward will become more dense than its surroundings and tend to descend to its original position, whereas a small parcel displaced downward will become warmer and rise to its original level.

4.1.7 Isothermal

When the ambient temperature is constant with height, the layer is termed isothermal, and as in the subadiabatic case there is a slight tendency for a parcel to resist vertical motion.

4.1.8 Inversion

A stable atmospheric layer in which the temperature increases with height strongly resists vertical motion and tends to suppress turbulence. It is therefore of particular interest in air pollution, since it allows very limited dispersion.

4.2 Atmospheric Turbulence

Turbulence is an irregular, random motion which in general makes its appearance in fluids, gaseous or liquid, when they flow past solid surfaces or even when neighbouring streams of the same fluid flows past or over one another. In the atmosphere, the interaction of all weather systems on all scales results, at a given point of observation, in a three-dimensional wind direction and speed that vary continuously with time. This continuous fluctuation, or turbulence, is the characteristic of the atmosphere that causes the diffusion of pollutants introduced into it and in general results in rates of momentum, heat and mass transfer that are many orders of magnitude greater than the corresponding rates due to pure molecular transport. These fluid properties can be thought of as being transported across the flow by irregular but somehow identifiable material wind structures called eddies.

A detailed discussion of turbulent flow is not attempted here and for a more detailed introduction to the subject the following references are useful; BATCHELOR (1953), TOWNSEND (1956), LUMLEY and PANOFSKY (1964) and PLATE (1971).

The fluctuating wind, observed at a point, can usually be divided into a mean motion and superimposed fluctuating motions with components along the direction of the mean wind and in the vertical and lateral perpendicular

directions. The distinction between the mean and turbulent motion may be determined on the basis of the dimensions of the diffusing system, e.g., a puff of smoke. Wind fluctuations larger than the puff tend to move it in its entirety and thus contribute to the mean motion. Fluctuations considerably smaller than the dimensions of the puff tear it apart and can thus be regarded as turbulent. The definitions of mean and turbulent quantities are somewhat arbitrary since they depend on the overall time and space scales of the specific problem.

Turbulence is dependent upon three factors; the mechanical effects of objects protruding into the air stream, such as the roughness of the earth's surface, the vertical rate of increase of wind speed, and the vertical temperature structure of the atmosphere. Generally, an increase in the gradient wind flow or an increase in the air temperature close to the earth's surface compared to that aloft creates a corresponding increase in turbulence.

The study of turbulent variations has usually proceeded via the application of statistical techniques rather than dynamical methods and frequently requires data that are in the form of a digital or analog time series especially for those techniques that relate diffusion to wind fluctuations. Section 4.3 presents definitions of some terms used in the discussion of time series and space series.

4.3 The Random process

The concept of a random process has been applied with considerable success to the problems in turbulence and diffusion in spite of the fact that meteorological occurrences are not strictly random (the wind speed at a given instant is correlated with the speed at the previous instant). The ensemble statistics resulting from numerous repetitions of an experiment carried out under the same conditions may be useful as a physical representation of the process being studied. Since the statistical characteristics derived from any one experiment would bear a distinct resemblance to the ensemble statistics, it is frequently only necessary to study one or a few of the experiments to derive some characteristics of the entire ensemble.

A type of random process that has found frequent application in turbulence and diffusion studies can be described as being stationary, homogeneous, isotropic and Gaussian. The property of stationarity implies that the statistical properties derived for a time series do not vary with time. Thus a variance computed from one hour of data would be similar to that computed from the next hour of the data if the turbulence were stationary.

If the random process is homogeneous, its statistical properties will not vary in space; that is, a measurement taken at a particular point will display

statistical characteristics identical to those taken at some neighbouring point in space.

Isotropy can be defined by the condition that the statistical properties of the field being studied are independent of the rotation of the co-ordinate axes. Although this condition may be met in a limited way in the atmosphere, such is generally not the case.

A Gaussian random process is one in which the frequency distribution of values of the variable of interest follows the Gaussian, or normal, curve. The distribution is completely specified by the mean and standard deviation.

4.4 Measurement of Wind Fluctuation

Atmospheric turbulence in the context usually encountered in diffusion literature consists of seemingly random fluctuations of the three dimensional wind vector which act in a highly organised manner to dilute an effluent or tracer injected into the atmosphere.

If, in an orthogonal co-ordinate system, u is the velocity component of the wind along the x-axis (usually assumed to coincide with the mean vector wind direction), v is the velocity component in the y direction, and w is the velocity component along the z-axis (assumed to be vertical), then the actual wind velocity components at any instant can be thought of as being composed of mean

values and deviations from the mean:

$$U = \bar{U} + U'$$
$$V = \bar{V} + V'$$
$$W = \bar{W} + W'$$

Here $\bar{u}$, $\bar{v}$ and $\bar{w}$ are mean velocities usually defined as a time-averaged value of the particular component and u', v' and w' are the fluctuations from the mean values and can be represented as time series' that pass through positive and negative values. These series' can be subjected to variance, spectral and autocorrelation analyses.

To aid discussion of the measurement and calculation of the variance, or standard deviation, of the wind fluctuations, the following concept is introduced: the intensity of turbulence.

The intensity of turbulence along each axis is defined by

$$i_x = \left[\frac{\overline{U'^2}}{\bar{U}^2}\right]^{\frac{1}{2}} = \frac{\sigma_u}{\bar{U}}$$

$$i_y = \left[\frac{\overline{V'^2}}{\bar{V}^2}\right]^{\frac{1}{2}} = \frac{\sigma_v}{\bar{U}}$$

$$i_z = \left[\frac{\overline{W'^2}}{\bar{V}^2}\right]^{\frac{1}{2}} = \frac{\sigma_w}{\bar{U}}$$

Where σ is the standard deviation of the velocity distribution. These statistics of turbulence bear a direct relation to the diffusing power of the atmosphere. The values of i_x, i_y and i_z are not constants for a particular set of meteorological conditions. Their values depend on sampling and averaging times that are inherent characteristics of a sample of data. In an Eulerian time series in which the properties of the fluid motion are measured at a particular point, the sampling and averaging times can be defined as follows:- the sampling time is that time during which the data are measured and is represented as the total period of the record; the averaging time is some time interval over which the fluctuation is represented by a constant (average) value. The standard deviation of the velocity distribution, whether of the u, v or w components, normally increases with increasing sampling time up to some point. Further, the standard deviation decreases with increasing averaging time. PASQUILL (1962) discusses the statistical effects of finite sampling and averaging in more detail.

4.5 Fluctuations of the Wind

Turbulence and diffusion studies frequently require a knowledge of the standard deviation of the U, V and W velocity component distributions. The following are general statements concerning the variation of σ_u, σ_v and σ_w with wind speed, stability and height (SLADE, 1968):

A. Standard deviation of the along wind component distribution σ_u.

1. At a fixed height σ_u is proportional to wind speed.

2. At a fixed height σ_u increases with increasing stability.

3. The value of σ_u is generally independent of height levels in the lower levels of the atmosphere during neutral and unstable conditions, but it decreases with height during stable conditions. Thus $\sigma_u/\bar{U}$ may be expected to decrease with height at all times.

B. Standard deviation of the crosswind component distribution σ_v.

1. At a given height during neutral conditions, σ_v is proportional to wind speed.

2. For a given wind speed and height, σ_v is greater during unstable than during stable conditions.

3. For a given stability condition and at a given height, σ_v increases with wind speed and surface roughness, most markedly during stable conditions.

4. The value of σ_v changes very little with height during any stability condition.

C. Standard deviation of the vertical component distribution σ_w.

1. Under neutral conditions σ_w is proportional to wind speed and displays little variation with height.

2. In a stable atmosphere σ_w generally decreases with height.

3. During unstable conditions σ_w increases markedly with height.

The capacity of the atmosphere for diffusing heat and matter is related not only to the value of the standard deviation, or variance, of wind fluctuations but also to the frequency or range of frequencies in the spectrum that makes the greatest contribution to the total standard deviation. Although two records of the fluctuation of a wind may have the same standard deviation, this would be caused either by a few fluctuations of long periods or by more numerous fluctuations of shorter period. Since long-period fluctuations tend to transport a small volume element of atmospheric pollutant in its entirety, whereas short-period fluctuations tend to tear it apart, the distribution of the energy within the different fluctuations periods is of great interest. This distribution has been studied by spectral analysis methods; the variance of a stochastic process is decomposed into contributions at a continuous range of frequencies. Prior to discussing meteorological spectra the following points are noted:

i. The atmospheric spectrum extends up to the large scales involved in the general circulation therefore the corresponding statistical properties depend considerably on the sampling duration, and in many practical situations the variance and autocorrelation do not reach their respective constant or zero limiting values.

ii. Because of the effects of variable terrain, diurnal heating or nocturnal cooling of the ground and of the continually changing large-scale pattern of air flow, turbulence in the atmosphere is neither stationary nor homogeneous i.e. the statistical properties depend on the particular time and place at which the observations are made. This feature is troublesome not only in the sense that extensive observations are required before any representative description can be assembled, but also because the most important assumption made about a time series is that the corresponding stochastic process is stationary.

Meteorological spectra are usually computed from time - rather than space - series data. The spectra now discussed relate to estimates of spectra at a point, as functions of frequency. These local spectra can be converted into spectra as functions of wave-number using the assumption of TAYLOR (1938) that the turbulence velocities are small compared to the mean wind.

Figures 4.1 and 4.2 present typical spectra of the vertical (w) and horizontal (u) velocity components respectively at a height of 91 metres in which the individual spectra for a series of experiments have been grouped by categories of thermal stability (PANOFSKY and McCORMICK, 1954). In both figures the logarithmic spectral density divided by the square of the mean wind speed for a particular stability category (ordinate) is plotted against a reduced frequency (abscissa) f ie

$$f = \frac{nZ}{\overline{U}}$$

the height Z being inserted to make the quantity non-dimensional.

The work by Panofsky and his coworkers using observations made at the Brookhaven National Laboratory since 1951 is very well documented especially in PASQUILL (1962), and the related papers PANOFSKY and McCORMICK (1952), PANOFSKY (1953), McCORMICK (1954), PANOFSKY and VAN DER HOVEN (1955) details all of the procedures and analysis carried out. A complete review of the work, including a reference to the spectrum of the lateral (V) component, has been given by PANOFSKY and DELAND (1959).

The general features notable in figures 4.1 and 4.2 are as follows:

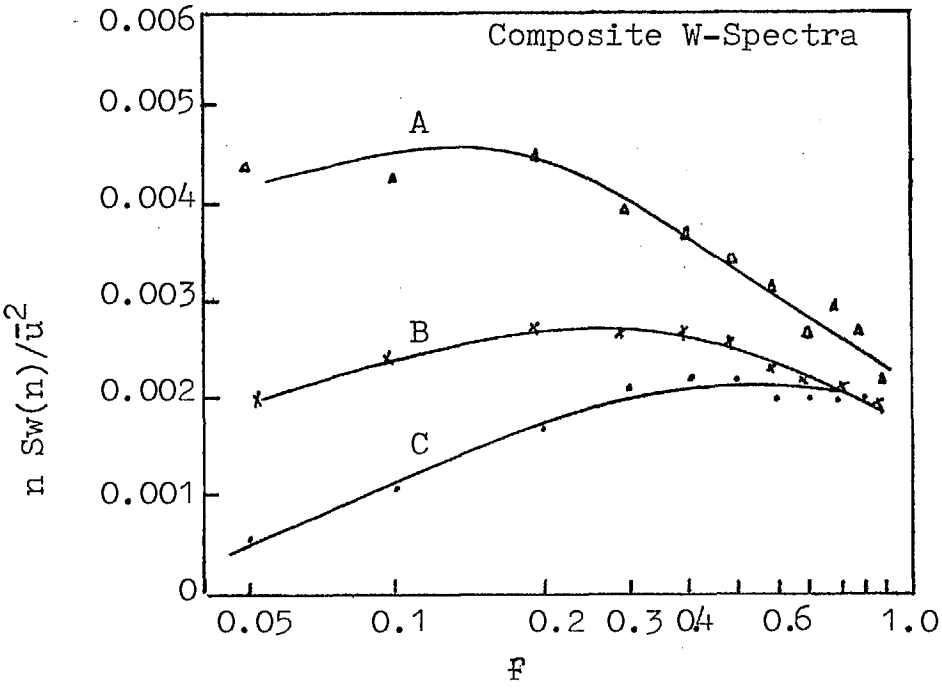

Figure 4.1 Composite logarithmic spectra of the vertical velocity at a height of 91m. Data groups correspond the incoming radiation: (A) $\geq_1$ 1.0; (B) $_2$ 0.3-0.9; (C) 0.2 cal cm^{-2} min^{-1} (PANOFSKY AND McCORMICK 1954).

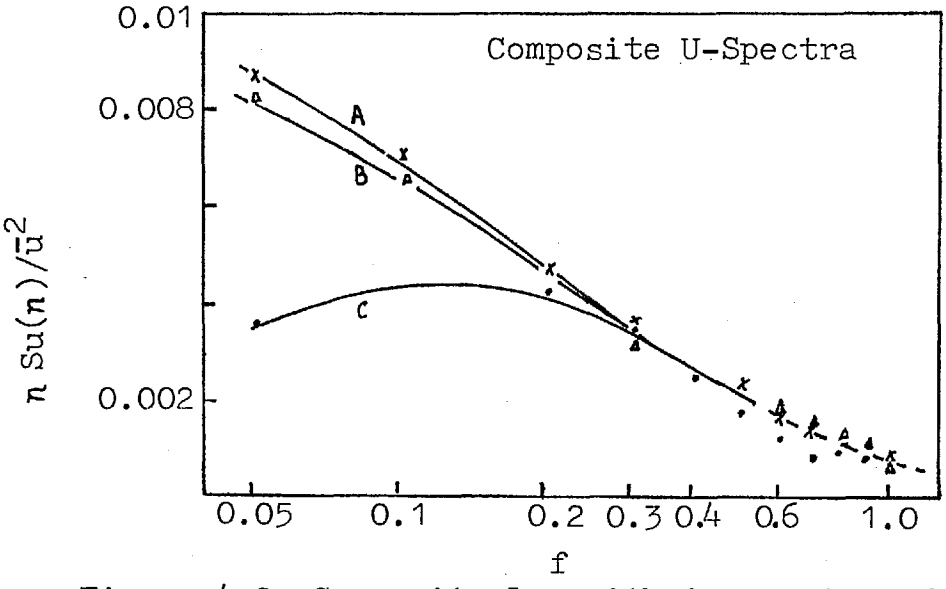

Figure 4.2 Composite logarithmic spectra of the horizontal velocity along the mean wind direction. Data groups as in figure 4.1 (PANOFSKY AND McCORMICK 1954).

a. At high frequencies the spectra are approximately independent of radiation implying that the turbulence here is of the mechanically-induced type.

b. At low frequencies the spectral density increases with increasing radiation implying that thermally-induced modifications of the turbulence appear only at a relatively large scale. Also the ratio of vertical to horizontal spectral density increases with increasing radiation and the spectral density of the horizontal velocity components is generally much larger than that of the vertical velocity.

c. With increasing radiation the maximum of the logarithmic spectral density occurs at a decreasing reduced frequency.

The preceeding work has been concerned with an "Eulerian" description of fluid motion in terms of the velocities or displacements of volume elements fixed in space - as measured by an instrument which is usually fixed. Such fixed point velocities are a result of many eddies randomly moving in a given volume element fixed in space. However, attention is often focussed on the velocity variations of individual tagged elements as measured by an instrument which is carried on a moving platform and this is known as a "Lagrangian" description. In the Lagrangian description, velocities of fluid elements

are determined by random eddies as in the Eulerian description, but in a somewhat different way because the element "travels with" the eddies. For both cases the measurements refer to a continually changing sample of air and the main difference between the Eulerian and Lagrangian velocity history is that at a fixed point the fluctuations appear rather more quickly as eddies are convected past the measuring instrument.

The Lagrangian properties of turbulence are less well known than the Eulerian ones. PASQUILL (1962) gives a good account of the Lagrangian properties of turbulence and their use in developing formal expressions of diffusion.

4.6 Atmospheric Diffusion

Knowledge of the configuration of the source of an effluent is a necessary starting point for describing atmospheric diffusion. For purposes of description it is assumed in the following discussion that the effluent is composed of a gas or of particles that faithfully follow the motions of the atmosphere. This implies that the effluent is neither negatively nor positively buoyant if it is a gas and that it has negligible settling velocity if it is composed of discrete particles.

The two idealised source types commonly used in atmospheric diffusions are the instantaneous point source and the continuous point source. An instantaneous point source

is the conventional idealisation of a rapid release of a quantity of material. Obviously, an "instantaneous point" is a mathematical idealisation since any rapid release has finite spatial dimensions. As the puff is carried away from its source by the wind, it will disperse under the action of turbulent velocity fluctuations. Figure 4.3 shows the dispersion of a puff under three different turbulence conditions, Figure 4.3a shows a puff embedded in a turbulent field in which all the turbulent eddies are smaller than the puff. The puff will disperse uniformly as the turbulent eddies at its boundary entrain fresh air. In figure 4.3b a puff is embedded in a turbulent field all of whose eddies are considerably larger than the puff. In this case the puff will appear to the turbulent field as a small patch of fluid which will be transported through the field with little dilution. Ultimately, molecular diffusion will dissipate the puff. Figure 4.3c shows a puff in a turbulent field of eddies of size comparable to the puff. In this case the puff will be both dispersed and distorted. In the atmosphere, a cloud of material is always dispersed since there are almost always eddies of size smaller than the cloud. From figure 4.3 it can be seen that dispersion of a puff relative to its centre of mass depends on the initial size of the puff relative to the length scales of the turbulence. Quantitatively, this relative diffusion should depend on the action of eddies approximately as large as a puff - or as large as the instantaneous width of the plume.

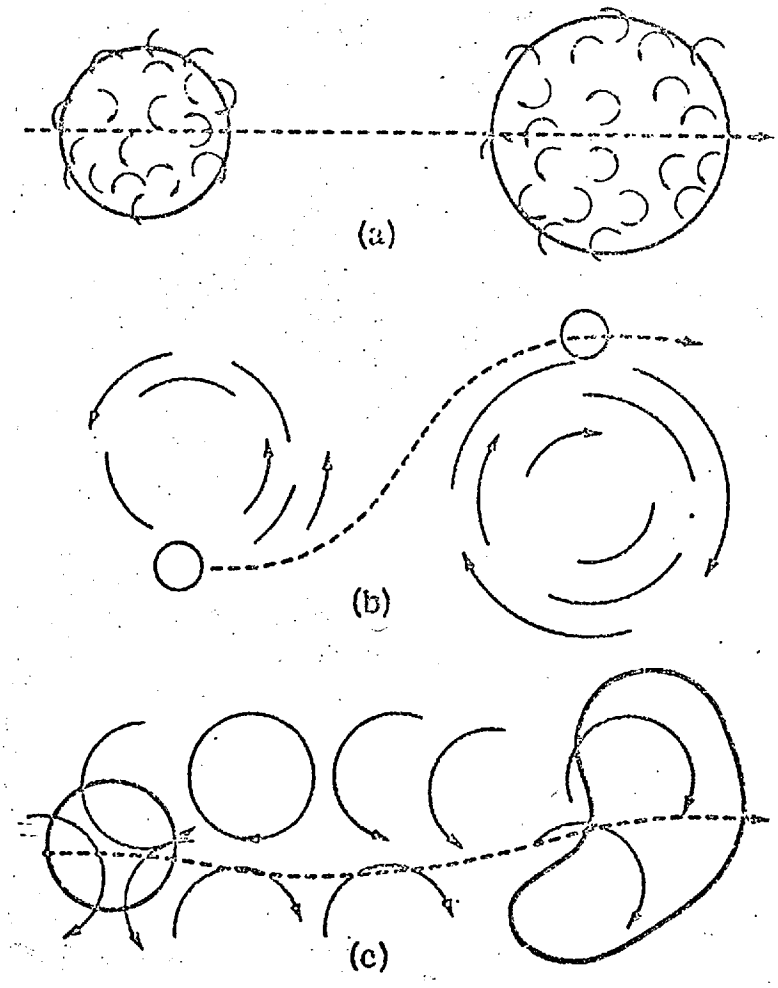

Figure 4.3 Idealised dispersion patterns. (a) A large cloud in a uniform field of small eddies. (b) A small cloud in a uniform field of large eddies. (c) A cloud in a field of eddies of the same size as the cloud.

A continuous source emits a plume which might be envisioned as an infinite number of puffs released sequentially with an infinitessimal time interval between puffs. Figure 4.4 shows the plume "boundaries" and concentration distributions as might be seen in an instantaneous snapshot and exposures of a few minutes and several hours. An instantaneous picture of a plume reveals a meandering behaviour with the width of the plume gradually growing downwind of the source. Longer-time averages give a more regular appearance to the plume and a smaller concentration distribution.

If a time exposure, say one hour or more, were taken of the plume at large distances from the source, the boundaries of the time-averaged plume relative to a final axis would begin to meander because the plume would come under the influence of larger and larger eddies, and the averaging time, say several hours, may still be too brief to time-average adequately the effect of these larger eddies. As already mentioned, eddies larger in size than the plume dimension tend to transport the plume intact whereas those that are smaller than the plume tend to disperse it. As the plume becomes wider, larger and larger eddies become effective in dispersing the plume and the smaller ones become increasingly ineffective.

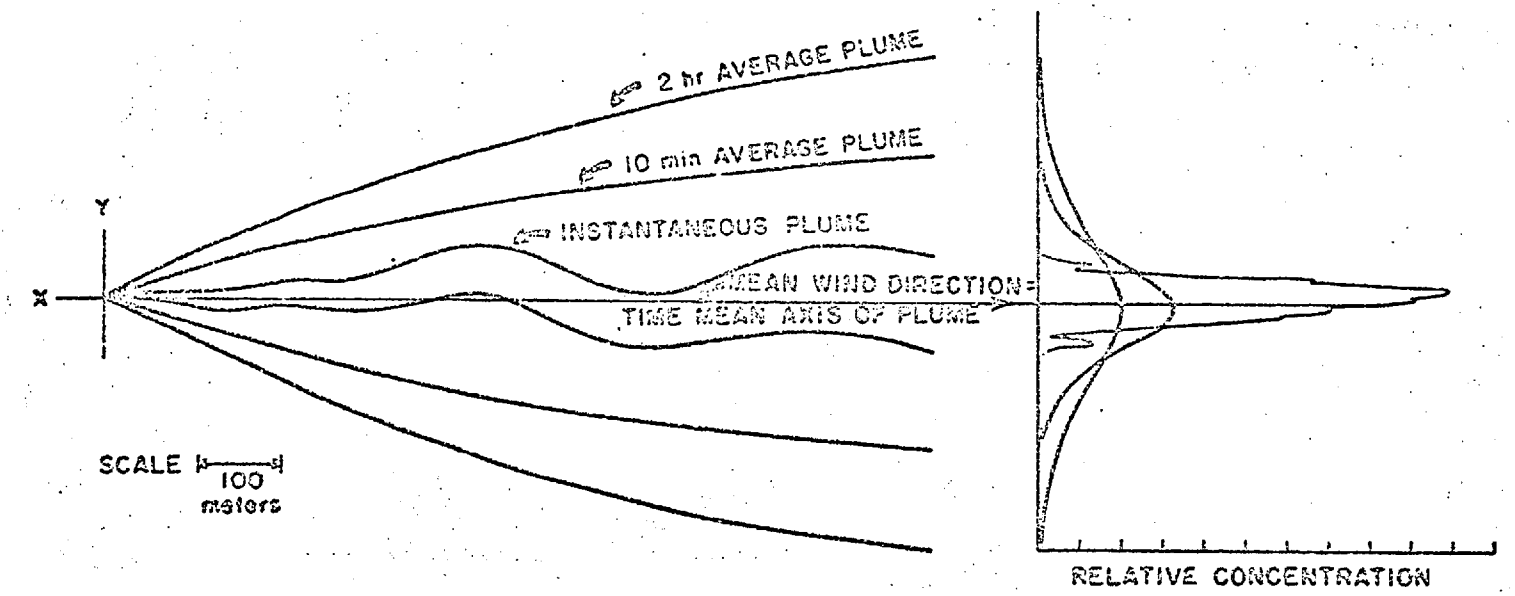

Figure 4.4 The diagram on the left represents the approximate outlines of a smoke plume observed instantaneously and of plumes averaged over ten minutes and two hours. The diagram on the right shows the corresponding cross plume distribution patterns.

Various types of smoke plume observed in the atmosphere are summarised in Figure 4.5 together with temperature profiles and the vertical (σ_ψ) and horizontal (σ_θ) wind-direction standard deviations (SLADE, 1968).

Several features of real atmospheric diffusion have been disregarded in the previous discussion. For example, effluents are often emitted with appreciable exit velocities and at temperatures considerably above ambient to ensure that the plume will travel upward to a certain height before it is carried downward and dispersed. It has also been assumed that the plume particles are of the same density as the air. In practice, the particles may be more dense, and thus the plume would have some constant downward motion superimposed on the turbulent mixing. The assumptions also apply to the following section on Atmospheric Diffusion Theories.

4.7 Atmospheric Diffusion Theories

4.7.1 Mean Field Theory

The problem of turbulent diffusion in the atmosphere has not yet been uniquely formulated in the sense that a single basic physical model capable of explaining all the significant aspects of the problem has not yet been proposed. Instead, there are available three approaches that have been used for calculating mean concentration of species in turbulence. The three approaches are the gradient transport theory, the statistical theory and the similarity

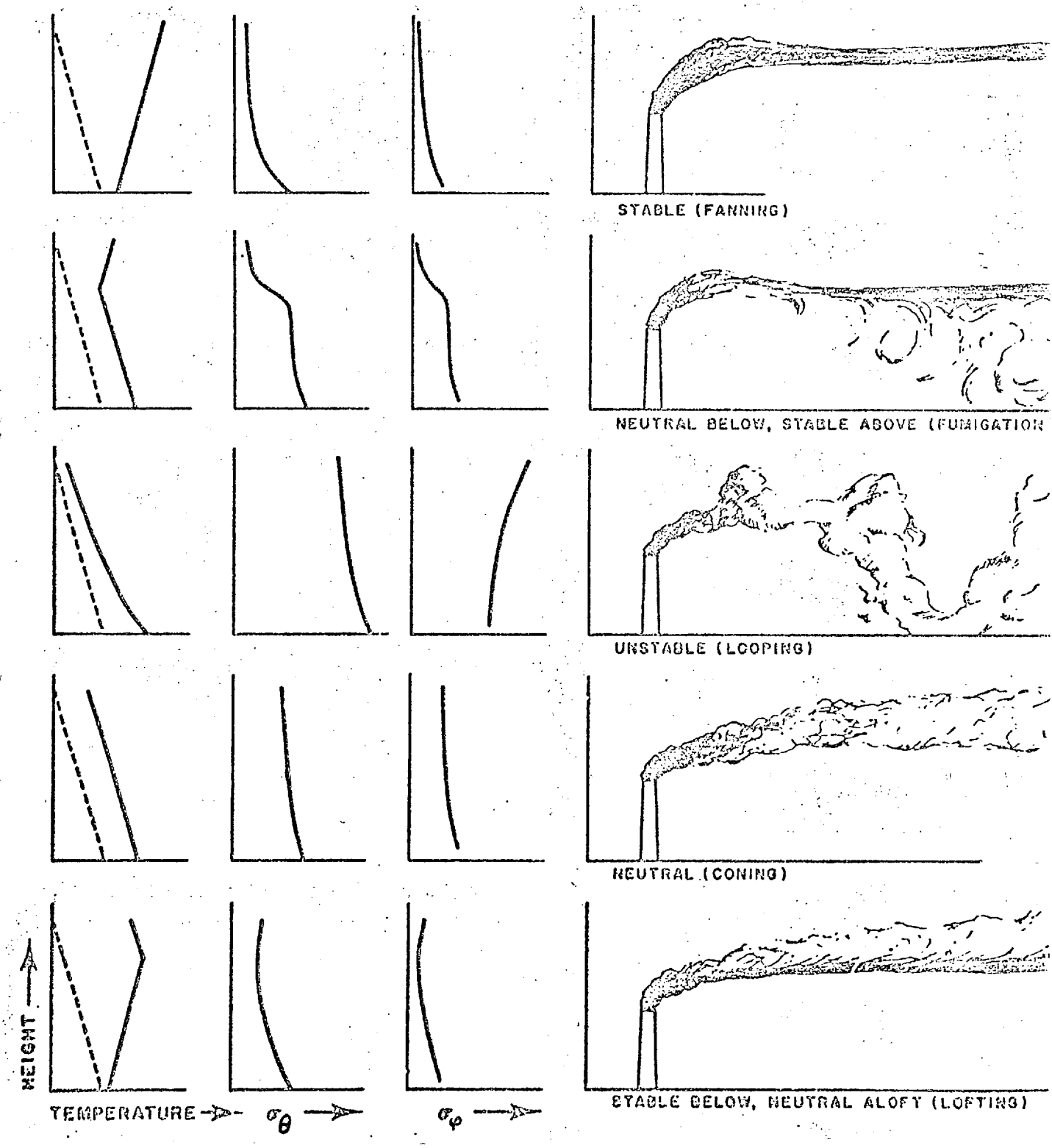

FIGURE 4.5 Various types of smoke plume patterns observed in the atmosphere. The dashed curves in the left hand columns of the diagrams show the adiabatic lapse rate and the solid lines are the observed profiles. The abscissas for the horizontal and vertical wind direction standard deviations (σ_θ and σ_φ) represent a range of 0° to 25°.

theory. Diffusion at a fixed point in the atmosphere, according to the gradient transport theory, is proportional to the local concentration gradient. Consequently it can be said that this theory is Eulerian in nature in that it considers properties of fluid motion relative to a spatially fixed coordinate system. On the other hand, statistical diffusion theories consider motion following fluid particles and thus can be described as Lagrangian.

ROBERTS (1923), RICHARDSON (1926) and CALDER (1949, 1965) are a few of the more basic references noted for their contribution to the development of gradient transport theory.

The study of the statistical theories of turbulent diffusion began with the investigation by TAYLOR (1921) and an extension of Taylor's model to represent average plume diffusion was proposed by SUTTON (1953).

The similarity theory originally developed by MONIN (1959) and BATCHELOR (1964) predicts the dependence of the mean downwind and vertical position of a particle released in the atmospheric surface layer. In this theory Lagrangian particle statistics depend on the same variables as the Eulerian velocity statistics.

The appearance of real plumes is quite different from that predicted by the application of the Gaussian diffusion model to average plume diffusion, especially during unstable conditions when the entire plume fluctuates about some mean positions - plume meander. The theoretical basis of fluctuating predictions is so far very incomplete. The first important contribution to the problem seems to have been a paper of GIFFORD (1959) in which a theory was developed that can be regarded as predicting the fluctuations due to plume meander. As yet, there seems to be no theoretical treatment available in the literature that discusses the effects of relative diffusion plus meandering. The following discussion pays attention to some of the important aspects of the fluctuating problem.

4.7.2 Probability Distribution of Concentration

If marked fluid is instantaneously released into some prescribed region of a turbulent field and the experiment repeated under identical environmental conditions and identical conditions of release, it is found that the measured concentration at a fixed position and after a fixed time after release is a random variable. The results of a large number of trials may be conveniently summarised in a probability distribution which specifies the probability that the observed concentration in a given trial at a fixed position and a fixed time after release is less than a certain value.

Often, models derived from both the gradient transport theory and the statistical theory lead to a Gaussian (normal) probability distribution of concentration. SLADE (1968) discusses the Gaussian diffusion model and its application in describing diffusion averaged over some period of time - usually at least several minutes. It is recognised by most workers that practically observable concentrations of a pollutant at some location in the environment are the general random variables about which it is only possible to be able to make probabilistic predictions. Fully satisfactory predictions of this sort would specify with what frequency given concentrations are exceeded for more than 1 second, 10 seconds, 1 minute and so on. Such information could be given in the form of suitable probability distributions.

Experimentally, the relevant information would have to be collected by carrying out large numbers of identical trials, a practically very difficult task on account of the natural variability of winds and currents. At present very little experimental information exists on such probability distributions, nor is the theory of turbulent diffusion far enough developed to predict them with any confidence. Effectively, the only quantity about which there is adequate evidence, both theoretical and experimental, is the first moment of the concentration probability distribution as predicted by the Gaussian diffusion model.

Similar ly, in relative diffusion a probability distribution can be defined where the concentration is measured at a fixed distance from the centre of gravity of a diffusing cloud.

The above discussion has been said (CSANADY, 1968) to apply to any specific release repeated exactly in successive trials, over a finite period. As yet, no serious theoretical discussion of the problem has been published that specifies the form of the probability distributions for results at a fixed point in space and results at a fixed distance from the centre of gravity. However, the logarithm of the concentration observed at a sampling instrument arranged as a cumulative frequency distribution and plotted on log - normal probability graph paper has been applied to some results yielding straight lines (CSANADY et al., 1968) - zero readings were first removed from the data.

LARSEN (1969) has described a mathematical model for the expression of air pollutant concentration as a function of averaging time and frequency. The model has the following characteristics:

a. Concentrations are approximately log-normally distributed for all averaging times for all pollutants and all cities that Larsen studied.

b. The median concentration (50^{th} percentile) is proportional to averaging time raised to an exponent (and thus plots as a straight line on log-normal probability paper).

BENCALA and SEINFELD (1976) analysed observed frequency distributions of air pollutant concentrations levels with respect to their statistical description. The authors demonstrate that several common distributions can be used to fit the observed data one of which is the log-normal distributions. Wind speed and mixing depth are discussed in the context of being the two factors most likely to influence air pollutant frequency distributions, for example, as Bencala and Seinfeld point out, the concentration of a pollutant near the centre of a uniform area source will not be sensitive to wind direction, whereas the concentration at a position near a single point source will be very sensitive to wind direction. Thus the impact of wind direction on concentration can range from negligible to significant and certainly varies from location to location.

In their work, Bencala and Seinfeld used information available from statistical correlations between wind speed and mixing depth (primarily wind speed). They found that in all cases, for both instantaneous and mean concentrations, if wind speeds are nearly log-normally distributed then resulting concentrations will be nearly log-normally distributed. Conventional models for mean concentrations, such as the Gaussian plume and eddy diffusion, can also lead to log-normality for concentration distributions if the wind speeds are log-normal. Bencala and Seinfeld conclude "that pollutant concentrations frequency distributions are the result of complex phenomena and cannot be predicted exactly,

but that the approximate log-normal character of the distributions is useful from a practical point of view and can be understood qualitatively on the basis of the relation between wind speed and concentration."

4.7.3 Intermittency

One obvious qualification about the use of a lognormal concentration probability distribution is that the pollutant must be received at a sampling instrument. In experimental studies of atmospheric diffusion periods of zero concentration are often encountered at a given instrument. This means that the sampled element contains no portion of the pollutant of interest. To describe this state of affairs an "intermittency factor" - γ - is introduced which specifies the fraction of the time in which the concentration is non-zero. The "time" can be conveniently defined as the time covered from the start of an experiment to the end of it. This is a somewhat arbitrary definition but it is nevertheless useful.

The intermittency factor discussed above is described by CSANADY (1973) and as Csanady notes is similar to that used by TOWNSEND (1956) for turbulent energy.

An early investigation of concentration probability distributions has been carried out by GOSLINE (1952) who measured "instantaneous" (10 second averages) ground level NO and NO_2 concentrations downwind of a 24 metre tall chimney

at distances of 5 to 10 chimney heights. Gosline noted that only 14 to 34% of the time was there a measurable concentration, i.e. χ at the sites ranged from 0.14 to 0.34. Also the duration of each NO bearing eddy at a given site was between 30 and 90 seconds. Zero concentration readings were removed from the data and a straight line was obtained when the data was plotted on log-probability paper.

4.7.4 Peak-Mean Concentration Ratio

A large amount of experimental information on atmospheric dispersion is available and widely used for predicting levels of atmospheric pollution but for practical reasons this relates to concentrations averaged over periods between about 10 and 100 minutes. Since some concentrations averaged over shorter periods may be many times higher than the mean and, further, since these relatively high concentrations may be important biologically, much work has been done attempting to characterise the relationship between the short-period concentrations and the longer term mean. Interest along these lines has focused particularly on the relationship between the highest concentration observed during a short averaging time and the long-term mean, the so-called peak-mean concentration ratio.

The problem of determining peak-mean air pollutant concentrations owing to plume meander has been treated analytically by GIFFORD (1959) in his fluctuating plume model.

The model suggested by Gifford considers the dispersion of air pollution from an isolated point source. The fluctuating plume is considered to be assembled from an infinite series of over-lapping puffs and it is a property of the model that both the mean concentration distribution and the instantaneous plume concentration distribution are assumed to be of a Gaussian form.

GIFFORD (1960) also has analysed peak-mean data and discusses the results of many measurements. From his study Gifford cites the following guides that can be laid down for the estimation of peak-mean air concentration ratios (P/M):

1. For a source and receptor located at the same level, P/M can be expected to be in the range from 1 to about 5.

2. For increasing difference in height between source and receptor or increasing distance from the plume axis, P/M increases, and values as great as 50 or 100 or greater may occur at the ground near a moderately tall stack (50 to 100 metres).

3. With increasing distance downwind from an elevated source, the ground-level P/M value will decrease toward its lower limit of unity but will attain values of this order only at considerable distances (perhaps 20 to 50 stack lengths or more) from the source.

CSANADY (1973) discusses and develops systematically much of the presently available theory concerning the "fluctuating problem in turbulent diffusion."

4.8 Conclusions

In general, the width of a plume - or puff - grows with distance from the source. The increase in width of the plume in a frame of reference moving with the centre of the plume is attributed to "relative diffusion." The growth of a plume in a fixed frame of reference (of an averaged concentration field) is termed average plume diffusion (also known as absolute diffusion).

In both situations - relative diffusion and absolute diffusion - the larger scale eddies have greater significance with respect to the growth of the plume as the plume travels further away from the source, whilst the smaller scale eddies being more important in the growth of the plume near the source when the plume width is - relatively speaking - narrower. Since the larger eddies take longer to pass a measuring site, for example, then the spatial and temporal distribution of the concentration of the pollutant within the plume will vary with the distance the plume has travelled. As the plume travels from the source, the variation of these spatial and temporal scales may be exhibited by, for example, a decrease in the extent of fluctuations - as measured by a fast response detector - as travel time increases.

Under unstable conditions, the growth of a plume is generally at a maximum and concentration measurements taken within plumes under such conditions could possibly be the most revealing in order to characterise plumes with respect to distance travelled. The same, more or less, applies to measurements in neutral conditions, however, under stable conditions the growth of the plume is much less extensive as the plume travels away from the source and the decrease in the extent of fluctuations is not so obvious because the concentration of a pollutant within a plume will be distributed over smaller spatial and temporal scales than would otherwise be the case under unstable conditions.

It is seen from the "U" and "w" spectra discussed in Section 4.5 that under unstable conditions the low-frequency long-period thermal components of turbulence contribute most to the diffusion process. Whilst under stable conditions the high frequency short-period mechanical components of turbulence predominates. This is interesting because it emphasises the difference between plume dispersion under these two stability conditions, especially at greater distances downwind from a source when the long-period fluctuations become more important as the plume width increases.

This research work may provide new data concerning log-normal concentration distributions, intermittencies and peak-mean ratios, however, it is recognised that important problems such as the variance of concentrations fluctuation

at a fixed point are relevant to the fluctuating problem of turbulent diffusion, but they have not been dealt with here.

Chapter 5

Experimental and Results

Chapter 5 is split into two parts:

5.1 Experimental
5.2 Results

The experimental section describes the set-up of the apparatus for field work. The choice of field sites in relation to the design of the experiments and the experiments carried out are also discussed. The results and calculations are presented in the Results Section.

5.1 Experimental

In order to record new information about the way that the concentration of air pollution fluctuates with time and so develop a relation between the concentration fluctuations and the source distance, it is necessary:

A. To measure the fluctuations and to develop a convenient means of characterising them.

B. To produce records of concentration as a function of time in a situation under conditions where virtually all of the pollution comes from a single identifiable source at a known distance. The experiment then has to be carried out with a variety of sources (or with one source) at a series of distances and under a range of meteorological conditions.

The experiments have been designed with the above aims in mind.

5.1.1 Set-up of the Apparatus

The set-up of the apparatus at any given site is shown in figure 5.1. The individual units making up the apparatus in figure 5.1 can be carried by one person over limited distances, if necessary. Transport to and from sites was by car.

In figure 5.1, a dexion frame supports the detector and ancillary apparatus. The gas cylinders are supported on the ground and are connected to the detector using 3.2 mm.i.d. stainless steel tubing with "Swagelock" connecting unions. A standard 7 kg cylinder of carbon dioxide and a 1.25 M^3 cylinder of hydrogen are used as gas supplies; these sizes being convenient for transport purposes. The electrical power requirement of the apparatus is 2 kilowatts and an extension lead carries either the mains electricity from the nearest available 13 amp ring main socket or electricity supplied from a 2 KW portable generator. A four way gang plug is used as the junction box for the electrical output to the following electrical units, as shown in figure 5.1:

A. A thermostatic water circulator connected to the detector via rubber tubing.

B. A Hewlett-Packard voltage stabilised power supply necessary to provide the high tension required for the photomultiplier tubes.

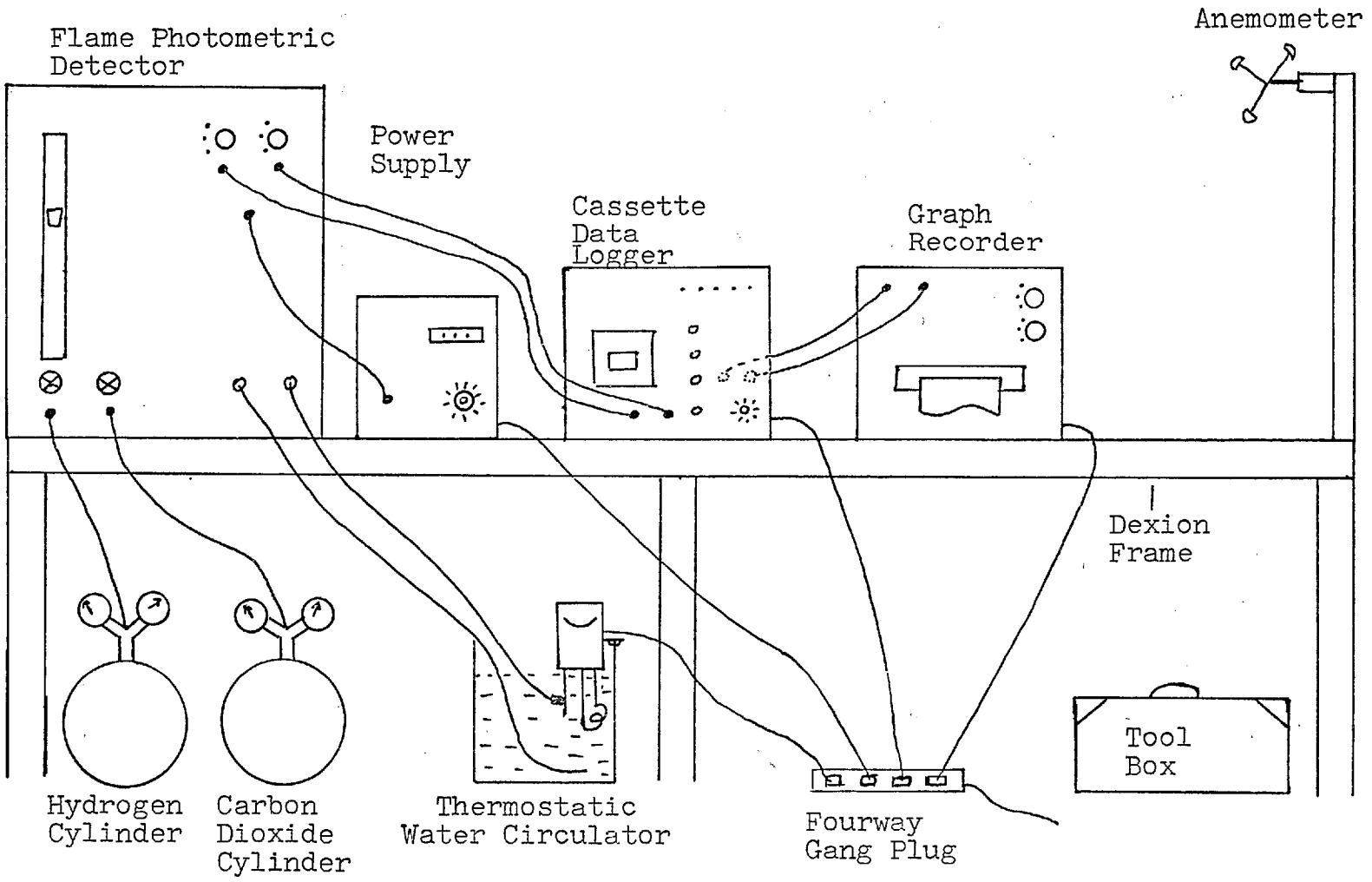

Figure 5.1 Apparatus set-up at a site.

C. A Philips double line fast-response graph recorder (PM 2000). In early work a Japanese TOA Model EPR-3T dual channel graph recorder was used.

D. A 2-channel Cassette Data logger.

A revolving three-cup anemometer is used to continuously record the wind speed on the graph recorder. The revolving mechanism of the anemometer short circuits a 9-volt battery every half revolution across one channel of the graph recorder, so that a series of counts are recorded. The number of counts per minute is proportional to the wind speed and the speed is read from a calibration chart.

5.1.2 Cassette Data Logger

The cassette data logger was designed and built in the electronic workshops of the Chemical Engineering Department specifically for use with the flame photometric detector. Originally the logger contained two easily-identifiable channels but was only used effectively with one channel for much of this work. This was the result of the logger being incompatible with a cassette-tape reader interface in the Computing Department at Imperial College, which was not in operation at the start of this project and only became operational as a direct result of the requirement created by this project for such a computing facility. This facility is discussed in more detail in the Results Section 5.2

Figure 5.2 shows a schematic diagram of the principle of operation of the cassette data logger.

The data logger was designed for medium speed data logging purposes. Portability was obtained by using a Racal Digideck Digital Cassette Tape Recorder. The device uses Philips type cassette as the data storage medium and data conversion rates from 100 channels/second to 100 seconds/channel are possible.

5.1.2.1 Principles of Operation

The various boxes shown in figure 5.2 are now discussed in detail.

Cassette Recorder

The recording device is a Racal P70 Digideck Recorder capable of accepting digital data in a 9 bit parallel format upon command and placing it on magnetic tape. A total number of 50000 9 bit words may be stored on one cassette.

Tape Control Unit

This unit is necessary to place the recorder in the correct mode of operation and to perform such functions as rewind tape, load tape, write tape etc.

The Tape Control Unit also acts as the interface between the Recorder and the Sequence Control unit and Signals from the Timebase Generator to the Tape Control unit are used to give some control of tape speed at the highest data rates.

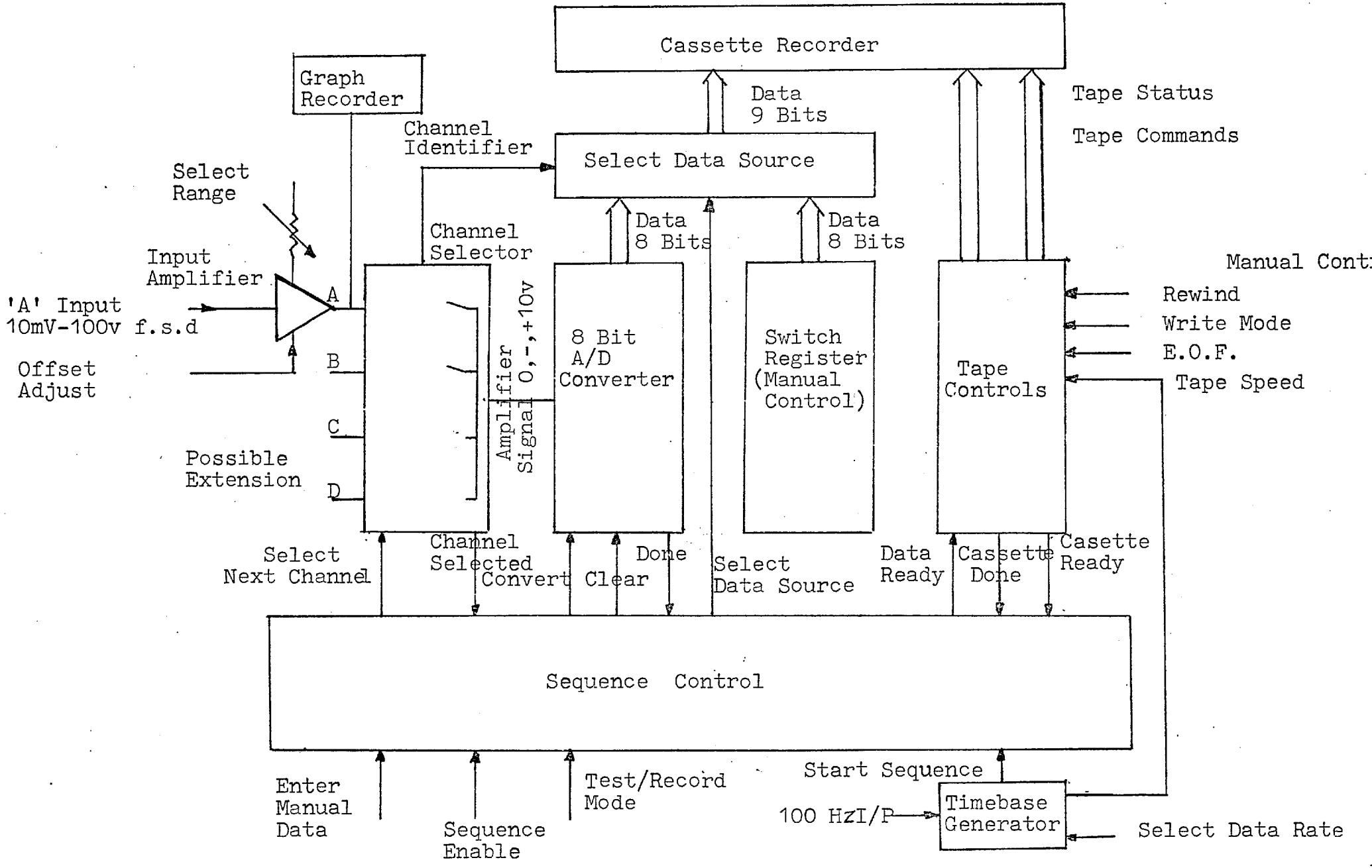

Figure 5.2 CASSETTE DATA LOGGER SCHEMATIC

Sequence Controller.

The Sequence Controller sequences the operation of the individual elements of the system ensuring that all operations take place in the right sequence by communicating with each element necessary for the performance of an operation.

Upon receipt of a pulse from the Timebase Generator the controller runs through the sequence of selecting the next analogue channel, initiating an Analogue to Digital conversion and commanding the Recorder to write the digital data onto tape.

On completion of the sequence, the control is left waiting for the next start sequence pulse.

Timebase Generator

This unit works from a 100 Hz source and contains frequency division circuits. Switch controls select the division rate and allow data conversion to be completed at rates between 100/SECOND and 1 every 100 SECONDS.

Input Amplifers

The amplifers convert input signals to the levels required for the Analogue/Digital converter system (0 to +10 volts) The amplifer gain is selectable to allow signals from 10 millivolts to 100 volts to give full-scale signals on the Analogue/Digital converter. The output from the Amplifers was used to drive the graph recorder via connecting pins at the back of the data logger.

Channel Selector

Under instructions from the Sequence Controller this unit selects the next analogue channel for conversion and feeds the analogue signal to the A/D converter through high speed relays.

Specific channels upon selection send a digital signal to the 9th data bit of the recorder for channel identification.

Analogue to Digital Converter

The A/D Converter converts analogue signals in the range 0 to +10 volts to 8 bit binary format, thus the converter is capable of resolving to 1 part in 255 i.e. a resolution of better than $\frac{1}{2}$ %.

Select Data Source

This unit has gates that "steer" digital data from either the A/D converter or from 8 manual switches in the Switch Register to the recorder.

Outputs from the gates also illuminate Light Emitting Diodes which allow interpretation of the data being presented to the recorder thus facilitating the setting up of the Input Amplifers. A "test mode" facility is available which inhibits cassette operation and allows setting up without the data being recorded.

Switch Register

This permits the entry of manually selected data onto the cassette for identification of blocks of data before the Recorder is placed in the data logging mode.

The whole unit is 32 cm x 18 cm x 24 cm and is light so that it can easily be carried by one person.

5.1.3 Start-Up Procedure

With the equipment set-up as in Figure 5.1 the following start-up procedure must be followed so that the burner can be safely lit and the apparatus made ready for experiments.

1. Check all electrical instruments are switched off and then switch on the mains electricity - a red light will glow on the 4-way gang plug. Check that the stainless steel tubing is securely connected to the hydrogen and carbon dioxide cylinders and to the detector with the regulator valves fully closed. Also, check that the water inlet and outlet taps on the detector are open and the hydrogen and carbon dioxide flow control valves are fully closed. Finally, check that the photomultiplier load resistances are set to 100 kΩ, the Hewlett-Packard power supply output is set to zero, the altimeter is set to zero and both channels on the graph recorder are set to maximum sensitivity.

2. With the thermostat on the water circulator set to 40C, switch on the thermostatic water circulator - a red light will glow brightly. Check that the water is circulating around the circuit by lifting the "outlet" rubber tubing out of the water tank to see if the water is issuing forth. If the water is not circulating then the system requires priming in the usual way. Leave this operating and after t en minutes or so the red light on the

circulator should be flickering - this is an indication that the thermostatic circulator is controlling.

3. Switch on the graph recorder and the power supply. Slowly increase the power supply voltage to 700 V noting that there is little or no deflection on the graph recorder. If there is significant deflection (more than 3 millivolts) then the detector is not light-tight and providing the signal is not greater than 1 volt then tests can be carried out to discover the leak with the power supply still on. If all is well, open the carbon dioxide valve on the detector by about three turns and open the carbon dioxide cylinder regulator valve (a pressure of 10 psig is adequate). The hydrogen valve on the detector can then be opened, again, by about three turns and open the hydrogen cylinder regulator slowly to 10 psig. Leave flushing for several minutes.

4. The hydrogen pressure regulator is adjusted to 30 psig and the carbon dioxide pressure regulator is adjusted to 40 psig. Using the carbon dioxide flow control valve the burner pressure is regulated to "1500 feet" and the hydrogen flow is regulated to 5 or 6 on the flowmeter (see graph 5.1 for calibration curve) using the hydrogen flow control valve. On depressing the piezoelectric igniter once or twice, the burner will light as signified by the sharp increase in signal as shown on the graph recorder.

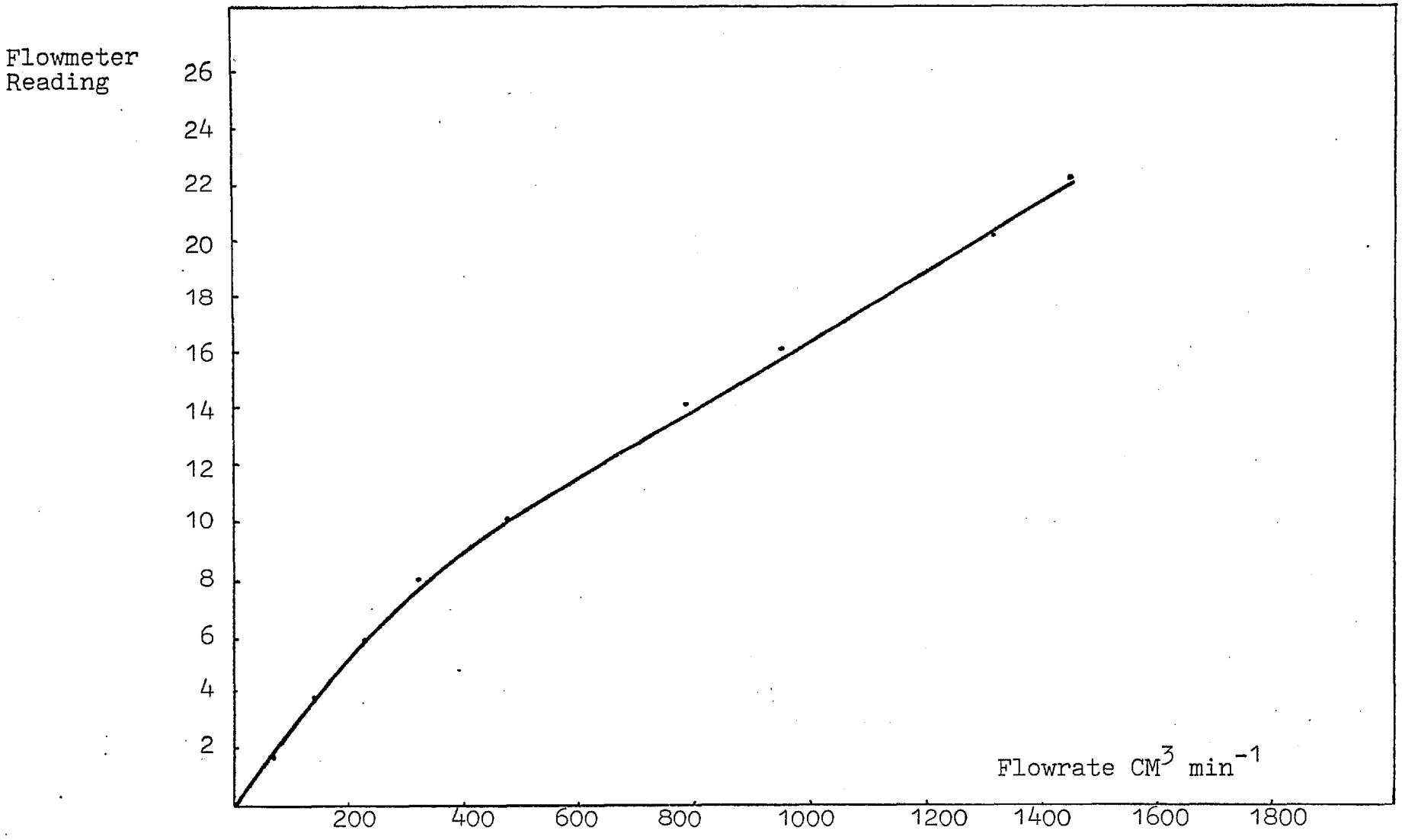

Graph 5.1 Calibration curve for Hydrogen Flowmeter

5. Increase the hydrogen flow to 20 on the flowmeter, slowly decrease the burner pressure by opening the carbon dioxide flow control valve until the altimeter registers 3000 feet (0.9 atmosphere) readjusting the hydrogen flow to 20, if necessary. The sensitivity on the graph recorder will require alteration under these operating conditions so that the pens are not off-scale. Leave for about 10-15 minutes to equilibrate.

6. The photomultiplier power supply can be adjusted from 600 v to a maximum of 940 v and the output of either photomultiplier (sulphur or phosphorus) with 100 kΩ load resistor must not exceed one volt so that operation is limited to these ranges. During operation the hydrogen flow and carbon dioxide may require adjustment to the stated operating conditions (in 5.)

7. At any time during operation the cassette data logger can be used as well as the graph recorder. The sensitivities of the data logger and graph recorder can be adjusted during operation so that the signals can be fully recorded without loss of the peaks. The output from the revolving cup anemometer is monitored on one channel of the graph recorder usually at the expense of the phosphorus channel.

5.1.4 Shut down

1. Switch off photomultiplier power supply, graph recorder and cassette data logger.

2. Turn off the hydrogen by reducing the regulator pressure to zero and do the same with carbon dioxide.

3. Switch off the thermostatic water circulator and switch off the electricity at the mains.

5.1.5 Experimental and Experimental Sites

The requirements of the sites from the point of view of experimental design is now considered together with experimental design.

A. Dover.

Advantages of recording pollution from moving sources over that from stationary sources are obvious; much time can be wasted in moving the apparatus in attempts to keep within a chimney plume from a source such as a power station, however, pollution from moving sources can be recorded without moving the apparatus, since the motion of the source across the wind sweeps the plume over the apparatus if sited downwind. At Dover, ships are a very convenient moving source since there are many of them covering a wide range of distance.

Permission was obtained from the Dover Harbour Board to place the apparatus on the end of the Admiralty Pier Extension. Figure 5.3 shows the layout of the Harbour and the experimental site is marked accordingly. In a 30° to 90° wind, pollution can be received at the site from Cross-Channel Ferries travelling in and out of the Eastern and Western entrances - both marked on Figure 5.3 There is also the possibility of recording pollution from ships moving along the channel in winds ranging from 90° to 270°, thus

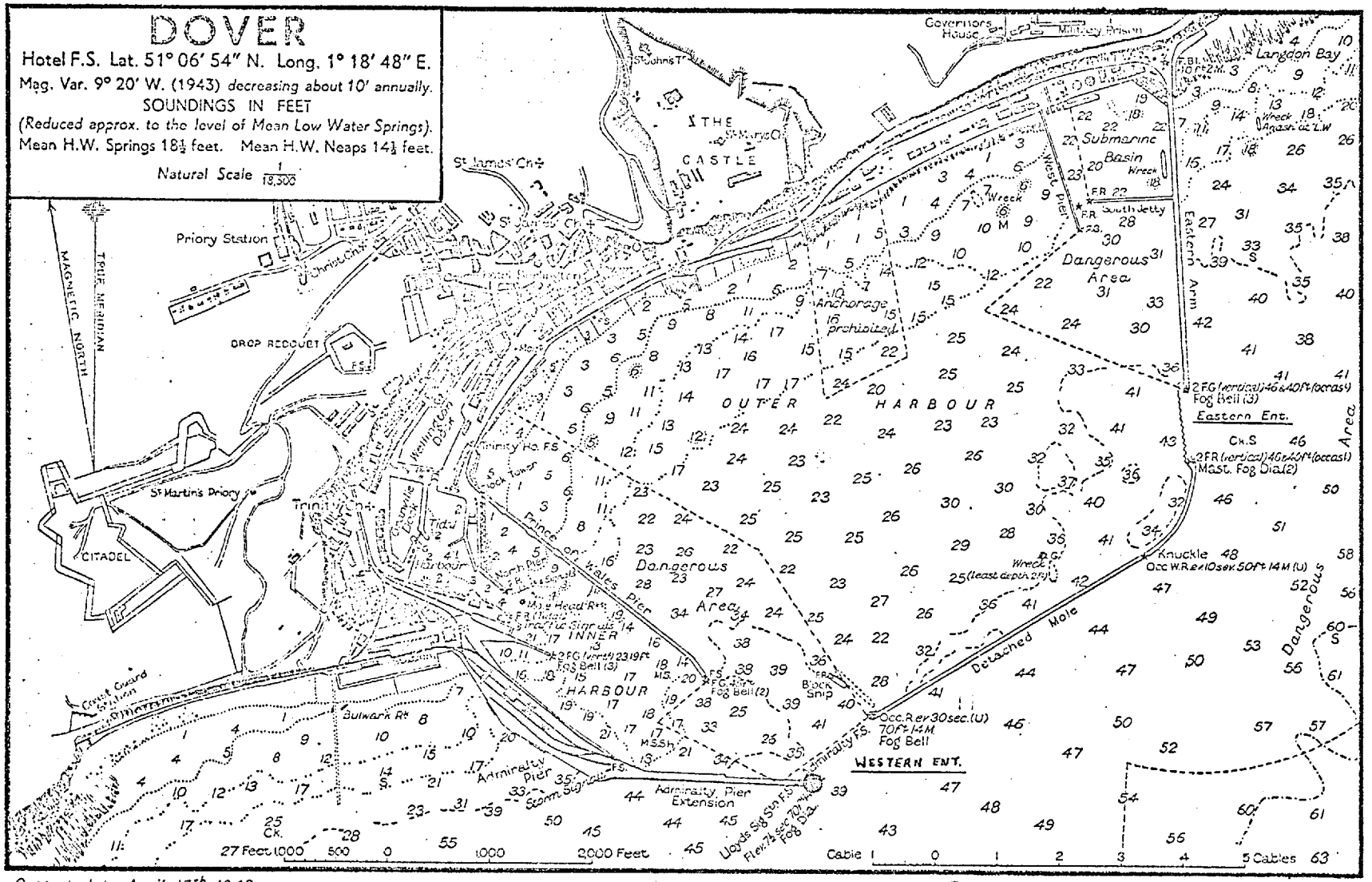

Figure 5.3 This figure shows the layout of Dover Harbour.

the Dover site offers a wide range of suitable operating wind directions combined with a frequent variety of moving sources, although it is probably not suitable to measure there with the atmosphere in unstable conditions.

The work at Dover involved travel by car or train - sometimes staying and working overnight - often with the apparatus, even though storage area for the equipment was available at Dover. The apparatus was set up in one of two wells on the end of the Admiralty Pier Signal Station - a matter of metres from the edge of the Channel. Information regarding any result was noted on a Data Sheet as in Figure 5.4. Weather data were obtained from the Lloyds Signal Station - both wind direction and wind speed (if the revolving cup anemometer was not available) and observations of cloud cover and insolation were also noted. Source distances were estimated from a knowledge of the distances of the various entrances and the wind direction.

B. Harlington

Harlington is the sports ground of Imperial College and is sited near Heathrow Airport. It offers a large area (15 - 20 acres) of fairly flat grass land upon which close range pollution studies were carried out in stable and unstable conditions, with the permission of the Head Groundsman. The site was also convenient because any wind direction was favourable.

DATE	GRAPH RECORDER	CASSETTE DATA LOGGER
TIME		
SENSITIVITY AT POWER = ...		
CHART/TAPE SPEED		
WINDSPEED AND DIRECTION		
WEATHER		
SOURCE DESCRIPTION AND POSITION		
MISCELLANEOUS OBSERVATION ETC.		

Figure 5.4 This is a Data Sheet upon which information concerning a particular result was recorded.

The work at Harlington involved the burning of sulphur candles at different distances from the detector upto about a maximum of 200 metres. The experiement involved two people; one to operate the apparatus, the other to carry the source at various distances from the apparatus. The sulphur candles were manufactured by melting and resolidyfing flowers of sulphur in glass petri dishes and were held within a storm lantern in the field. The candles were easily lit using a match. Both day and night work was done at this site and as with the Dover experiments, the results were recorded on the data sheet whilst distances were paced out and converted to metres using an appropriate conversion specific to the person who paced out the distance.

C. London.

During the early stages of field work the Aeronautics roof at Imperial College provided a suitable testing site to gain operating experience. However, the site also proved to be useful for recording pollution from the nearby College boiler Chimney and from Lotts Road power station. Meteorological information - wind speed and direction - was obtained from the Meteorological Department at the College. Source distances were estimated from maps of the area.

D. Drax.

As part of its Environmental Research Programme the Committee for the European Commission devoted funds to organise a "Remote Sensing of Air Pollution" campaign, held

at Drax Generation Station in Yorkshire during 9th-21st September, 1976. The stated overall objectives were two-fold; namely "to compare and evaluate remote sensing techniques for measuring airbone concentrations of gaseous emissions and to obtain basic information on the dispersion of tall stack plumes over flat terrain." The collaborative field trials involved teams from E.E.C. countries who for their own part could meet, compare results and evaluate their techniques at Drax.

The campaign was directed from a control room at the power station camp site where computer services and a radio communications system were installed with links to a number of measuring sites. Briefing sessions in the early morning were used to give the latest meteorological information - wind speed and direction up to a height of about 1000M and vertical profiles of temperature and humidity all provided by a Meteorological Office team - and the predicted power station emissions for the day. Five mobile survey vehicles operated on the road network around Drax measuring ground level concentrations of SO_2 and NO_x and correlation spectroscopy was used to measure the integrated concentration of SO_2 and NO_x along lines between a given vehicle and the top of the plume. The direction of the plume was measured using LIDAR and the positions of the mobile vehicles were co-ordinated from the control room.

In addition to ground based survey vehicles a Norwegian aircraft belonging to the Norsk Institutt for Luftforskning (NILU) traversed the plume in the air,

carrying instruments to measure SO_2 concentration, integrated values of SO_2 and NO_x concentrations along flight paths, aerosol concentration, air temperature and turbulence.

There were several groups whose instruments were fixed for the duration of the measurement period. A large number of different sites were made available for teams wishing to use them and instruments to measure the position and dimensions of the plume (LIDAR, correlation spectrometer s and SODAR), concentrations at ground level (point samplers), concentrations above ground level (long-path spectrometers, LIDAR and differential LIDAR) and meteorological conditions such as depth and structure of the mixing layer as well as those previously mentioned (SODAR and LIDAR) were all part of the campaign.

A team from Imperial College (Dr. M.J.G. Wilson and myself) participated in the campaign in a "non-official" capacity. An operating site at Burn Airfield (disused) was chosen because it offered a large area of open land with very few people where experiments both with sulphur and phosphorus tracer compounds could be carried out, and was also in a good strategic position to record pollution from any four power stations sited at Drax (2000 megawatt; 6.5 KM 92°) Eggborough (2000 Megwatt; 4.5 kM 220°), Ferrybridge C (2000 Megawatt; 13 kM 254°) and Thorpe Marsh (1800 Megawatt; 18.5 kM 180°). Unfortunately, for the duration of the campaign the wind never blew from any power station to the site. However, this site provided the first real opportunity to operate the detector using two channels simultaneously to monitor both sulphur and phosphorus.

The experiment involved releasing Sulphur dioxide and phosphorus trichloride (PCl_3) together at a suitable distance from the detector and recording the concentration of each simultaneously on the graph recorder and cassette data logger. The sulphur source was a lecture bottle of sulphur dioxide (with a control valve) while Helium bubbled through a wash bottle of phosphorus trichloride was used as a phosphorus source. The concentrations of both tracers could be varied sufficiently to obtain adequate sulphur and phosphorus signal on the sulphur and phosphorus channnels respectively with as little cross-channel interference as possible.

After sufficent data was recorded with the sources together (actually they were separated by a distance of 3 mm) the two sources were moved apart in a crosswind direction by a known distance (0.7 metres) and the concentration of the two species again recorded simultaneously on the graph recorder and the cassette data logger. Wind speed could not be measured at the same time as the experiment and so it was recorded after.

5.1.6 Stability Classification

In order to classify the results at different sites according to atmospheric stability the "Modified Pasquill Stability Categories" were used - as supplied by the Meteorological Office. Briefly, the method (PASQUILL, 1961) uses commonly observed surface meteorological variables, wind speed and cloud cover. Pasquill's method was based

primarily on observations of the spread of pollution on particular occasions from a source on or near the ground, averaged over times of the order of an hour. His method assumes that vertical diffusion in the lowest layers is strongly influenced by the vertical flux of sensible heat due primarily to daytime heating of the ground by solar radiation or radiative cooling of the ground at night, and that the ground conditions are effectively uniform. The most unstable category, A, is associated with strong sunshine/low wind speed conditions during the daytime, conditions in which the lapse rate in the lowest 50 metres or so often exceeds the dry adiabatic lapse rate (DALR) and approximates to it above this, up to about 300 metres. The most stable category, G, is associated with clear sky/light wind conditions at night, with a surface-based inversion extending up to 150-200 metres or higher, Category D is the "neutral" category. Table 5.1 shows the modified Pasquill stability categories.

5.2 Results

The use of the data logger digitising at 50 times a second provides 3000 readings every minute. One tape cassette can hold approximately 50,000 readings from seventeen minutes operating time, whilst a typical day of experiments may produce six or seven cassettes. The procedures for systematic handling and processing of this data base are now described, the primary objective of which is to convert the digitised readings to concentrations in μgM^{-3}.

WIND SPEED M SEC^{-1}	DAYTIME (EXCLUDING 1 HOUR AFTER SUNRISE AND 1 HOUR BEFORE SUNSET				WITHIN ONE HOUR BEFORE SUNSET OR AFTER SUNRISE	NIGHT TIME		
	INCOMING SOLAR RADIATION ($MW.cM^{-2}$)					CLOUD AMOUNT (OKTAS)		
	STRONG (≥ 60)	MOD (30-60)	SLT (<30)	OVERCAST		0-3	4-7	8
2	A	A - B	B	C	D	F or G See Note 2 below	F	D
2 - 3	A - B	B	C	C	D	F	E	D
3 - 5	B	B - C	C	C	D	E	D	D
5 - 6	C	C - D	D	D	D	D	D	D
6 - 7	C	D	D	D	D	D	D	D

Table 5.1 Modified Pasquill Stability Categories.

Notes

1. Night was originally defined to include period of one hour before sunset and after sunrise. These two hours are always categorised here as D.
2. Pasquill stated that in light winds on clear nights the vertical speed might be less than for category F but such cases have been excluded because the surface plume is unlikely to have any definable travel. However, they are important from the point of view of the build up of pollution and category G (night time, 0 or 1 okta of cloud, wind speed 0 or 0.5 M Sec^{-1}) has been added.

The results of concentrations from each site are then used to establish a relation between concentration fluctuations and source distance and the section is finally devoted to a wider examination of the results.

5.2.1 Data Handling and Processing

The Imperial College Computer Centre facility for reading cassette tapes prepared on a Racal p70, 71, 72 or Termicette Recorder uses a UT-1 terminal containing a Data General "NOVA" series computer. Remote job entry (R.J.E.) using cassette tapes and program decks is controlled by a "terminal emulator" program running in the NOVA and by IMPORT/EXPORT system running in the CDC 6400/CYBER 70 system at Imperial College. Connected to the R.J.E. station at the Computer Centre is a 300 card minute^{-1} card reader, 300 line minute^{-1} printer, a paper tape reader and a Racal cassette tape reader.

Each cassette tape is marked with a six character identifier e.g. HADJO1, HADJO2 and is labelled so as to identify whether the cassette is recorded with side A or side B facing. A file on the tape contains many subfiles each separated by a known label inserted on the tape using the Switch Register (5.1.2.1.) on the Data Logger e.g. 111, 254 254 254, the sequence always occurring in groups of identical numbers. These labels are also recorded on the Data Sheet along with the six character identifier and the file on the tape is terminated by a sequence of at least 256 NULL characters.

In order to process a cassette tape recorded in Binary Mode the deck set-up must conform to the structure outlined in figure 5.5. "EITAPE" is a procedure file that takes the contents of the Cassette Tape and formats them in a suitable way for processing. The parameter "FN = filename" is used to indicate what "filename" the Cassette Tape will be known by in the job. The Kronos (the Computer Operating System used at Imperial College) Control Language statements LIBFILE (EITAPE) and CALL, EITAPE must be the first two cards after the Password Card. The file produced by the parameter "CD = UD" is a single record file, where each "character" on the Cassette Tape requires one 60-bit word, and the value is stored in 12-bits in the right-hand-end of the word. The program to process this file is compiled with a Fortran compiler and a library routine "READB" is used to read the file.

The first card after the Kronos Control Language Record must contain)(B in columns 1,2,3. This Card must not contain any other information and must be followed by an end-of-record or end-of-file card. The function of the information on this card is to pass control from the card reader to the Cassette Tape Recorder and does not become part of the input file.

As the data is read from the cassette it is stored on Disk and also printed onto computer paper via the line printers. The data on the paper output is matched to the results on the graph recorder output using the labels -

```
JOB  (job number ...)

PASSWOR (pass word)

LIBFILE (EITAPE)

CALL, EI TAPE (FN = filename, CD = UD)

.
.
.
.          other user Kronos Control Language statements
.
.
.
.
7-8-9      End of Record

) ( B      These characters must appear in columns 1,2,3
7-8-9      End of Record
.
.
.
.          Possibly, program and data records.
.
.
.
.
6-7-8-9    End of file
```

Figure 5.5 Job deck set-up used to process a Cassette Tape.

previously mentioned - as an aid to identification. A reference number is then given to the matched results and this same number is also entered onto the appropriate Data Sheet. On any computer paper output there may be up to 70% of the data requiring further processing - the remainder is baseline data and is not useful as such - therefore an editing facility available on the Kronos system is used to edit the files on disk and "queue" the edited version to punch card output. The card output is used as the data input to subsequent processing.

To convert the digitised readings into concentrations a Fortran program was written that uses constants obtained from calibration curves as in Chapter 3. As an aid to developing techniques for characterising the data the following calculations are also performed.

A. The concentration of sulphur dioxide (μgm^{-3}) is plotted against time (seconds). This plot is confusing if there are more than about 1000 points to be plotted because of space limitations on the line printer.

B. A cumulative frequency distribution is calculated.

C. The gradients for the rises and falls are found (change in concentration per change in time).

D. The gradients for the rises and falls divided by the mean of the respective rise or fall are calculated.

E. Basic descriptive statistics are evaluated; mean, standard deviation, skewness and Kurtosis. This was only added to the program in the last stages of the work.

Except for the plotting routine, the above computation is carried out for different averaging times - usually from 20 milliseconds to one second in steps of 100 milliseconds.

When the data logger output was not available the processing had to be done by hand using the graphical output.

5.2.2 Calculated Results

Table 5.2 contains the concentration/time results of a puff obtained from the work at Harlington (reference number ID9509) and figure 5.6 shows the concentration results plotted against time. Various features of the concentration/time results that might be useful to quantify are now discussed, together with the technique used to analyse the results. The results in Table 5.2 are referred to, to exemplify some of the points made.

A striking feature of the results in Table 5.2 is the change in concentration between 18.5 μgM^{-3} and 35 μgM^{-3}. As explained in the Experimental section, there is a need to adjust the sensitivity of the graph recorder and data logger so that the peaks of signals can be recorded. This, combined with the effects of the square law, means that

CONCENTRATION $\mu g\ M^{-3}$	18.5	35.2	46.8	46.8	78.4	182	133.1	84.7	56.2	56.2
TIME SECONDS	0.05	0.1	0.15	0.2	0.25	0.3	0.35	0.4	0.45	0.5
CONCENTRATION $\mu g\ M^{-3}$	75.4	120.4	106.4	76.7	64.4	56.2	46.8	46.8	56.2	56.2
TIME SECONDS	0.55	0.6	0.65	0.7	0.75	0.8	0.85	0.9	0.95	1
CONCENTRATION $\mu g\ M^{-3}$	71.7	64.4	56.2	46.8	46.8	46.8	56.2	69.4	78.9	202.5
TIME SECONDS	1.05	1.1	1.15	1.2	1.25	1.3	1.35	1.4	1.45	1.5
CONCENTRATION $\mu g\ M^{-3}$	155.7	245.8	221.2	115.9	78.4	56.2	46.8	35.2	35.2	35.2
TIME SECONDS	1.55	1.6	1.65	1.7	1.75	1.8	1.85	1.9	1.95	2
CONCENTRATION $\mu g\ M^{-3}$	35.2	18.5								
TIME SECONDS	2.05	2.1								

Table 5.2 This table shows a concentration/time signal obtained from a puff of pollution at Harlington.

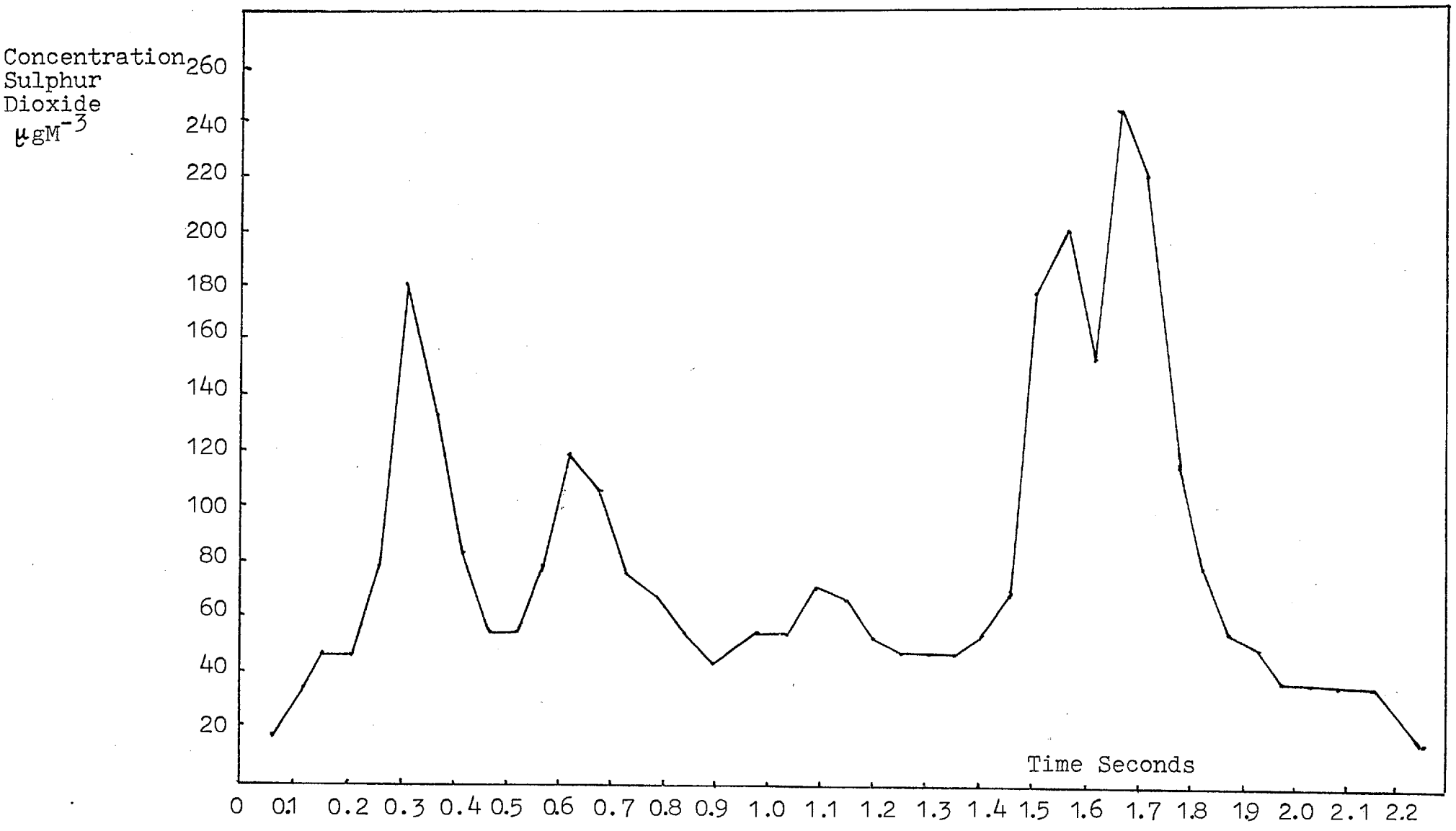

Figure 5.6 This is a Plot of the Concentration/Time results listed in Table 5.2.

for much of the time the instrument operates at the lower end of the sensitivity scale. As a result the digitised readings - when converted to concentration - are liable to change between 18.5 μgM^{-3} and 35 μgM^{-3} as seen in the concentration/time results in Table 5.2. This change which represents the increment of the digitised voltage could be due to a large change in concentration or to instrument behaviour. The estimation of baseline concentration under these conditions is not very reliable.

The first attempts to analyse the data included the use of spectral analysis. The method used is described in JENKINS and WATT (1968) Chapter 7. The variance of a record is decomposed into contributions at a continuous range of frequencies. The results were examined to see if the variance would shift to values with greater contributions at the lower frequencies than at the higher frequencies as the source distance increased. After some preliminary computation the analysis was terminated because many of the records from sources especially at near distance, last a few seconds. The confidence interval for the spectral density at a given frequency is very large for records lasting only a few seconds thus making interpretation of the spectrum impractical.

Further data analysis used the results to calculate differences and variations of concentrations with time. Preliminary analysis using differences revealed the following as useful guidelines in selecting a suitable relation between source distance and concentration fluctuations - the relation selected is termed a "statistic":

1) The statistic should not be too sensitive to the form of the leading edge of the signal, for example, to the concentration rise from 18.5 μgM^{-3} to 35.2 μgM^{-3} as seen in table 5.2.

2) The statistic should not be affected by changes in source strength and the background concentration.

3) The statistic should reflect the main part of the rise(s) and/or the fall(s) of concentration and not be unduly influenced by slowly varying parts of the signal. For example, from the results in table 5.2, the rise in concentration between 46.8 μgM^{-3} and 202.5 μgM^{-3} is considered more important than the changes in concentration occurring in the time interval 0.9 seconds to 1.15 seconds.

4) The statistic should account for wind speed and atmospheric stability.

Some of the attractions of differences are:

i) They retain information concerning the rises and falls that is lost in spectral analysis.

ii) Differences are easily computed with no apparent mathematical difficulties of principle and can be determined "on-line" in the field.

However, there are features of differences, especially when calculated from digitised readings, that are not so attractive. For example, consider the change in concentration from 56.2 μgM^{-3} to 71.7 μgM^{-3} in 0.05 seconds,

as shown in Table 5.2. This gives a nominal increase of $15.5\mu g m^{-3}$ in 0.05 seconds. The real increase might have been much lower depending on the size of the digitising interval and the relation between these intervals and the actual concentration.

At the other extreme the actual increase might have been infinitely fast if the actual concentration followed a step change placed exactly right in line in relation to the moment at which readings were digitised and recorded.

These effects may have many statistical implications, for example, the distribution of the results may be skew rather than normal and digitising effects may contribute to the variance of the results.

5.2.3 The Statistic

A statistic that substantially fulfils the guidelines previously given can be calculated from the rises in concentration actually occurring within the puff or plume and not from the background concentration. The determination of concentration changes as calculated from the background has an inherent disadvantage if the portion of the signal of interest rises from the background because the value of the statistic becomes independent from the concentration changes.

The statistic utilises 50% of any given concentration change occurring within a rise. Fifty per cent was chosen as a compromise between using the concentration change calculated in one time interval (the interval determined by the data logging speed) and that calculated over a rise. Under these circumstances it is essential to log data at high speeds otherwise vital information at the beginning of the rise may be lost.

The value of the statistic is calculated as follows:

$$\text{Statistic} = f(s) = \frac{C_2 - C_1}{\frac{C_2 + C_1}{2} . \Delta t . U} \text{ metres}^{-1} \qquad \text{Equation 5 .1}$$

where

C_1 = Initial concentration at the start of a rise within the puff or plume.

C_2 = 50% of the concentration change as calculated from the final concentration at the end of a rise subtracted from the initial concentration C_1.

Δt = The time for this 50% concentration change to occur in seconds.

U = Wind velocity as determined during the period of the concentration change, metres second.$^{-1}$

The following procedure is used to determine a value of f(s):

1. The data logger output is converted to concentration in μgM^{-3} using the computer program described in 5.2.1. The resulting concentration/time record is then matched up with the corresponding graphical record in millivolts. This procedure is very time consuming and requires much effort due to the effect of the square law and the large amounts of data needed to be examined. For a signal of interest in the matched record, the most significant rises above the noise level are identified using both the graphical record and computer output, if available, as a check on the match. If the data logger output is not available, the graphical output is used to produce a concentration/time record, which has worse time-scale resolution than the data logger output.

2. For any given significant rise the local peak and trough concentrations are determined and by subtraction the concentration change is calculated, (C_2-C_1 in equation 5.1).

3. Fifty per cent of the concentration change is calculated and the corresponding time for the 50% concentration change is found using linear interpolation (Δt in equation 5.1).

4. The wind speed is determined from the graphical record for the period covering the rise. On occasions when the instantaneous wind speed record at the sampling site was not available, then either an average wind speed, as obtained from say the Meteorological Department at Imperial College, was used or the wind speed was obtained from measurements taken at the sampling site after the experiments.

5. On substitution for C_2-C_1, t and U in equation 5.1, f(s) is then calculated. Steps 2 to 5 are carried out for all of the significant rises in the signal.

6. In a signal with more than one significant rise, the maximum value obtained for the statistic is chosen to characterise the signal. This value of the statistic is then recorded together with the source distance, the Pasquill stability category and the sampling site.

The results in table 5.2 are used in the following calculation example.

Using the concentration change occurring after 0.2 seconds and lasting for 0.1 seconds,

$$C_2-C_1 = \left[\left(\frac{50}{100}\right)(182-46.8)+46.8\right] - 46.8$$

$$= 114.4 - 46.8 \ \mu g M^{-3}$$

The time t seconds for the concentration to reach 114.4 $\mu g\ M^{-3}$ is

$$\Delta t = 0.05 + \frac{(114.4-78.4)}{(182-78.4)} \times (0.05)$$

$$= 0.067 \quad \text{seconds}$$

The wind speed U = 4.26 metres second $^{-1}$

$$\therefore f(s) = \frac{114-46.8}{\frac{114+46.8}{2} \times 0.067 \times 4.26}$$

$$= 2.9 \text{ metres}^{-1}$$

The above calculation has been applied to the results from Dover, Harlington and London. In total approximately 250 results have been processed leaving many more unprocessed. The unprocessed results include signals that went off - scale because the data logger sensitivity was too high, signals that were logged with a data logger sensitivity that was too low, signals that could not be matched up with graphical output. Appendix A1 contains tables showing all of the calculated results from the various sites. Table A1.1 contains the calculated results from Dover and tables A1.2 and A1.3 contain the calculated results from Harlington - Unstable and stable respectively.

The results have been grouped according to the Pasquill stability categories and then each group has been regressed using a first order linear model. Graph 5.2 is a log-log plot of the statistic (f (s) metres $^{-1}$) against distance (s metres) for different stability categories and different sites. The lines plotted are regression lines and are now discussed individually along with the two sets of points plotted on graph 5.2 - labelled as "Lotts Road" and "College."

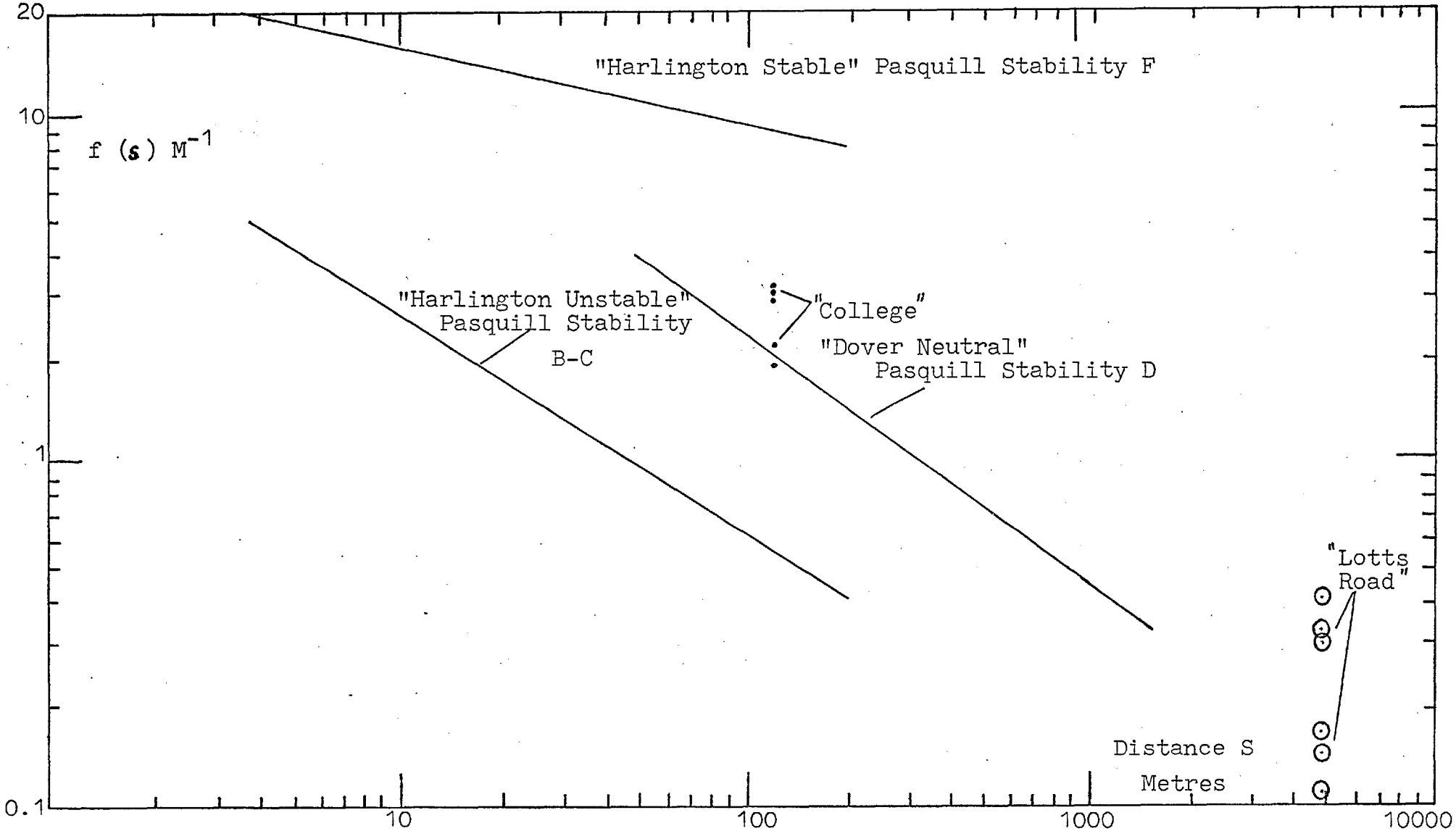

Graph 5.2 A plot of the statistic (f(s) against distance (s) for different Pasquill stability categories and different sites.

5.2.4 Dover Results

Table 5.3 shows a sample of the Dover results. The results from Dover have been regressed and the resultant regression line is plotted on graph 5.2 and labelled "Dover Neutral." The results have been grouped together with a Pasquill stability category of D because the average wind speed on different occasions was normally in excess of three metres per second and the air flow was always over at least a 1500 metre stretch of sea.

The results were regressed using a model of the form:

$$\log f(s) = \log a + b \log s$$

where all logs are to base 10 and

$f(s)$ = Value of statistic (Dependent Variable) metres $^{-1}$

s = Distance (Independent Variable) metres.

a = Intercept of regression line.

b = Slope of regression line.

Table 5.4 is a summary of the results from the regression analysis. On substitution of the gradient and intercept from table 5.4 into the regression model the following is obtained:

$$\log f(s) = 1.87 - 0.75 \log S$$

$$f(s) = 73.8\ s^{-0.75} \qquad \text{Equation 5.2}$$

INDEX REFERENCE NUMBER	DISTANCE S Metres	LOG DISTANCE	WIND VELOCITY M S^{-1}	50% RISE $\frac{c_2-c_1}{\frac{c_1+c_2}{2}\Delta t}$	TIME INTERVAL Δt Secs*	f (S) M^{-1}	Log [f(S)]
M 1**	35	1.54	1.37	8.9	0.1	6.5	0.81
ID 1A	100	2	7.16	1 7.4	0.02	2.39	0.39
ID 2A	100	2	2.65	4.92	0.02	1.86	0.27
ID 6C	100	2	4.21	18.4	0.03	4.37	0.64
ID 6D	100	2	4.26	12.8	0.015	3.00	0.48
ID 7D	150	2.18	3.81	3.6	0.02	0.95	-0.25
M 7**	150	2.18	9.3	18.7	0.07	2	0.3
M 3**	175	2.24	3.65	4.5	0.04	1.2	0.09
M 4**	175	2.24	2.68	9.6	0.04	3.58	0.55
M 2**	200	2.3	2.25	3.15	0.09	1.40	0.15
M 5**	200	2.3	3.26	4.9	0.2	1.5	0.18
ID 6E	1300	3.11	3.26	1.27	0.06	0.39	-0.41
ID 7H**	1300	3.11	2.19	0.45	0.4	0.21	-0.69
ID 6B**	1300	3.11	3	1.2	0.2	0.4	-0.4
M 11**	1300	3.11	2.29	0.51	0.4	0.22	-0.65
M 13**	1300	3.11	2	0.33	0.1	0.17	-0.78

* Quoted to within 5 milliseconds

** Calculated from graphical record

Table 5.3 Some results from Dover under neutral conditions.

SOURCE OF VARIATION	DEGREE OF FREEDOM	SUM OF SQUARES	MEAN SQUARE	F VALUE
DUE TO REGRESSION...	1	5.21	5.21	90.2
DEVIATION ABOUT REGRESSION...	31	1.79	0.058	
TOTAL...	32	7.00		

SAMPLE SIZE N	33
X MEAN.. ($\overline{\log x}$).....	2.51
Y MEAN.. ($\overline{\log y}$).....	-0.026
INTERCEPT. (log a value)	1.87
REG. COEFFICIENT. (b value).....	-0.75
STD. ERROR OF REG. COEF. $S.e_b$	0.079
STD. ERROR OF INTERCEPT $S.e_{\log a}$..	0.20
STD. ERROR OF ESTIMATE S.e.	0.24
CORRELATION COEFFICIENT r	-0.86

Table 5.4 The analysis of variance and regression analysis results for the data obtained from Dover (Neutral).

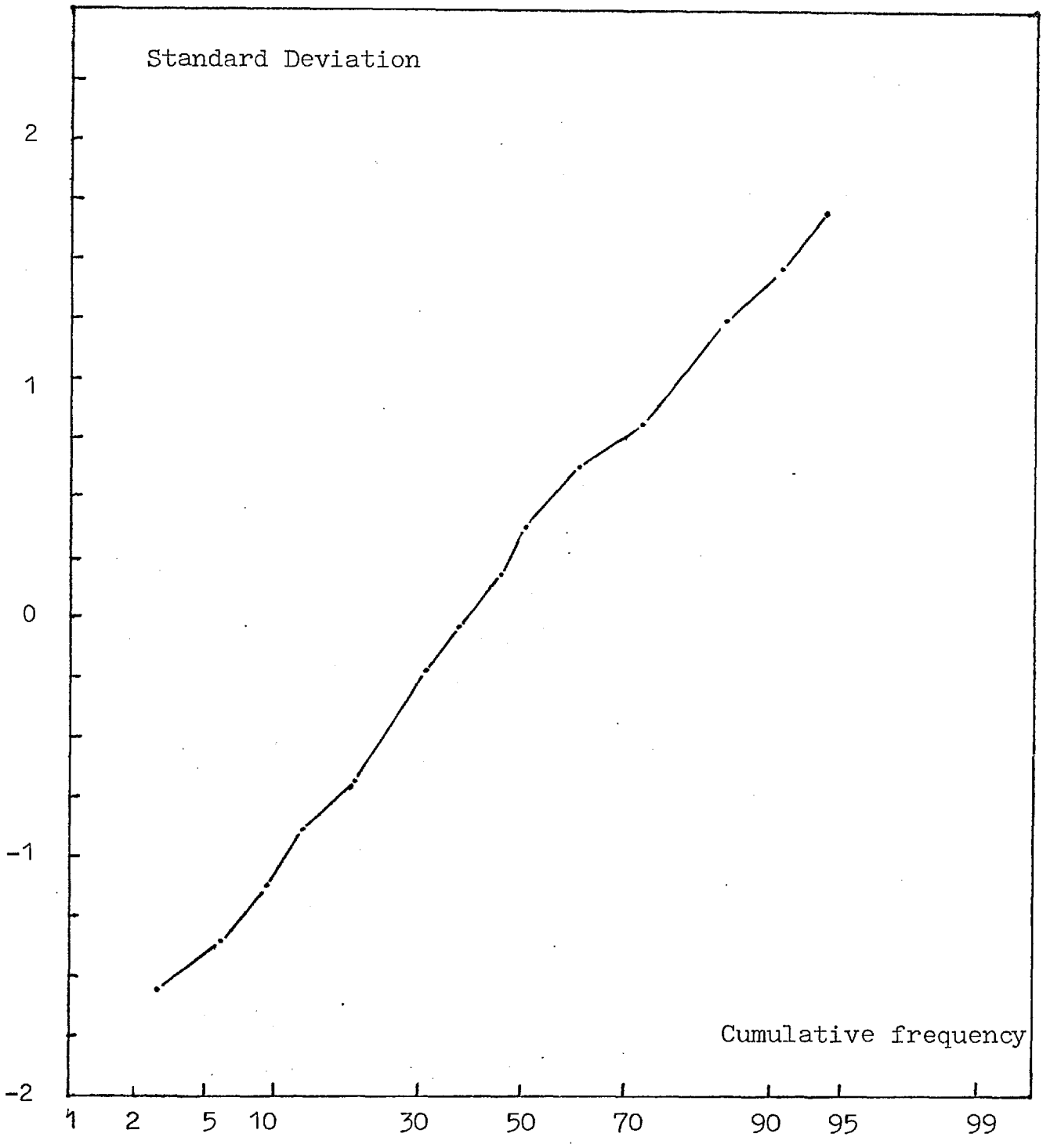

Graph 5.3

Plot of the cumulative frequency for a standardised distribution of the values of the statistic - f(s) - as obtained from the DOVER results.

Graph 5.3 is a plot of the cumulative frequency for a standardised distribution of the values of the statistic obtained from the Dover results.

Using the t-test, both the regression coefficient, b, and the correlation coefficient, r, are found to be significant at the 0.01 level. Using the F-test, the regression is found to be significant at the 0.01 level.

Finally, the relationship between the statistic, f(s), and distance, s , over the range spanned by the results may be expressed as

$$\log f(s) = \left[\log a \pm s.e._{\log a}\right] - \left[b \pm s.e._{b}\right] \log s$$

where the limits of the slope and intercept are standard errors obtained from table 5.4.

i.e. $\log f(s) = (1.87 \pm 0.2) - (0.75 \pm 0.08) \log s$

5.2.5 Harlington Results (Unstable)

Table 5.5 shows a sample of the results obtained at Harlington. The results from Harlington have been regressed and the resultant regression line is plotted on graph 5.2 and labelled "Harlington Unstable." The results have been grouped together with a Pasquill stability Category of B-C. These results were obtained during the afternoon of 1st June 1976 at about 16.00 hours onwards. During the day there had been strong sunshine but the sky became cloudy about 15.00 hours and the winds became stronger rising to approximately four metres per second.

INDEX REFERENCE NUMBER	DISTANCE S Metres	LOG DISTANCE	WIND VELOCITY $M\ S^{-1}$	50% RISE $\frac{c_2-c_1}{\frac{c_2+c_1}{2}}\Delta t$	TIME INTERVAL Δt_* Secs	f(S) M^{-1}	Log[f(S)]
ID 9501	3.8	0.58	4.35	11	0.14	2.5	0.4
ID 9506	3.8	0.58	4.26	19.9	0.09	4.67	0.67
ID 9509	3.8	0.58	4.1	12.5	0.07	3.05	0.48
ID 960E	3.8	0.58	3.98	23.6	0.05	5.93	0.77
ID 96010	3.8	0.58	3.98	28	0.05	7.04	0.85
ID 9604	6.1	0.79	3.29	9	0.16	2.74	0.44
ID 9607	6.1	0.79	3.93	20.5	0.06	5.22	0.72
ID 9608	6.1	0.79	3.47	9.6	0.09	2.77	0.44
ID 960H	6.1	0.79	3.62	18.4	0.05	5.08	0.71
ID 960I	6.1	0.79	4.6	39.6	0.03	8.6	0.93
ID 9501A	15.2	1.18	4.29	7	0.08	1.63	0.21
ID 960A	15.2	1.18	3.62	9.18	0.09	2.53	0.4
ID 960D	15.2	1.18	3.44	4.4	0.17	1.28	0.11
ID 95016	15.2	1.18	5.24	11.3	0.05	2.16	0.33
ID 9705	76	1.88	4.27	2.9	0.17	0.68	-0.17
ID 97011	76	1.88	4.6	4.78	0.23	1.04	0.02
ID 9706	76	1.88	3.96	3.1	0.04	0.78	-0.11
ID 97019	214	2.33	4.92	2.3	0.17	0.47	-0.33
ID 97020	214	2.33	3.47	0.68	0.07	0.19	-0.71
ID 970C	214	2.33	4.26	1.5	0.1	0.35	-0.45

* Quoted to within 5 milliseconds

Table 5.5 Some results from Harlington under unstable conditions (B-C stability Category)

Regression analysis of the results using the same model as for the Dover results yields

$$f(s) = 11.04\ s^{-0.63} \qquad \text{Equation 5.3}$$

Table 5.6 is a summary of the results from the regression analysis.

Graph 5.4 is a plot of the cumulative frequency for a standardised distribution of the values of the statistic obtained from the Harlington (Unstable) results. The straight line graph shows that the distribution is normal.

As for the Dover results, the use of the t-test reveals that both the regression coefficient, b, and the correlation coefficient, r, are significant at the 0.01 level. The F-test shows that the regression is significant at the 0.01 level - the mean square due to regression is significantly greater than the mean square about the regression line.

The relationship between the statistic, f(s), and distance, s, over the range spanned by the results can be expressed as

$$\log f(s) = (1.04 \pm 0.04) - (0.63 \pm 0.03) \log S$$

where the limits of the slope and intercept are standard errors obtained from table 5.6.

SOURCE OF VARIATION	DEGREE OF FREEDOM	SUM OF SQUARES	MEAN SQUARE	F VALUE
DUE TO REGRESSION...	1	14.04	14.04	448.4
DEVIATION ABOUT REGRESSION...	83	2.59	0.031	
TOTAL...	84	16.64		

SAMPLE SIZE N	85
X MEAN ..($\overline{\log x}$).....	1.24
Y MEAN ($\overline{\log y}$).....	0.27
INTERCEPT (log a value)	1.04
REGRESSION COEFFICIENT (b value)	-0.63
STD. ERROR OF REG.COEF. $S.e._b$.....	0.029
STD. ERROR OF INTERCEPT $S.e._{\log a}$	0.04
STD. ERROR OF ESTIMATE S.e.	0.18
CORRELATION COEFFICIENT r	-0.92

Table 5.6 The analysis of variance and regression analysis results for the data obtained from Harlington - Pasquill Stablility Category B-C (Unstable).

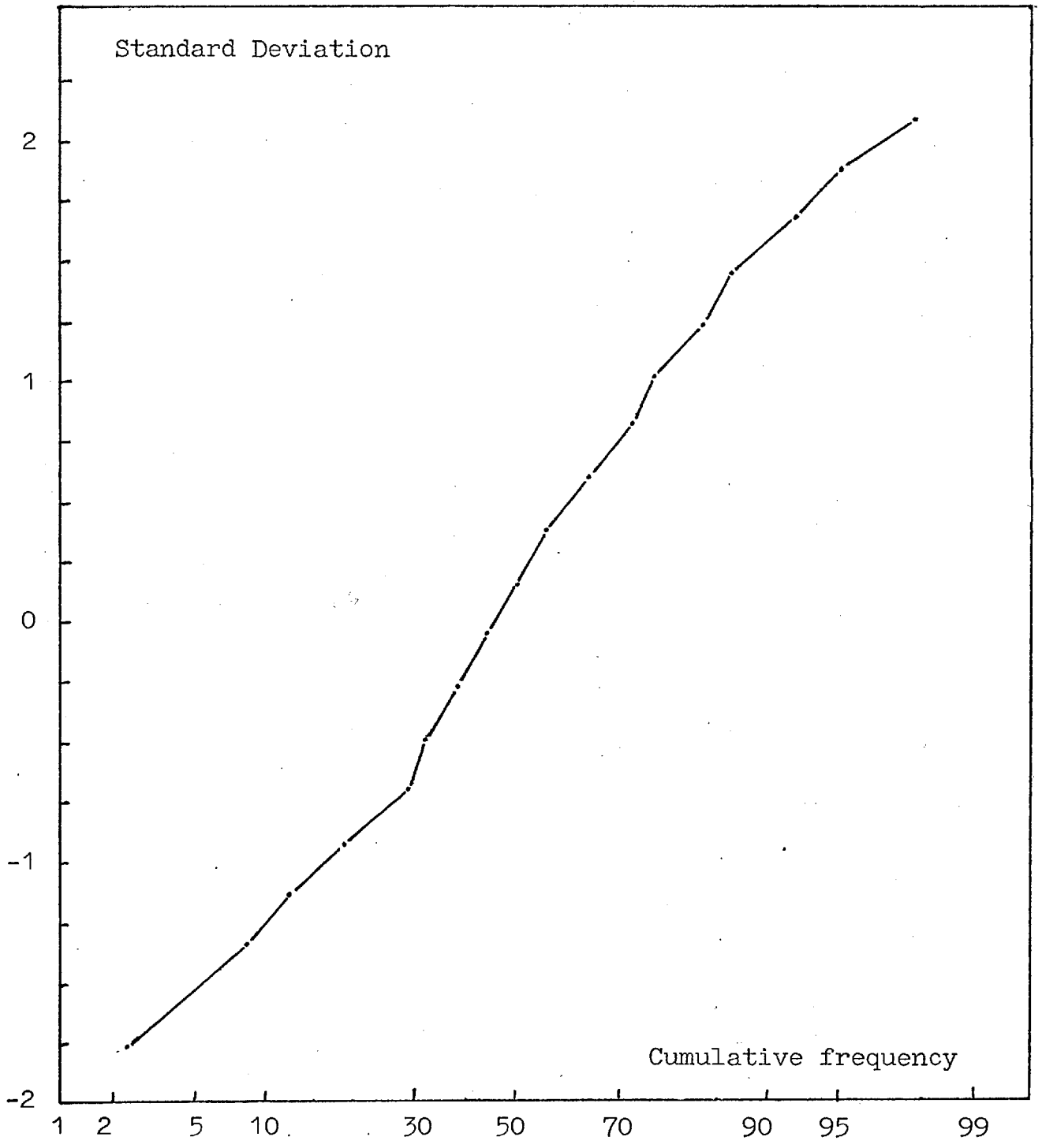

Graph 5.4 Plot of the cumulative frequency for a standardised distribution of the values of the statistic - f(s) - as obtained from the Harlington unstable results.

5.2.6 Harlington Results (Stable)

Table 5.7 shows a sample of the results obtained at Harlington. The results were obtained from about midnight onwards on August 21, 1976. The day had been very hot and the clear evening skies and little wind were ideal for operation in stable conditions. Therefore, the results have been grouped together with a Pasquill stability category of F.

The results have been regressed and the resultant regression line is plotted on graph 5.2 and labelled "Harlington Stable."

The regression analysis gives

$$f(s) = 27.15\ s^{-0.23} \qquad \text{Equation 5.4}$$

Table 5.8 is a summary of the results from the regression analysis.

Graph 5.5 is a plot of the cumulative frequency for a standardised distribution of the values of the statistic obtained from the Harlington (stable) results. The distribution is approximately normal.

Using the t-test, both the regression coefficient, b, and the correlation coefficient, r, are found to be significant at the 0.01 level. Also, the t-test shows that the regression is significant at the 0.01 level.

As with the Dover and Harlington (unstable) results, representing the limits of the slope and intercept as standard errors from table 5.8 gives

$$\log f(s) = (1.44 \pm 0.04) - (0.23 \pm 0.03) \log s.$$

INDEX REFERENCE NUMBER	DISTANCE S Metres	LOG DISTANCE	WIND VELOCITY M S^{-1}	50% RISE $\frac{c_2-c_1}{\frac{c_2+c_1}{2}}\Delta t$	TIME INTERVAL* Δt Secs	f (S) M^{-1}	Log [f(S)]
N11	3.8	0.58	1.2	20.9	0.08	17.4	1.24
N19	3.8	0.58	1.24	48	0.02	38.7	1.59
N1 16	3.8	0.58	1.1	16.7	0.02	15.18	1.18
N1 21	3.8	0.58	0.99	3 3	0.04	33	1.52
N1 26	11.4	1.06	1.16	17.1	0.06	14.7	1.17
N1 36	11.4	1.06	1.23	49	0.03	39.8	1.6
N1 42	11.4	1.06	1.07	11.8	0.07	11.0	1.04
N1 45	11.4	1.06	0.87	21	0.03	24.1	1.38
N2E	61	1.78	1.7	11.2	0.05	6.59	0.82
N2J	61	1.78	1.2	10.5	0.1	8.75	0.94
N2K	61	1.78	1.1	7.3	0.07	6.6	0.82
N2L	61	1.78	1.2	14.5	0.05	12.1	1.08
N2U	91.2	1.96	1.19	9.1	0.04	7.65	0.88
N2V	91.2	1.96	1.47	25	0.03	17	1.23
N3E	91.2	1.96	0.95	9.1	0.09	9.6	0.98
N2T	91.2	1.96	1.2	5.7	0.04	4.75	0.68
N5B	144	2.16	1.1	12.1	0.03	15.1	1.18
N5C	144	2.16	0.85	9.3	0.02	10.9	1.04
N5A	144	2.16	0.85	5.3	0.04	6.2	0.79

* Quoted to within 5 milliseconds

Table 5.7 Some results from Harlington under Stable Conditions.

SOURCE OF VARIATION	DEGREE OF FREEDOM	SUM OF SQUARES	MEAN SQUARE	F VALUE
DUE TO REGRESSION...	1	1.63	1.63	4 69
DEVIATION ABOUT REGRESSION ...	123	4.27	0.03	
TOTAL...	124	5.89		

SAMPLE SIZE N.....	125
X MEAN.. ($\overline{\log x}$)	1.19
Y MEAN.. ($\overline{\log y}$)	1.16
INTERCEPT (log a value)	1.44
REG. COEFFICIENT. (b value)	-0.23
STD. ERROR OF REG. COEF. $S.e_b$.....	0.034
STD. ERROR OF INTERCEPT S.e . log a.	0.04
STD. ERROR OF ESTIMATE S.e	0.19
CORRELATION COEFFICIENT r.....	-0.53

Table 5.8 The analysis of variance and regression analysis results for the data obtained from Harlington - Pasquill stability Category F (Stable).

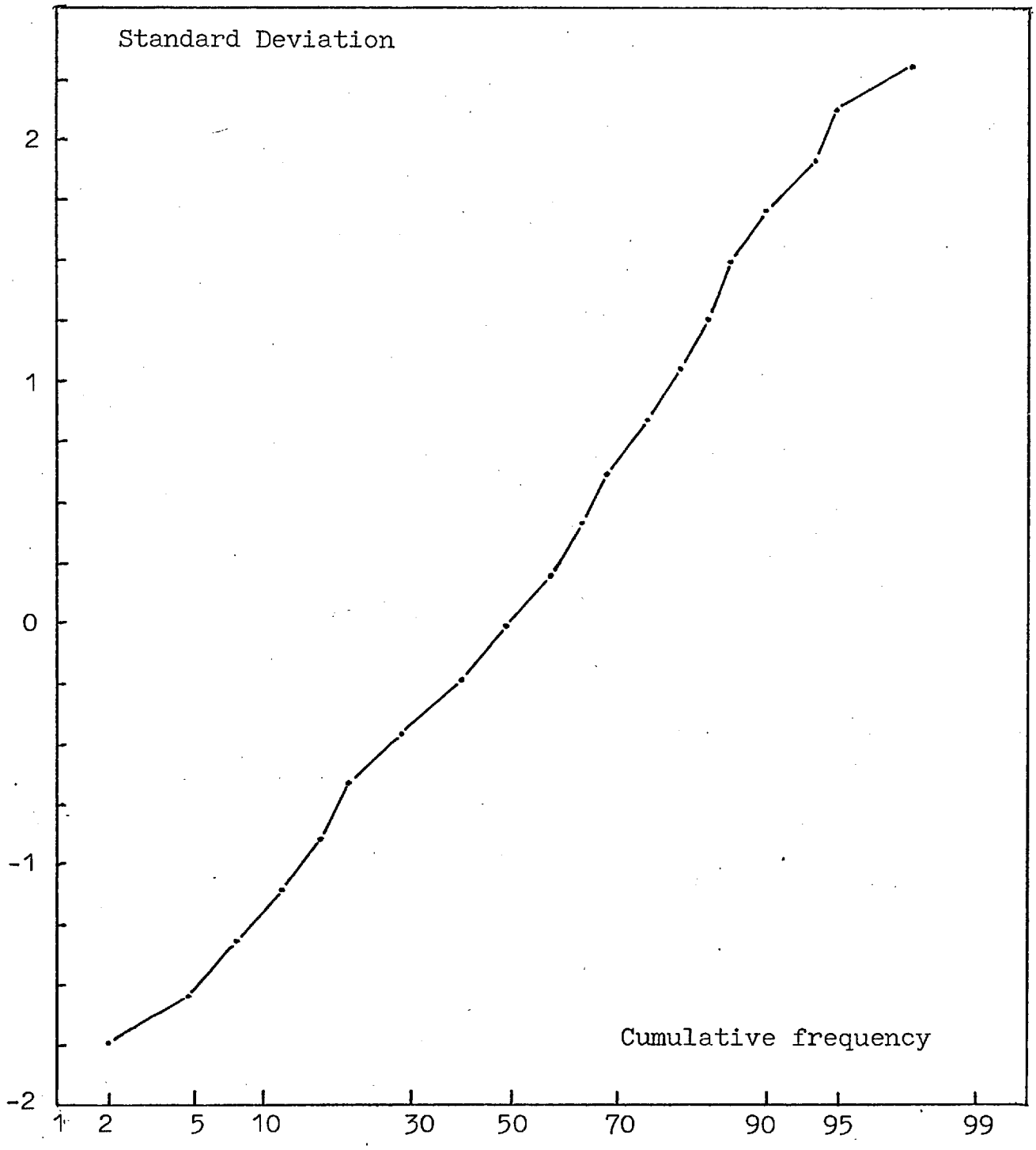

Graph 5.5 Plot of the cumulative frequency for a standardised distribution of the values of the statistic - f(s) - as obtained from the Harlington stable results.

5.2.7 London Results

The results obtained on the Aeronautics roof at Imperial College are shown in table 5.9. The results have not been regressed and are plotted as on graph 5.2 according to the following headings:

a. College.

This refers to signals recorded from pollution emitted by the college boiler's chimney under a cold clear night sky in March 1976 at about 18.00 hours.

b. Lotts Road.

This refers to signals recorded from pollution emitted by Lotts Road power station under a cloudy sky in May 1976 with a southerly wind of 6-8 m sec $^{-1}$. The results shown in table 5.9 are split according to morning and afternoon periods. The morning results were obtained at about 11.00 hours and the afternoon results were obtained around 17.00 hours.

5.3 Further Results

5.3.1 Signal Fluctuations

The fluctuation relative to a local mean calculated for one rise in a signal - f(s) - is only one of many possible statistics that may be useful in characterising a signal. One particular feature apparent in the results is illustrated in graphs 5.6 A-F; the amount of change in the signal per unit time varies for sources at different distances. These graphs relate to results obtained at Harlington with a Pasquill stability category B-C. The following technique is used to

EMISSION SOURCE DESCRIPTION	INDEX REFERENCE NUMBER	DISTANCE S Metres	LOG DISTANCE	WIND * VELOCITY M Sec^{-1}	50% RISE $\frac{c_2-c_1}{\frac{c_1+c_2}{2}} \Delta t$	TIME INTERVAL Δt Secs **	f(S)	Log[f(S)]
COLLEGE	ID 30D	125	2.09	4.2	15.3	0.01	3.64	0.56
COLLEGE	ID 30aa	125	2.09	4.2	13.1	0.01	3.12	0.49
COLLEGE	ID 30bb	125	2.09	4.2	10.4	0.02	2.48	0.39
COLLEGE	ID 30cc	125	2.09	4.2	8.8	0.03	2.09	0.32
COLLEGE	ID 30I	125	2.09	4.2	12.6	0.02	3.00	0.48
LOTTS ROAD MORNING	ID 9302	4800	3.68	6.94	2.19	0.16	0.32	-0.5
LOTTS ROAD MORNING	ID 9303	4800	3.68	6.94	1.2	0.45	0.17	-0.76
LOTTS ROAD MORNING	ID 9304	4800	3.68	6.94	1.0	0.14	0.14	-0.84
	ID 9306	4800	3.68	6.94	0.78	0.19	0.11	-0.95
LOTTS ROAD AFTERNOON	ID 9401	4800	3.68	6.94	1.16	0.14	0.17	-0.78
LOTTS ROAD AFTERNOON	ID 9402	4800	3.68	6.94	2	0.22	0.29	-0.54
LOTTS ROAD AFTERNOON	ID 9403	4800	3.68	6.94	2.7	0.15	0.39	-0.41

Table 5.9 This table shows the results obtained from the College boiler's chimney and from Lotts Road power station.

* Wind velocity as determined from the Meteorology Department, Imperial College.

** Quoted to within 5 milliseconds.

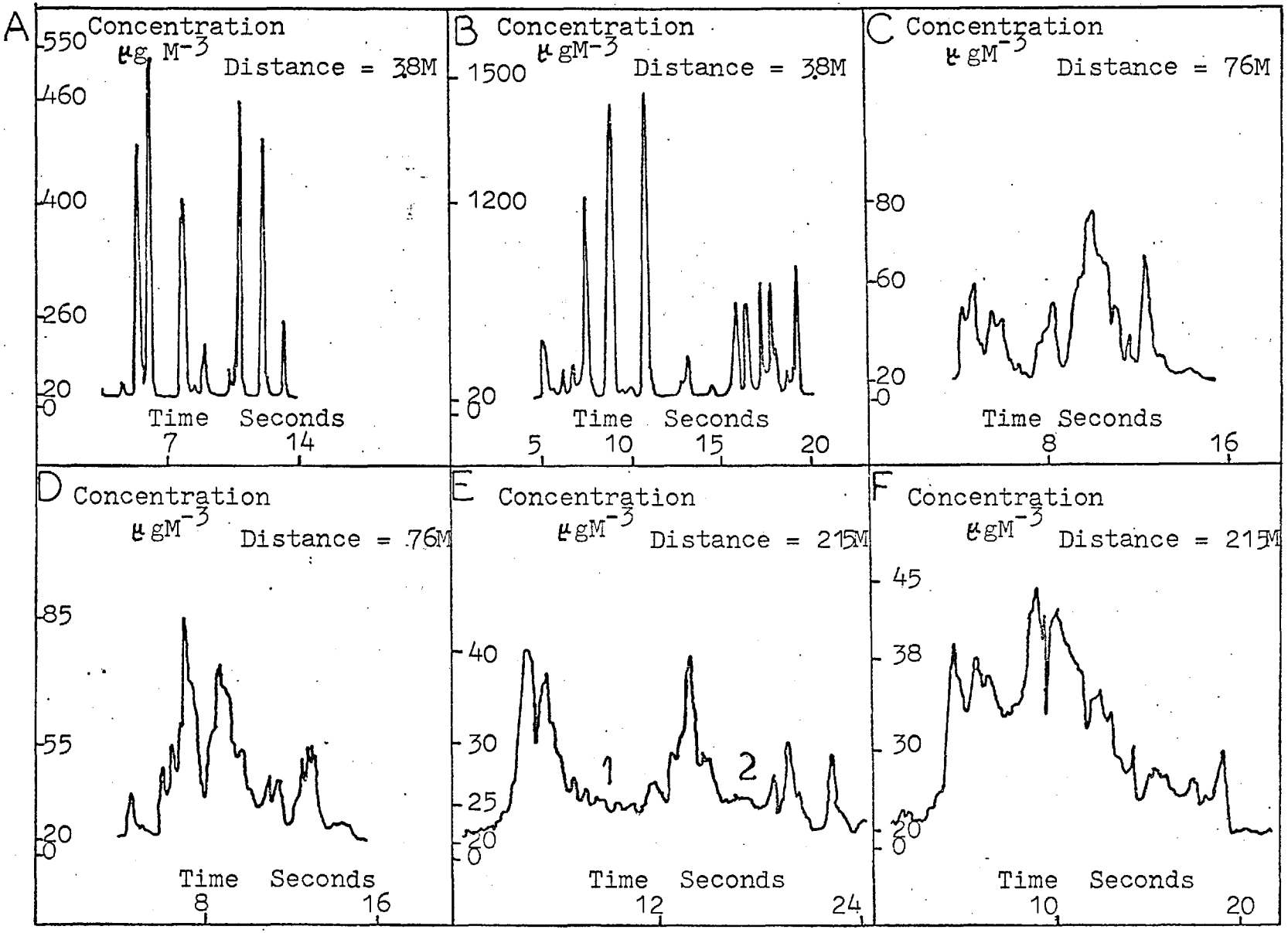

Graph 5.6A-F Results from Harlington (Unstable) Pasquill stability Category B-C.

estimate the percentage change relative to the mean signal level occurring per second. The technique utilises only the significant rises and falls in a signal and slowly varying portions of the signal like regions "1" and "2" in graph 5.6 E are not used:-

1. From the concentration - time output calculate the arithmetic mean concentration for the entire signal .

2. Sum the percentage changes relative to the mean for the significant rises and falls occurring above the noise level.

3. Divide the total sum by the time T in seconds for which the significant rises and falls last and also divide by the average wind velocity $\bar{u}$ i.e.

$$F(s) = \frac{1}{\bar{u}\,T} \sum_{rise}^{fall} \frac{\Delta c}{mean} \cdot (100) \qquad \text{Equation 5.5}$$

where Δ c refers to the difference in concentration between a local peak and trough in a given part of the signal.

Table 5.10 shows values of F(s) calculated for a range of distances at different sites. Also listed in the table are the following:

a. The background concentration for each site in $\mu g\ M^{-3}$.

b. The maximum rate of change for a rise and fall in a signal calculated from $\Delta C/\Delta T$ where ΔC - as in equation 5.5 - is the difference in concentration between a local peak and trough in a given part of the signal lasting for ΔT seconds.

INDEX REFERENCE NUMBER	SITE	PASQUILL STABILITY CRITERIA	BACKGROUND CONCENTRATION $\mu g\ M^{-3}$	$\frac{C_2-C_1}{\Delta T}\ \mu gM^{-3}\ s^{-1}$ RISE	FALL	DURATION PUFF SECONDS	DISTANCE S Metres	F(S)
ID 9501	HARLINGTON	B - C	18	1961	1423	2	3.8	150
ID 9502				2821	1122	1.1		136
ID 9509				1802	936	2.2		167
ID 95012				872	596	1.2		151
ID 9602				1044	542	0.5	6.1	252
ID 9604				6995	7794	1.2		156
ID 970A				180	226	5.3	7 6	60
ID 9703				164	222	22		53
ID 97013				56	74	5		35
ID 97017				70	88	25	215	23
ID 970C				146	116	21.5		27
ID 970D				104	114	17.5		27
N1 5	HARLINGTON	F	20	62605	39615	2.5	3.8	670
N1 11				33090	47175	1.5		326
N1 14				86582	35902	12		196
N 3D				4657	2870	11	91	220
N 5C				545	491	220	144	280
ID 1A	DOVER	D	14	356	242	40	100	53
ID 6C				1257	603	19		66
ID 6B				543	305	50	1300	2
ID 6E				330	345	60		16
ID 9303	LOTTS ROAD		60	209	157	160	4800	24
ID 9403				581	597	410		14

Table 5.10 This table shows the statistic F(S) and other puff characteristics for a variety of distancds at different sites.

c. The duration of the signal in seconds.

F(s), in table 5.10, shows a marked decrease as source distance is increased from 3.8 metres to 215 metres for the results at Harlington - unstable. This is also the case for the results at Dover, however, for the results at Harlington - Stable - there is no obvious decrease in F(s) with increasing distance. Two results are also shown for Lotts Road power station. It is recognised that only a small sample of the total results have been treated in this way.

5.3.2 Graphical Results

The two statistics f(s) and F(s) so far used go some way in characterising the signals obtained at different sites from sources at different distances. At the same time visual description of the signals, although often made difficult because of the effect of the square law, is also useful when discussing the results. To aid in a discussion use is made of the intermittency factor and the peak-mean ratio, as described in Chapter 4.

Graphs 5.6 to 5.19 show the graphical records that will be referred to in the following discussion - they have been reproduced here for illustrative purposes.

A) Dover.

Graphs 5.7 to 5.9 show three signals received from ships passing to within 100 metres of the detector. The values of f(s) are calculated from the parts labelled A B and C on graphs 5.7, 5.8 and 5.9 respectively. Values of F(s) have been estimated for graph 5.7 (ID1A in table 5.10) and for

graph 5. 9 (ID6C in table 5.10). The calculation of F(s) typically involves the most striking peaks and troughs visible, particularly in the leading edge of all three graphs, but neglecting regions such as those labelled D on graph 5.7 and E on graph 5.8.

These three graphs serve to illustrate one obvious disadvantage of using a statistic as calculated from equation 5.5. The mean signal level will be strongly influenced by the slowly varying tail-portions in graphs 5.7, and 5.9, even though these portions contribute little to the amount of change in concentration per unit time.

Graphs 5.10 and 5.11 show two signals received from ships at a distance of approximately 1300 metres from the detector. Both signals contain noise from the photo-multiplier. The rises labelled F on graph 5.10 and G on graph 5.11 have been used to calculate values of f(s). A difficulty encountered in determining a value of F(s) is highlighted in these two graphs; namely the presence of photomultiplier noise. A rise for which Δ C can be calculated for use in equation 5.5 is taken from point 1 to point 2 on graph 5.10, similarly for a fall, Δ C is calculated over the portion 4 to 3 on graph 5.11. Therefore, the noise is effectively numerically filtered by averaging the concentration changes ΔC over times greater than the period of the noise fluctuations.

A notable feature concerning the work at Dover was the shape and position of the sampling site. The apparatus was placed in a well about 0.7 metres deep at the end of the Admiralty Pier Extension. The Pier is approximately 10 metres above sea level and extends to about 1500 metres from the shore into the English Channel. The presence of this bluff structure in an otherwise fairly open terrain would have produced an aberration in the background wind flow - the flow which would have existed in the absence of structure - around and over the Pier.

The main characteristic of the flow over the Pier was probably a highly turbulent wake usually associated with such flow disturbances. The characteristic of the turbulent wake would be dependent upon the free air stream speed and direction relative to the pier. Generally with such flows, there is an upwind portion of the wake adjacent to the lee walls and top of the structure called a cavity in which the mean flow is toroidal. The particular flow structure existing around the pier extension may have been such that the sampling area was in a cavity. The result of this would be that plumes from ships may have been distorted by their passage over the pier and this would affect the concentration fluctuations recorded. An attempt was made to position the detector beyond the front end of the pier so as to clear the cavity but fear of losing the equipment, to say the least, in the English Channel together with practical difficulties prevented the attempt from succeeding.

Out of all of the signals recorded from ships at Dover, the highest concentrations were detected from British Rail Car Ferries - the "Caesarea" in particular at distances of 50 metres. On occasions, concentrations well in excess of 2500 $\mu g\ M^{-3}$ were recorded from the Caesarea at this distance and fits of coughing were experienced. Often, whilst waiting for pollution to reach the detector from a known ship, a smell - possibly of diesel fuel - could be perceived a few seconds before the detector responded.

Finally, peak-mean ratios of about 1.4 to 2.8 for far sources and 1.8 to 5 for near sources have been recorded. These values are not representative of a distribution of peak-mean values at different distances but are the maximum and minimum values obtained.

B) Harlington Unstable.

A noticeable feature concerning the results at different distances for Pasquill stability category B-C is the difference in the shape of the signals, as seen in graph 5.6 A - F. At very near distances- 3.8 metres - the signals are very spiky in appearance lasting about one second or less. The signals received from a distance of 215 metres last for about twenty seconds or more having a "peaky" appearance as opposed to the spikes at 3.8 metres.

The intermittency factor at a distance of 3.8 metres is 0.56 falling to 0.3 at 215 metres and peak-mean ratios vary from a maximum of 4.8 at 3.8 metres to a minimum of 1.3 at 215 metres.

Values of f(s) for graph 5.6 C - F have all been found for the rises on the leading edge of the signal. For graph 5.6 A -B there are several distinct signals for each of which a value of f(s) has been calculated.

C) Harlington Stable.

Graph 5.12 - 5.17 show some signals received from a variety of distances at Harlington for a Pasquill stability category F.

Under the stable night conditions at Harlington, the recorded signals have a peaky appearance at 3.8 M with a duration of five seconds or more and still retain a similar shape at greater distances but, generally, of duration of 30 seconds or more, in fact at 150 metres a plume was sampled for more than two minutes. Also, at this distance a narrow "ribbon-like plume" could clearly be seen in the moonlight moving towards the detector showing little meander. Unfortunately, the plume passed to within about 15 metres of the detector and was not detected.

At a distance of 3.8 metres the intermittency factor is 0.64 but for distances of 100 metres or more intermittencies vary from very low values, where no sulphur was measured, to very high values when sulphur dioxide was sampled continuously for minutes.

D) Lotts Road Power Station.

Graph 5.18 and 5.19 show two signals received from pollution emitted from Lotts Road power station detected on the Aeronautic's roof at Imperial College.

The leading edge of graph 5.18 is clearly the most significant part of the signal from the point of view of calculating f(s). However, this signal is not typical of the other signals detected from Lott's Road because of the appearance of the "decaying" trailing edge labelled "A" on graph 5.18. Graph 5.19 shows only part of the signal actually recorded but the whole signal does not exhibit this decaying tendency. Accompanying the periods where there are the rises and falls notable in graphs 5.18 and 5.19, there are periods when the concentration changes much less with time and in some cases the signal above the background is so steady - for about 20 seconds - that it looks like a baseline signal.

5.3.3 Logarithmic Probability Distributions

The cumulative probability distribution of concentration of any signal or series of signals was obtained from the computer output, however, this distribution invariably contained background readings. The background readings were subsequently subtracted from the original distribution and a new distribution was formed by hand. Graphs 5.20 to 5.22 show the distributions plotted on log-normal probability graph paper where the concentration - ordinate - is the concentration above the background concentration. A total of 68 distributions were plotted but only five are shown here.

The necessary information relating to each curve is shown on the respective graphs and it is left just to mention the following:

The curve labelled "sum of 8 signals" on graph 5.21 has been produced by cumulating the concentration distribution from eight individual signals received at the detector from a distance of 3.8 metres. The graph shows the distribution of the 8 signals to be approximately log-normal.

Generally the 68 distributions plotted display greater deviations from the approximate "sum of 8 signals" straight line plotted on graph 5.21. The deviations from a straight line are similar to those deviations illustrated in the lines plotted on graphs 5.20 to 5.22 and are to be found on the plots produced from signals received at both near and far distances.

5.3.4 Effect of Averaging Time on Maximum Concentration

A small sample of results have been plotted from a range of distances to show the effect of a change in averaging time on the maximum concentration. Graph 5.23 shows three such results.

In each case the maximum concentration has been determined from the computer output using averaging times varying from concentrations averaged every 20 readings/sec. down to 1 reading/sec.

The results clearly show from this small sample that the change in averaging time from 20 readings/sec to 1 reading/sec has a large effect on the maximum concentration from sources at near distances and only a small effect on sources at large distances (>400 m).

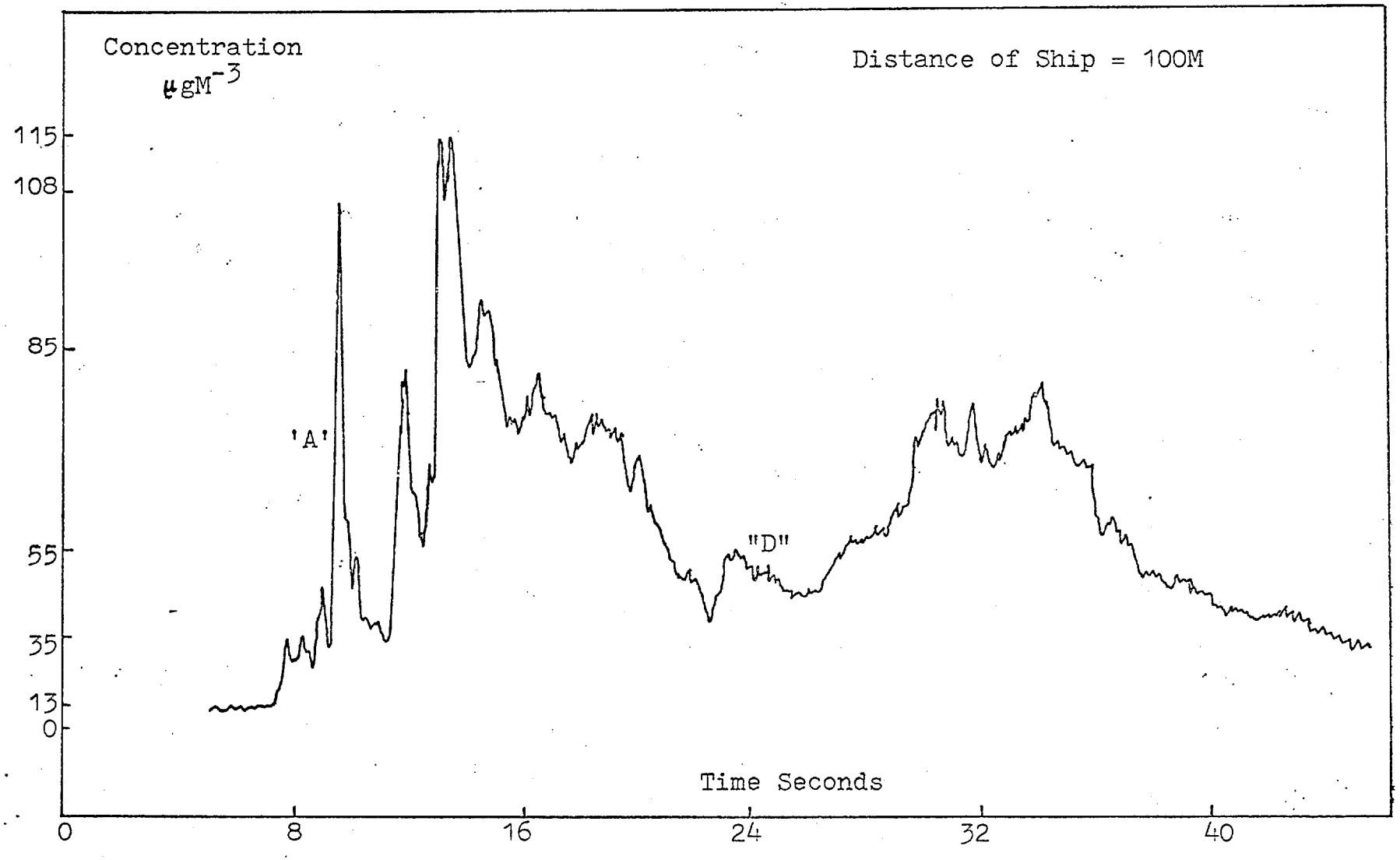

Graph 5.7 This is a puff from a ship travelling to within 100 metres of the detector at Dover.

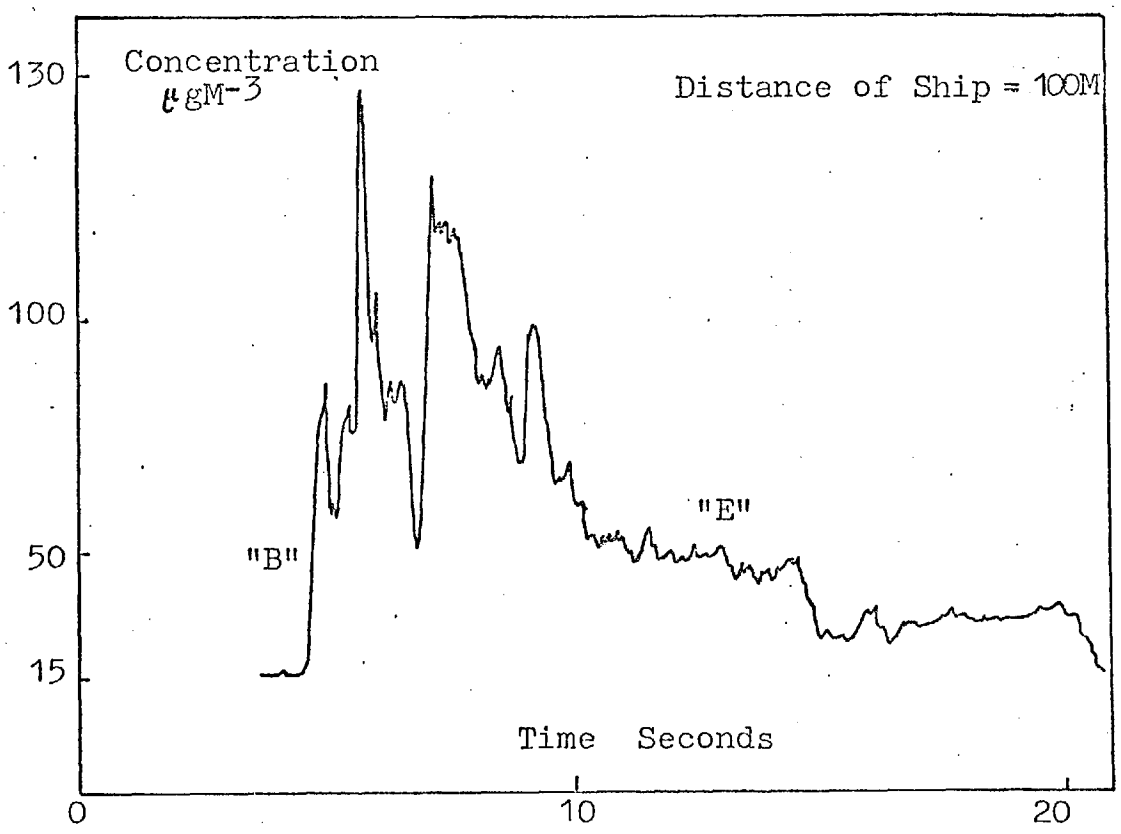

Graph 5.8 This a puff received from a ship travelling to within 100 metre of the detector at Dover.

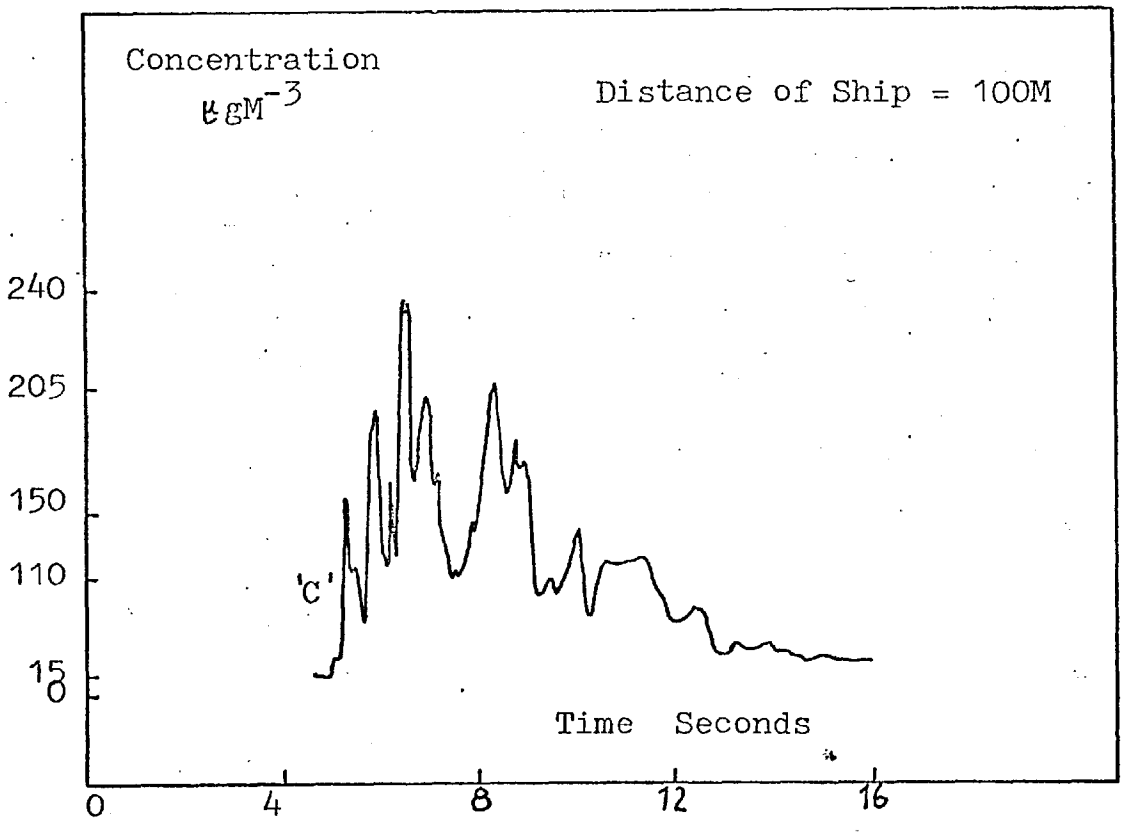

Graph 5.9 This shows a puff received from a ship travelling to within a 100 metre of the detector at Dover.

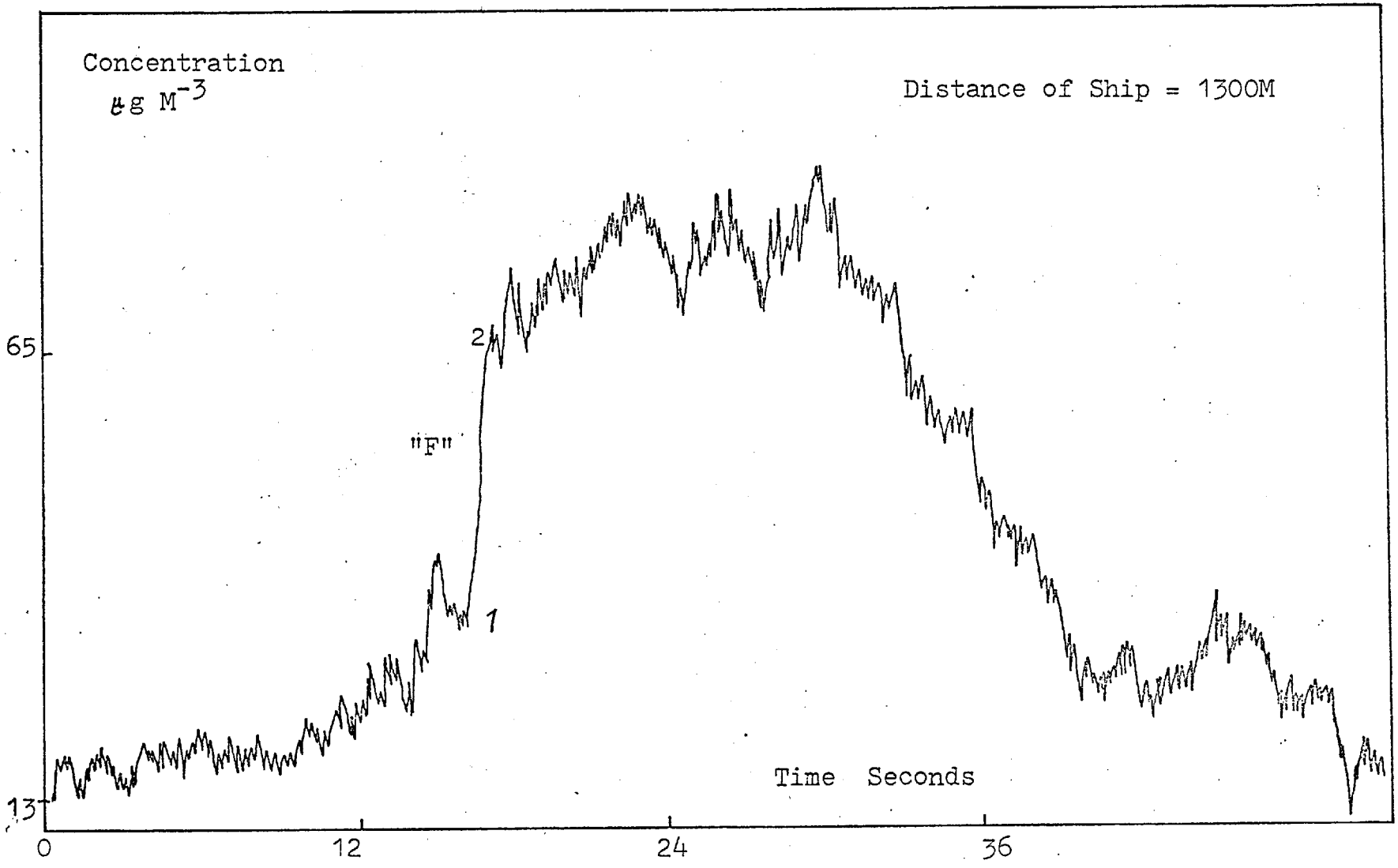

Graph 5.10 This graph shows a puff received from a ship 1300 metres from the detector at Dover.

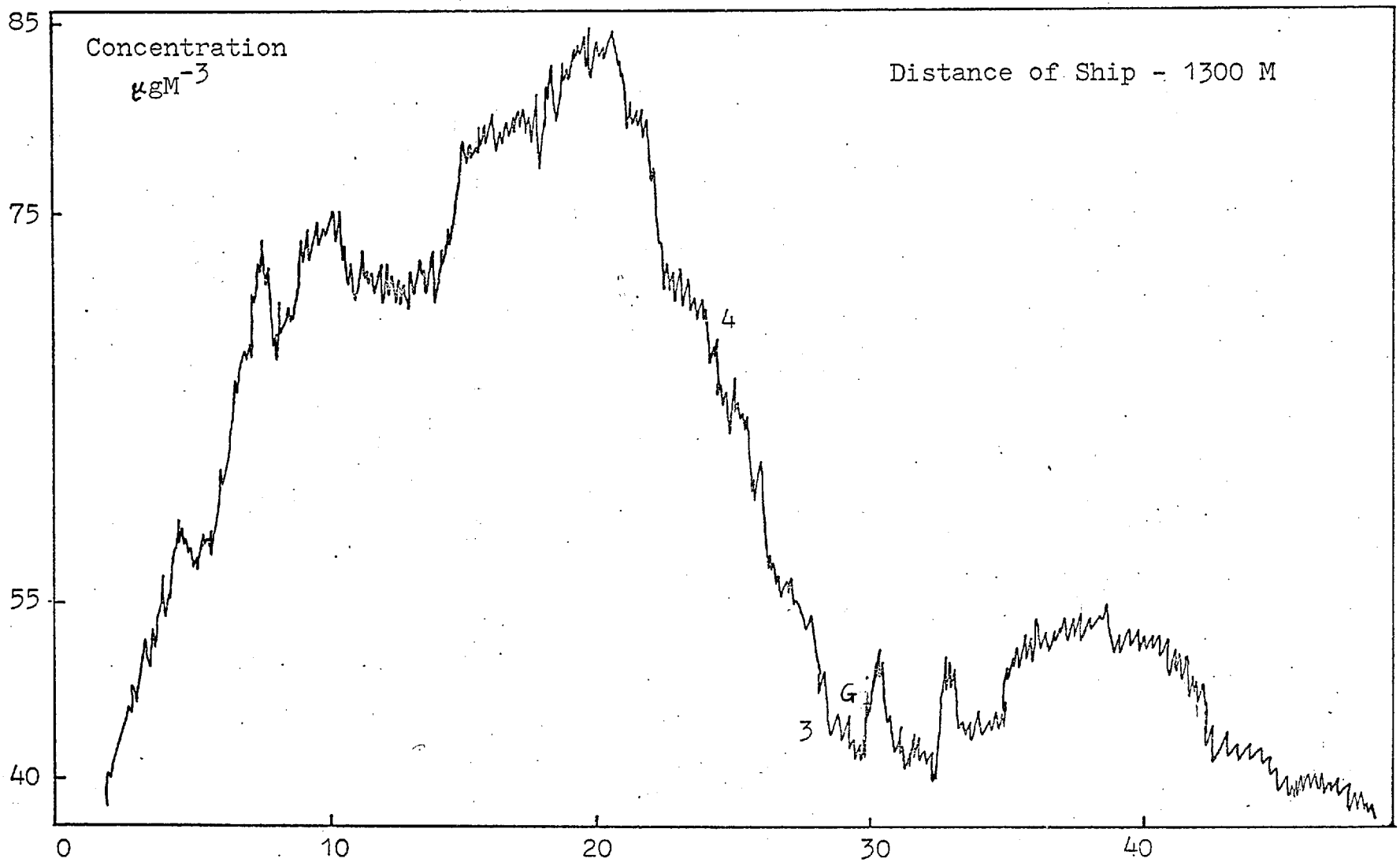

Graph 5.11 This graph shows a puff received from a ship 1300 metres from the detector at Dover.

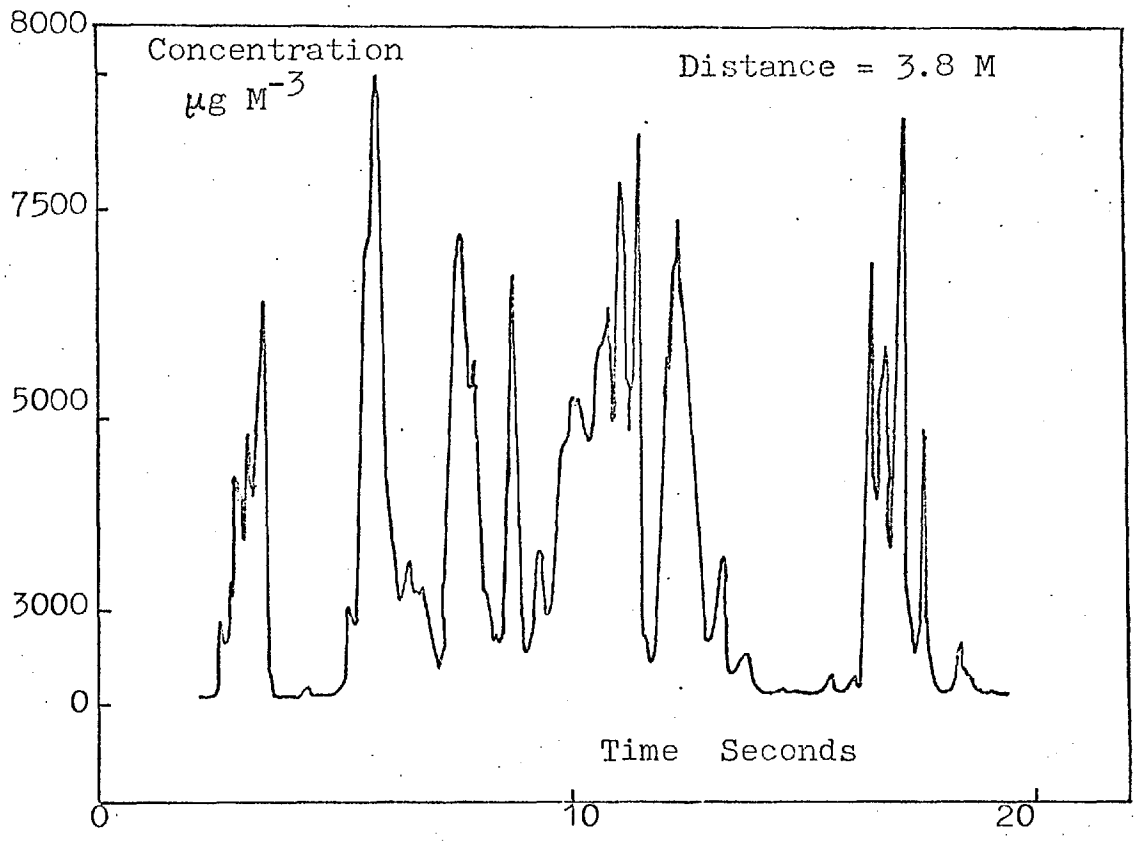

Graph 5.12 This shows a puff from a sulphur source at 3.8M at Harlington (Stable) with a Pasquill Stability Category F.

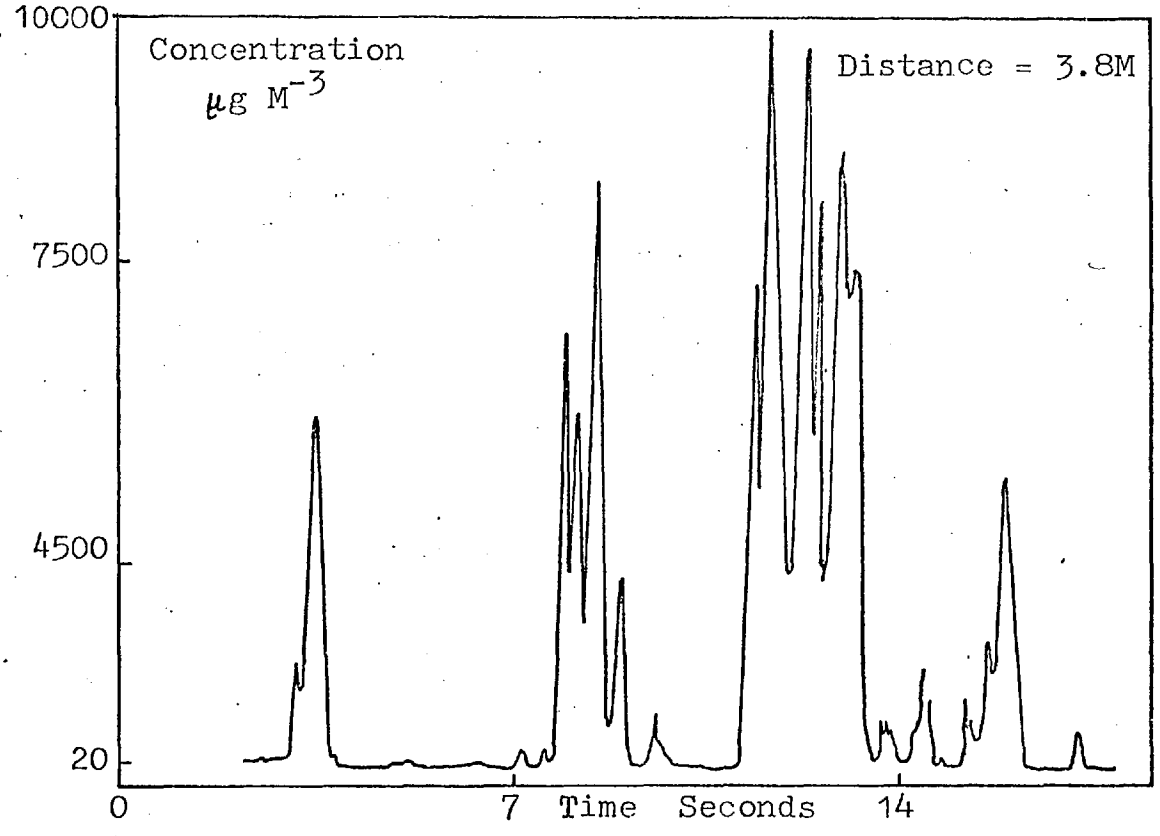

Graph 5.13 This shows a puff from a sulphur candle at 3.8M at Harlington (Stable) with a Pasquill stability Category F.

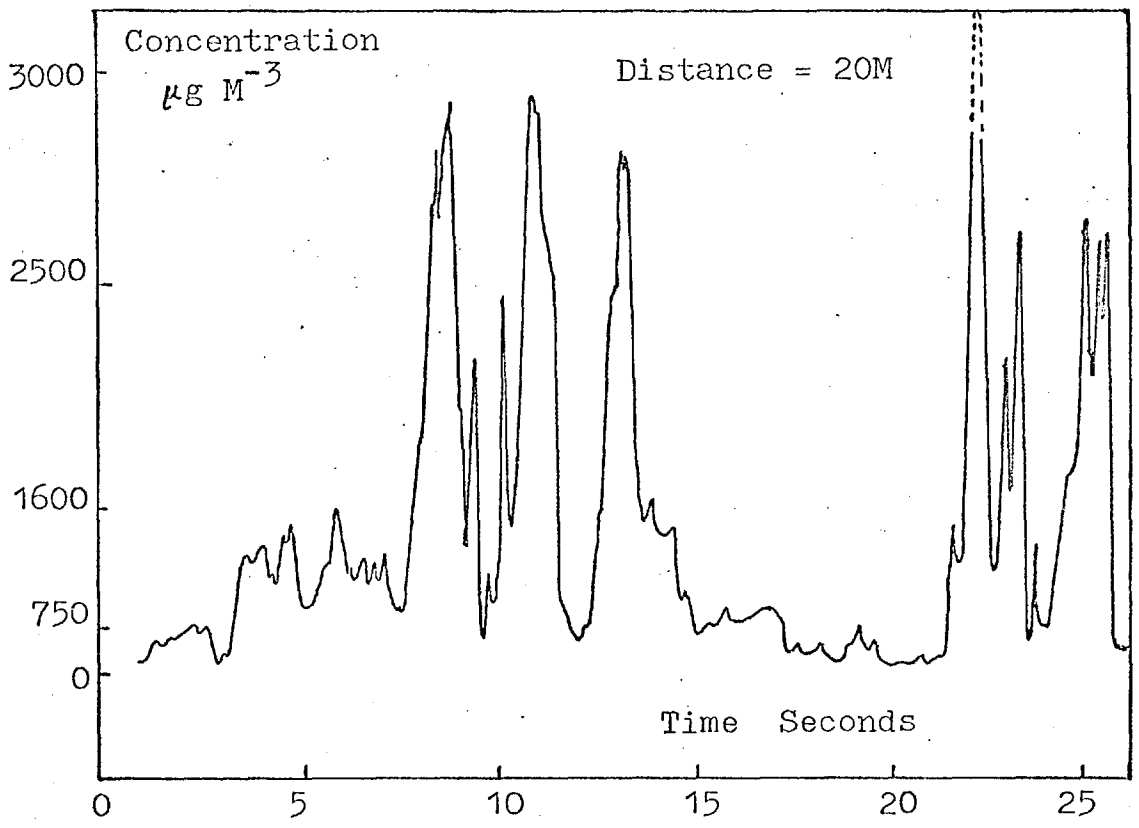

Graph 5.14 This graph shows a puff received from a sulphur candle at a distance of 20 M - Harlington Stable.

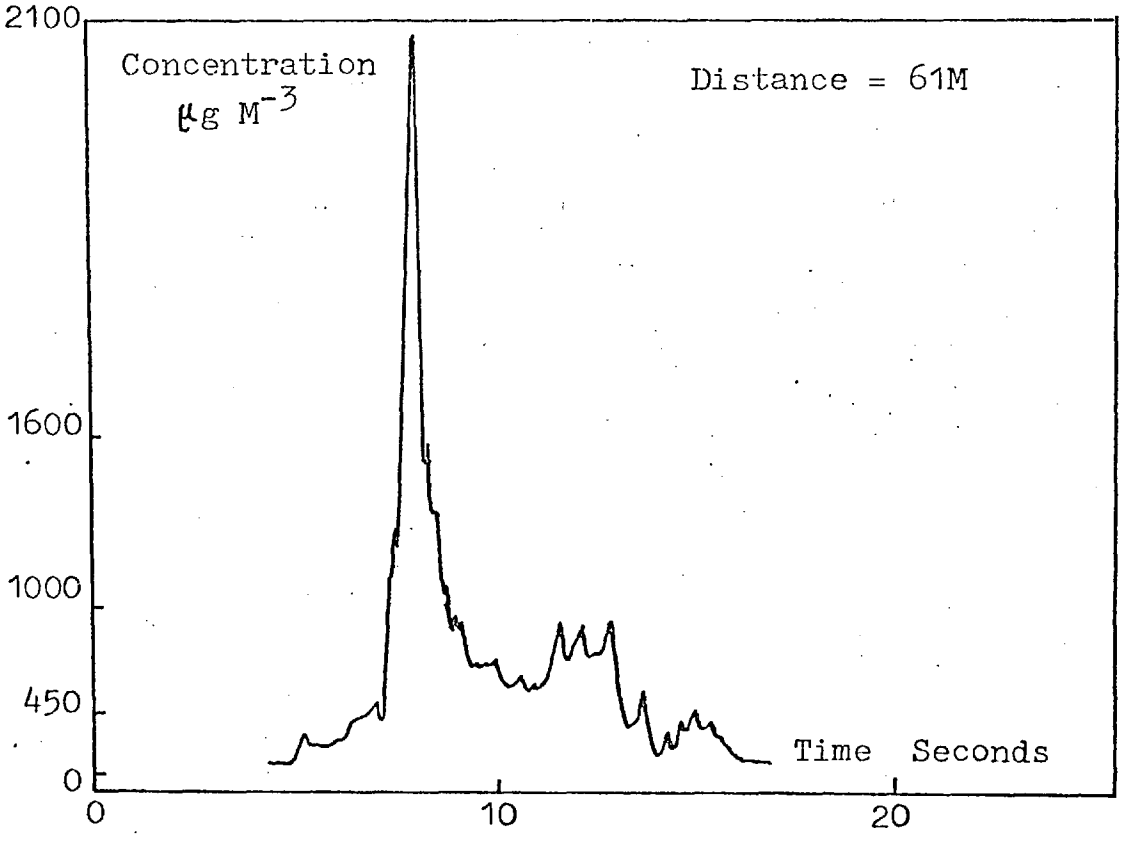

Graph 5.15 This graph shows a puff received from a Sulphur candle at a distance of 61 M - Harlington Stable.

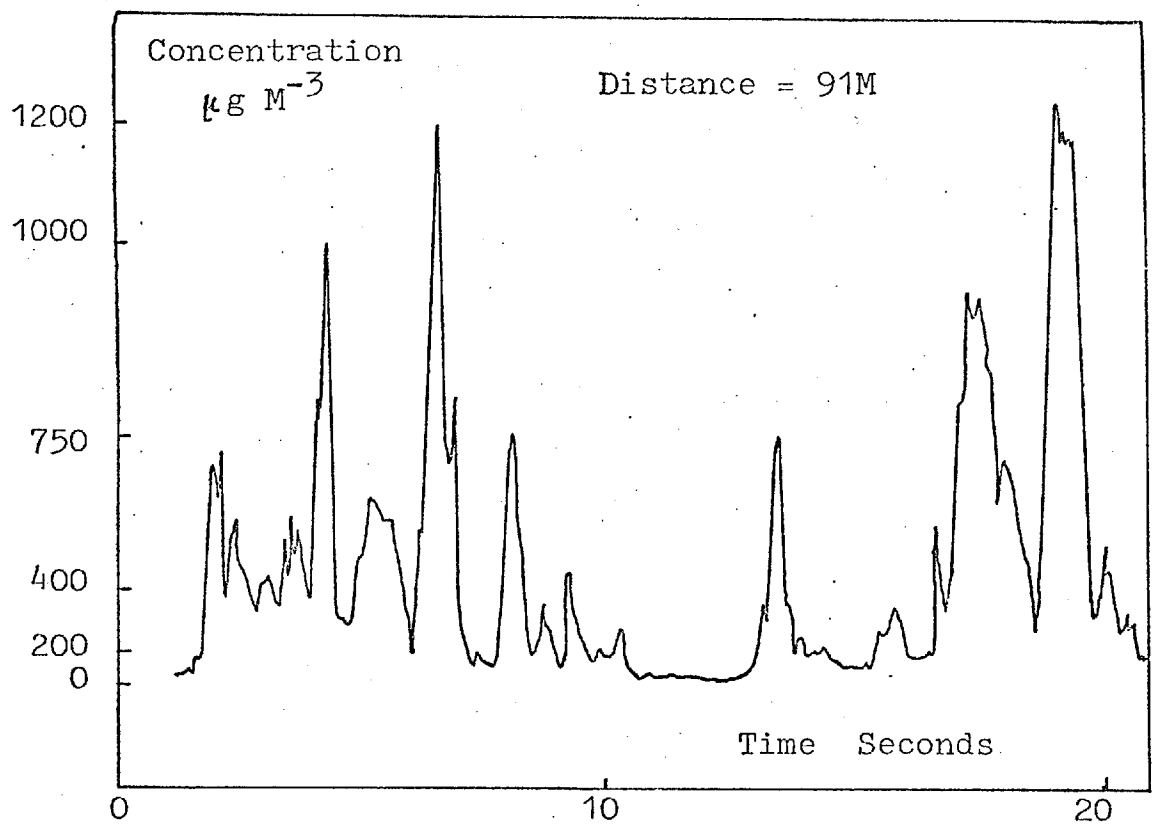

Graph 5.16 This shows a puff received from a sulphur source at a distance of 91M - Harlington Stable.

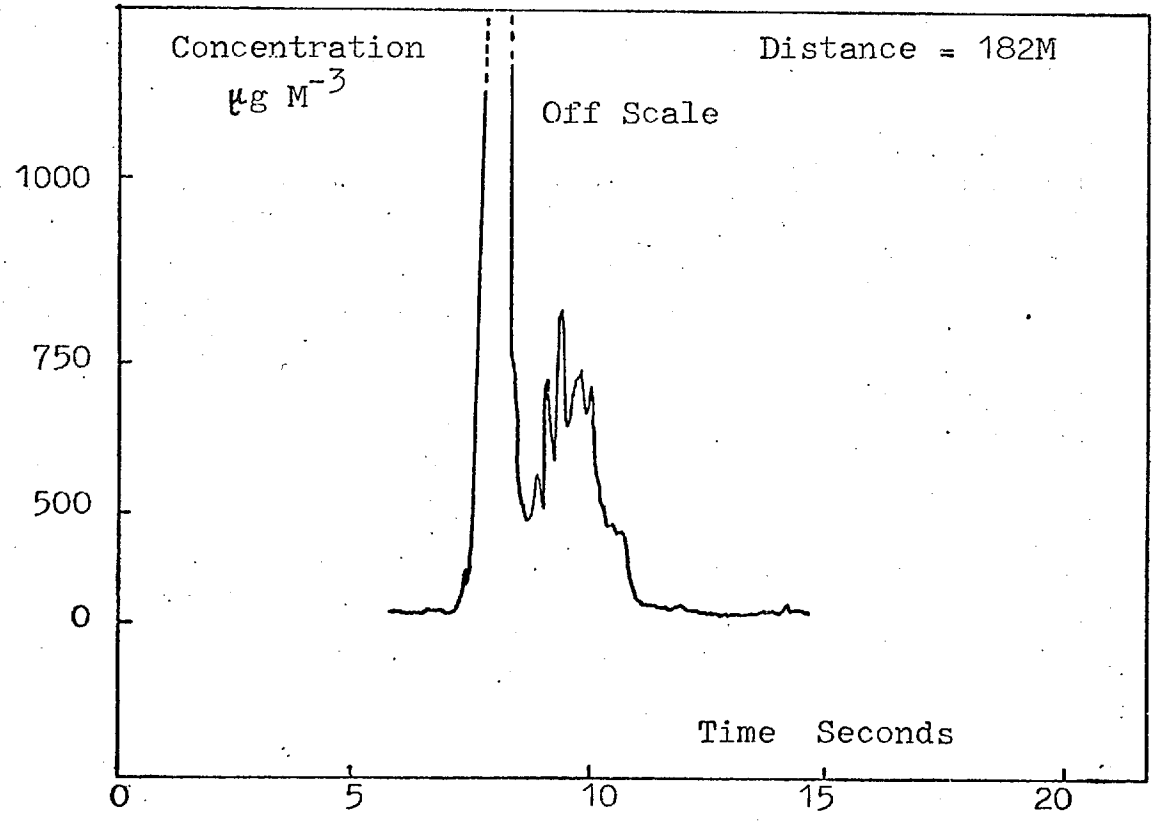

Graph 5.17 This is a puff received from a sulphur candle a distance of 182 M - Harlington Stable.

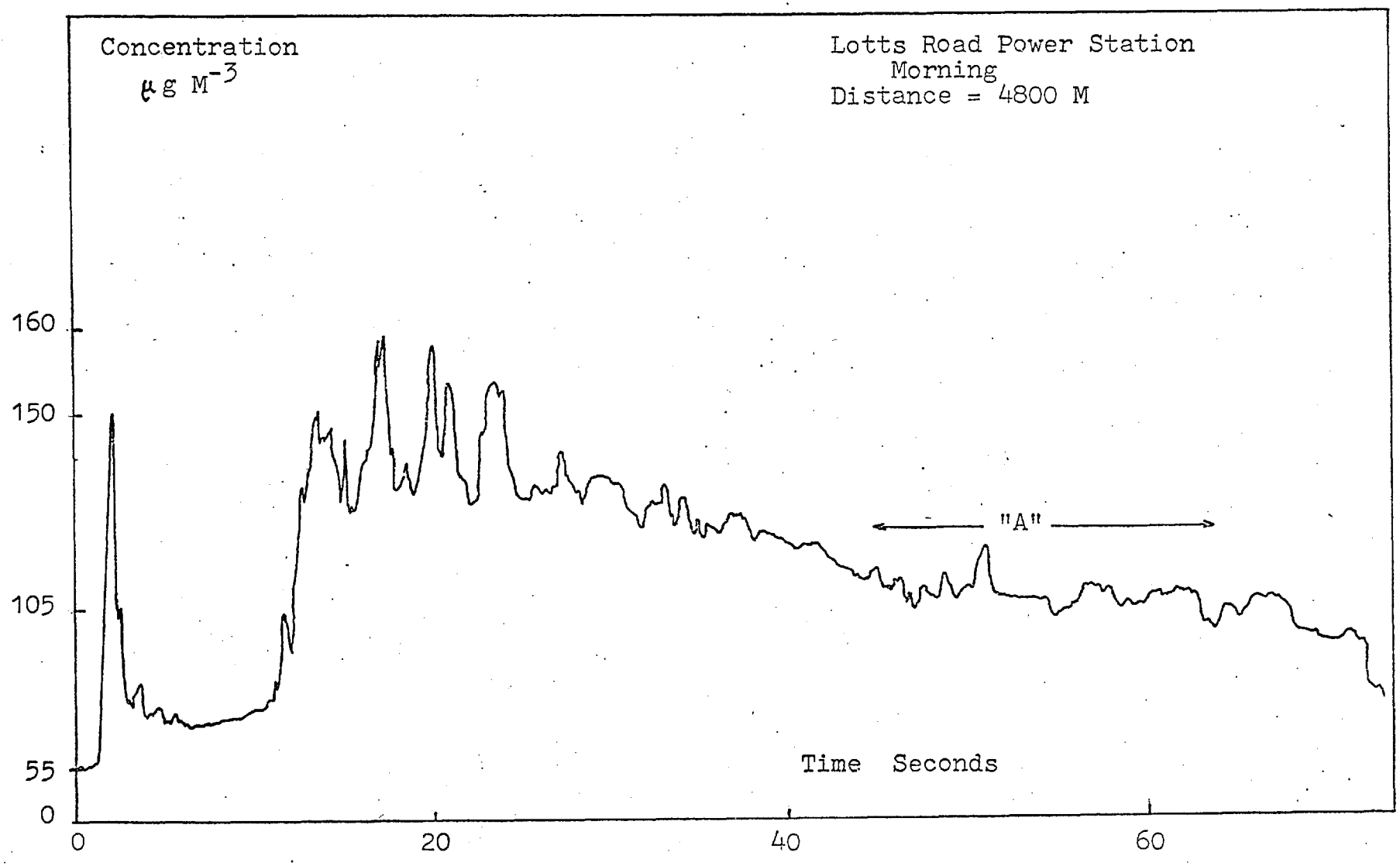

Graph 5.18 This graph shows part of a puff received from Lotts Road Power stations detected on the Aeronautics roof at Imperial College.

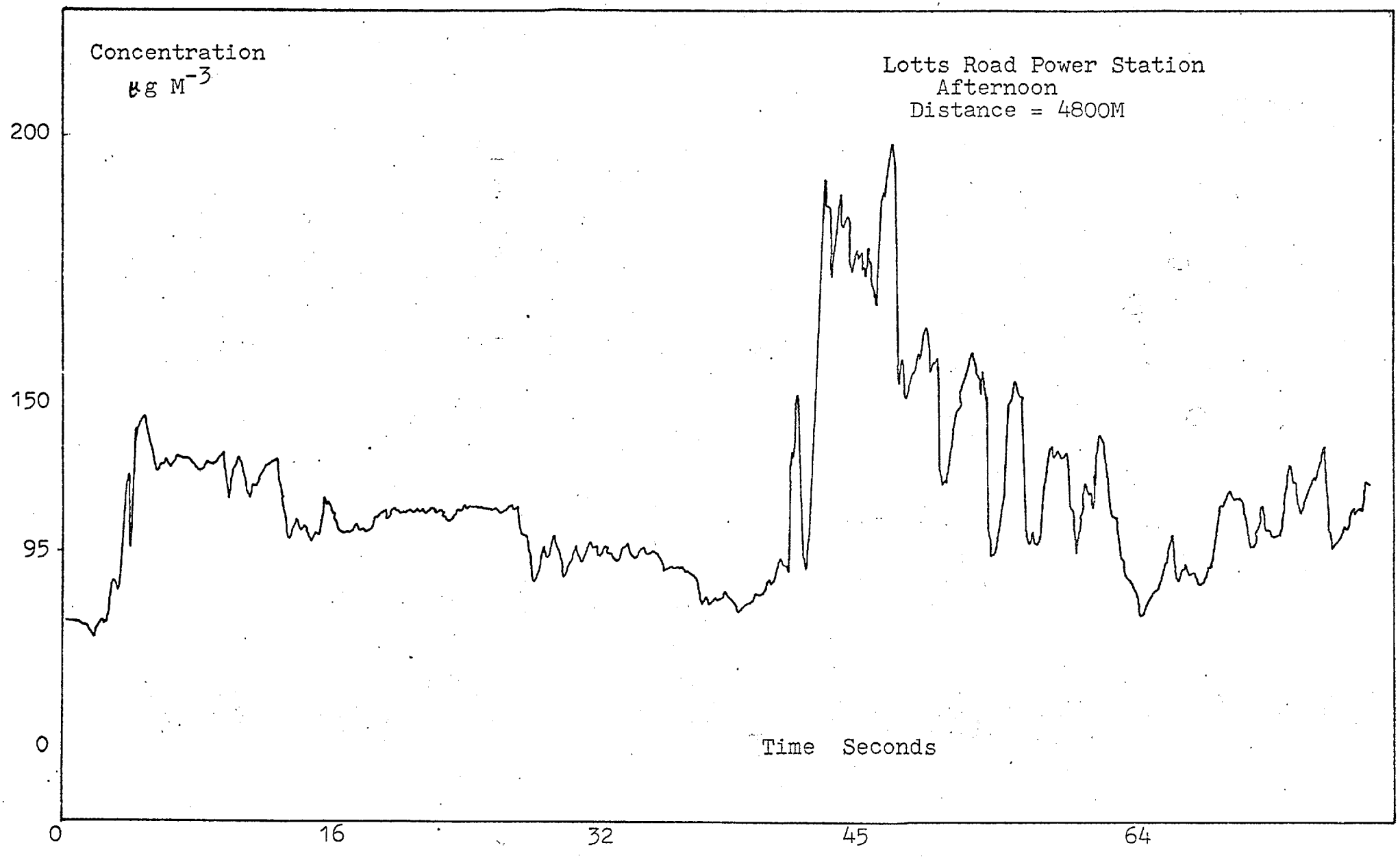

Graph 5.19 This shows part of a puff received from Lotts Road Power Station detected on the Aeronautics roof at Imperial College.

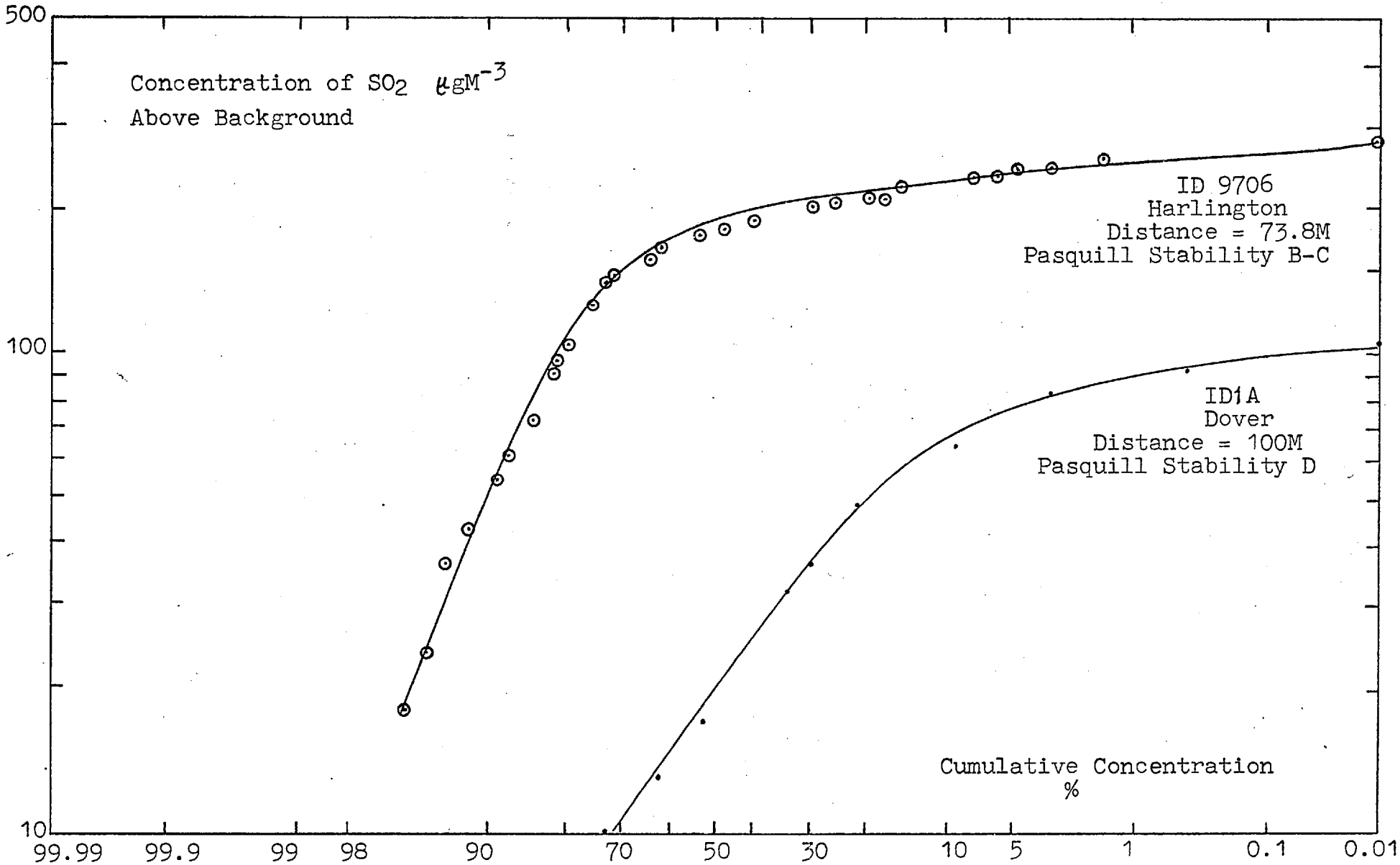

Graph 5.20 This is a plot of the concentration of SO_2 above the background against cumulative concentration distribution (%) plotted on a log-normal probabilit scale.

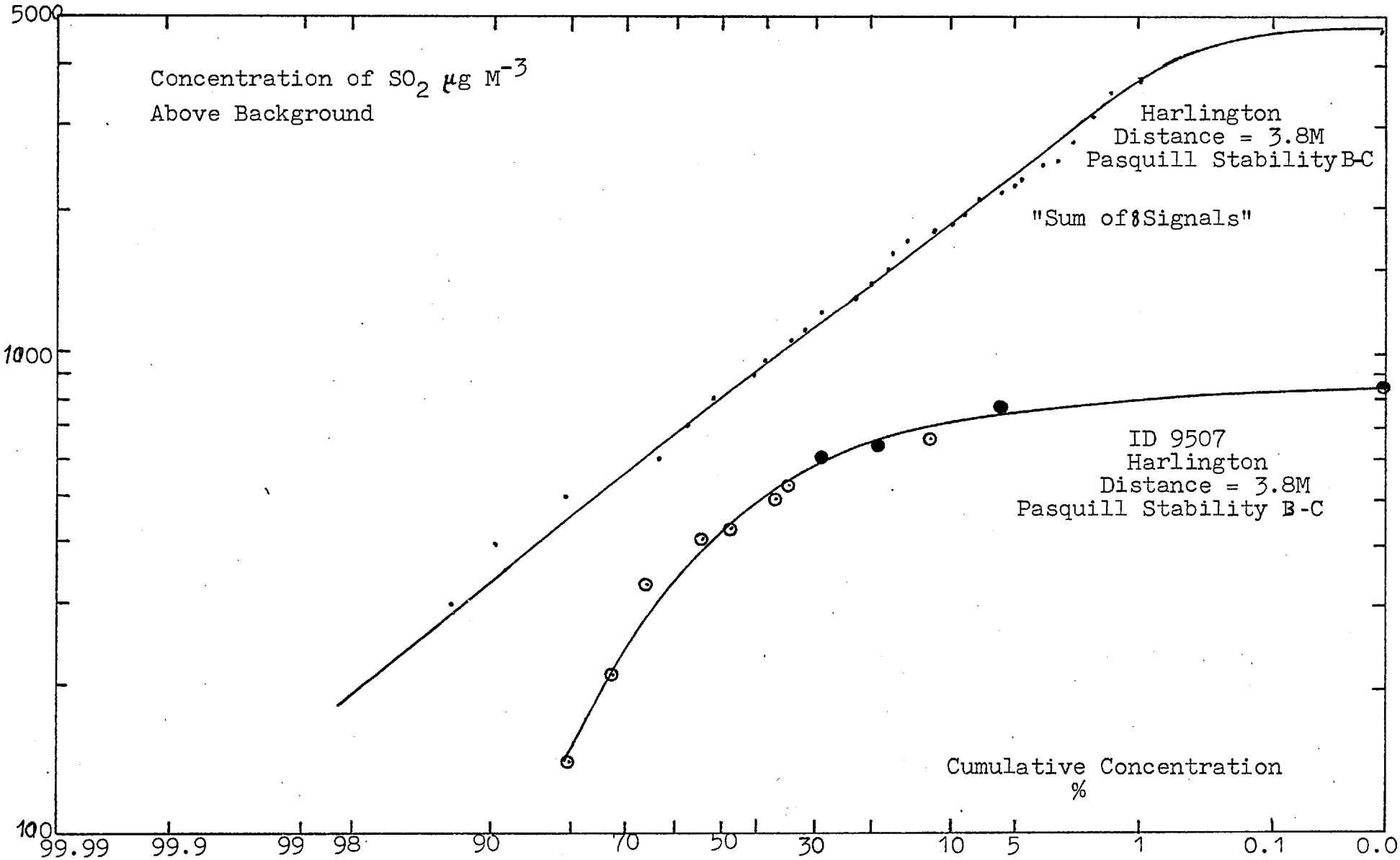

Graph 5.21 This is a plot of the concentration of SO_2 above the background against cumulative concentration distribution (% lotted on a lo -normal robabilit scale.

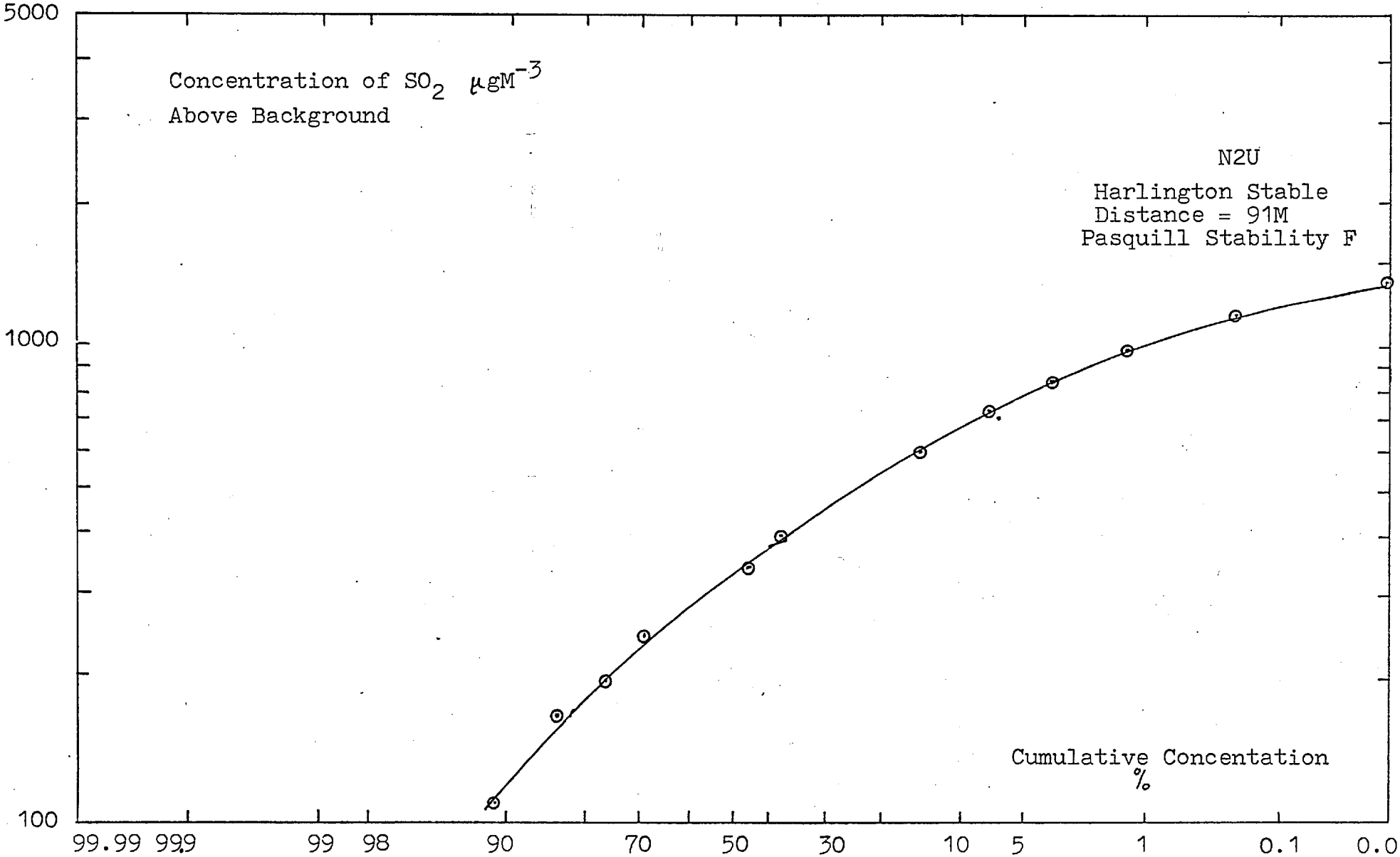

Graph 5.22 This is a plot of the concentration of SO_2 above the background against cumulative concentration distribution (%) plotted on a log-normal probability scale.

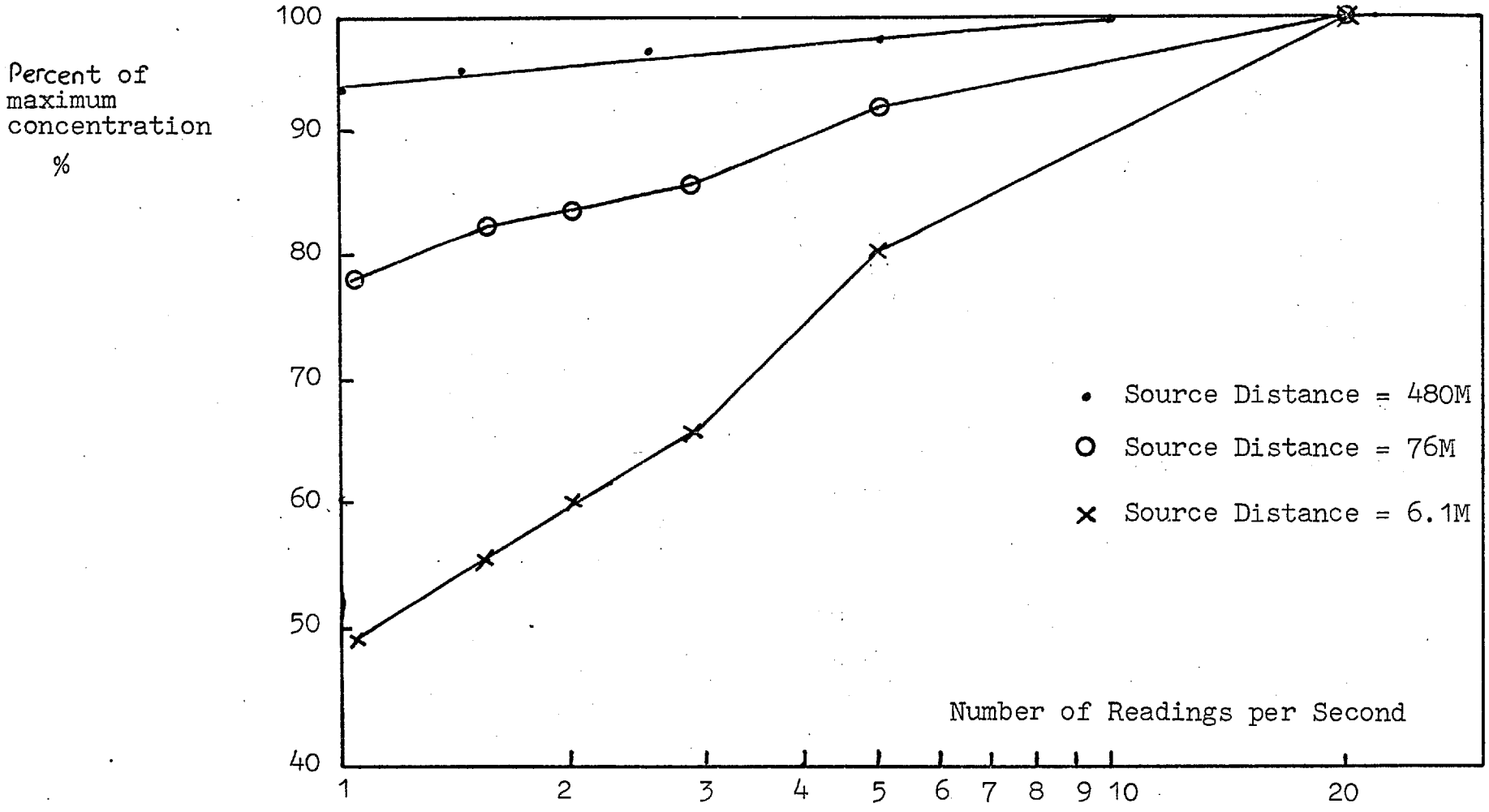

Figure 5.23 Effect of averaging time on maximum concentration.

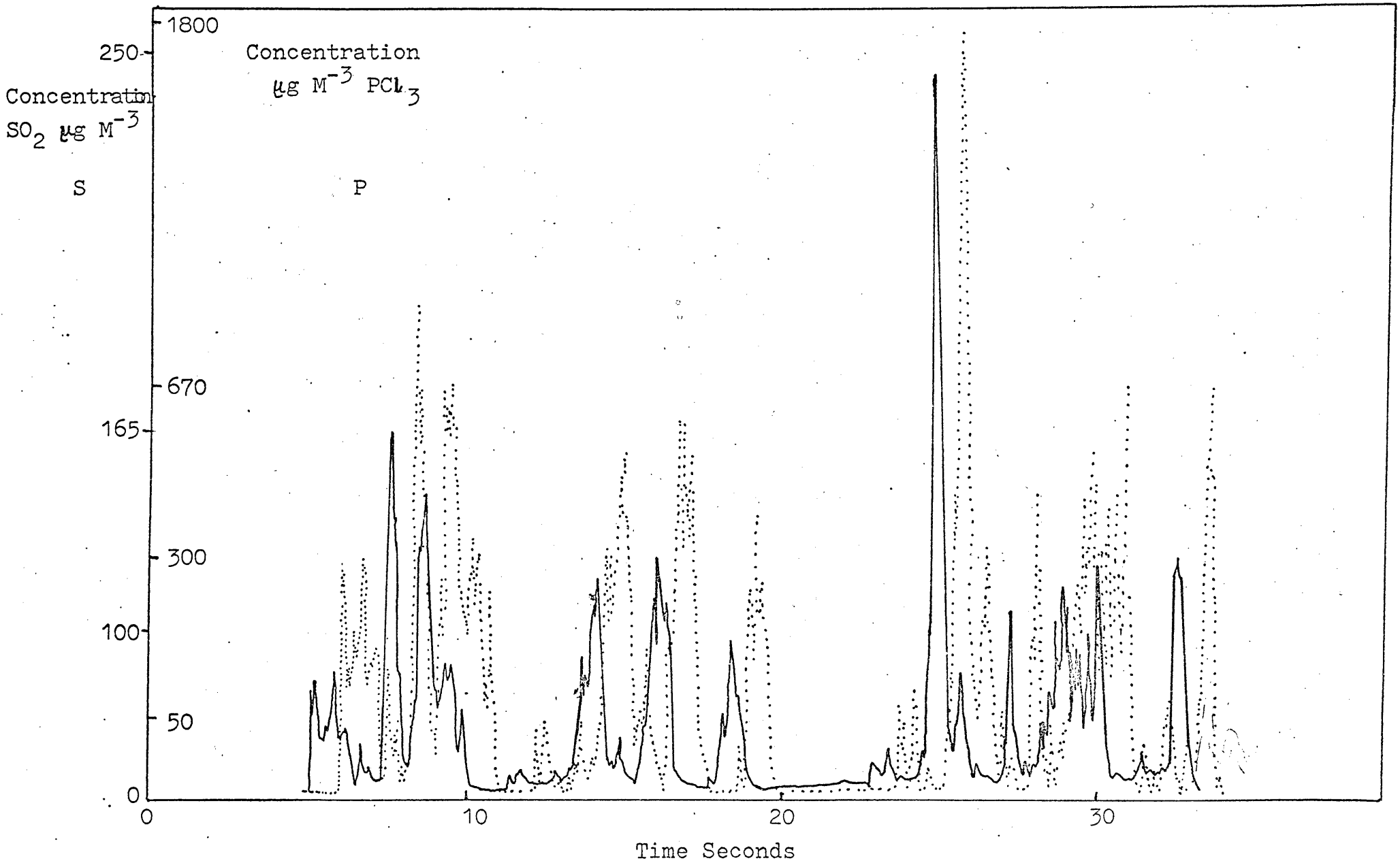

Graph 5.24 This is a graph of the concentration of sulphur dioxide (full line) and phosphorus trichloride (dotted line) against time.

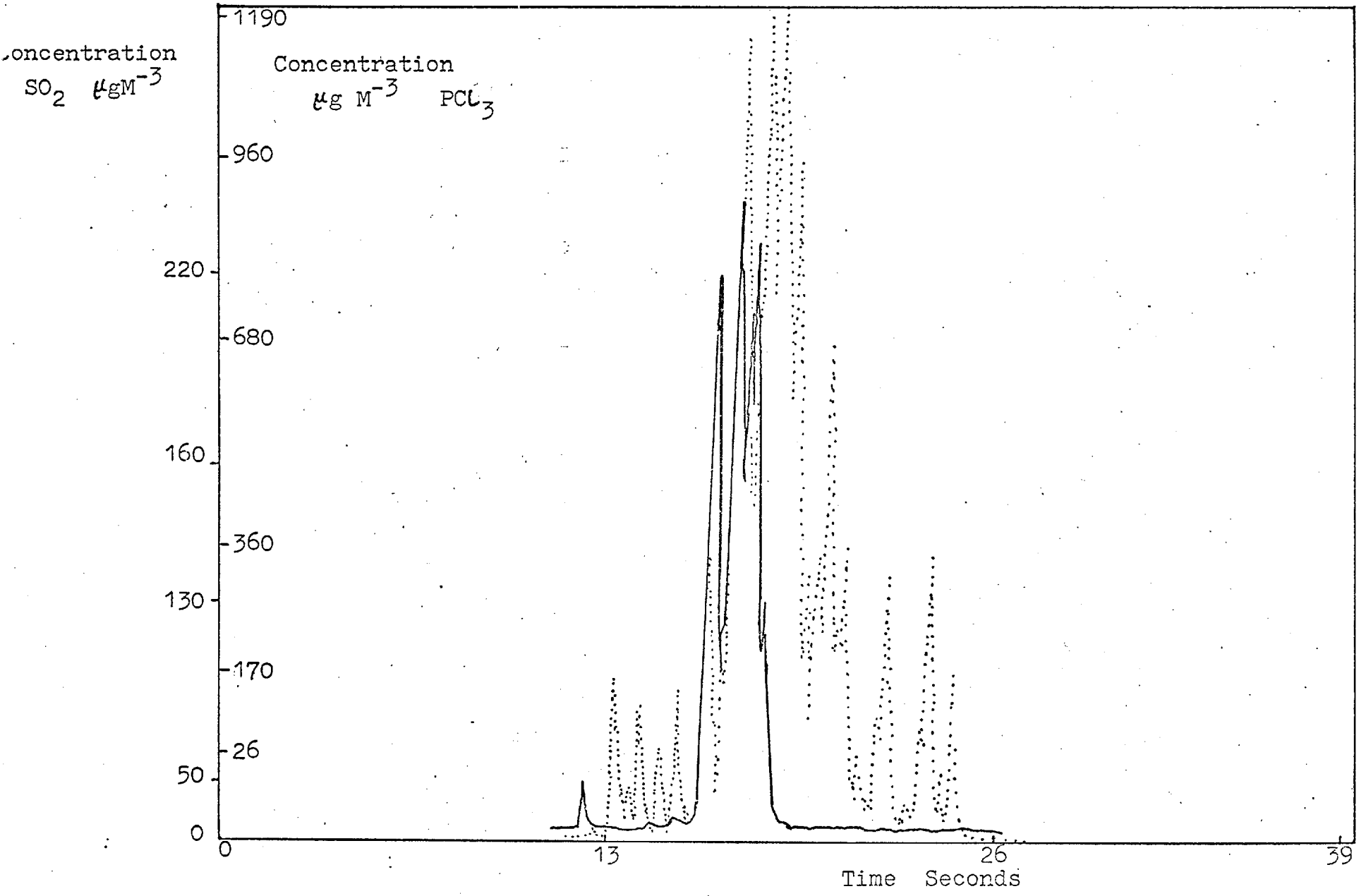

Graph 5.25 This is a graph of the concentration of sulphur dioxide (full line) and phosphorus trichloride (dotted line) against time.

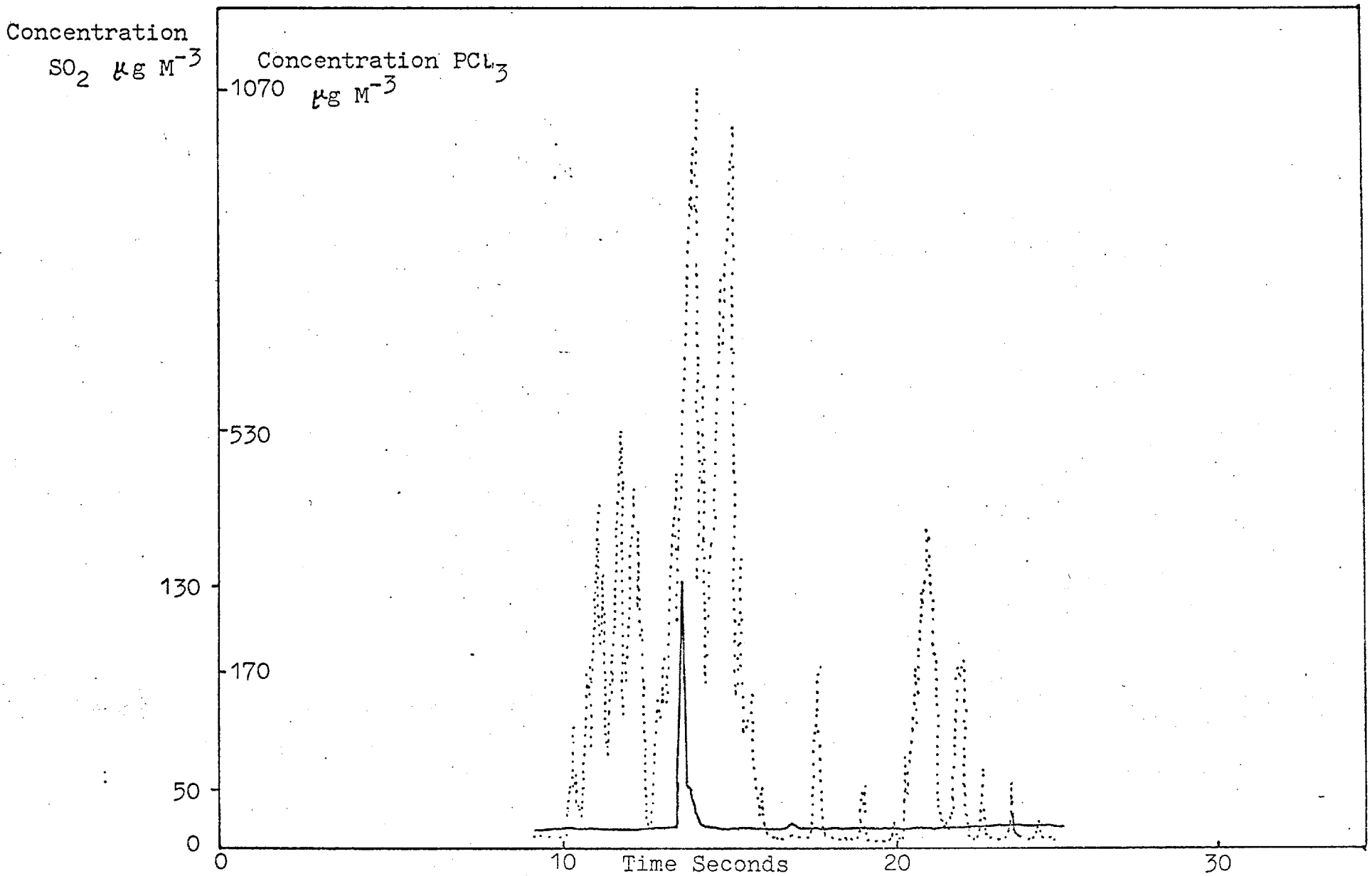

Graph 5.26 This is a graph of the concentration of sulphur dioxide (full line) and phosphorus trichloride (dotted line) against time.

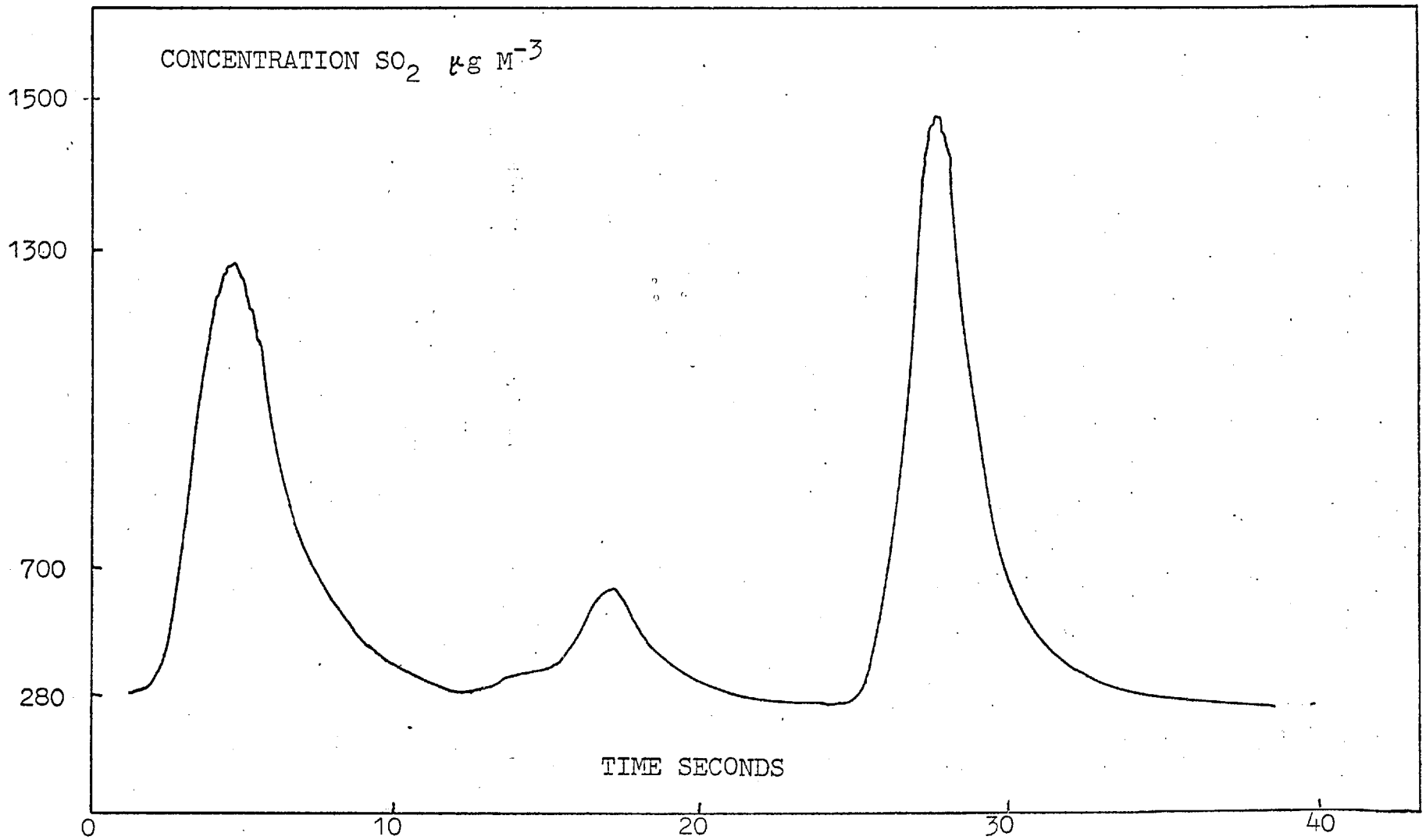

Graph 5.27 This is a graph of the concentration of SO_2 μgM^{-3} against time in seconds with a piece of silicon tubing inserted over the inlet of the detector.

5.3.5 Twin Channel Results

All of the twin channel work was carried out at Drax during the "Committee for the European Commission" campaign. The following account is descriptive and is aided by the use of graphs.

The experiments at Drax (Chapter 5.15 D) were carried out in conditions of a light variable wind, 7/8 cloud cover and slight to overcast insolation (Pasquill stability Criteria C or D). The background concentration at Burn airfield - the operating site - was about 30 $\mu g\ M^{-3}$. The results now described were recorded on 15 September 1976 from 11.00 hours onwards and are particularly convenient for description because of the freedom from cross-channel interference. The sulphur and phosphorus sources were placed 20 metres from the detector with as little separation as was possible (3mm) between the two sources' outlet pipes.

Graph 5.23 shows a piece of graphical record; the full line indicating sulphur leads the dotted line, phosphours because of the fixed separation between the pens pre-set by the design of the graph recorder writing mechanism. As can be seen from the graph, the two signals follow each other very closely and this is evident in the whole of this particular record which lasts about thirteen minutes. The fraction of time for which the concentration of sulphur dioxide is non-zero is about 0.74 i.e. γ is 0.74 for this site and for the above meteorological conditions.

The two sources were then separated by 0.75 metres across wind as accurately as was possible. Graph 5.25 and 5.26 show three distinct stages:

A. The full line - sulphur - is low and constant and there is no correlation with the dotted line - phosphorus.

B. The full line then shows response from sulphur dioxide and there is correlation with the dotted line.

C. Finally, the full line returns to its low constant value and there is no correlation with the dotted line. Throughout the period shown in Graph 5.25 and 5.26 the detector is responding to phosphorus.

The periods when there is zero correlation between the sulphur and phosphorus signals are more the exception than the rule in this record which lasts 2.7 minutes. It is difficult to be more precise about the periods when there is correlation or lack of it. Interpretation of the graphs is made confusing because of the effect of the different speed of response of the two pens enhanced by grease and dirt on the pens' guide lines and because of the fixed separation between the two pens. Despite this, the periods when there is an obvious lack of correlation occupy approximately 5% of the time for which the concentration is non-zero.

Further analysis of the results utilising the correlation coefficient would be justified so as to report more precisely periods when there is negative zero or positive correlation between the two signals.

Generally, for all of the records, the duration of the signals range from under one second to one minute at the distance of 20 metres under the specified meteorological conditions.

The use of two channels recording simultaneously can also provide a means of differentiating between a particle and a sulphur response because the cross-channel interference on the phosphorus channel is different for the two components, therefore enabling better judgement as to the nature of a response in the sulphur channel. Of course, if the detector is operated so that cross-channel interference is negligible then the advantages of differing responses of a particle and sulphur on the phosphorus channel are lost.

5.3.6 Effect of silicon tubing on detector response in the field

The effect on the detector's response to a 50 cm long 5 mm. i.d. section of silicon tubing when inserted onto the detector inlet is shown in Graph 5.26. This graph shows a puff received at the detector from a sulphur candle about six metres away at Harlington under stable conditions. The signal has lost all of the high frequency content that is usually recorded on signals received from such a distance. Also, the signal is significantly attenuated as was verified by the fact that when the tubing was removed, the signal on the sulphur channel immediately exceeded the selected full-scale deflection. The tubing was removed several times to test that the attenuation was real and not due to a sudden change in output of sulphur dioxide from the sulphur candle. Every time the concentration greatly exceeded the selected full-scale deflection.

CHAPTER 6

Discussion

The work previously described has involved two broad areas:-

1. The development and use of the fast-response detector.

2. Experimental work in the field and subsequent data analysis.

The following discussion encompasses these two areas and also involves some wider implications of the work.

6.1 The detector

The detector proved to be a robust and reliable instrument. On only one occasion during the early stages of the work did the instrument require internal maintenance. The maintenance involved replacing an "OVI" light filter with an interference filter on the sulphur channel because of the appearance of "signal blips", as shown in figure 3.11, on the detector's output.

In the field, the hydrogen flowmeter was sensitive to wind gusts. The float in the flowmeter could be seen to bob up and down especially with a strong wind. However, no effect could be seen on the detector's output signal.

The step and frequency response tests discussed in Chapter 3 show that the response-time of the sulphur channel is flat up to 5 HZ and attenuates signals of a frequency of 50 HZ by 20%. Although the transfer function has been calculated for the detector it has not been used to calculate the concentrations of the recorded signals. However, it is likely that a correction would be necessary for the concentrations calculated from signals received from sources at very near distances because of the fast rises and falls occurring in such signals.

The high sensitivities available on the graph recorder and data logger were often sacrificed for lower sensitivities so that the full peak heights could be recorded. This would lead to errors when calculating concentrations, particularly baseline concentrations, from small deflections on the graph recorder or data logger. Signals from low concentration sulphur sources recorded with a high sensitivity on the graph recorder and data logger and with a high photomultiplier sensitivity were often "polluted" with noise. The presence of noise on such signals makes the determination of the beginning and end of the rises and falls more difficult than would otherwise be the case without the noise.

The detector's calibration was checked after each trip and any changes in the calibration curves were noted. These small changes in the calibration curves may have been the result of wear and tear due to transporting the apparatus to and from sites.

Difficulties encountered during operation of the detector often involved the supporting apparatus. The supporting apparatus in this case includes the graph recorder and power supply. Both of these instruments gave trouble at one time or another.

The Phi lips chart recorder - a 25cm 2 channel recorder with full scale deflection in 0.25 seconds and chart speeds up to 320 mm./minute - although new suffered from two distinct disadvantages:

A. The pen s' guide lines and the electrical slide wires required careful cleaning - a clean tissue, and not oil, should be used to clean the guide lines - because of the presence of dirt and grease on them. The effect of dirt and grease on the guide lines drastically slowed down the movement of the pens across the chart. This problem gave considerable trouble whilst at Drax during the C.E.C. Campaign. Operating the graph recorder in the field did not particularly help matters. However, after careful and persistent cleaning the effect of the problem was less inconvenient from the operating point of view, but of course, the speed of response of the two pens was still slightly affected.

B. The second disadvantage of the graph recorder in the field involved the use of Z-fold chart paper. Z-fold chart paper is very convenient for use in the laboratory because the graph recorder can be left switched on with the chart paper neatly folding in its outlet compartment. However, in the

field, especially in humid conditions, the paper becomes limp and does not fold neatly into its compartment. The result of this, especially when operating at Dover, is either the chart paper proceeds to overflow from the compartment and is invariably scavenged by the wind thus creating a nasty mess or the chart paper becomes entangled within the chart drive mechanism of the graph recorder and so the trace of a recording is lost. These problems, naturally, have their greatest effect when a signal of interest is being recorded. Careful vigilance is necessarily kept whilst signals are being recorded.

The power supply became a little troublesome whilst at Drax in the rather damp conditions. The instrument short circuited and had to be kept for 5 or 10 minutes in a relatively warm place. Otherwise, the power supply was reliable.

Generally, the field work involved the use of an apparatus that was not designed for open-air use. The detector worked quite happily in the open and was not affected by rain and sun, although, the electrical connections had to be covered in wet conditions. The field work also involved the use of a great deal of apparatus. The inventory includes dexion, a heavy well-equipped tool box, a gallon of water, a circular glass tank and a whole variety of necessary equipment including, of course, the hydrogen and carbon dioxide cylinders. Fortunately, a good sized car was available for the transportation of the apparatus. To erect and switch on the apparatus to make ready for experiments took approximately 1½ hours at any given site.

It is also noted that although experiments carried out under a clean moonlit sky on a warm night or on a warm summer's day as at Harlington, can be very enjoyable, they are hard work. When the conditions are not so appealing, as was very often the case at Dover, the experiments can be very de-moralising and this is when the hospitality of the "Pilots" was much appreciated.

6.2 Data Analysis

The fast response time of the detector has enabled the concentration fluctuations of sulphur and phosphorus compounds released into the atmosphere to be followed much more closely than has been done in the past. The data obtained from the experiments at different sites has been examined with the following objectives:

A. Generally, to describe both qualitatively and quantitatively the results.

B. Specifically, to examine a possible relation between concentration fluctuations and source distance.

These two objectives are now discussed.

The cumulative distributions of concentrations of sulphur dioxide above the background obtained from point sources and plotted on log-normal probability graph paper have some interesting features. The "trailing off" characteristics exhibited at the top end of the curves on graph 5.20 is visible in the majority of the distributions plotted. This characteristic - which is particularly noticeable in the upper 5 per cent of the distributions - does not have a simple correlation with source distance since distributions obtained from results of near and far sources display similar deviations. There are straight line portions of the graphs and these - generally - occupy 70 per cent to 80 per cent of the total distribution.

In contrast, LARSEN's (1969) plots of concentration (sulphur dioxide, nitrogen dioxide etc.) against frequency (% of time concentration exceeded) on log normal probability graph paper were constructed from data recorded from pollution emitted from large area sources such as cities and straight lines were obtained. Also, CSANADY (1973) obtained straight lines in replots of concentration against cumulative percentage on log-normal probability graph paper using GOSLINE's (1952) and RAMSDELL and HIND's (1971) data obtained from point sources.

BENCALA and SEINFELD (1976) point out that several concentration distributions can be used to fit observed data one of which is the useful log-normal distribution. Up to the present time concentration distributions plotted from data

obtained with instruments having averaging times of 100 milliseconds are non-existent and so comparison is not practical. The effect of changing the averaging time on the concentration distributions has not been examined but this might produce interesting results.

The distribution plotted by summing the distributions from eight signals received at the detector from a distance of about 4 metres fit closely to a straight line - Graph 5.21. The deviations of the concentration distributions from straight lines may be due to several factors including effects of data logging with low sensitivity, data logging with a high sensitivity, instrumental effects such as attenuation by the detector of rapidly rising signals or the inapplicability of the log normal distribution to the results.

The effect of changing the averaging time on the maximum concentration is shown in graph 5.23 and shows that for sources at near distances the maximum concentration is reduced by 50% when the averaging time is increased from 20 milliseconds to 1 millisecond. For sources at far distances the effect of changing the averaging time on the maximum concentration is much less.

The intermittency factor, although only calculated for a few of the results (Chapter 5.3.2) warrants a mention in the discussion. The factor, defined as the fraction of time for which the concentration is non-zero during an experiment,

as reported in the Results was calculated from isolated records of the data. The whole record for say a day's operation at a given site could not usually be used to calculate an intermittency factor. This is because the factor as then determined would merely reflect the success or failure of the experimenter to ensure that the detector was continuously sampling from the sulphur dioxide source i.e. by moving the source across wind. Therefore, the records selected for the calculation involved periods of steady operation without any experimenter interference.

However, for those limited results it is interesting to examine the variability of the intermittency factor especially in stable conditions. For stable conditions at Harlington and with a source distance of about 100 metres, the high values of 0.9, obtained from sampling a plume continuously for several minutes prior to a sulphur dioxide candle being exhausted are in contrast to the zero values when the plume travelled past the detector and nothing was detected. At a distance of 3.8 metres, again for the stable case, the intermittency factor was calculated to be 0.64. Plume meander in the stable conditions may be the most important factor that contributes to the large variability in the intermittency factor obtained from the experiments carried out during the night.

Comparison of the above results with those reported by CSANADY (1973) is avoided because of the different definition

of the intermittency factor used in this work. Also, CSANADY briefly discussed intermittency factors for the two following cases:

a. In relation to a frame of reference moving with the centreline of a continuous plume. For this case CSANADY says that the intermittency factor is known to be unity in the centre portion of the plume and to be zero outside the plume.

b. In a fixed frame of reference the intermittency factor can be as low as 0.65 at the axis of a plume and much lower at the fringes.

However, the work presented here exemplifies the difficulties in defining a so-called plume axis or fringe because of the discrete puff nature of the signals received at the detector.

Some peak/mean values have been calculated and presented in the Results together with the effect of averaging time on the peak concentrations calculated for several results at different distances - figure 5.23. A study of the ratio of peak/mean concentration with different averaging periods has not been carried out. However, the results are available for this to be done and it could be useful because the results may help to deduce short period peak concentrations from long period averages in areas where only long period averaged concentration data are available. SHIRUAIKAR and PATEL (1977)

recently reported the ratios of peak/mean concentration from a single source computed from hourly meterological data for various sampling and averaging periods from 1 hour to 1 year. BARRY(1971) describes the peak to mean concentration ratio obtained from observations near a point source of pollution as being a particular example of the ratio of any short period concentration to the long term mean. BARRY also presents a probability distribution function to calculate the value of this ratio. The data produced from the work presented here can be used to calculate peak to mean concentration ratios at different averaging times (20 milliseconds up to say 20 seconds) and so evaluate the applicability of the distribution function used by BARRY.

The data analysis concerning the investigation of a possible relation between source distance and concentration fluctuations initially involved making the use of observation and, after some experience, it was not difficult to see that rises in recorded signals were faster when received from near sources as opposed to far sources. This was particularly evident in the Dover results when it was noticed that ships entering the Eastern dock, more than 1,500 metres from the detector, produced signals that contained slower rises than the fast rises obtained from signals received from ships entering the Western dock some 70 metres away.

The so-called statistic chosen to help quantify this observation (f(s)) has some distinct attractions;

i) It is simple and can be easily calculated either in the field or in the laboratory. Computer printout or graphical output can be used to provide a value of the statistic.

ii) A simple account is made for wind speed and stability i.e. the results are divided by wind speed and classified by Pasquill stability categories. This is particularly useful in the on-line situation.

The statistic is calculated as detailed in Chapter 5 taking into account some of the difficulties of using output from the digitised recording or graphical output i.e. signals from particles entering the burner. The value of f(s) depends on the relative, not the absolute, values of concentration, having units m^{-1}. For a doubling of concentration $f(s) = \frac{2}{3}\Delta tu$ and for an infinite rise $f(s) = \frac{2}{\Delta tu}$.

The equations produced from regressed values of the statistic show that there is a difference in the results from operation in a stable and an unstable atmosphere. The difference being that the relative rate of change of concentration varies approximately with $(\text{distance})^{-0.6}$ having a correlation coefficient of -0.92 and significant at the 0.01

level for the unstable case, whilst for the stable case the relative rate of change of concentration varies approximately with $(\text{distance})^{-0.2}$ having a correlation coefficient of -0.53 and significant at the 0.01 level. The results for the neutral case are more closely related to the unstable case with the relative rate of change of concentration varying with $(\text{distance})^{-0.75}$ having a correlation coefficient of -0.86 and significant at the 0.01 level.

The regressed results calculated using the statistic f(s) and plotted on Graph 5.2 display a significant difference in that the slope of the line for the stable case (Pasquill Stability Category F) relative to those for the neutral and unstable cases (Pasquill stability categories D and B-C respectively) is smaller. The steeper slope for the neutral and unstable cases may be the result of the greater dispersion of a plume occurring in such conditions so that the pollutant is distributed over larger spatial and temporal scales relative to the stable case. However, it is recognised that effects of, for example, wind variability will influence the signals recorded and hence the concentration fluctuations. These effects will be discussed after discussing the use of various techniques to characterise the signals. Another distinct feature of the results as shown in Appendix A1.1 is the consistent difference in the values of the statistic obtained from sources at near distances (100 metres) and for distances (1300 metres) at Dover.

More statistical stability could be obtained in the results by producing a distribution of say f(s)'s. A distribution would help to characterise the whole of a signal as opposed to a small part as is the case with f(s). For example, for any given signal the statistic f(s) could be calculated for each rise in millivolts that is large compared to the noise i.e. 2 to 3 times the noise. The wind speed would have to be determined as a function of time for the whole signal so that the effect of changing wind speed, during different parts of the record, can be accounted for. The distribution can be plotted using log normal probability graph paper. It is possible that distributions using the falls alone or both the rises and falls may be worthwhile calculating. The distributions can be particularly useful for long records and a series of distribution plots could help to characterise signals from sources at different distances and signals from a single source at one site could be easily summed.

No such plots have been produced for the work reported here. However, Dr. M.J.G. Wilson, in a private communication, has found that values of a statistic, in this case f(s) multiplied by the wind velocity, greater than 0.2 were log normally distributed in many experiments. The difference between the values of this statistic at different distances was striking when expressed in terms of the proportion of values of the statistic above certain levels.

For example, one plot for a distant source revealed values of the statistic equal to 1.43 for the highest 10% and 3.2 at 1% compared with the observed maximum of 4.65 among 342 values of the statistic. If therefore, a maximum value of the statistic of 10 or 20 were determined in a brief experiment, the source would be unlikely to be as distant as the above plot.

The simple statistic f(s) uses only a little of the information available in a signal - usually the information contained in the leading edge of the puff. For signals recorded from puffs or plumes lasting tens of seconds, another statistic - F(s) - has also been calculated but only for a small sample of the results. This statistic is designed to account for the amount of change occurring in the signal per second utilising the major rises and falls not including the noise. The statistic has only been calculated for a few records and table 5.10 shows those values that have been calculated. As with f(s) there is a significant difference in the value of F(s) as calculated for sources at near distances and far distances.

The statistic can be adversely affected i.e. reduced by trailing edges in signals, for example, the trailing edge as seen in figure 5.18, which has been recorded from a plume that has travelled over London from Battersea power station, and may have been affected by top ography and local climate. The trailing edge will contribute significantly to the mean

concentration level determined for the signal but contributes little to the amount of change occurring in the signal per unit time as calculated by the statistic F(s).

Previous work (GRAEDEL, 1977) uses normalised concentration roses and concentration box plots (using hourly averaged values of hydrogen sulphide concentrations) as techniques for remote identification and semiquantitative estimation of both sporadic and continuous sources. However, the techniques assume constancy of wind vector during travel time in the atmosphere from source to detector and in Graedel's words "the technique would be expected to be most useful for simple source matrices."

It must be borne in mind that the statistics and distributions mentioned are attempts to quantify in simple terms an inter-related multi variable problem. Many factors will affect the fluctuations in concentration in a signal received at the detector and therefore affect both the derived distributions and values of the statistic that are calculated. The following factors, other than the distance travelled, wind speed and atmospheric stability, may affect the results:

1. The nature of the source of which some important factors are:

    a) Stack effluent temperature

The stack effluents from many industries are quite warm relative to the atmosphere. The buoyancy resulting from the reduced density of the effluent permits the plume to rise above the stack top. As it rises it cools primarily by entrainment of the cooler air until eventually the temperature differential is dissipated and the buoyant rise ceases. The existence of the temperature differential in buoyant plumes will affect the growth and the distribution of pollutant particularly in relation to that in non buoyant plumes.

b) Stack effluent exit velocity

The beneficial effect of a significant exit velocity is primarily to prevent the downwash of effluent in the lee of a stack. The momentum given the stack effluent by a large exit velocity will also provide additional elevation of the plume before atmospheric turbulence becomes important. However, the incremental height increase is not usually great unless the exit velocity is quite high and an exit plume takes on the characteristics of a jet.

The existence of a high exit velocity, especially if a jet occurs, will influence the growth and therefore the concentration fluctuations in the plume particularly at near distances to the stack.

c) Size of the source.

Both the diameter and height of the stack will affect the dispersion of the plume or puff. Diameter

is important because, for example, the ratio of the area of the plume envelope to its volume increases with a decrease in width of the plume and this will determine how fast buoyancy is dissipated thus affecting plume growth. The height at which a pollutant is introduced into the atmosphere is important because of the variation of atmospheric turbulence with height above the ground.

In the experiments carried out the diameter of the source varied from several millimetres (a match) to several metres (a ship's funnel, a 'Battersea power station' chimney). Source height above the ground varied from less than ten metres to over 70 metres.

d) Position of the source.

On many of the ships large structures - derricks and masts - near to the source can affect the growth and travel of the plume. Several ships have twin funnels both emitting pollution and Hovercraft's have propellors all of which will produce aberrations in the air thus affecting plume behaviour.

2. Influence of buildings and terrain.

Surface irregularities range from an isolated projection or depression on level ground to a dense succession of such features - buildings. Generally, thermal and topographic irregularities occur simultaneously and it is

difficult to distinguish their separate influences on plume behaviour. Most cities create their own modifications of the weather. The most notable of these is the Urban heat island. The bulk heat emissions from fuel consumption and the stored heat in buildings and streets warm the Urban area more than the surrounding countryside. The effect on a plume from a stack located in the Urban area is to enhance vertical spreading. The mechanical turbulence created by the buildings also enhances mixing. The signals recorded from pollution emitted by Battersea powere station are likely to have been influenced by such effects similarly the puffs detected from Imperial College's boiler chimney would have been affected by the wake structure associated with the Electrical Engineering building.

Small volume emissions occurring as short duration puffs released near ground level (as from matches) are also affected by local terrain - induced differences in atmospheric turbulence.

4. Relative velocity of source and wind.

Generally, for the work at Dover, the results will depend upon the relative velocity of source (moving ships) and wind because this will determine the angle at which the plume cross section is sampled.

Two extremes can be envisaged:

a) If there is infinite speed of travel across the plume then all of the variance on the signals recorded comes from this source.

b) If the plume is sampled continuously on the axis for a long enough period then all of the variance on the signal recorded comes from plume variance.

The case of the ships at Dover is intermediate between 4a and 4b because the ships were moving past the detector with the wind blowing the plumes over the detector. Therefore, differences in appearance, as shown on the graph recorder output, and differences in the concentration gradients sampled are expected from signals recorded from stationary and moving sources.

5. Wind Variability.

Variability of the wind particularly under stable conditions with light winds where plume meander is evident will influence the signals recorded at the detector, For example, a plume may be swept to and fro across the detector at varying intervals or it may be sampled continuously for many minutes. The concentration fluctuations recorded at the detector will depend on how the plume is sampled i.e. along the plume axis, at the plume fringes or from both regions of the plume.

The statistics used in this work - f(s) and F(s) - may not necessarily characterise any of the effects of the above factors. For example, f(s) only makes use of the fastest rise occurring in a puff or plume and so is not capable of describing the entire event for which time a plume

is being sampled. This statistic,can therefore, have limited use in describing the effects of wind variability on concentration fluctuations as recorded at the detector. F(s) is better from this point of view because it considers changes in concentration in the whole signal but care has to be exercised in discriminating between noise and major rises and falls, particularly occurring in slowly varying signals. The slowly varying portion of a signal may be important in describing the history of the plume, however, F(s) as already explained only considers the significance of the slowly varying portions in the calculation of the arithmetic mean concentration level of the entire signal. The contribution of the slowly varying portion of the signal to the amount of change in concentration per unit time is not accounted for in F(s).

6.2.1. Twin Channel Work

The twin channel experiments carried out at Burn airfield, Drax, Yorkshire are interesting. Graph 5.24 shows the concentration of sulphur and phosphorus dioxide and phosphorus trichloride. The graph shows a strong positive visible correlation between the two traces - correlation coefficients have not been calculated for this work. When the two sources are separated by a small distance of 0.75 metres across wind, periods are visible in graph 5.25 where no correlation is apparent from inspection of the two traces on the chart. Further detailed examination of the traces obtained from the Drax experiments may provide graphs that

show negative correlation between the two traces for the separated sources. No experiments were carried out by separating the sources along the wind.

This experiment works well for the two sources at a distance of 20 metres from the detector because the atmosphere brings a great deal of information in the form of concentration fluctuations. However, for slowly varying signals received from different sources at different distances the experimenter would have to wait longer to collect the same amount of information and the effect of noise would have to be accounted for noisy signals.

6.3 Future Work

In previous work DESJARDINS and LEMON (1974) used a modified infrared carbon dioxide gas analyser in an experiment designed to measure the eddy fluxes of heat and carbon dioxide above corn crops. Experimental results of the fluxes and the limitations of an eddy correlation technique are discussed in the paper. The carbon dioxide gas analyser had a time constant of 0.5 seconds and this time appeared to be just enough to detect most of the vertical carbon dioxide transfer so long as the sensor was located at least 1 metre above the corn surface.

Over the past year or so the flame photometric detector developed for this work has made it possible to successfully measure sulphur dioxide flux to a forest. This

work is being carried out in conjunction with a team from Harwell and another team from the Institute of Terrestrial Ecology.

Pheromones have been used in population monitoring traps for insects (CAMPION, 1975) and in control by confusion (CAMPION, 1973); a good understanding of how the male finds the female is of great importance in the development of these techniques. Wind tunnel experiments (KENNEDY and MARSH, 1974) have shown that moths fly upwind in a series of horizontal zig-zags which decrease in amplitude as the source is approached. Field observations (SHOREY, 1973) support these general findings. Recent techniques for observing and recording the details of the behaviour of night flying insects in attractant plumes have also been described (MURLIS and BETTANY, 1977). Briefly, the observations of Murlis and Bettany, as they explain, suggest that the flight of male spodoptera littoralis to a pheromone source is made in discrete stages with different flight patterns and also perhaps different orientation mechanisms. The flight paths observed also showed a strongly vertical undulation pattern which contrasts with the horizontal zig-zagging more generally seen. Murlis and Bettany suggest that this may be due in some way to differences in the structure of the pheromone plume.

The presence of concentration fluctuations from a pheromone emitted into the atmosphere and the variation of these fluctuations with distance may contribute to the flow of information available to an insect thereby helping to determine the insect's flight path. An insect such as

Spodoptera littoralis may be able to detect changes in the concentration both in time and space to help determine its distance from the source, possibly responding to slowly varying concentration gradients with the undulating flight at far distances from the source and to fast varying concentration gradients with the hovering flight at near distances to the source. It may be an interesting exercise to calculate the flow of information represented by the records collected in various conditions, distances, sources etc. and so determine an upper limit of what is available to an animal.

Finally, measurements of concentration recorded from fast-response instruments might be useful in the area of conditional sampling. A decision to trap a sample from a nearby source in the presence of emissions from more distant sources could be taken automatically by a suitably designed instrument according to the rate of rise of the concentration from the baseline. If this rate of rise is below a certain level then the sample is not taken thereby reducing, to any desired level, the risk of sampling in error from a distant source. The problem of sampling from the more distant sources can be dealt with by trying to find sufficiently long slow rises but the chance of success may be less than in the former case because nearby sources do produce slow rises.

CHAPTER 7

Conclusions

A fast response flame photometric detector has been developed for measuring the concentration of sulphur and phosphorus compounds in the atmosphere.

The response-time of the detector to 90% of a rise in a step input signal of sulphur dioxide is 80 milliseconds and to 100% in 900 milliseconds. This response time is essentially composed of two time constants; the first describing a fast initial 90% of the rise and the second describing the slower rise to 100% of the input signal. The response time of the sulphur channel for a rise in the concentration of sulphur dioxide is slower and of a different form to that for a fall in sulphur dioxide concentration. These results may be due to the effect of the chemiluminescent reaction occurring within the burner.

The response time of the detector to 90% of a rise or fall in a step input signal of phosphorus pentafluoride is 8 milliseconds and to 100% in 15 milliseconds. These times, as for the sulphur channel, represent maximum limits for the response times because of the non-ideal step input signal generated by the response-time testing apparatus - the Oscillating calibrator. The response time for the phosphorus channel as determined from the tests may be limited by this apparatus.

The amplitude of the output signals from the sulphur and phosphorus channels of the detector shows no significant attenuation at frequencies of 5Hz and 15 Hz respectively.

The fast response detector is capable of responding to fast fluctuating concentration signals in the atmosphere in a way that has not been possible with slower responding instruments developed in the past.

The detector together with a cassette data logger, graph recorder and supporting apparatus have been used for experiments in the field.

The results from the field experiments have been used to produce concentration-time records. The concentration-time records have subsequently been used to quantify the effect of changes in concentration fluctuations with sources at known distances. A statistic has been developed that uses the fastest 50% of a rise above the background concentration - taking into account limitations in the recordings such as noise and digitising effects. This statistic - f(s) - is sutiable for calculation in the field and it generally utilises the changes in concentration occurring in the leading edge of a signal.

In using this statistic it is usually possible to distinguish between recorded signals that originate from known sources at near distances - ten or twenty metres - and

signals from known sources at far distances - about 1000 metres or more - in unstable and neutral atmospheric conditions; the relative rate of change of concentration of calculated using the statistic f(s) varies approximately with $(\text{distance})^{-0.6}$. The results obtained at Dover illustrate this for the neutral case. For stable conditions the relative rate of change of concentration varies approximately with $(\text{distance})^{-0.2}$.

Plots of the concentration of sulphur dioxide against the cumulative percentage on log normal probability graph paper show deviations from a straight line. The intermittency factor - as calculated in this work - exhibits wide variability for the results obtained under stable conditions.

The detector has also been used to record the concentration of both sulphur and phosphorus compounds in the atmosphere.

When the two sources - at a distance of 20 metres from the detector and in neutral atmospheric conditions - were coincident the signals received at the detector displayed persistent high positive "visible correlation" on the graph recorder output. When the two sources were separated by 0.75 a metres across the wind, periods of zero "visible correlation" were in evidence.

The results of this work show locally-emitted pollutants generally carry information about their distance of origin. It may be possible to estimate the proportion of

pollution which originates from sources at any given distance from the measuring site. This information can be useful in assessing how representative are the results from a measuring site relative to the experiences of the local population. The utilisation of a twin or multi-channel instrument may be useful in differentiating between two sources at the same distance but with different emission characteristics i.e. one source emitting sulphur dioxide and another source emitting both sulphur dioxide and NO_x .

The response time of the detector makes it worthwhile of consideration for the following:

1) Experiments used to record the deposition velocity of sulphur dioxide above forests.

2) Experiments in conditional sampling where a decision can be taken to accept or reject a sample from a source of pollution according to the concentration fluctuations measured.

3) Describing signal characteristics in the atmosphere thereby adding to an understanding of these characteristics and help to explain, for example, how insects detect and assimilate information derived from pheromones emitted into the atmosphere.

Finally, information has been recorded approximately 100 times faster than previous workers in this field have achieved but without a proportionate increase in cost.

Some of this information has turned out to be sufficiently useful to make it seem worthwhile to make a further, more deliberate, search for possible applications of this information, or of similar results yet to be collected.

APPENDICES

APPENDIX A1.1 Appendix A1.1 shows the results calculated using the statistic f(s) obtained at Dover. The results were intended for data obtained during the period March to October 1976. The pollutant was emitted from ships moving in and out of the Eastern and Western docks at Dover. The air flow was always over at least a 1500 metre stretch of sea. The results have been grouped together with a Pasquill Stability Category D.

LABEL	WIND VELOCITY M SEC^{-1}	DISTANCE M	f(s)	LABEL	WIND VELOCITY M SEC^{-1}	DISTANCE M	f(s)
M1	1.37	35	6.49	ID 7H	2.19	1300	0.21
ID 1A	7.16	100	2.43				
ID 3B	4.26	100	1.88				
ID 1	2.2	100	3.36				
ID 6C	4.21	100	4.37				
ID 6D	4.26	100	3.0				
ID 6F	3.66	100	3.17				
ID 7J	3.54	100	2.91				
ID 2A	2.65	100	1.87				
ID 7G	4.17	100	2.08				
M9	2.2	100	2.73				
ID 7D	3.81	150	0.95				
M2	2.5	150	1.64				
M6	6.0	150	1.58				
M7	9.3	150	2.01				
M3	3.65	175	1.23				
M4	2.68	175	3.58				
M2	2.25	200	1.4				
M5	3.26	200	1.5				
ID 6E	3.26	1300	0.39				
ID 7A	2.65	1300	0.22				
ID 6B	3.0	1300	0.4				
ID 5A	2.62	1300	0.68				
ID 3C	1.74	1300	0.32				
M8	2.8	1300	0.17				
M10	0.64	1300	0.77				
M11	1.70	1300	0.58				
M11A	2.29	1300	0.22				
M12	1.89	1300	0.79				
M12A	2.34	1300	0.21				
M13	2.0	1300	0.17				
ID 7I	2.62	1300	0.33				

APPENDIX A1.2 Appendix A1.2 shows the results calculated using the statistic f(s) obtained at Harlington. The results were calculated from data obtained on the afternoon of 1st June, 1976. The pollutant detected was emitted from a variety of sources including Ship's Lifeboat Matches and sulphur candles. The land is appreciably flat in and around Heathrow Airport and Harlington has flat grass land of about 15 acres situated near to the Airport. The results have been grouped together with a Pasquill Stability Category B-C.

LABEL	WIND VELOCITY M SEC $^{-1}$	DISTANCE M	f(s)	LABEL	WIND VELOCITY M SEC $^{-1}$	DISTANCE M	f(s)
ID 951	4.35	3.8	2.53	ID 963D	5.5	6.1	4.27
ID 952	4.27	3.8	4.19	ID 9605A	5.24	6.1	2.0
ID 952A	3.8	3.8	2.18	ID 9605B	5.24	6.1	3.32
ID 953A	4.26	3.8	4.67	ID 9606	3.60	6.1	7.50
ID 953B	4.26	3.8	7.5	ID 967	3.93	6.1	5.22
ID 956	4.26	3.8	4.67	ID 968	3.47	6.1	2.77
ID 958	3.76	3.8	6.9	ID 960L	3.62	6.1	6.57
ID 957	4.26	3.8	2.2	ID 960J	5.5	6.1	5.18
ID 959	4.1	3.8	3.05	ID 960K	3.63	6.1	7.52
ID 95013A	4.9	3.8	2.35	ID 960H	3.62	6.1	5.08
ID 95013B	4.9	3.8	5.10	ID 960I	4.6	6.1	8.61
ID 95013C	4.9	3.8	3.32	ID 9609A	3.1	6.1	2.87
ID 95014	5.05	3.8	3.8	ID 9609B	3.1	6.1	2.92
ID 95015	3.93	3.8	3.0	ID 9609C	3.1	6.1	2.55
ID 95012	3.96	3.8	2.93	ID 9501A	4.29	15.2	1.63
ID 960E	3.98	3.8	5.93	ID 95017	5.3	15.2	1.51
ID 960F	3.98	3.8	3.42	ID 9601AB	3.2	15.2	1.81
ID 960G	3.98	3.8	5.18	ID 9601AA	3.1	15.2	3.65
ID 9601A	4.26	3.8	3.62	ID 960A	3.62	15.2	2.53
ID 9601B	4.26	3.8	6.69	ID 960B	3.0	15.2	3.06
ID 96012A	3.98	3.8	3.84	ID 960C	2.98	15.2	2.19
ID 96012B	3.98	3.8	5.95	ID 960D	3.44	15.2	1.28

LABEL	WIND VELOCITY M SEC^{-1}	DISTANCE M	f(s)
ID 96010	3.98	3.8	7.04
ID 9602A	4.26	6.1	3.52
ID 9602B	4.26	6.1	4.46
ID 9602C	4.26	6.1	5.87
ID 964	3.29	6.1	2.74
ID 963A	5.5	6.1	2.8
ID 963B	5.5	6.1	3.73
ID 963C	5.5	6.1	4.29
ID 9703B	3.96		0.91
ID 9705	4.27	76	0.68
ID 97011	4.60	76	1.04
ID 97012A	3.96	76	0.88
ID 97012B	3.96	76	0.76
ID 97013A	4.26	76	0.61
ID 97013B	4.26	76	0.47
ID 97014A	4.08	76	0.39
ID 97014B	4.08	76	0.51
ID 97015A	4.6	76	0.83
ID 97015B	4.6	76	1.37
ID 9706	3.96	76	0.78
ID 97016A	4.6	76	1.58
ID 97016B	4.6	76	0.71
ID 97017A	4.92	214	0.19
ID 97017B	4.92	214	0.22
ID 97018A	4.26	214	0.21
ID 97018B	4.26	214	0.38
ID 97018C	4.26	214	0.33
ID 97019A	4.92	214	0.47
ID 97019B	3.96	214	0.45
ID 97020	3.47	214	0.19
ID 970CA	4.26	214	0.35
ID 970CB	4.26	214	0.42
ID 970D	4.15	214	0.51

LABEL	WIND VELOCITY M SEC^{-1}	DISTANCE M	f(s)
ID 95016	5.24	15.2	2.16
ID 95018	3.96	15.2	1.15
ID 95020	4.96	15.2	1.48
ID 970A1	4.26	76	0.59
ID 970A2	4.26	76	0.99
ID 970B1	4.6	76	0.65
ID 970B2	4.6	76	1.13
ID 9703A	3.96	76	0.81

APPENDIX A1.3 Appendix A1.3 shows the results calculated using the statistic f(s) obtained at Harlington. The results were calculated from data obtained during the night and early morning of July 13, 1976. The pollutant detected was emitted from a variety of sources including ship's lifeboat matches and sulphur candles. The results have been grouped together with a Pasquill Stability Category F.

LABEL	WIND VELOCITY M SEC^{-1}	DISTANCE M	f(s)	LABEL	WIND VELOCITY M SEC^{-1}	DISTANCE M	f(s)
N 11	1.2	2.8	17.4	N 5F	1.6	3.8	10.1
N 12	1.2	3.8	17.2	N 5G1	1.7	3.8	15.9
N 13A	1.2	3.8	14.9	N 5G2	1.7	3.8	18.8
N 13B	1.2	3.8	12.17	N 5H	1.7	3.8	18.2
N 15	1.37	3.8	15	N 5K	1.4	3.8	29.3
N 16	1.70	3.8	12.9	N 125A	1.2	11.4	14.9
N 18	1.5	3.8	15.3	N 125B	1.2	11.4	11.9
N 19	1.24	3.8	38.7	N 125C	1.2	11.4	11.2
N 110A	1.2	3.8	14.9	N 126	1.16	11.4	14.7
N 110B	1.2	3.8	19.2	N 127A	1.09	11.4	15.4
N 111A	1.0	3.8	17.9	N 127B	1.09	11.4	18.3
N 111B	1.0	3.8	14.5	N 128A	1.1	11.4	17.3
N 112A	1.25	3.8	13.5	N 128B	1.1	11.4	19.1
N 112B	1.25	3.8	14.3	N 128C	1.1	11.4	13.1
N 112C	1.25	3.8	23.6	N 129A	1.17	11.4	21.4
N 114A	1.10	3.8	15.4	N 129B	1.17	11.4	9.06
N 1141	1,10	3.8	34.5	N 130A	1.1	11.4	22.1
N 1142	1.10	3.8	39.7	N 130B	1.1	11.4	36.1
N 116	1.10	3.8	15.2	N 131	1.07	11.4	15.2
N 117A	1.10	3.8	12.7	N 132	0.9	11.4	19.9
N 117B	1.10	3.8	16.3	N 135	0.96	11.4	28.6
N 118A	1.10	3.8	28.2	N 136	1.23	11.4	39.8
N 118B	1.10	3.8	25.6	N 138	1.1	11.4	17.8
N 120	1.20	3.8	14.9	N 140	0.7	11.4	16.6
N 121A	0.99	3.8	33.3	N 141	1.02	11.4	17.5
N 121B	0.99	3.8	17.2	N 143	1.02	11.4	14.0
N 122	0.99	3.8	17.1	N 145	0.87	11.4	24.1
N 123	1.06	3.8	43.4	N 146	0.87	11.4	19.5
N 124	1.04	3.8	40.9	N 142	1.07	11.4	11.03
N 5E	1.5	3.8	18	N 134	0.73	11.4	11.10

LABEL	WIND VELOCITY M SEC^{-1}	DISTANCE M	f(s)
N 625	1.29	11.4	8.2
N 626	2.04	11.4	12.06
N 627	1.91	11.4	9.74
N 628	1.05	11.4	12.8
N 629	0.85	11.4	10.1
N 618A	1.16	23	28.4
N 618B	1.16	23	13.79
N 619	1.34	23	11.8
N 620A	0.99	23	17.98
N 621B	0.99	23	9.7
N 621	1.25	23	12.8
N 622	1.34	23	10.4
N 623	0.83	23	15.8
N 624	1.04	23	11.25
N 624B	1.04	23	15.4
N 5U	2.0	23	4.55
N 5W	1.9	23	8.7
N 148	0.82	23	7.26
N 151A	0.82	23	28.05
N 151B	0.82	23	21.3
N 151C	0.82	23	17.1
N 150A	0.98	23	32.4
N 150B	0.98	23	14.18
N 152	0.91	23	11.76
N 153A	0.91	23	27.9
N 153B	1.07	23	27.4
N 154	0.85	23	38.4
N 155	0.85	23	20.7
N 156	0.79	23	6.96
N 162	1.28	23	6.64
N 157	0.82	23	13.17

LABEL	WIND VELOCITY M SEC^{-1}	DISTANCE M	f(s)
N 158	0.91	23	15.16
N 159	0.91	23	19.1
N 160	0.95	23	22.5
N 161	1.13	23	14.7
N 163A	1.3	23	7.15
N 163B	1.3	23	13.5
N 2A	1.2	61	10
N 2D	1.3	61	5.9
N 2E	1.7	61	6.59
N 2J	1.13	61	8.75
N 2K	1.1	61	6.64
N 2L	1.2	61	12.08
N 614	1.67	61	10.78
N 2P	1.13	61	8.58
N 2Q	1.06	61	16.98
N 2R	1.0	61	13.7
N 2M	1.2	61	12.1
N 2UA	1.19	91.2	7.65
N 2UB	1.19	91.2	13.4
N 2V	1.47	91.2	17
N 2W	1.30	91.2	9.23
N 2X	1.26	91.2	7.46
N 3A	1.22	91.2	4.84
N 3B1	1.14	91.2	12.02
N 3B2	1.14	91.2	14.9
N 2T	1.2	91.2	4.75
N 3F	1	91.2	7.7
N 3D	1.1	91.2	12.7
N 3E	0.95	91.2	9.58
N 5B	0.8	144	15.13
N 5C	0.85	144	10.9
N 5A	0.85	144	6.24
N 5C1	0.98	144	4.59
N 5B1	1.1	144	5.36

REFERENCES

ALDOUS, K.M., DAGNALL, R.M., & WEST, T.S., 1970, ANALYST 95 417

BARRINGER, A.R., 1968, 23RD ANNUAL ISA INSTRUMENTATION CONFERENCE, OCTOBER

BARRINGER, A.R., McNEIL, J.D., 1969, ISA-AID SYMPOSIUM, NEW ORLEANS, MAY

BARRINGER, A.R., NEWBURY, B.C., & ROBBINS, J., 1969, AIR POLLUTION CONTROL ASSOCIATION, 62ND ANNUAL MEETING, JUNE

BARRY, P.J., 1971, BOUNDARY LAYER METEOROLOGY, 2, 122

BA RYNIN, J.A.M., 1970, Ph.D. THESIS, UNIVERSITY OF LONDON, THE MEASUREMENT AND PERCEPTION OF SULPHUROUS ODOUR POLLUTANTS

BATCHELOR, G.K., 1953 THE THEORY OF HOMOGENEOUS TURBULENCE, CAMBRIDGE UNIVERSITY PRESS

BATCHELOR, G.K., 1964, ARCH. MECH. STOSOWANEJ, 3, 661

BENCALA, K.E., SEINFELD, J.H., 1976, ATMOSPHERIC ENVIRONMENT, 10 941

BRINSLEY, F., STEPHENS, S., 1946, NATURE, 157, 1946

BRODY, S.S., CHANEY, J.E., 1966, JOURNAL OF GAS CHROMATOGRAPHY, FEBRUARY, 42

CALDER, K.L., 1949, Q.J. MECH. APPL. MATH., 2, 153

CALDER, K.L., 1965, Q.J. ROY. METEOROL. SOC., 91, 514

CAMPION, D.G., et al, 1973, BULL. ent. RES., 64 39

CAMPION, D.G., 1975, PROC. EIGHTH BR. INSECTICIDE FUNGICIDE CONF., 939

CRIDER, W.L., 1965, ANALYTICAL CHEMISTRY, 37, 1770

CRIDER, W.L., SLATER, R.W., 1969, ANALYTICAL CHEMISTRY, 41, 531

CSANADY, G.T., 1973, TURBULENT DIFFUSION IN THE ENVIRONMENT, D. REIDEL, HOLLAND

CSANADY, G.T., HILST, G.R., & BOWNE, N.E., 1968, ATMOSPHERIC ENVIRONMENT, 2, 273

CULLIS, C.F., MULCAHY, M.F.R., 1972, COMBUSTION AND FLAME, 18, 225

DAGNALL, R.M., THOMPSON, K.C., & WEST, T.S., 1967, ANALYST, 92, 506

DAGNALL, R.M., THOMPSON, K.C., & WEST, T.S., 1968, ANALYST, 93, 72

DAVIES, J.H. 1970, ANALYTICAL CHEMISTRY, 42 101A

DESJARDINS, R.L., LEMON, E.R., 1974, BOUNDARY-LAYER METEOROLOGY, 5 451

DRAEGERWERK, H., DRAEGER, B., 1962, W. GERMAN PATENT 1, 133, 918

ENVIRONMENTAL INSTRUMENTAL GROUP, 1972, 1973, INSTRUMENTATION FOR ENVIRONMENTAL MONITORING AIR, LBl-1, LAWRENCE BERKELEY LAB, CALIF. UNIV., BERKELEY, 1

EVERETT, G.L., WEST, T.S., WILLIAMS, R.W., 1974, ANALYTICA CHIMICA ACTA, 68 387

FAIR, R.W., THRUSH, B.A., 1969A, TRANS. FARADAY SOC., 65, 1208

FENIMORE, C.P., JONES, G.W., 1964, COMBUSTION AND FLAME, 8, 133

FORREST, J., NEWMAN, L., 1973, JOURNAL OF AIR POLLUTION CONTROL ASSOCIATION, 23 761

FOWLER, A., VAIDYA, V.M., 1931, PROC. ROY. SOC., A132 310

FOWLES, P., DESORGO, M., YARWOOD, A.J., STRAUSZ, O.P., GUNNING, H.E., 1967, JOURNAL OF AMERICAN CHEMICAL SOCIETY, 89 1352

FROSTLING, H., BRANTTE, A., 1972, JOURNAL PHYS. E : SCI INSTRUM, 5 251

GAYDON, A.G., 1974, THE SPECTROSCOPY OF FLAMES, CHAPMAN & HALL, LONDON

GAYDON, A.G., WHITTINGHAM, G., 1947, PROC. ROY. SOC., A189, 313

GAYDON, A.G., WOLFHARD, H.G., 1952, PROC. ROY. SOC., A213, 366

GEU TER, R., 1907, ZWISS. PHOTOG., 5, 33

GIFFORD, F., 1959, ADV. IN GEOPHYSICS, 6, ACADEMIC PRESS

GIFFORD, F., 1960, INT. JOURNAL OF AIR POLLUTION, 3, 253

GILBERT, P.T., SEE SYTY, A. & DEAN, J.A.

GLOVER, J.H., 1975, THE ANALYST, 100, 449

GOSLINE, C.A., 1952, CHEM. ENG. PROG., 48, 165

GRAEDEL, T.E., 1977, ATMOSPHERIC ENVIRONMENT, 11, 313

HALL, H.J., 1974, ANALYSIS INSTRUMENTATION, 12, 1

HAMILTON, P.M., 1969, ATMOSPHERIC ENVIRONMENT, 3, 221

HEALY, C., ATKINS, D.H.F., 1975, ENVIRONMENTAL & MEDICAL SCIENCES DIVISION, AERE, HARWELL, AERE - R7956

HODGESON, J.A., McCLENNY, W.A., HANST, P.L., 1973, SCIENCE, 182, 248

ISACSSON, V., WETTERMARK, G., 1974, ANALYTICA CHIMICA ACTA, 68, 339

JENKINS, G.M., WATT, D.G., 1968, SPECTRAL ANALYSIS AND ITS APPLICATIONS, HOLDEN AND DAY

KARMARKAR, K.H., WEBBER, L.M. & GULBAULT, G.G., 1976, ANALYTICA CHIMICA ACTA, 81, 265

KATZ, M., 1969, MEASUREMENT OF AIR POLLUTANTS, W.H.O., GENEVA

KAY, R.B., 1967, APPLIED OPTICS, 6, 776

KENNEDY, J.S., MARSH, D., 1974, SCIENCE, 189, 999

KILDAL, H. , BYER, R.L. , 1971 , PROC. I EEE, 59, 1644-1633

KONDRATIEV, V.N., 1962, KINETICS OF CHEMICAL GAS REACTIONS (TRANSLATION OF RUSSIAN EDITION OF 1958) A.E.C. - tr - 4493

LAM THANH MY, PEYRON, M.J., 1963, J. CHIM PHYS, 60 1289

LARSEN, R.I., 1969, JOURNAL OF AIR POLLUTION CONTROL ASSOCIATION, 19, 24

LINDQUIST, F., LANTING, R.W., 1972, ATMOSPHERIC ENVIRONMENT, 6, 943

LUDLUM, E.B., 1935, J. CHEM. PHYS., 3 617

LUMLEY, T.L., PANOFSKY, H.A., 1964, THE STRUCTURE OF ATMOSPHERIC TURBULENCE, INTERSCIENCE PUBLISHERS, NEW YORK

McCORMICK, R.A., 1954, QUARTERLY JOURNAL OF THE ROYAL METEOROLOGICAL SOCIETY, 80, 359

MEASURES, R.M., PILON, G., 1972, OPTO-ELECTRONICS, 4, 141

MONIN, A.S., 1959, SMOKE PROPAGATION IN THE SURFACE LAYER OF THE ATMOSPHERE IN FRIENKEL F.N. AND SHEPPARD (EDS), ACADEMIC PRESS, NEW YORK, "ADVANCES IN GEOPHYSICS", 6

MUELLER, P.K., KOTHNY, E.L., 1973, ANALYTICAL CHEMISTRY 45, 1R

MURLIS, J., BETTANY, B.W., 1977, NATURE, 268 433

PANOFSKY, H.A., 1953, QUARTERLY JOURNAL OF THE ROYAL METEOROLOGICAL SOCIETY, 79, 150

PANOFSKY, H.A., DELAND, R.J., 1959, ADV. GEOPHYS., 6 41

PANOFSKY, H.A., McCORMICK, R.A., 1952, GEOPHYS. PAPER G R D, CAMBRIDGE (USA) No. 19, 359

PANOFSKY, H.A., McCORMICK, R.A., 1954, QUARTERLY JOURNAL OF THE ROYAL METEOROLOGICAL SOCIETY, 80, 557

PANOFSKY, H.A, VAN DER HOVEN, I., 1955, QUARTERLY JOURNAL OF THE ROYAL METEOROLOGICAL SOCIETY, 81, 350

PASQUILL, F., 1961, THE METEOROLOGICAL MAGAZINE, 90, 34

PASQUILL, F., 1962, ATMOSPHERIC DIFFUSION, D. VAN NOSTRAND CO. LTD., NEW YORK

PLATE, E.J., 1971, AERODYNAMIC CHARACTERISTICS OF ATMOSPHERIC BOUNDARY LAYERS, U.S. ATOMIC ENERGY COMMISSION, OAK RIDGE, TENN.

RAMSDELL, J.W., Jr., HINDS, W.T., 1971, ATMOSPHERIC ENVIRONMENT, 5, 483

RICHARDSON, L.F., 1926, PROC. ROY. SOC., A110, 709

ROBERTS, O.F.T., 1923, PROC. ROY. SOC., 104A, 640

RUDOLF SEITZ, R., NEARY, M.P., 1974, ANALYTICAL CHEMISTRY, 46, 188A

RUMPF, K.Z., 1938, Z. PHYS. CHEM. B, 38 469

SALET, G., 1869, BULL. SOC. CHIM. FRANCE, 11, 302

SALTZMAN, B.E., CUDDEBACK, J.E., 1975, ANALYTICAL CHEMISTRY, 47, 1R

SCHWARZ, F.P., OKABE, H., WHITTAKER, J.K., 1974, ANALYTICAL CHEMISTRY, 46, 1024

SHACKELFORD, W.M., GULBAULT, G.G., 1974, ANALYTICA CHIMICA ACTA, 73 383

SHAW, M., 1968, PROC. 1ST NATIONAL SYMPOSIUM HETEROGENEOUS CATALYSIS FOR CONTROL OF AIR POLLUTION, NOVEMBER 21-22

SHILLER, J.W., CAMPBELL, D.N., WINTER 1971, BENDIX TECHNICAL JOURNAL, 51

SHIRUAIKAR, V.V., PATEL, P.R., 1977, ATMOSPHERIC ENVIRONMENT, 11, 387

SHOREY, H.H., 1973, A. REV. ENT., 18, 349

SLADE, D.H. (ed.), 1968, METEOROLOGY AND ATOMIC ENERGY, U.S. ATOMIC ENERGY COMMISSION, OAK RIDGE, TENN.

STEVENS, R.K., HODGESON, J.A., 1973, ANALYTICAL CHEMISTRY, 45, 443A

STEVENS, R.K., MULIK, J.D., O'KEEFFE, A.E., & KROST, K.J., 1971, ANALYTICAL CHEMISTRY, 43, 827

STEVENS, R.K., O'KEEFFE, A.E., 1970, ANALYTICAL CHEMISTRY, 42, 143A

SUGDEN, T.M. BULEWICZ, E.M., DEMERDACHE, A., 1962, CHEMICAL REACTIONS IN THE LOWER AND UPPER ATMOSPHERE, WILEY, NEW YORK, 89

SUGDEN, T.M., DEMERDACHE, A., 1962, NATURE, 195, 596

SUTTON, O.G., 1953, MICROMETEOROLOGY, McGRAW-HILL, NEW YORK

SYTY, A., DEAN, J.A., 1968, APPLIED OPTICS, 7, 1331

TAYLOR, G.I., 1921, PROC. LONDON MATH. SOC., SER. 2, 20, 196

TAYLOR, G.I., 1938, PROC. ROY. SOC., A164, 476

TOWNSEND, A.A., 1956, THE STRUCTURE OF TURBULENT SHEARFLOW, CAMBRIDGE UNIVERSITY PRESS, LONDON, 315

VEILLON, C., PARK, J.Y., 1972, ANALYTICA CHIMICA ACTA, 60, 293

WEST, P.W., GAEKE, C.C., 1956, ANALYTICAL CHEMISTRY, 28, 1816

WILLIAMS, D.T., HAGGER, R.N., Jr., 1970, APPLIED OPTICS, 9, 1597

WILLIAMS, D.T., KOLLITZ, B.L., 1968, APPLIED OPTICS, 7, 607

WOHLERS, H.C., TRIEFF, N.M., NEWSTEIN, H., & STEVENS, W., 1967, ATMOSPHERIC ENVIRONMENT, 1, 121